

**Novel, Differentiated
Antibody Drug Conjugate
Warheads from Analysis of
the NCI Screening Database**

This thesis is submitted to Newcastle University for the
degree of Doctor of Philosophy

Daniel Brough

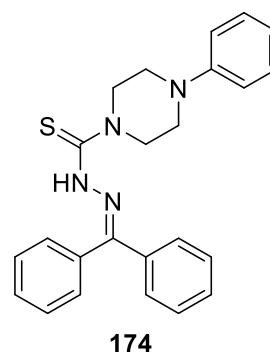
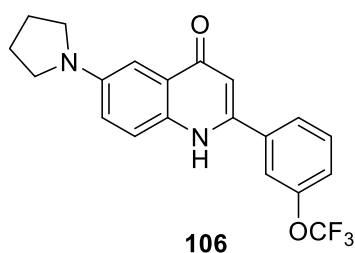
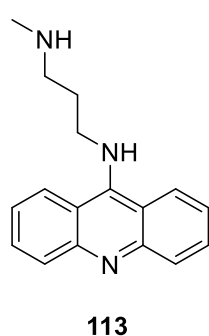
Northern Institute for Cancer Research

September 2019

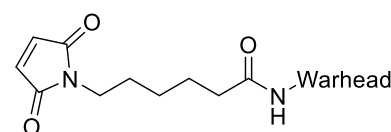
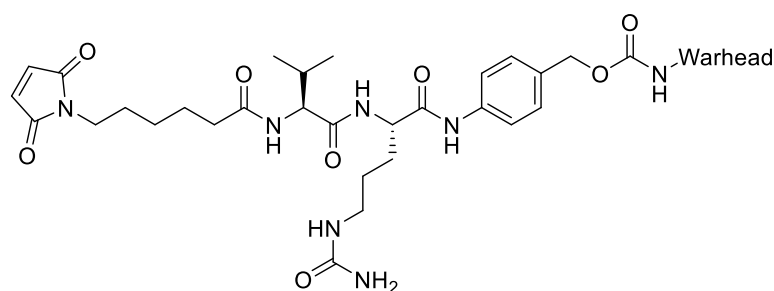
Abstract

Antibody-drug conjugates (ADCs) combine the selective nature of targeted therapies with potent cytotoxic warheads utilising linker technology to deliver selectively the warhead to the target. Proof of concept has already been observed with five licensed ADCs on the market, giving confidence to the use of ADCs in cancer treatment, with multiple ADCs in clinical testing. Many of these ADCs consist of cytotoxic payloads derived from complex natural products, consequently leading to synthetically long and complicated routes.

To address this problem, novel warheads have been identified through screening the NCI database, that are structurally simpler drugs with differing cellular activity profiles. This may also address resistance issues. Out of the seven that were identified, three series have been explored; the nitroacridines (**113**), the quinolones (**106**) and thiosemicarbazones (**174**). Nitroacridines inherently target hypoxic cells and are known to intercalate with DNA. Quinolones are known tubulin binders and compounds synthesised have been evaluated in biological studies. Thiosemicarbazones are metal chelators, sequestering iron and copper. They inhibit ribonucleotide reductase, inactivating the enzyme leading to cell death.



Work has been carried out to optimise and resynthesize these parent warheads as well as analogues. The warheads have been coupled to non-cleavable and cleavable dipeptide linkers (examples shown below) and subsequent conjugation to an antibody, which have been assessed in cell assays.



Declaration

The work described in this thesis was carried out between September 2015 and August 2019 in the Northern Institute for Cancer Research Medicinal Chemistry Laboratories (Bedson Building, School of Chemistry, Newcastle University, Newcastle upon Tyne, UK, NE1, 7RU). All the research described in this thesis is original and does not incorporate any material or ideas previously published or presented by other authors, except where acknowledged by references. Compounds which were biologically tested was performed by me with help from Nicole Phillips. Compounds **106** and **157** were further tested by Dr Lisa Prendergast and Joshua Fayers. Analysis of the NCI database was done by Professor Mike Waring and Dr. Alfred Rabow.

No part of this thesis is being, or has been previously, submitted for a degree, diploma or any qualification at any other university.

Acknowledgements

First and foremost, I would like to thank my supervisor Professor Mike Waring for his generous support and guidance over the years, for which I'm very thankful for. I would also like to thank Dr Céline Cano, Dr Ian Hardcastle and Professor Bernard Golding for their expertise and knowledge throughout my degree.

I'd like to thank everyone from the NICR Medicinal Chemistry Laboratory past and present for making my time so enjoyable; Dr Harry Shrides, an inspiration to us all, Dr Stephen Hobson, for inspiring confidence and his excellent mentorship, Dr Greg Aldred, Ayaz Ahmad, Dr Duncan Miller, for his endless source of knowledge, Dr Hannah Stewart, Dr Kirsty Wilson, Dr James Sanderson, Dr Cinzia Bordini, Dr Shaun Stevens, Dr Suzannah Harnor, Edwige Picazo, Dani Lopez Fernandez, Mélanie Uguen, Luisa Camarin, Shaimaa Khalifah, Islam Al-Khawaldeh, Gemma Davison for her excellent punctuality, James Hunter, for his mass spec expertise, Dr Christine Basmadjian, Harriet Stanway, Shengying (Lish) Lin, Dr Marion Prieri, Dr Anne-Sophie Marques, Ziwei Jiang, Selma Dormen, Rosie Bannister, Dr Jennyfer Goujon-Ricci, Conghao Gai, Dr Amy Heptinstall, Dr Mohammed Al Yasiri, Lukas Sprenger, Dr Lauren Molyneux, Jade Hooper, Charlotte Rayburn and Jessica Graham. I also want to thank my tumour targeting team of Pasquale Morese for his great musical taste and comedy style that I had to endure.

Special thanks goes to the best lab partner I never had, Dr Alfie Brennan for being the best drunk and making any conference more enjoyable and Dr Alexia Papaioannou for being a true friend over the years and always instilling fun and joy to work.

I would like to thank AstraZeneca and my industrial supervisor Dr Jeremy Parker

I would also like to thank our bioscience colleagues at the NICR; Nicole Phillips in particular for helping me perform the cell assays, Dr Lisa Prendergast and Dr Claire Jennings.

Finally, I would like to thank all my friends and family who have supported me and kept me sane over these past few years.

Abbreviations

5-Fu	-	5-Fluorouracil
Ab	-	Antibody
Ac	-	Acetyl
AcOH	-	Acetic acid
ADC	-	Antibody-drug conjugate
Ala	-	Alanine
ALL	-	Acute Lymphoblastic Leukaemia
AML	-	Acute Myeloid Leukaemia
Aq	-	Aqueous
Ar	-	Aryl
Arg	-	Arginine
Asn	-	Asparagine
ATP	-	Adenosine Triphosphate
AzAb	-	Antibody containing an azide residue
B-ALL	-	B-Acute Lymphoblastic Leukaemia
Bcr-Abl	-	Kinase encoded by the BCR-ABL1 gene
BEP	-	2-Bromo-1-ethyl-pyridinium tetrafluoroborate
Boc	-	<i>tert</i> -Butyloxycarbonyl
Br	-	Broad
CA6	-	Carbonic anhydrase 6 encoded by the CA6 gene
CA9	-	Carbohydrate antigen 10
CAN	-	Ceric ammonium nitrate
CBI	-	1,2,9,9a-tetrahydrocyclopropa[c]benz[e]indol-4-one
CD30	-	Cluster of differentiation antigen 31

CD33	-	Cluster of differentiation antigen 33
CD70	-	Cluster of differentiation antigen 70
CDR	-	Complimentary determining region
CHO	-	Chinese hamster ovary cells
CHOP	-	Combination therapy with cyclophosphamide, vincristine, prednisone and doxorubicin
Cit	-	Citrulline
Conc.	-	Concentrated
COSHH	-	Control of Substances Hazardous to Health
COSY	-	Correlation spectroscopy
CTLA-4	-	Cytotoxic T-lymphocyte-associated protein 4
CVP	-	Combination therapy with cyclophosphamide, vincristine and prednisone
Cys	-	Cysteine
DABCO	-	1,4-Diazabicyclo[2.2.2]octane
DAR	-	Drug to antibody ratio
DCC	-	<i>N, N'</i> -Dicyclohexylcarbodiimide
DCM	-	Dichloromethane
DCU	-	Dicyclohexylurea
DDQ	-	2,3-Dichloro-5,6-dicyano-1,4-benzoquinone
DHFR	-	Dihydrofolate reductase
DIC	-	<i>N, N'</i> -Diisopropylcarbodiimide
DIPEA	-	<i>N-N</i> -diisopropylethylamine
DLBCL	-	Diffuse Large B-cell Lymphoma
DLL3	-	Delta-like 3 encoded by the DLL3 gene

DM1	-	Mertansine
DM4	-	Ravtansine
DMAP	-	4-Dimethylaminopyridine
DMB	-	2,4-Dimethoxybenzyl ether
DME	-	Dimethoxyethane
DMED	-	<i>N,N'</i> -Dimethylethylenediamine
DMF	-	<i>N,N</i> -Dimethyl formamide
DMSO	-	Dimethylsulfoxide
DNA	-	Deoxyribosenucleic acid
DTT	-	Dithiothreitol
EDC	-	1-Ethyl-3-(3-dimethylaminopropyl)carbodiimide
EEDQ	-	<i>N</i> -Ethoxycarbonyl-2-ethoxy-1,2-dihydroquinoline
ELSD	-	Evaporative Light Scattering Detector
ES	-	Electrospray ionisation
Et ₃ N	-	Triethylamine
EtOAc	-	Ethyl Acetate
EtOH	-	Ethanol
Fc	-	Fragment crystallisable region
FDA	-	Food and Drug Administration
FGE	-	Formylglycine-generating enzyme
Fmoc	-	Fluorenylmethyloxycarbonyl
FTIR	-	Fourier-Transform Infra-Red spectroscopy
GI ₅₀	-	Concentration for 50% of maximal inhibition of cell proliferation
Glu	-	Glutamic acid
Gly	-	Glycine

HATU	-	(1-[Bis(dimethylamino)methylene]-1H-1,2,3-triazolo[4,5-b]pyridinium 3-oxide hexafluorophosphate, Hexafluorophosphate Azabenzotriazole Tetramethyl Uronium
HBTU	-	(2-(1H-benzotriazol-1-yl)-1,1,3,3-tetramethyluronium hexafluorophosphate
HER2	-	Human epidermal growth factor receptor 2
HIV	-	Human immunodeficiency virus
HMBC	-	Heteronuclear Multiple Bond Coherence
HOBt	-	Hydroxybenzotriazole
HPLC	-	High-Performance Liquid Chromatography
HRMS	-	High-Resolution Mass Spectrometry
IC ₅₀	-	The half maximal inhibitory concentration
IgA	-	Immunoglobulin A
IgD	-	Immunoglobulin D
IgE	-	Immunoglobulin E
IgM	-	Immunoglobulin M
IPA	-	Isopropyl alcohol
IR	-	Infrared
KHMDS	-	Potassium bis(trimethylsilyl)amide
λ _{max}	-	Wavelength for an absorption maximum
LC ₅₀	-	Lethal concentration required to kill 50% of the population
LC-MS	-	Liquid Chromatography Mass Spectrometry
Lys	-	Lysine
m.p.	-	Melting point
mAb	-	Monoclonal antibody

mal	-	Maleimide
MDR	-	Multi drug resistance protein
MeCN	-	Acetonitrile
MeI	-	Iodomethane
MeOH	-	Methanol
Mep	-	5-ethyl-2-methylpyridine
MMAE	-	Monomethyl aurastatin E
MMAF	-	Monomethyl aurastatin F
MoA	-	Mechanism of action
MS	-	Mass spectrometry
MTD	-	Maximum tolerated dose
MW	-	Microwave
NCI	-	National Cancer Institute
NHL	-	non-Hodgkin lymphomas
NICR	-	Northern Institute for Cancer Research
NMM	-	<i>N</i> -Methylmorpholine
NMR	-	Nuclear magnetic resonance
PAB-OH	-	para-aminobenzyl alcohol
pAMF	-	para-azidomethyl-L-phenylalanine
PBD	-	Pyrrlobenzodiazepine
PEG	-	Poly(ethylene glycol)
PMB	-	4-Methoxybenzyl ether
Pro	-	Proline
PROTAC	-	Proteolysis targeting chimera
Quant.	-	Quantitative

Rb	-	Retinoblastoma tumour suppressor protein
R-CHOP	-	Combination therapy with cyclophosphamide, vincristine, prednisone, doxorubicin and rituximab
R_f	-	Retention factor
RNA	-	Ribonucleic acid
RT	-	Room temperature
SARs	-	Structure Activity Relationship Studies
S_N1	-	Nucleophilic Substitution with one component in the rate determining step
S_N2	-	Nucleophilic Substitution with two components in the rate limiting step
S_NAr	-	Nucleophilic Aromatic Substitution
SRB	-	Sulforhodamine B
Sulfo-SPDB	-	<i>N</i> -Hydroxysuccinimydyl-4-(2-pyrridyldithio)-2-sulfobutane
TBAF	-	Tetra- <i>n</i> -butylammonium Fluoride
<i>t</i> -BuOK	-	Potassium <i>tert</i> -butoxide
TCDI	-	1-1'-Thiocarbonyldiimidazole
TCEP	-	Tris(2-carboxyethyl)phosphine
TDC	-	THIOMAB antibody-drug conjugate
<i>t</i> -BuOH	-	<i>tert</i> -Butanol
TES	-	Triethylsilyl ether
TFA	-	Trifluoroacetic Acid
TFE	-	Tetrafluoroethylene
THF	-	Tetrahydrofuran
Thr	-	Threonine
TLC	-	Thin layer chromatography

Trop2	-	Tumour-associated calcium signal transducer 2
TsOH	-	p-Toluenesulfonic acid
UV	-	Ultraviolet
Val	-	Valine
vmax	-	Vibrational Frequency for an absorption maximum
VOD	-	veno-occlusion disease
VT	-	Variable temperature

Contents

Abstract	i
Declaration	iii
Acknowledgements.....	v
Abbreviations.....	vii
Chapter 1: Introduction to cancer	1
1.1. Cancer.....	1
1.2. Hallmarks of cancer.....	1
1.1.2. Sustaining proliferative signalling.....	1
1.2.2. Evading growth suppressors.....	2
1.3.2. Enabling replicative immortality	3
1.4.2. Angiogenesis and metastasis.....	3
1.5.2. Resisting cell death.....	3
1.6.2. Emerging hallmarks.....	3
1.7.2. Enabling Characteristics	4
1.3. Treatments for cancer	4
1.1.3. Cytotoxic Chemotherapy	4
1.4. Targeted therapy.....	8
1.5. Other modalities for the treatment of cancer	8
Chapter 2: Antibody-Drug Conjugates	10
2.1. Introduction to ADCs	10
2.1.1. ADC components	10
2.2.1. Internalisation mechanism for ADC.....	11
2.2. Introduction to Antibodies	11
2.3. Linkers	13
2.1.3. Non-cleavable linkers	13
2.2.3. Hydrazone linkers.....	14
2.3.3. Cathepsin B-responsive linkers	15

2.4.3. B-glucuronides as linkers.....	15
2.5.3. Disulfide linkers	16
2.4. Payloads.....	16
2.1.4. Calicheamicin.....	17
2.2.4. Aurastatins	19
2.3.4. Maytansinoids	22
2.4.4. Tubulysins.....	23
2.5.4. Duocarmycins, Pyrrolobenzodiazepines and Psymberin.....	26
2.5. Conjugation sites and attachment groups	27
2.1.5. Lysine conjugation	27
2.2.5. Cysteine conjugation	28
2.3.5. Glutamine conjugation.....	29
2.4.5. Site specific conjugations	29
2.5.5. Unnatural amino acid engineering.....	30
2.6.5. Enzymatic conjugation	31
2.7.5. N-glycan engineering.....	32
2.6. Early ADCs.....	33
2.7. First generation ADCs.....	33
2.1.7. cBR96	33
2.2.7. Gemtuzumab ozogamicin	35
2.3.7. Inotuzumab ozogamicin.....	36
2.8. Second generation ADCs.....	37
2.1.8. Brentuximab vedotin	38
2.2.8. Trastuzumab emtansine	39
2.9. Third generation ADCs	41
2.1.9. Vadastuximab talirine.....	41
2.2.9. Rovalpituzumab tesirine	41
2.3.9. Sacituzumab Govitecan	42

2.4.9. Multi-drug resistance proteins.....	43
2.5.9. Biparatopic antibodies	44
Chapter 3: Aims and objectives.....	46
Chapter 4: Identifying suitable cytotoxic warheads.....	47
4.1. Current problems with cytotoxic warheads	47
4.2. Screening the NCI database	47
4.3. Selected cytotoxic drugs	48
4.1.3. Overview of selected warheads.....	48
4.2.3. Nitroacridines	49
4.3.3. Quinolones	52
4.4.3. Thiosemicarbones	54
Chapter 5: Nitroacridine series	57
5.1. Resynthesis plan for nitroacridines	57
5.1.1. Synthesis optimisation of 2-((3-nitrophenyl)amino)benzoic acid 125	58
5.2.1. Synthesis of 9-chloro-1-nitroacridine, 126	60
5.3.1. Synthesis of 2-nitro-6-(phenylamino)benzoic acid, 132.....	63
5.4.1. Synthesis of amino-nitroacridines	65
5.2. Synthesis of <i>N</i> ¹ -methylpropane-1,3-diamine, 138	66
5.3. Biological testing of compound 114	71
5.4. Nitroacridine dimers.....	71
5.1.4. Synthesis of nitroacridine dimers	71
5.2.4. Biological testing of nitroacridine targets.....	73
Chapter 6: Quinolone series	76
6.1. Resynthesis of quinolone.....	76
6.2. Biological testing of quinolones.....	80
6.3. Design of PROTAC with 2-phenyl-4-quinolone, 157.....	84
Chapter 7: Thiosemicarbazone series	87
7.1. Synthesis of <i>N</i> -(diphenylmethylene)piperazine-1-carbothiohydrazide, 173.....	87

7.1.1. Synthesis of methyl hydrazinecarbodithioate	88
Chapter 8: Preparation of payloads.....	95
8.1. Non-Cleavable linkers	95
8.2. Synthesis of amino acid backbone	102
8.3. Biological evaluation of non-cleavable linkers.....	106
8.4. Cleavable linkers.....	108
8.5. Urea Linker	117
8.6. Model System for Release Mechanism	118
Chapter 9: Conjugations to the Antibody.....	121
Chapter 10: Conclusions and Future work.....	126
Chapter 11: Experimental and Analysis.....	129
9.1 Safety	129
11.1. Conjugations	130
11.2. SRB assay	130
11.3. Compound Data	131
11.1.3. General Procedures.....	131
References	202

Chapter 1: Introduction to cancer

1.1. Cancer

Cancer can be described as the uncontrolled abnormal proliferation of any cell in the body and can lead to the development of a malignant tumour.¹ As it can affect any cell, there are more than a hundred different types of cancer, which are described by their origin of source.

Despite the variety of different cancers, most fall into three main groups, carcinomas (90% of human cancers), sarcomas and leukaemias or lymphomas.¹ Because of the many types of cancers, it can be difficult to treat, and cancer cells can spread to other parts of the body through the lymphatic system or bloodstream.

Globally, cancer is the second leading cause of death, causing 9.6 million deaths in 2018 and 163,444 deaths in the UK alone in 2016.^{2,3} Up to 300,000 new cases of cancer are diagnosed each year in children aged 0-19 worldwide. These figures show that there is a clear need for effective cancer treatments not just in the UK but worldwide. Improvements have been made, for example, 84% of men diagnosed with prostate cancer in England and Wales will survive their disease for 10 years or more (2010-11) compared to only 25% in the 1970s. However, other cancers are not so positive. For example, only 5% of people will survive lung cancer for 10 years or more and 57% in bowel cancer which have the third and fourth highest incident rates after breast and prostate cancer (47,235 and 42,042 new cases between 2014-2016 respectively) in the UK.³ There is still a real need to treat these patients and improve survival rates.

1.2. Hallmarks of cancer

The hallmarks of cancer were proposed in 2000 by Hanahan and Weinberg.⁴ The six hallmarks allow tumour cells to grow and spread through the body and make essential changes to overcome the natural anticancer defence mechanisms the body employs in its cells and tissues. Initially six hallmarks of cancer were described, but further work has led to a total of 10 hallmarks of cancer to be identified (Figure 1.1).⁵

1.1.2. Sustaining proliferative signalling

One of the most fundamental hallmarks is sustaining proliferative signalling. Normal cells carefully control proliferation through growth-promoting signals, allowing the cell cycle only to progress when needed. However, cancer cells can disrupt this process and have several ways to obtain and maintain excessive proliferation.⁴ They can increase the number of growth factor receptors on the cell surface leading to overexpression and hyperresponsivity, allowing signals to be received, even when there are low concentrations of growth factors available

outside of the cell. They can also stimulate nearby cells to produce growth factors for them or synthesise growth factors themselves to self-stimulate. Independence of growth factors themselves is also possible by activation of downstream components, allowing growth factor receptors to no longer need activation to induce a growth signal.⁴

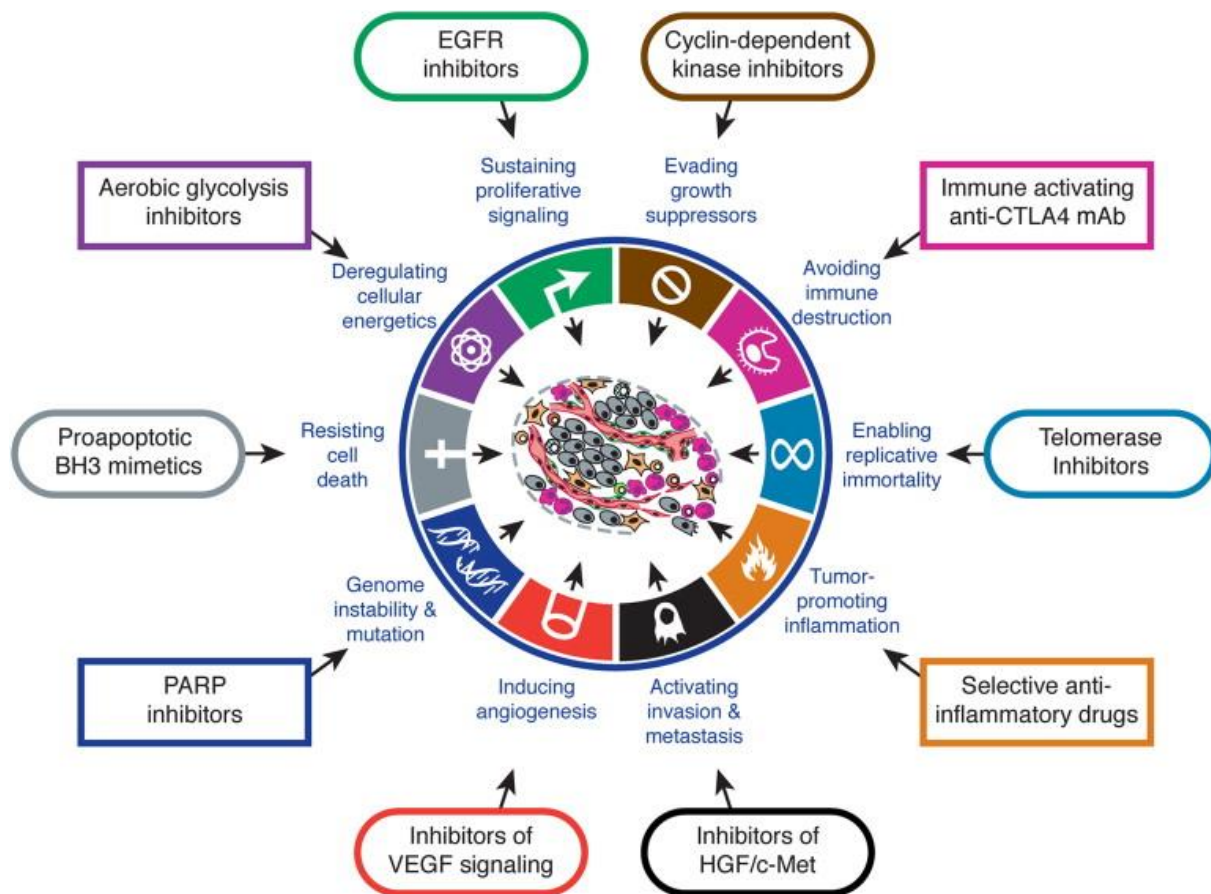


Figure 1.1: Therapeutic targeting of the hallmarks of cancer⁶.

1.2.2. Evading growth suppressors

Evading growth suppressors is also vital and allows cancer cells to avoid the mechanisms in place to stop uncontrolled proliferation. Tumour suppressor genes, such as retinoblastoma protein (Rb) can stop cells proliferating by acting as a cell cycle gatekeeper.⁴ However, in cancer cells, these genes can become damaged and are no longer active, thus the usual mechanism cannot prevent tumour cells from proliferating. Cancer cells can also disrupt the pathways of tumour suppressors.⁵

1.3.2. Enabling replicative immortality

Normal cells have a finite number of replications and have two barriers to prevent them replicating, senescence and crisis, the latter of which leads to cell death and is the safety net if senescence fails. If cells can bypass both barriers, they become immortalised and many cancer cells achieve this state. At the end of every chromosome is a repetitive non-coding sequence of nucleotides called a telomere which protects the chromosome during DNA replication. Every time a cell proliferates, the telomeres shorten and so over time they eventually stop protecting the chromosome.⁷ The enzyme telomerase can restore telomeres after replication and is expressed in 90% of immortal human cell lines, cancerous or not but is not found in normal cells.⁸ Inhibiting telomerase can lead to telomeres shortening as further replication will decrease the telomeres length, thus removing their protection of the chromosome, leading to cell death. Cancer cells use telomerase to allow them to continually replicate.⁴

1.4.2. Angiogenesis and metastasis

All cells require blood vessels to enable them to grow. Tumours require a considerable network of blood vessels to manage their demand of nutrients and oxygen, which they require to proliferate quickly. Early on in growth, cells develop their vasculature through vasculogenesis where endothelial cells are formed into tubes. New vessels are then spawned from existing ones, a process known as angiogenesis.⁴ This is constantly induced through the lifetime of a tumour, allowing it to continually grow and receive the necessary nutrients and oxygen. After angiogenesis is invasion and metastasis which is where the cancer can spread around the body through the bloodstream leading to a secondary site. This can cause the cancer to spread around the body, making it difficult to treat.⁶

1.5.2. Resisting cell death

Apoptosis is a vital process for cell death in response to physiological stresses cancer cells may undergo during tumorigenesis or DNA damage. Although the sequence of apoptosis is not fully understood, it is thought to involve proteases associated with cell death and caspase enzymes which facilitate the degradation of key organelles in the cell, leading to cell death. Cancer cells can resist cell death by increasing the expression of anti-apoptotic proteins and down regulation of pro-apoptotic factors to do so.⁶

1.6.2. Emerging hallmarks

Hanahan and Weinberg described the emergence of two new hallmarks on top of the six existing ones: avoiding immune destruction and deregulation of cellular energetics. Cancerous cells can hijack the normal mechanisms of immune checkpoint control to help evade the immune system and thus avoid immune destruction.⁶ Otto Warburg first observed over 70

years ago that cancerous cells favour anaerobic glycolysis even in the presence of oxygen, which is a more inefficient process of metabolism compared to aerobic glycolysis. The rationale for this is that this can lead to the formation of metabolites which are important in cell proliferation.⁹

1.7.2. Enabling Characteristics

It is given that genome instability exists in tumour cells because of the number of mutations required to observe tumour traits. In healthy cells, there are multiple pathways for DNA repair but in tumour cells, DNA repair can be limited which increase the chances of further mutations occurring and can provide a competitive advantage for the cancer cell survive.¹⁰ A limitation to this is that they have heightened sensitivity to DNA damaging agents and so inhibiting the DNA repair pathways can be an effective strategy in treating cancer cells.¹¹

Tumour-promoting inflammation is another enabling characteristic of tumour progression. It has been observed that tumours are infiltrated by immune cells. It was originally thought this was because the immune system was attempting to remove the tumour which while true there is also growing evidence that tumour-associated inflammatory response can lead to an increase in bioactive molecules into the tumour microenvironment which can help cell proliferation and survival.¹²

1.3. Treatments for cancer

There are a variety of treatments available for cancer, depending the stage and the type. For solid tumours, surgery can be an option to remove most of the cancer and is carried out alongside a course of chemotherapy or radiotherapy after surgery. This is only effective before invasion and metastasis has occurred. There are now more drugs than ever on the market to treat a huge array of cancers involving cytotoxic agents and targeted therapies.

1.1.3. Cytotoxic Chemotherapy

Classical chemotherapy employs the use of cytotoxic agents, which target the biological processes that a cancer cell needs to grow and proliferate. This can be done by causing damage to their DNA, prohibiting them from being able to replicate DNA and therefore leading to cell death. Normal cells are also affected by this as they follow the same process and this can cause side effects. There is a narrow therapeutic window for these types of agents. Since cancer cells replicate at a much faster rate than that of normal cells, they are more susceptible to damage to DNA as they go through the cell cycle more frequently. These types of treatments usually have severe side effects but are still used in first line treatment for certain cancers.

One early class of chemotherapy agents extensively studied was DNA alkylators (Figure 1.2). It was observed from the effects of poison gas in World War 1 and the effects of an accidental spill of sulfur mustards such as **1** in World War 2, that soldiers exposed to mustard gases used at the time had lymph nodes and bone marrow significantly depleted compared to those soldiers who had not been exposed.¹³ This led to further studies in mice, which showed regression in mice and later in humans with lymphomas. This was short lived however as remissions were brief.¹⁴ This work also included the nitrogen mustards such as HN1 **2** and, due to their lesser toxicities and not being a gas, the sulfur mustards were derivatised. Oral derivatives such as chlorambucil **3** (approved in 1957) and cyclophosphamide **4** (1959) were developed. These DNA alkylators worked by cross-linking DNA irreversibly and causing apoptosis. Other DNA alkylators have also been used such as procarbazine **5** which was approved in 1969.¹⁵

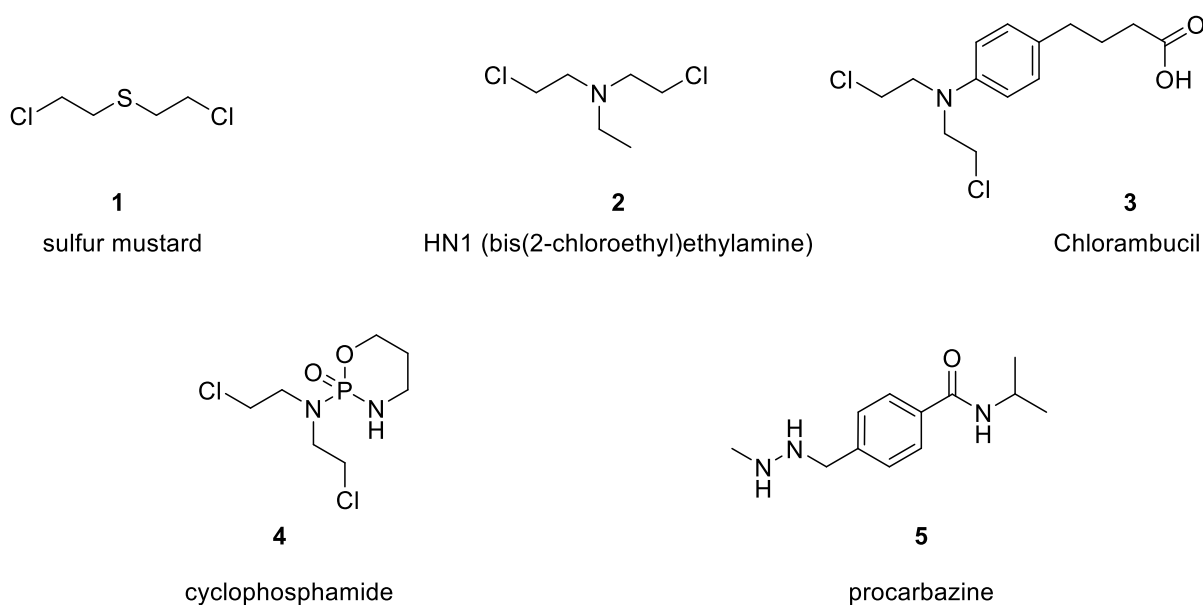


Figure 1.2: DNA alkylating agents

Other chemotherapies include cisplatin **6** and carboplatin **7** (Figure 1.3). Cisplatin was discovered in 1845 but its anticancer activity was only elucidated much later and was used medicinally in the late 70s. These agents crosslink DNA by reacting with the DNA bases, such as guanine and interfere with DNA replication. DNA repair is impossible and leads to cell apoptosis. They have been indicated for the use in various cancers such as testicular, ovarian and breast cancer.¹⁶

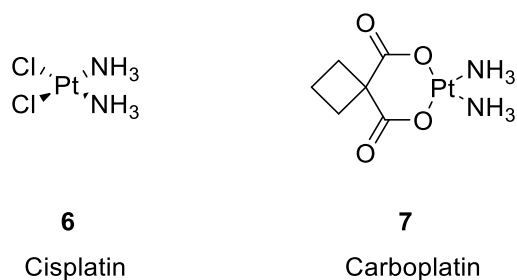


Figure 1.3: DNA intercalator agents cisplatin 6, carboplatin 7

Methotrexate **8** was developed in the 1940s and 50s and is an antimetabolite and inhibits dihydrofolate reductase (DHFR) by mimicking folic acid and blocking its binding. DHFR is needed in the biosynthesis of thymidine and purine and pyrimidine bases, which are needed for DNA synthesis (Figure 1.4). Use of methotrexate has shown remission in leukaemia.¹⁷

The antimetabolite 5-fluorouracil (5-FU) **9** was developed in the 50s. It acts as a thymidylate synthase inhibitor, blocking the synthesis of thymidine needed for DNA replication. This results in cancer cells undergoing thymineless death. It was shown to be active in a broad range of cancers and is still used in the treatment of colorectal cancer. 5-FU does show a wide range of adverse side effects such as nausea and diarrhoea.¹⁸

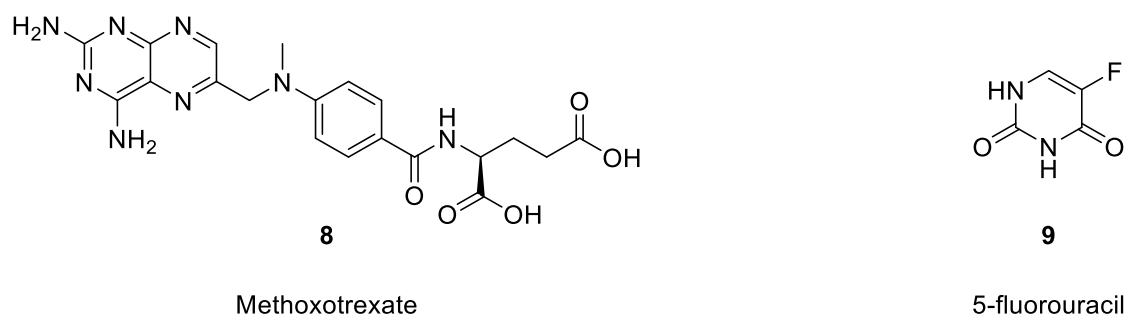


Figure 1.4: Antimetabolites methotrexate and 5-fluorouracil

The discovery of the vinca alkaloids led to a major breakthrough in using natural products in chemotherapies as tubulin binders. They bind to tubulin and prevent microtubule formation leading to cell death. Multiple alkaloids have been used clinically including vinblastine **10** and vincristine **11** (Figure 1.5).¹⁹ Other natural products derived from plants have been discovered which do not necessarily have the same MoA such as Taxol (paclitaxel) **12**, isolated in 1971 from the Pacific yew. Taxol stabilises microtubule formation and prevents its disassembly and thus blocks progression of mitosis leading to cell death. Vinca alkaloids and taxane derivatives remain commonly used cancer treatments to this day.²⁰

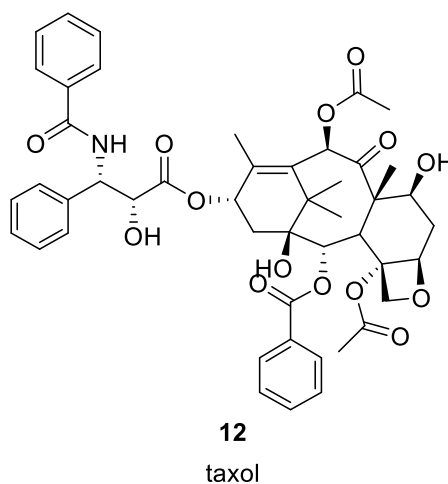
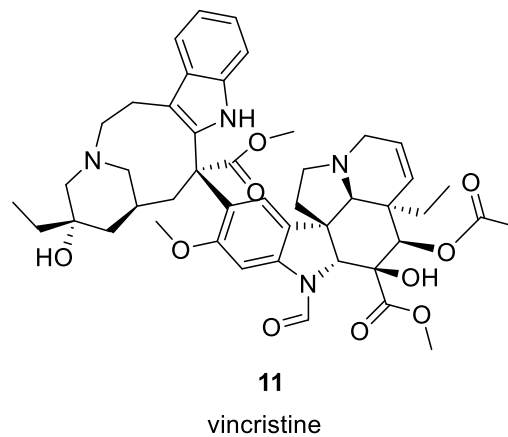
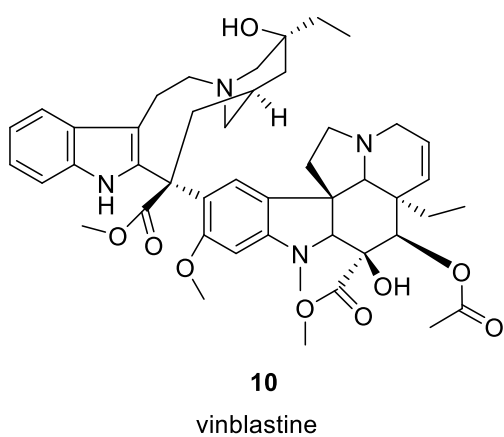


Figure 1.5: Chemotherapies derived from plants, vinca alkaloids **10** and **11** and taxol **12**

There are also other cytotoxins such as doxorubicin, which intercalates with DNA and inhibits the enzyme topoisomerase II (Figure 1.6). It is often used in combination with other chemotherapies and is used for the treatment of breast and bladder cancers as well as ALL amongst others.

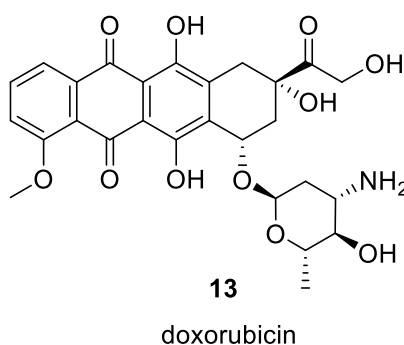


Figure 1.6: Structure of doxorubicin, **13**

Most of these chemotherapies rely on their ability to affect rapidly dividing cells more than those that do not as their mechanism of actions affect DNA replication and cell division. Since cancer cells rapidly divide, this is where their selectivity comes from. However, these

treatments affect all cells and these treatments can cause a wide range of side effects including hair loss and nausea and vomiting. Most of these treatments such as the DNA alkylators of the mustard gases also were confirmed to cause secondary cancers later as damage to DNA can lead to cancers. Resistance is also an issue but that is not exclusive to these treatments. To help mitigate against resistance, combination therapies are used to maximise the therapeutic window and prevent resistant cancer cells surviving.²¹

1.4. Targeted therapy

Targeted therapy relies on the use of specifically targeting cancer cells over normal cells. This would help reduce the side effects commonly seen in chemotherapies as healthy cells would be less affected by these treatments. A number of targeted therapies are now entering the clinic.

One of the first and best examples of targeted therapy is imatinib **14** (Figure 1.7). This is a Bcr-Abl tyrosine kinase inhibitor for the treatment of chronic myelocytic leukaemia and acute lymphocytic leukaemia with Philadelphia chromosome positive (Ph⁺). The kinases require binding of ATP in order to allow the kinase to phosphorylate and activate other proteins, some associated in cancers. Imatinib was licensed as Gleevec in 2001.²² The abnormal fusion gene, BCR-ABL1 codes for a hybrid tyrosine kinase signalling protein that is always switched on and is important in cell proliferation and can be selectively targeted. Other similar drugs to imatinib like dasatinib have been developed to overcome resistance. This has now led to more drug discovery projects in this field to develop kinases inhibitors and other targets.

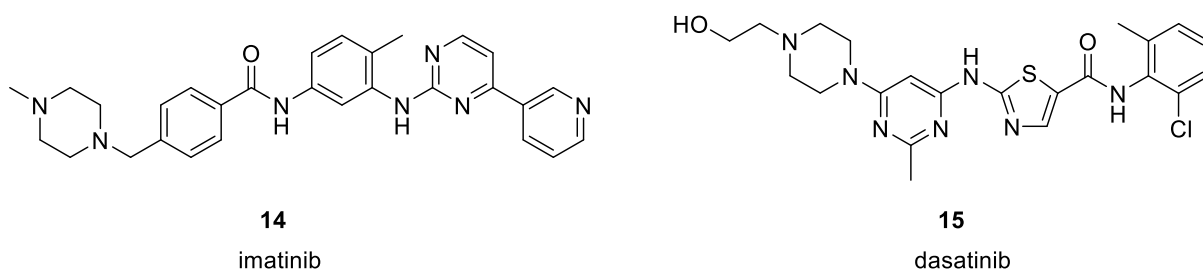


Figure 1.7: Bcr-Abl tyrosine kinase inhibitors imatinib **14** and dasatinib **15**.

1.5. Other modalities for the treatment of cancer

Other modalities have also been developed in the treatment of cancer. This can include immunotherapies such as the use of monoclonal antibodies. One example is Ipilimumab, a checkpoint inhibitor and targets CTLA-4.²³

Monoclonal antibodies have also been used as chemotherapy such as trastuzumab, or Herceptin, which targets HER2 positive breast cancer.²⁴ This works by exploiting the

overexpression of HER2 in cancerous cells relative to that of normal healthy cells.²⁵ HER2 is an epidermal growth factor receptor which regulates cell growth in breast cells and is present in 20 – 30 % of breast cancers and due to amplification of the HER2 gene can promote uncontrolled cell proliferation in breast cells.²⁶ Trastuzumab works by binding to the extracellular domain of the HER2 receptor and prevents the activation of its intracellular tyrosine kinase. Several mechanisms of action have been proposed which decrease the signalling of the HER2 pathway and inhibiting growth signalling. Prevention of dimerization of the HER2 receptor, immune activation, inhibition shedding of the extracellular domain and increased endocytotic destruction of the receptor are some of the mechanisms proposed.²⁷ Trastuzumab is clinically used from early stages of HER2 positive breast cancer to metastatic HER2 positive breast cancer.

There is also much work in other modalities such as PROTACs and modified RNA for example as well as other biologics which are drugs extracted from or are semi synthesised from biological sources.²⁸ A variety of new treatments could help to personalise treatments to specific cancers as well as help to counter resistance issues.

Chapter 2: Antibody-Drug Conjugates

2.1. Introduction to ADCs

2.1.1. ADC components

Antibody-drug conjugates (ADCs) are designed to selectively deliver a potent payload to a specific target and can do this by consisting of three key components, an antibody, a linker and a payload (Figure 2.1). Selectivity can be achieved as some cancers overexpress certain receptors which can be targeted with an antibody. Once the antibody has bound to the receptor, the ADC can be internalised where the payload can be released in the cell causing cell death.

Each have strict criteria that have evolved over time. Antibodies are very selective towards their target and ADCs exploit this to selectively deliver a payload towards a targeted cell. For the antibody, target antigens should be differentially overexpressed in cancer cells relative to healthy cells. The target antigen also needs to be present on the cell surface so that an Ab in circulation can access it. Finally, the target antigen needs to internalise the antibody upon binding

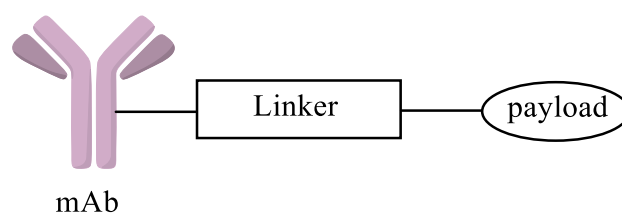


Figure 2.1: Basic components making up an ADC

Linkers must be stable while the ADC is in the blood but allow for easy release of the warhead within the targeted cell. It should also have attachment handles to conjugate with the antibody. Optimisation of linkers is important for successful ADCs such as aiding bioconjugation and avoid forming inactive aggregates.²⁹

Payloads used are often highly potent compounds with sub-nM potencies. This is because for tumours with low levels of expression, the payloads should be sufficiently potent to kill the cancer cells at low concentrations. Often the payload is a drug which has failed clinical trials due to adverse side effects and poor drug-like properties which would not cause issues when incorporated into an ADC. The payload should contain a functional group which acts as a handle for linker attachment and optimisation of the linker-payload is critically important to

ensure a good safety profile with limited toxicities from systemic release of the payload. The payload also needs to be soluble and stable under physiological conditions.

2.2.1. Internalisation mechanism for ADC

The postulated mechanism of action is broadly common to all ADCs (Figure 2.2).³⁰ The antibody binds to its receptor where it is internalised through receptor mediated endocytosis. Once in the cell, the antibody is broken down in endosomes and lysosomes and the payload is released. There is also a chance that the payload will diffuse out into the extracellular space leading to the bystander effect.³⁰ The bystander effect is where the internalised drug diffuses out of the cell and can affect nearby cells and cause cell death, regardless of whether they are the target or not. This can be a useful phenomenon as tumours can be heterogenous with not all cells expressing the same antigens. A drug released into the extracellular space can kill nearby antigen null tumour cells. However, this can also lead to killing neighbouring healthy cells, potentially causing adverse effects.³¹

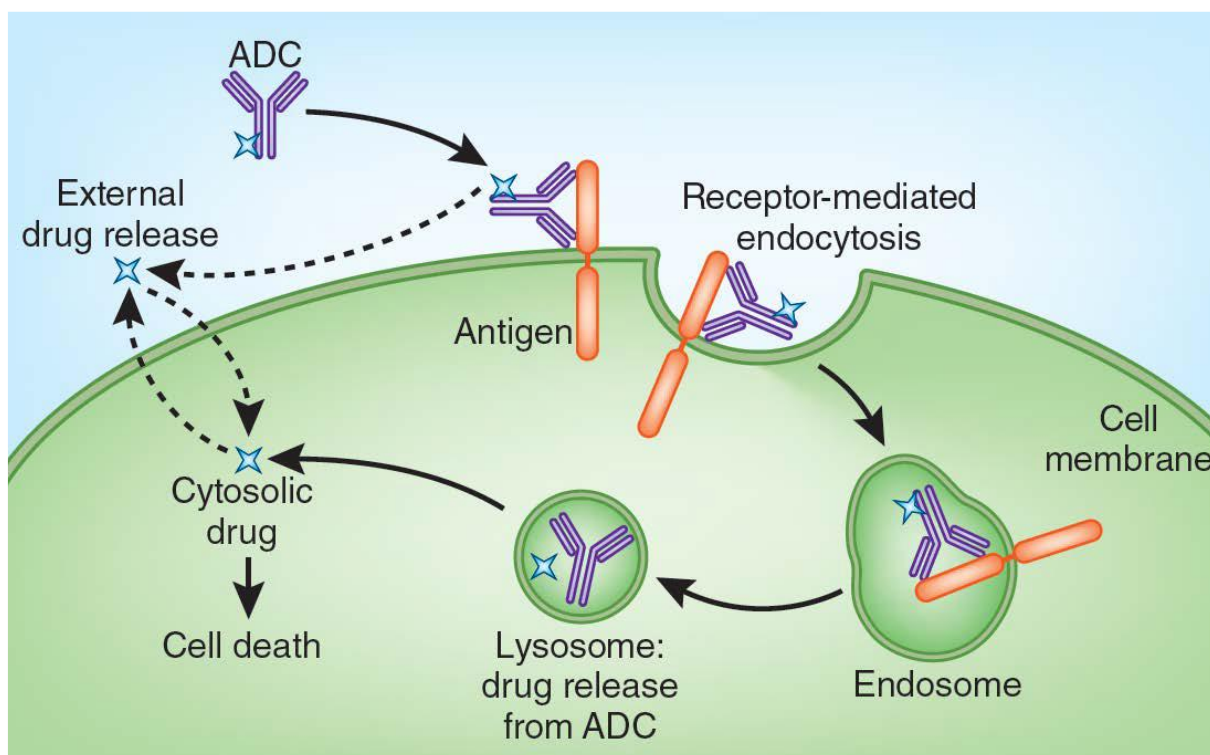


Figure 2.2: Internalisation mechanism of an ADC³⁰

2.2. Introduction to Antibodies

Antibodies, also known as immunoglobins, are glycoproteins produced by the immune system. In the body, they are produced by differentiated B cells called plasma cells and used to neutralise pathogens that present specific antigens which the antibody can target.³² There

are five classes according to their constant region, IgG, IgM, IgA, IgD and IgE. IgG is the most common with IgG1, IgG2 and IgG4 the most commonly used subclasses in ADCs.³³

Monoclonal antibodies are made up of four polypeptide chains to produce a flexible Y shaped protein consisting of two heavy and two light chains (Figure 2.3). The heavy chains are linked together, and each is linked to a light chain through another disulphide bridge. In most cases, the chains are identical to each other and within a class are highly homologous to each other. This region of the antibody is called the constant region for this reason and it is here where the antibody can bind to a white blood cell through the complementary determining region (CDR).³⁴

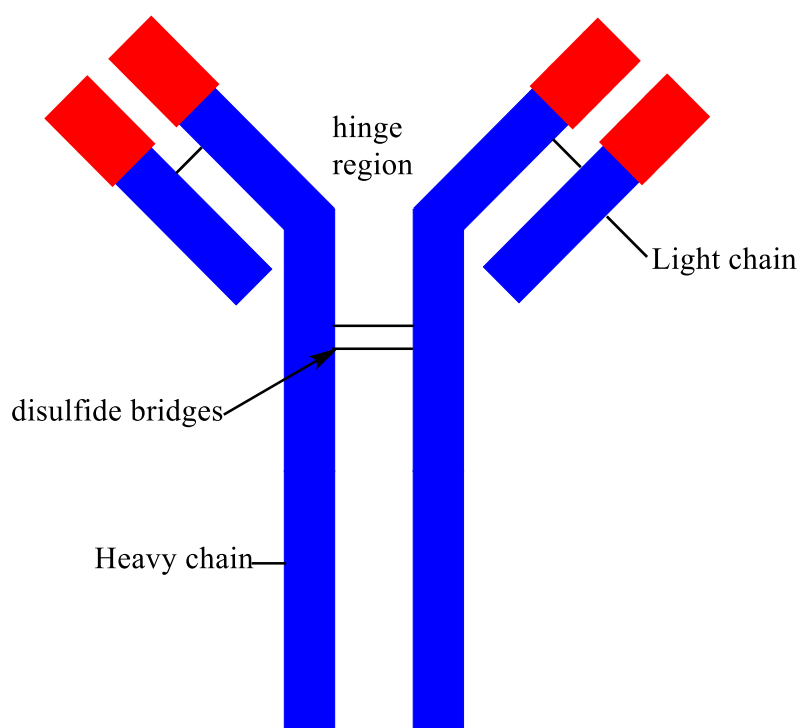


Figure 2.3: Basic structure of an antibody, in blue is the constant region, and red the variable region.

The tips of the arms, at the end of the heavy and light chains, are highly variable between each antibody and thus called the variable region. This allows the immune system to have a huge diverse range of antibodies targeting a vast number of antigens. The paratope, the tips, act like a lock that is specific to an epitope (part of an antigen which the immune system can recognise). Once bound, it can either tag the cell for the immune system to kill it such as through the action of macrophages or directly neutralise the cell by impeding the cell's biological functions.³⁴

Monoclonal antibodies, often produced from cell cultures in labs, are monospecific, i.e. they target the same epitope on an antigen and are made by identical immune cells which are clones of a single parent cell. Monoclonal antibodies often slow down and stop progression but do not eliminate the disease. There are many available therapeutic mAbs such as trastuzumab and adalimumab. These treatments have long half-lives and are given intravenously or through subcutaneous injection.³⁵

Early technologies applied the use of polyclonal antibodies, which differ from monoclonal antibodies as they are produced by different clones of B cells and bind to different epitopes in the same antigen. The use of polyclonal antibodies led to variations in the antibody drug ratio as well as reproducibility issues leading to a lack of efficacy.³⁶ The development of monoclonal antibodies came in 1975 by Kohler and Milstein and replaced the use of polyclonal antibodies.³⁷

Initial ADCs used murine derived antibodies but this led to immunogenicity problems as the immune system would generate antibodies to combat these mouse antibodies, resulting in an increase in clearance and lowered efficacy of these drugs.³⁸ It also led to systemic release of the payload in the body due to the instability of these antibodies in the blood leading to a need for higher dosing, leading to an increase in adverse effects.³⁹ Since then, chimerised (where the variable regions of heavy chain and light chain are murine based), humanised (which contains mouse CDR regions found at the very tips of the Ab) and now fully human antibodies have been developed and are used in newer generations of ADCs with improved stability and reduced risk of immunogenicity.⁴⁰

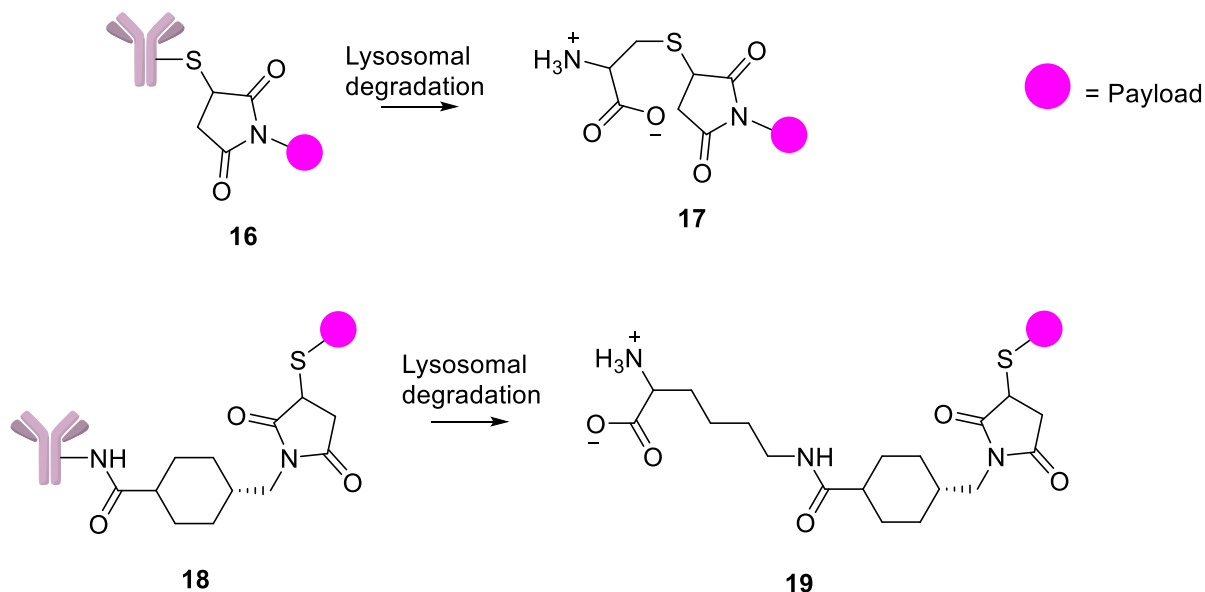
2.3.Linkers

2.1.3.Non-cleavable linkers

Non-cleavable linkers are formed of stable bonds, which are resistant to cleavage in the cell leading to greater stability than cleavable linkers. It requires complete lysosomal degradation of the antibody in the cell to release a drug-derivative payload consisting of the payload, linker and amino acid residue from the antibody. It is important to consider the selection and design of the payload with non-cleavable linkers as the modified payload needs to retain or improve its activity in the cell. The release of the amino acid residue from the antibody creates a charged drug-derivative and reduces the cell permeability of the drug, decreasing the bystander effect.

The most common non-cleavable linker is a thioether. The thioether can be formed either by cysteine conjugation to a maleimide, **16**, or through a succinimidyl-4-(*N*-maleimidomethyl)

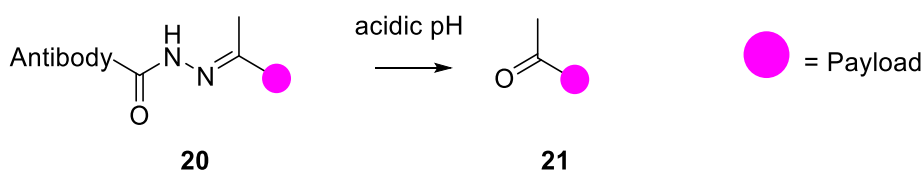
cyclohexane-1-carboxylate linker allowing for lysine conjugation, **18** (Scheme 2.1). There has been success with these linkers in the clinic.



Scheme 2.1: General scheme of non-cleavable linkers with lysosomal degradation leading to charged species containing the amino acid residue. **16** and **18** showing a maleimide linker. Magenta circle represents a payload.

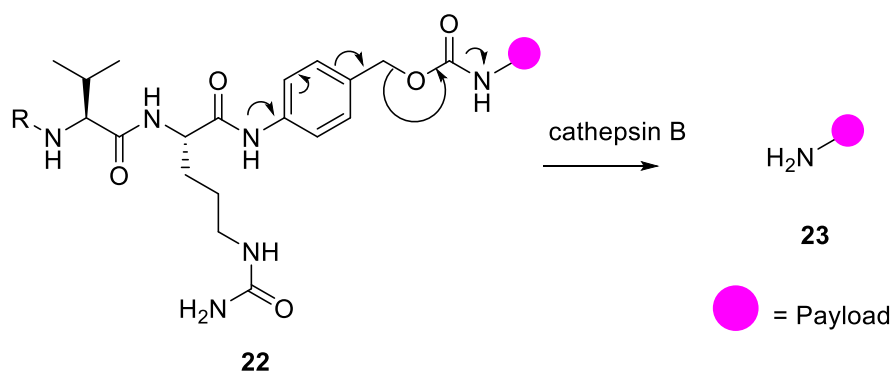
2.2.3. Hydrazone linkers

Early generations of ADCs use a hydrazone linker, which works as an acid-labile group and the free drug can be released through hydrolysis once the ADC has entered the cell and is exposed to endosomes or lysosomes, which have an acidic pH of around 5-6 and 4.8 respectively (Scheme 2.2).⁴¹ Hydrazones have been shown to undergo slow hydrolysis at pH 7 at 37 °C which can lead to premature release of the drug in the cell.⁴²



Scheme 2.2: Hydrazone linker release mechanism through acidic hydrolysis. Magenta circle represents payload.

2.3.3. Cathepsin B-responsive linkers



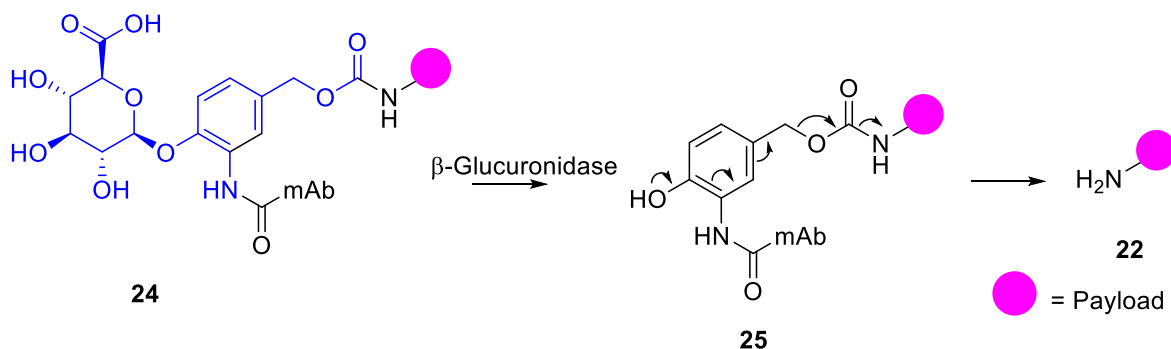
Scheme 2.3: Cathepsin B release mechanism of Val-Cit linker. Magenta circle represents payload.

Bristol Myers Squibb introduced a novel type of linker, now widely employed in later generations of ADCs. It involves the use of cathepsin B which is a lysosomal protease and is an effective biomarker for cancers due to its overexpression (Scheme 2.3).⁴³ It has a varied scope for substrates but recognises certain sequences such as valine-citrulline and phenylalanine-lysine as its preferences. Val-Cit and Val-Ala are commonly used in ADCs as cleavable linkers. These peptides showed good plasma stability as proteases are inactive at higher pH like that found in serum which is at physiological pH.⁴⁴ Cathepsin B can also be found on the cell surface of some cancer cells so there can be premature release of the payload outside of the cell, leading to the bystander effect.⁴⁵ Many linkers which employ these dipeptide chains also use a spacer in order to allow for better facile proteolysis from cathepsin B. This is normally a self-immolative linker such as a para-aminobenzyl alcohol, PAB-OH, group which can release the payload after cleavage of the amide bond.⁴⁶ The release mechanism is shown in Scheme 2.3 in which proteolysis occurs allowing for spontaneous cleavage of the payload, releasing CO₂ in the process.

2.4.3. *B*-glucuronides as linkers

To combat the high hydrophobicity of payloads and some linkers, polar linkers have been developed using β -glucuronides. The use of β -glucuronides has been successful in a few prodrugs and has been developed with MMAE and tubulysin. β -Glucuronidase is found in lysosomes and high levels can be found in solid tumour cells making it an attractive mechanism for cleavage.⁴⁷ It is active at pH 5 found in lysosomes but inactive at higher pHs so allows for selective cleavage of payloads in the cell, as is the case for the cathepsin B cleavable linker as the pH is higher outside of the cell.⁴⁸ An advantage of this kind of linker is the high hydrophilicity, increasing the aqueous solubility of the linker-payload as well as allowing for much more hydrophobic drugs like duocarmycin to be used. For example, high

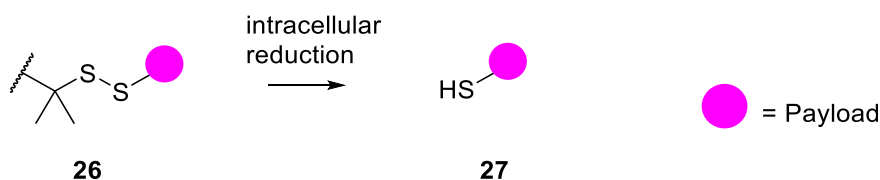
aggregation was seen with PABC-dipeptide conjugates with CBI based conjugates but not with a β -glucuronide linker.^{49,50} The mechanism of cleavage is shown in Scheme 2.4 with the glucuronide linker shown in blue. Cleavage of the glucuronide by glucuronidase reveals a free phenol, which triggers the elimination of the drug with loss of CO₂ in a similar manner to the cathepsin cleavable linker (Scheme 2.4).



Scheme 2.4: Release mechanism of payload with a β -glucuronide linker in blue and magenta circle represents payload.

2.5.3. Disulfide linkers

Disulfide linkers are glutathione sensitive and rely on the higher concentration of glutathione found in the cell (1-10 mmol/L) relative to the extracellular concentration (5 μ mol/L) and allows reduction of the disulphide bond to the thiol (Scheme 2.5). To increase the stability of these linkers, methyl groups are often installed adjacent to the disulphide bond.⁵¹



Scheme 2.5: Reduction of disulphide linker to free thiol. Magenta circle represents payload.

2.4. Payloads

Payloads used for ADCs are often drugs which have failed clinical trials as they were deemed too unsafe with adverse toxic effects associated with them. They are often sub-nM to pM in potency. Despite most tumours not being intrinsically sensitive to anti-microtubule agents, over 70% of ADCs in clinical development use these types of agents, mostly containing aurastatins and maytansinoids.⁵² Robust activity for antimicrotubule agents has only been seen in ALL, Hodgkin's disease and non-Hodgkin's lymphoma. There has been limited evidence of activity in breast and lung cancer as well as other solid tumours. The obvious reason for the

use of these drugs is the expectation that cancers will be sensitive to potent cytotoxic agents if delivered by an ADC. This is not always the case, e.g. SAR566658 **28** (Figure 2.4), an anti CA6 DM4 ADC using the maytansinoid payload DM4, had no activity in pancreatic cancer, even though the target antigen expression was high compared to healthy cells. Further studies to breast cancer are ongoing.⁵³

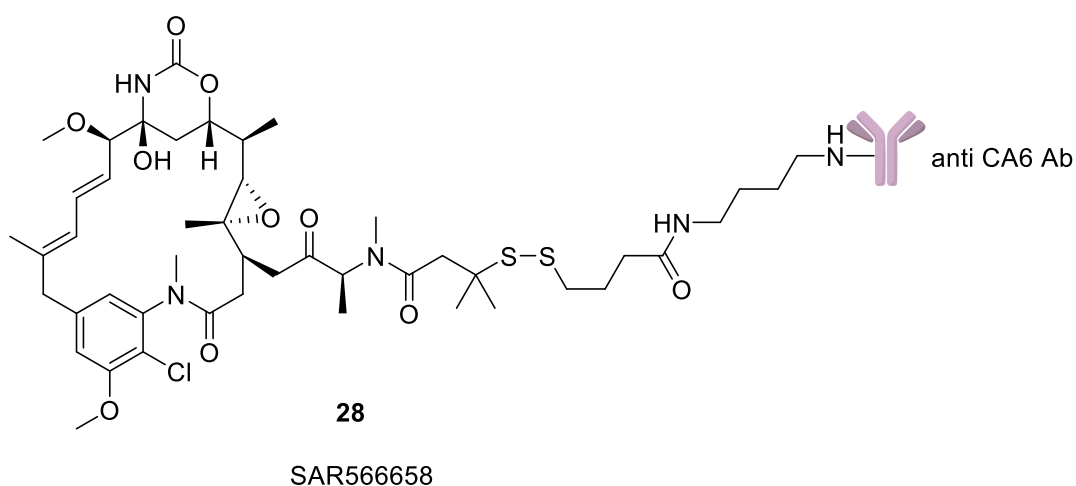


Figure 2.4: Structure of SAR566658, 16

It might be because of the strict criteria needed to identify suitable warheads, which give rise to the same compounds being reused as they have high potency, relative hydrophilicity, lack of susceptibility to MDR1 mediated efflux (a common resistance issue to ADCs) and a chemical handle to allow for a site of conjugation.

2.1.4. Calicheamicin

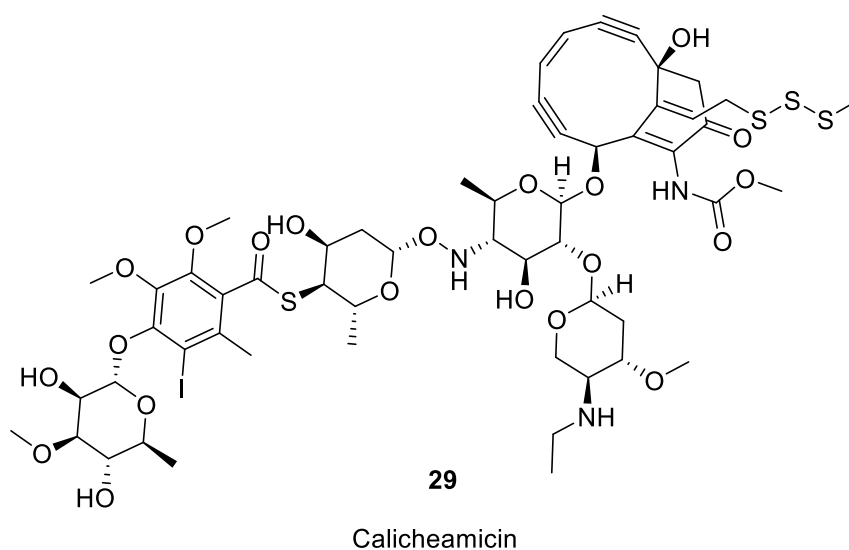


Figure 2.5: Structure of calicheamicin γ_1 **29**.

Calicheamicins are a class of antitumor antibiotics containing an enediyne group and are naturally occurring compounds isolated from the fermentation broth of a soil bacterium *Micromonospora echinospora*. Calicheamicin γ_1 **29** (Figure 2.5) is one such example and this class of drugs are highly potent DNA damaging agents and bind at the minor groove of the DNA, with high specificity for sequences such as 5'-TCCT-3' through hydrophobic interactions. In the presence of DNA, glutathione can attack the trisulfide group leading to the free thiol, **22** (Figure 2.6).⁵⁴ An intramolecular Michael addition then occurs which causes significant strain on the 10 membered-ring which can undergo the Bergman cyclisation to completely relieve the strained system to produce a diradical 1,4-didehydrobenzene, **23**. The diradical can then abstract hydrogen from the deoxyribose ring in DNA and causes a DNA break and cleavage of both strands.⁵⁵ This reaction is akin the Bergman cyclisation mechanism.⁵⁶

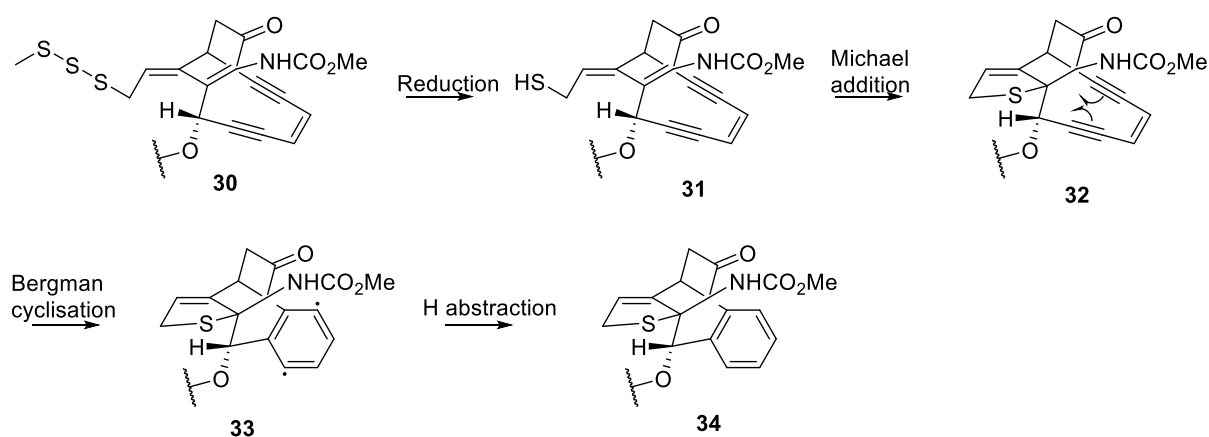


Figure 2.6: Mechanism of action for calicheamicin

The main issue with this class of compounds is the high hydrophobicity that it brings, meaning that only a few molecules can be conjugated to an antibody before high levels of aggregation are seen.⁵⁷

The total synthesis of calicheamicin γ_1 was achieved from the Nicolaou group in 1992 (Figure 2.7). It required the key fragments **35** and **36** which could be obtainable in gram quantities.⁵⁸ Calicheamicin γ_1 is costly due to its challenge of synthesis and extraction with 1 g costing upwards of \$24450. Due to its complexity, it is hard to modify and optimise its physical properties.

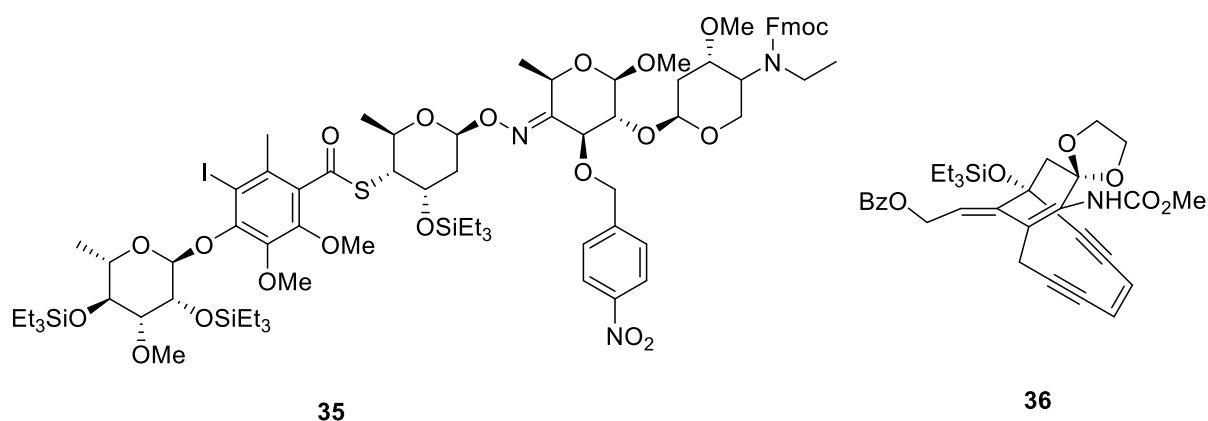


Figure 2.7: Key intermediates in Nicalaou's total synthesis of calicheamicin γ 1

2.2.4. Aurastatins

Aurastatins are derived from dolastatin 10, **37**, a marine natural product isolated from the extract of a sea hare, *Dolabella auricularia* in extremely low abundances, as well as in cyanobacteria that they feed on.⁵⁹ In preclinical studies, it had subnanomolar potencies in solid tumours as well as lymphomas and leukaemias. Results from Phase I trials of dolastatin 10 showed that 40% of patients developed moderate peripheral neuropathy and Phase II studies failed to demonstrate activity in solid tumours despite initial studies showing wide range of anticancer activity in the sub-nM range in lymphomas, leukemia and solid tumours.^{60, 61} A narrow therapeutic window and high cytotoxic activity with non-specific toxicity meant the drug was not progressed further.

Dolastatin-10 is a linear peptide chain consisting of dolavaline, valine, dolaisoleuine, dolaproine (Figure 2.8). Its mechanism of action is like that of the vinca alkaloids, sharing the same tubulin binding site, blocking their binding in a non-competitive manner.⁶² Issues with dolastatin-10 include its complexity and low yield of synthesis coupled with its poor water solubility making it a poor drug choice.

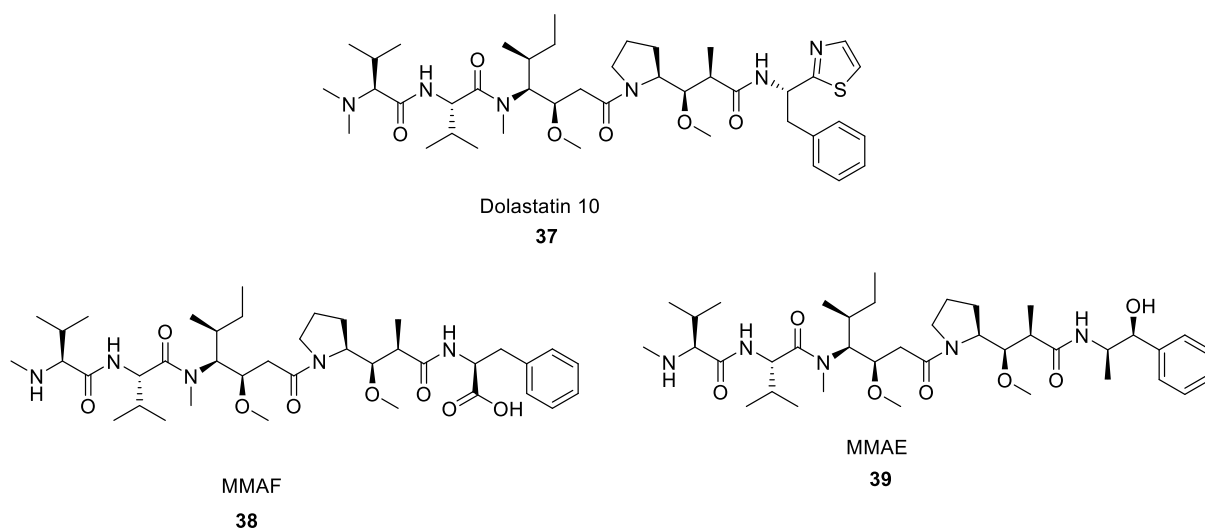
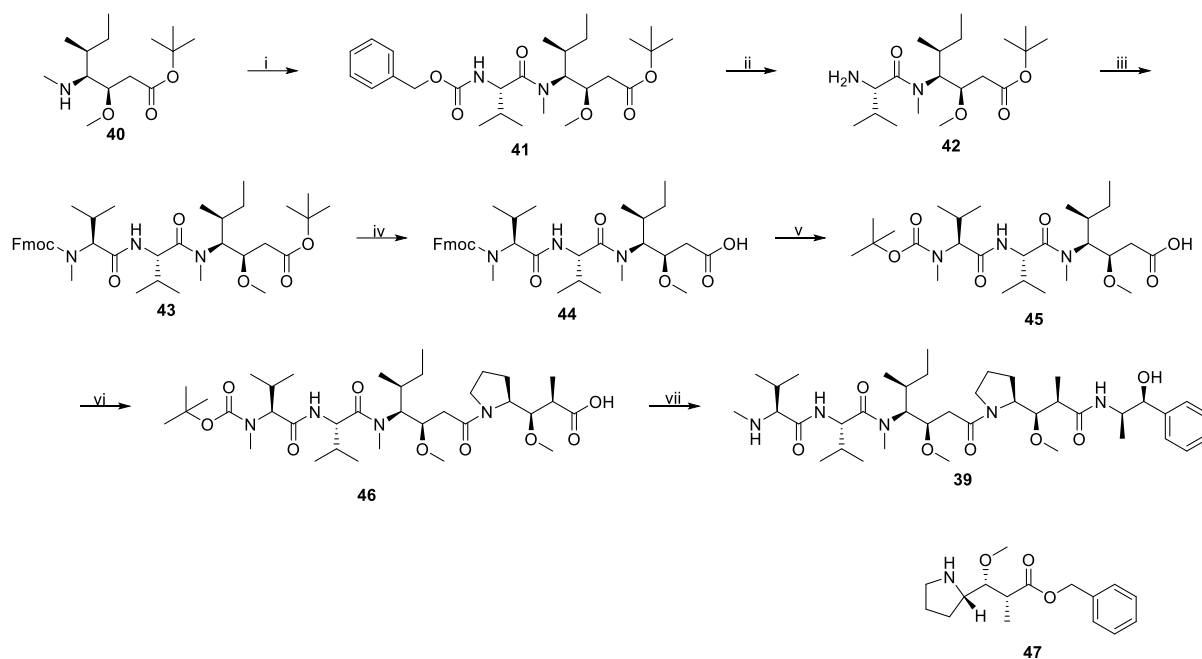


Figure 2.8: Structures of aurastatins, Dolastatin 10, **37**, MMAF, **38** and MMAE, **39**

MMAF, **38** and MMAE, **39** are both stable in plasma, human liver lysosomal environments and through proteases but are both less potent than dolastatin 10 in lymphoma cells in vitro.⁶³ MMAF is also less cytotoxic than MMAE as it is proposed the carboxylic acid functional group in MMAF reduces the cell permeability of the compound. MMAE is also capable of causing the bystander effect while MMAF however cannot as the metabolite produced in the cell is less permeable than MMAE.^{64, 65}

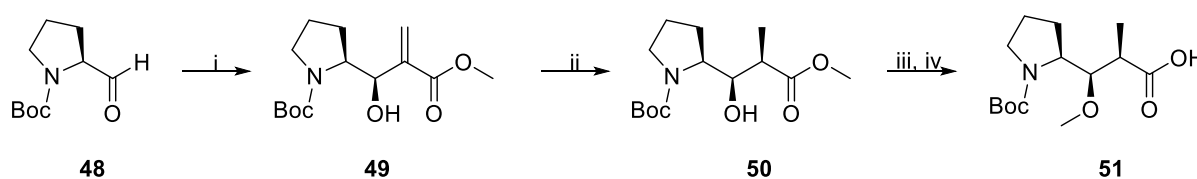
Efforts were made for synthetic analogues of dolastatin 10 and in contrast, its fully synthetic derivatives, MMAE and MMAF are widely used payloads in ADCs in development and have increased water solubility, with two FDA-approved ADCs using MMAE in particular. A useful feature to these payloads is the synthetic route which allows for easy modification of the payload if needed with many analogues having been made and synthesised.

MMAE can be synthesised starting from **40** (Scheme 2.6). BEP is used to facilitate the coupling of **40** with *N*-benzyl-L-valine followed by the removal of the benzyl protecting group by hydrogenation. EDC is used to couple Fmoc-L-valine with subsequent hydrolysis of the *tert*-butyl ester in compound **43**. Fmoc protecting group is removed with piperidine followed by subsequent protection of the amine with Boc. HBTU is used to couple **46** with **47** and the product undergoes hydrogenation to remove both the benzyl group. Finally, an amide coupling between **47** and (1*S*,2*R*)-2-amino-1-phenylpropan-1-ol followed by deprotection of Boc with TFA/DCM to yield MMAE **39**.⁶⁶



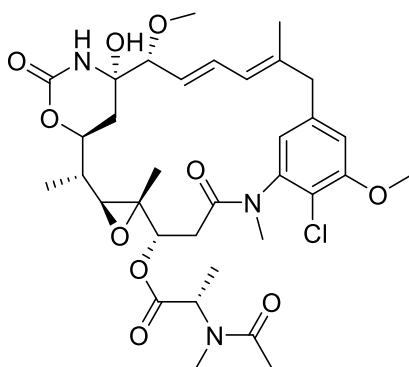
Scheme 2.6: Synthetic route to MMAE, allowing for derivatisation. *Reagents and Conditions:* i) *N*-benzyl-L-valine, DCM -10 °C, BEP, DIPEA, 20 h, 51%; ii) MeOH, 10% Pd/C, H₂, quant; iii) EDC.HCl, Fmoc-L-valine, DMF, HOBT, 16 h RT, quant 60% pure; iv) DCM, TFA 2h, RT, 86%; v) a) 5% piperidine in DMF, RT, 10 min; b) Boc₂O, NaOH, dioxane, 90% over two steps; vi) a) HBTU, **47**, DIPEA, DMF, RT 55%; b) MeOH/DCM 20:1, 10% Pd/C H₂, 30 min RT, 91%; vii) a) HBTU, DIPEA, (1*S*, 2*R*)-2-amino-1-phenylpropan-1-ol, RT 5 min, 81%, b) TFA/DCM, RT, 2 h, 52%.⁶⁶

One method of synthesising **47** is from *N*-Boc-dolaproline by first undergoing a Baylis-Hillmann reaction, followed by a diastereoselective hydrogenation. The alcohol can then be methylated, and the acid hydrolysed to give **51** (Scheme 2.7).⁶⁷ The acid can then be benzylated and the Boc group removed.



Scheme 2.7: Synthetic route to *N*-Boc-dolaproline. *Reagents and Conditions:* i) Methyl acrylate, DABCO, DCM, RT, 7 days, (3:1 diastereomeric mixture), 70 %, ii) H₂, 5% Pd/C, EtOAc, RT, (83:17 diastereomeric mixture), 79 %; iii) Me₃OBf₄, DCM, proton sponge, RT, 18 h, 70%. iv) LiOH-H₂O/THF, RT, 87%.⁶⁷

2.3.4. Maytansinoids

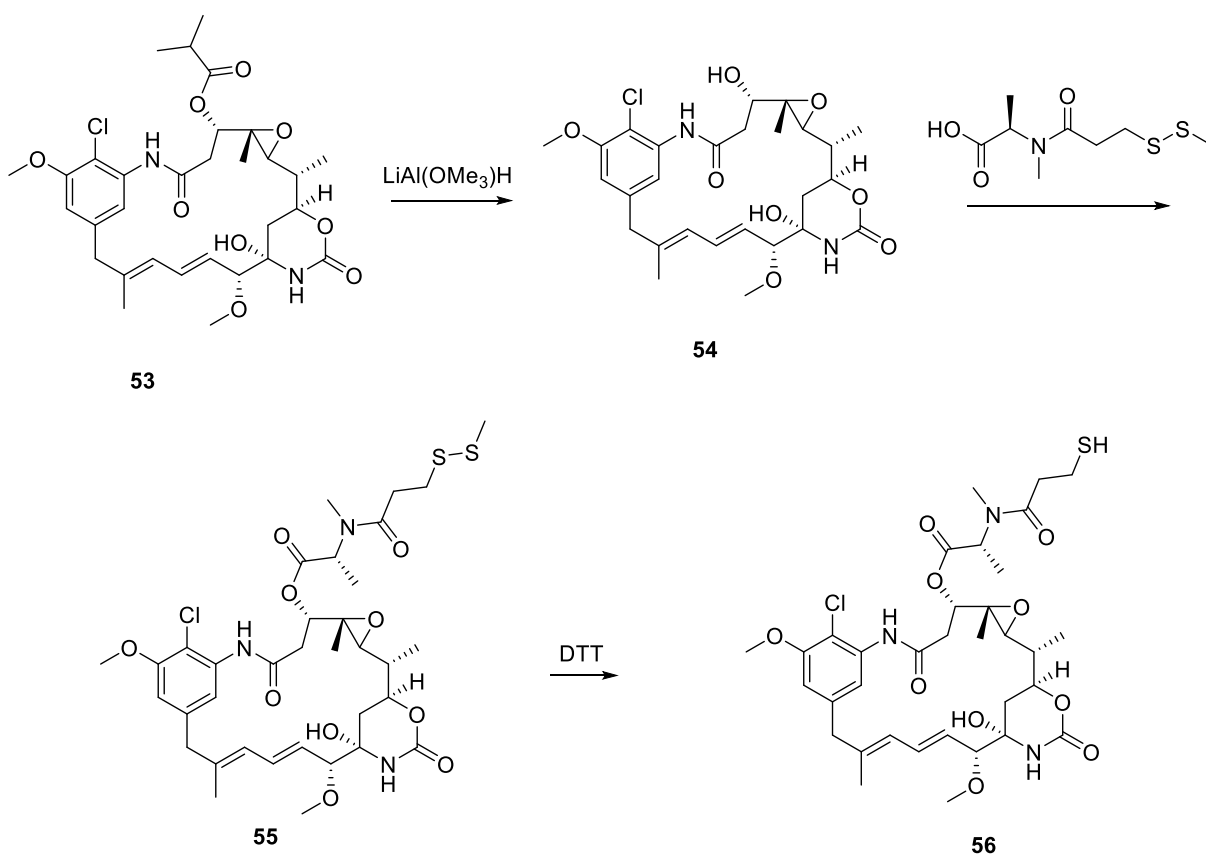


52

Figure 2.9: Structure of Maytansine **42**

Maytansinoids are derivatives of maytansine, **52**, and have similar function to vinca alkaloids. Maytansine was initially isolated in 1972 from an alcoholic extract in the bark of the African shrubs *Maytenus serrata* and *Maytenus buchananii* (Figure 2.9).⁶⁸ Maytansine has been demonstrated to be highly potent against several breast cancer cell lines such as SK-Br3 and MCF-7 with an IC₅₀ of 30-40 pM.⁶⁹ Despite its cytotoxicity, it is ideal as a potent payload which is why it has been used extensively with ADCs. Derivatives such as DM1, **56** and DM4 are often used as they have been modified to incorporate a free thiol which can be used as a linker attachment site, and can be made from maytanisol **42** which is an ester hydrolysed analogue of **52**.

The complexity of maytanisol with its multiple stereocentres makes the commercial production by total synthesis cost prohibitive. Numerous groups have attempted and succeeded at the total synthesis such as the Corey group in 1980.⁷⁰ Therefore, its derivatives are often semi-synthetic, derived from Ansamitocin P-3, **53** and analogues have been made this way (Scheme 2.8).⁶⁹ Only three steps are needed from **53** and involves a LiAl(OMe)₃H mediated ester cleavage followed by an esterification and a reduction of the disulphide to the free thiol, **56**.



Scheme 2.8: Semisynthetic general route to DM-1, **56**⁶⁹

2.4.4. Tubulysins

Tubulysins were originally isolated from myxobacteria, discovered in 2000 and act as antimetotics by inhibiting tubulin polymerisation. They are tetrapeptides composed of D-methylpipercolate, L-isoleucine, L-tubovaline and L-tubuphenylalanine residues. They exert potent anti-proliferative activity against cancer cell lines with tubulysin D, **57** the most potent (IC₅₀ values between 0.01 and 10 nM). Derivatives have been made such as **58** (Figure 2.10).^{71, 72}

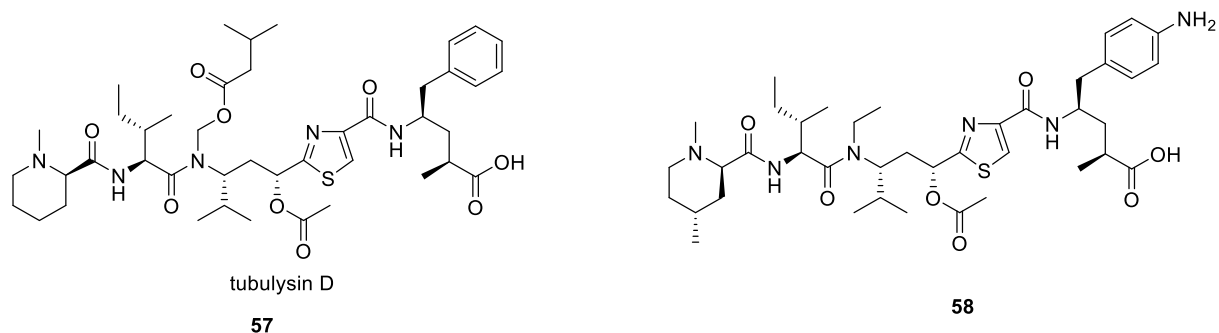
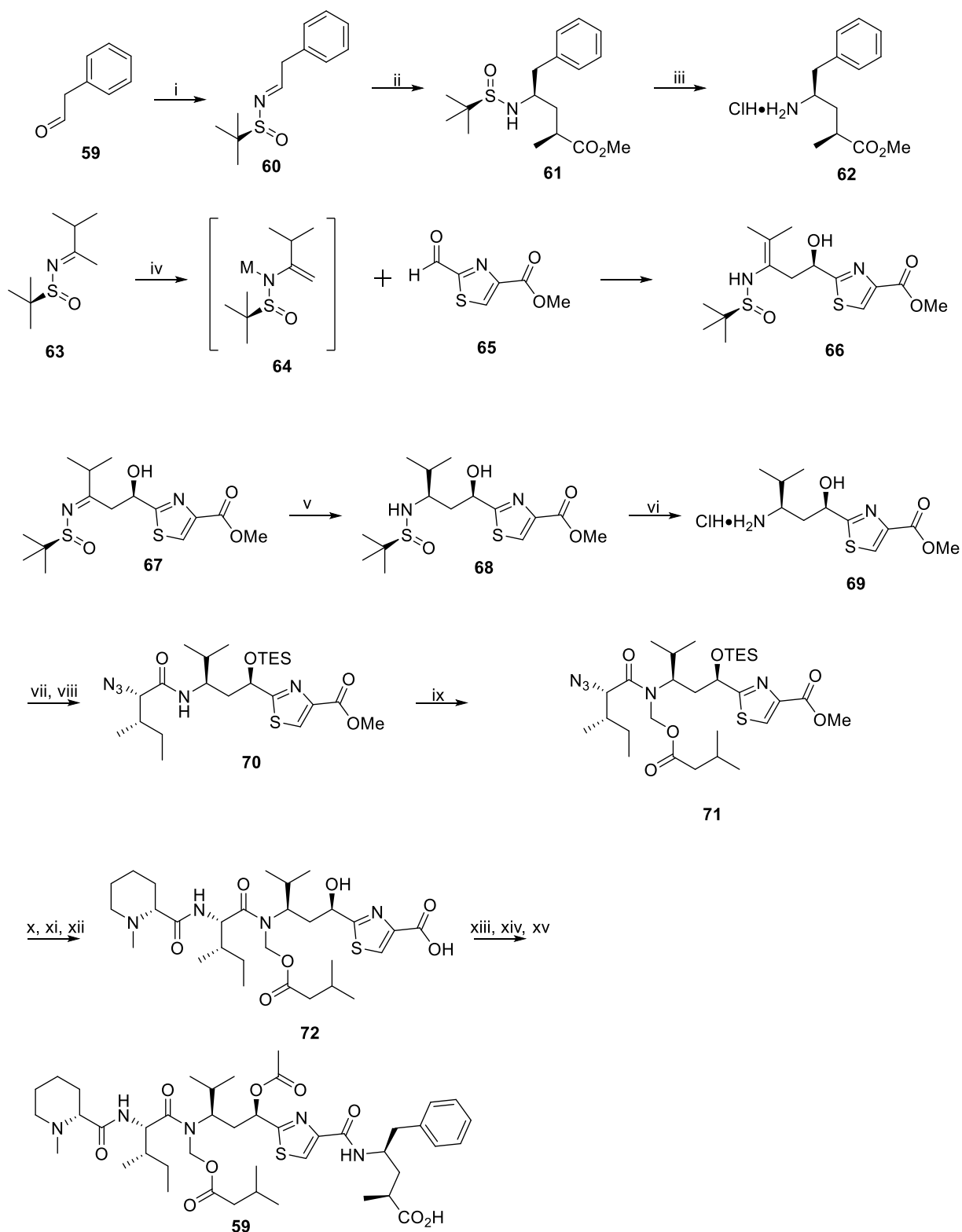


Figure 2.10: Structures of tubulysin derivatives, tubulysin D, **57** and AZ13599185, **58**

The total synthesis of tubulysins has been achieved, with a convergent synthesis of tubulysin D reported by Ellman *et al.*⁷³ Fragment **62** could be synthesised from commercially available

59 which undergoes a condensation with (R)-*tert*-butanesulfinamide to form **60**. An SmI₂ reductive coupling of methyl methacrylate and **60** gave **61** which was heated in aq HCl to give the HCl amine salt **62**.

With fragment **62** synthesised, attention switched to the other fragment. Metalloenamine **64** was formed from ketimine **63** and was reacted with thiazoline aldehyde **65**. Stereoselective reduction was achieved with NaBH₄ with the Lewis acid Ti(OEt)₄. The amine was obtained with treatment of HCl to **68**. Using α -azido acid chloride with **69** led to amide formation, followed by protection of the alcohol with TES to give **70**. *N*-alkylation with chloromethyl isobutyl carbonate was achieved with KHMDS to form **71** and subsequently the azide was reduced by hydrogenation in the presence of the pentafluorophenyl ester of Mep followed by deprotection of the silyl ether to form **72**. From here, the ester was selectively hydrolysed with Me₃SnOH followed by incorporation of fragment **57** using the activated acid of **72** and finally acetylation of the alcohol.



Scheme 2.9: Total synthesis of tubulylin D, **58**. *Reagents and Conditions*: i) (*R*)-*tert*-butanesufinamide, $\text{Ti}(\text{OEt})_4$, THF, RT, 6 h, 84%; ii) Sml_2 , LiBr, H_2O , THF, -78°C , 55%; iii) HCl, dioxane/ H_2O , reflux, quant.; iv) LDA, $\text{CITi}(\text{O}-i\text{-Pr})_3$, ether, -78°C , 90%; v) NaBH_4 , $\text{Ti}(\text{OEt})_4$, THF, -78°C , 88%; vi) HCl, dioxane/MeOH, RT, quant.; vii) (3*S*)-2-azido-3-methylpentanoyl chloride, *i*-Pr₂Et₂N, DCM, 93%; viii) TESOTf, lutidine, DCM, 98%; ix) KHMDS, THF, -45°C , then $\text{ClCH}_2\text{OCOCH}_2\text{CH}(\text{CH}_3)_2$, 73%; x) Mep pentafluorophenyl ester, H_2 , Pd/C, RT, EtOAc; xi) AcOH/THF/ H_2O , RT, 73% over two steps; xii) Me_3SnOH ,

Cl(CH₂)₂Cl, 60 °C, 67%; xiii) pentafluorophenol, DIC, DCM, RT; xiv) **63**, *i*-Pr₂EtN, DMF, RT, 85% over two steps; xv) Acetic anhydride, pyridine, then H₂O/dioxane, RT, 82%.

2.5.4. Duocarmycins, Pyrrolobenzodiazepines and Psymberin

Duocarmycins (e.g. duocarmycin A, **73**, Figure 2.11) are natural products first isolated from *Streptomyces* bacteria in 1978. They are DNA minor groove binders and alkylate the nucleobase adenine at the N3 position. Unlike tubulin binders, they can affect the cell at any stage of the cell cycle and are becoming more common as payloads in ADCs.⁷⁴

Pyrrolobenzodiazepine (PBD) dimers like SG3199, **74** (Figure 2.11) are an interesting class of alkylating agents being used in early clinical development of ADCs. PBDs were discovered in *Streptomyces species*, and are produced by actinomycetes and are DNA minor groove binders and bind to a particular sequence, forming an aminal bond to the N2 of guanine bases.³⁸ They disrupt the DNA structure, prohibiting transcription and translation. Dimeric PBDs have picomolar activity against a broad array of cancers and are implicated in the bystander effect. They also show no cross-resistance with other chemotherapies like cisplatin indicating a separate mechanism of action to other DNA binders and so could avoid emergent drug resistance.⁷⁵ *In vitro*, they possess IC₅₀s in the low nM to pM range.⁷⁶

Psymberin **75**, also known as irciniastatin A is derived from the sea sponges *Ircinia ramose* and *Psammocinia sp.* and exhibits potent antitumor activity.⁷⁷ When tested against 60 cell lines, it displayed cytotoxicity against breast, colon and melanoma cancers with LC₅₀ < 2.5 nM. It is postulated that works as a translation inhibitor, primarily targeting the ribosome and disrupts the synthesis of new proteins leading to inhibition of cell growth or proliferation.⁷⁸ Psymberin does this by disrupting protein synthesis after the formation of the ternary complex between the ribosome, aminoacyl-tRNA and messenger RNA.⁷⁹

β-Glucuronidase cleavable linkers have been used with phenolic cytotoxic agents like Psymberin, **75**, from Seattle Genetics as well as duocarmycins. In this, a DMED self-immolative spacer (Figure 2.11, **76**) was used to allow for stable linkage and facile release, working by cyclising to eliminate CO₂ along with the payload. This drug-linker was conjugated to cAC10 mAbs (anti-CD30) and h1F6 (anti-CD70) via reduced interchain disulfides. Exposure to a CD30 expressing line such as L540cy (Hodgkin lymphoma) to cAC10-**77** gave an IC₅₀ of 0.15 nM, compared to the CD30 negative cell line Caki-1 giving an IC₅₀ of 62 nM. H1F6 conjugated payload was also tested against the CD70 cell line of Caki-1 giving good activity but significantly reduced activity on L540cy. The payload is highly potent in both cell lines, indicating selectivity.⁵⁰

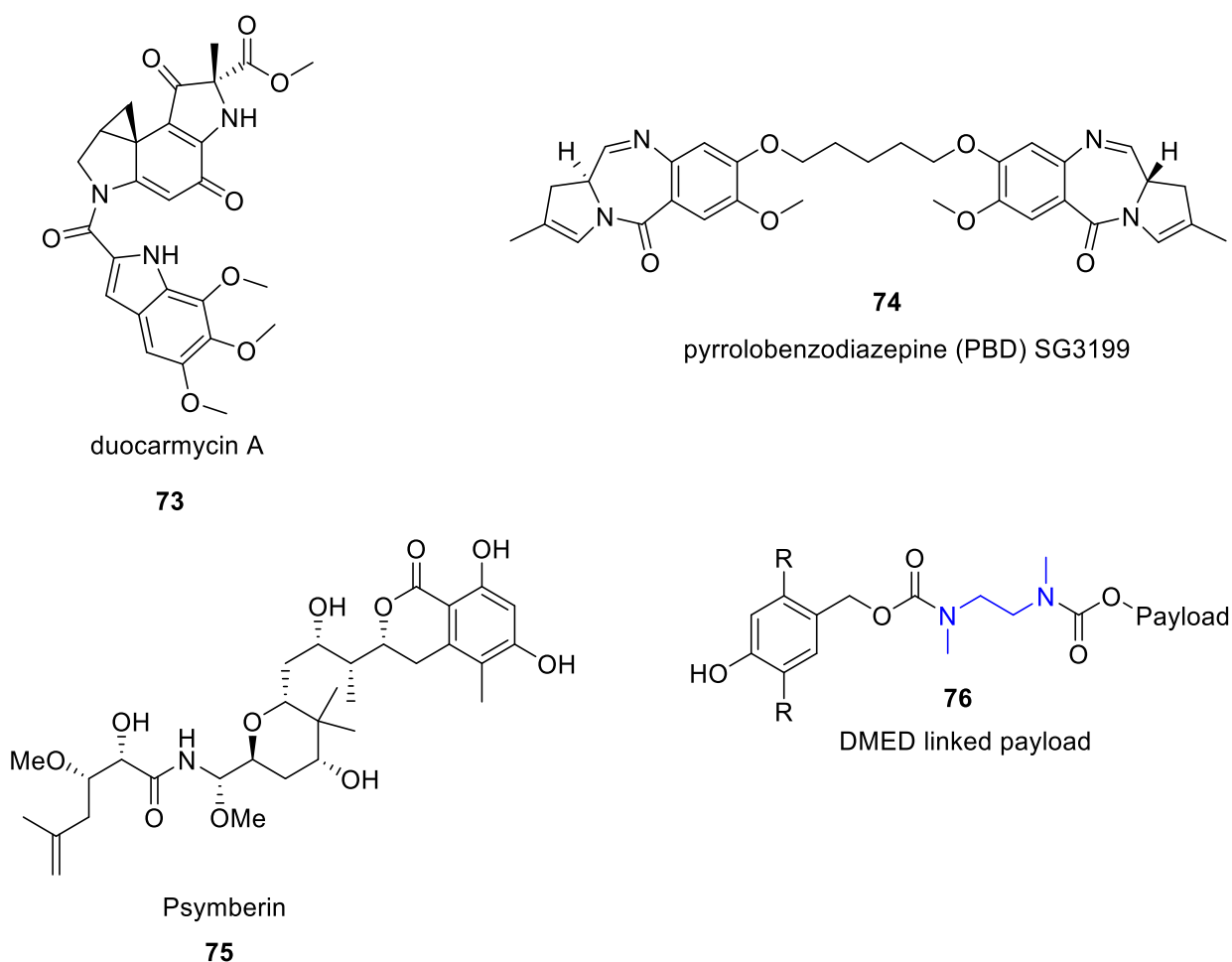
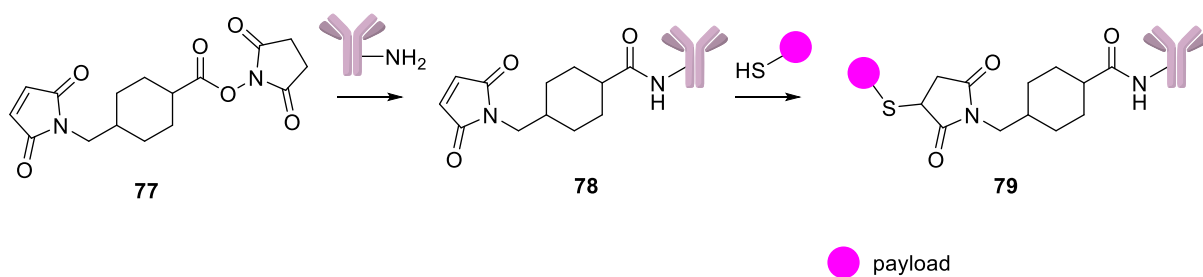


Figure 2.11: Structure of DMED linker in blue and the structures of duocarmycin A, pyrrolobenzodiazepine (PBD) SG3199 and Psymberin.

2.5. Conjugation sites and attachment groups

The use of conjugation sites is important to ideally ensure high homogeneity in ADCs with uniform DAR. ADCs with high DAR values often show greater potency *in vitro* but *in vivo*, there is a significant loss of potency. This is because an increase in hydrophobicity causes the antibody to be cleared rapidly and drive antibody aggregation and fragmentation especially through ionic or thermal stress. The increase in hydrophobicity stems from the increase in lipophilicity generated from the addition of lipophilic drug-linker moieties⁸⁰ Attempts have been made to limit and strictly control the DAR.

2.1.5. Lysine conjugation



Scheme 2.10: General scheme for the conjugation of lysines to a linker followed by linkage to a payload. Magenta is a payload.

Early generation ADCs used lysines to conjugate the linker to the antibody through a stable amide bond (Scheme 2.10). Lysine-based conjugation is a widely used non-specific conjugation strategy. An IgG can contain over 80 lysine residues with around 10 of these solvent accessible.⁸¹ The reactive amine can be coupled with activated carboxylic acids such as succinimide esters in high yields. A variety of succinimide esters are used for this conjugation and have thiol sensitive sites such as maleimides and disulfides that can be used to couple with a payload. (Figure 2.12). Lysine conjugation can lead to highly heterogeneous mixtures, with DARs ranging from 0-7.⁸² This method represents an easy and reliable way for conjugation but critical lysines in the antigen binding region could be altered leading to loss of affinity and efficacy.

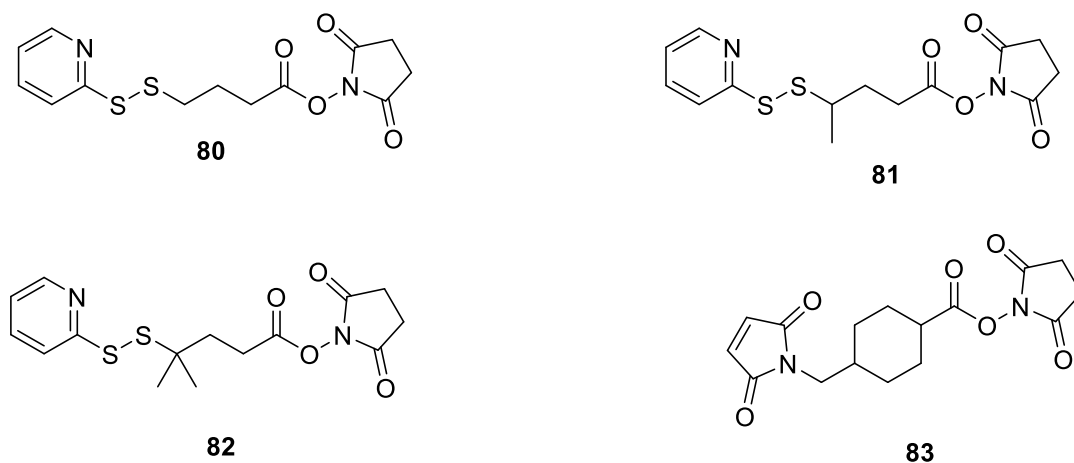


Figure 2.12: Structures of some succinimide esters used for Lysine conjugation

2.2.5. Cysteine conjugation

In most antibodies, the thiols of cysteine residues are not available to react as they are involved in disulphide bridges and so require partial reduction to reveal the free thiol residues for conjugation. There is a total of 16 disulphide bonds in an antibody, 4 interchain and 12 intrachain.⁸³ The 4 interchain disulphide bridges are normally not critical to antibody stability

and are more susceptible to mild reduction using chemicals such as DTT and TCEP.⁸⁴ Therefore, conjugations with DAR of 0, 2, 4, 6 and 8 are obtained. It is deemed more superior to lysine conjugation due to improved control of DAR and heterogeneity owing to its more uniform products.³⁰ It requires a thiol-reactive functional group on the payload, and in many cases, maleimide is used as an attachment group but maleimides are susceptible to deconjugation in the serum which can lead to off-target toxicity through a retro-Michael reaction.⁸⁵ Many mAbs are engineered to have a restricted number of free cysteine or lysine residues and so DAR can be more tightly controlled.⁸³

2.3.5. Glutamine conjugation

A primary amine-containing linker can be covalently attached to a native glutamine (Q295) through a catalysed transpeptidation by a transglutaminase derived from the bacteria *Streptomyces mobaraensis*. DARs of two can be obtained, with one conjugation site on each heavy chain. The antibody must be deglycosylated for the conjugation to be possible but no genetic engineering is required.⁸⁶

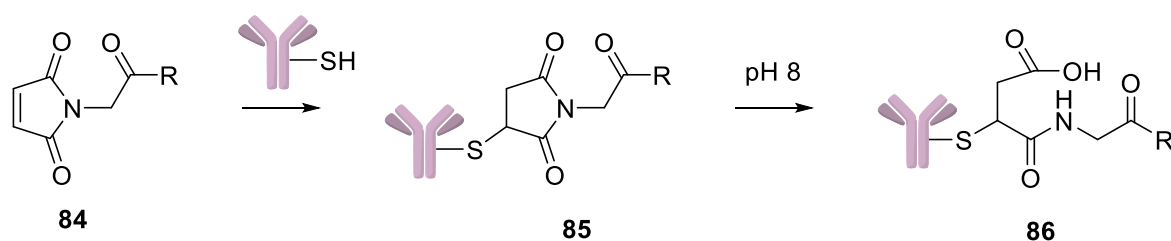
2.4.5. Site specific conjugations

Multiple companies have developed ADCs that use additional cysteines engineered into the antibody at different sites that have different free solvent accessibility. This has allowed for complete uniform stoichiometry with DARs of 2 or 4 exclusively, depending on how many new cysteines are added.

One of these new technologies is THIOMAB™, which uses site-directed mutagenesis to incorporate two new cysteines into the antibody.⁸⁷ This allows for complete control of the DAR and was originally used with the classical maleimide group to give a TDC (THIOMAB™ antibody-drug conjugate). TDCs are better tolerated with improved therapeutic indices than their classical ADC counterparts.⁸⁸ The cysteines of the antibody can undergo controlled reduction. After reduction to the free thiols, the non-engineered thiols can be oxidised back to their interchain disulphide bridges but the engineered cysteines are kept reduced allowing for conjugation.⁸⁴

A problem in this design is succinimide conjugates can undergo retro-Michael reactions and so TDCs would often rapidly lose the conjugated thiol-reactive linker in the plasma releasing the payload systemically. The engineered sites are highly accessible to solvent and are susceptible to the reactive thiols found in albumin, free cysteines and glutathione, leading to premature release of the payload.⁸⁹ It was found that hydrolysis of the maleimide to the

succinamic acid derivatives (Scheme 2.11, **86**) could stabilise the succinimide conjugates against the retro-Michael reaction. The hydrolysis can be facilitated by adding a LC-V205C mutation in the light chain leading to improved second-generation TDCs.⁸⁹



Scheme 2.11: Structure of the hydrolysed product of maleimide

2.5.5. Unnatural amino acid engineering

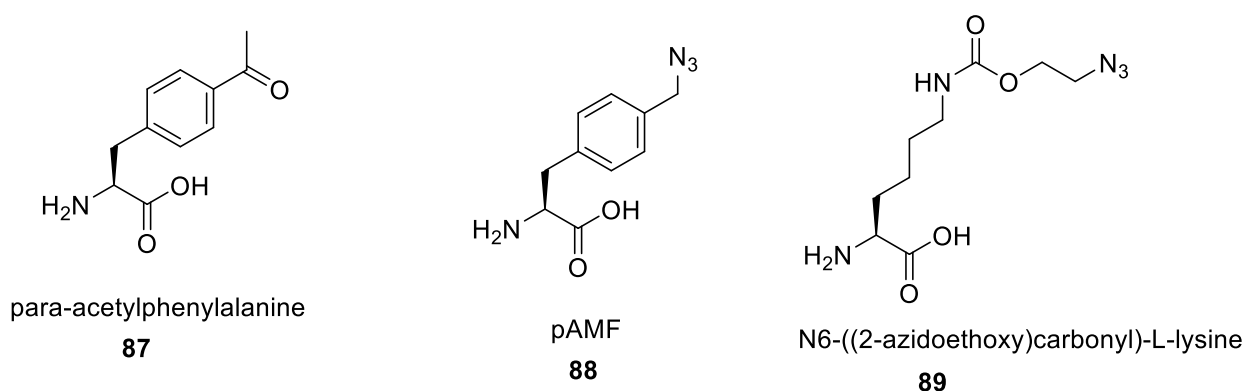
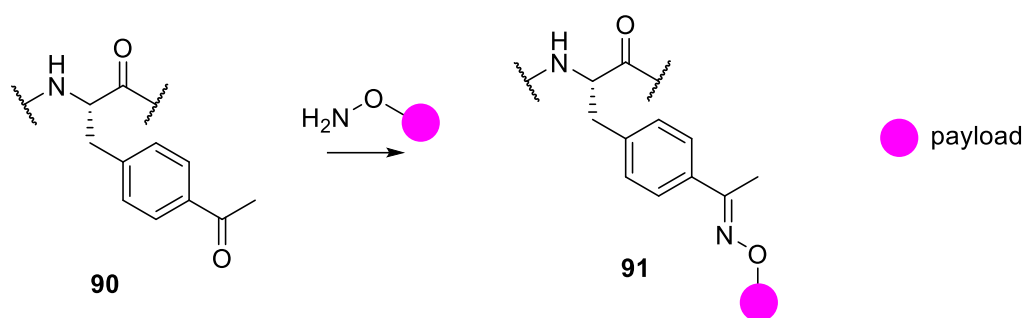


Figure 2.13: Unnatural amino acids engineered into antibodies

Incorporation of unnatural amino acids in an antibody can be used to install a residue containing a reactive handle which can be used to conjugate with a linker. This allows for biorthogonal chemical reactivity of the amino acids and so strictly controlled DARs can be achieved.⁹⁰ This has been shown with aurastatins and conjugations only occurred on the unnatural amino acid and none of the other 20 naturally occurring amino acids found in the antibody. This involved the use of para-acetylphenylalanine, **87** (Figure 2.13) as the unnatural amino acid.⁹¹ The ketone of para-acetylphenylalanine can then be reacted with a hydroxylamine functionalised nitroxide and the subsequent oxime can be used for conjugations (Scheme 2.12).



Scheme 2.12: General scheme for the condensation of a hydroxylamine functionalised nitroxide with para-acetyl phenylalanine residue. Magenta circle is a linker-payload derivative.

Antibodies incorporating para-azidomethyl-L-phenylalanine (pAMF) **88** and N6-((2-azidoethoxy)carbonyl)-L-lysine **89** are azide antibodies that have azide handles for bioconjugation allowing for copper free click chemistry. It was shown that after completion of the click bioconjugation to the AzAb, the aromatically stabilised linker was 10-fold more stable than a cysteine-maleimide linker and DAR could be tightly controlled.^{92, 93}

2.6.5. Enzymatic conjugation

Genetically encoded amino acid tags inserted into the mAb sequence can be recognised by specific enzymes such as formylglycine-generating enzyme (FGE) or sortases allowing for site specific conjugation. Essentially, an enzyme will modify a specific point encoded on the antibody based on a specific amino acid sequence and so only this specific amino acid will be modified into a reactive functional group for conjugation.

SMARTag™ is one such technology and involves the use of FGE which acts on the specific amino acid sequence Cys-X-Pro-X-Arg (where X is any amino acid) and modifies the cysteine to a formyl-glycine.^{94, 95} This can then be reacted with aldehyde reactive amino acid residues in a hydrazine-Pictet-Spengler ligation (Figure 2.14).⁹⁶

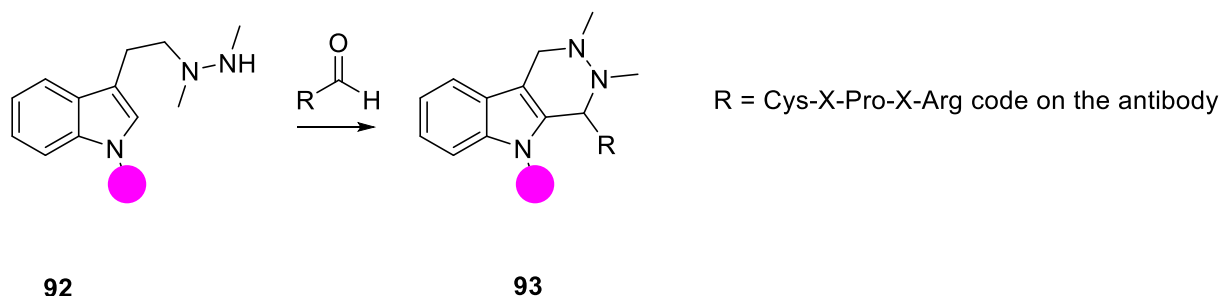


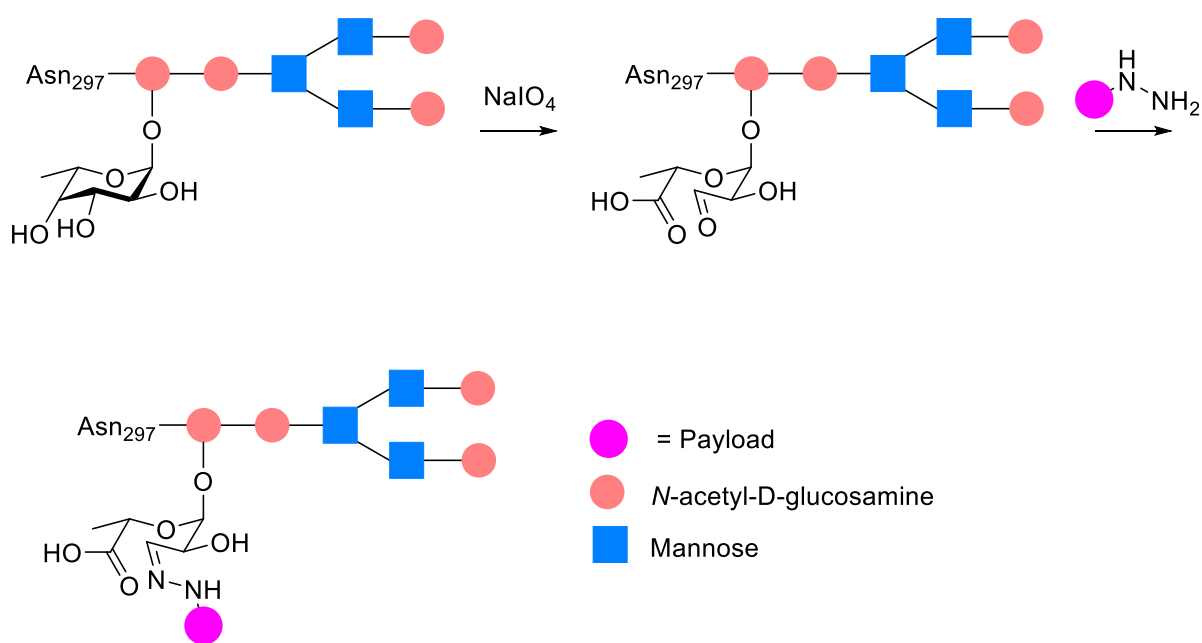
Figure 2.14: Hydrazine-Pictet-Spengler ligation involving tryptamine with an aldehyde. Magenta circle represents linker-payload

Sortase A can also be used as an enzyme and recognises the Lys-Pro-Glu-Thr-Gly sequence. It cleaves the Thr-Gly bond undergoing a transpeptidation reaction with an oligoglycine. A

payload such as MMAE or maytansine can be coupled to a pentaglycine peptide and subsequently can undergo another transpeptidation-like reaction to link the antibody to the payload. This has been developed by NBE therapeutics.⁹⁷

2.7.5. *N*-glycan engineering

N-glycan engineering involves the *N*-glycan Asn297 found in the Fc domain. It is conserved in all IgG classes and is situated away from the antigen binding site. This makes it an ideal target as it can be broadly used across all antibodies and also minimise the risk of affecting binding affinity.⁹⁸ Multiple approaches to modifying *N*-glycan have been employed such as introducing sialic acid or fucose to the *N*-glycan terminus through enzymes such as β -1,4-galactosyltransferase. For example, the cis diol of fucose can undergo oxidative cleavage with NaIO_4 to an aldehyde, which can be further modified through hydrazone linkers to a payload (Scheme 2.13). However, a downfall with this method is the use of NaIO_4 which can oxidise methionine residues and DAR distribution is wide due to low conversion.⁹⁹



Scheme 2.13: Schematic representation for fucose-specific conjugation of hydrazone-derivatives. Circles represent *N*-acetyl-D-glucosamine, squares represent mannose and x as a payload.

Metabolic glycoengineering has also been suggested. Instead of using fructose, unnatural fructose derivatives such as 6-thiofructose can be added to the culture media which is then incorporated into the *N*-glycan. The resulting unnatural thio-glycan can then be used to conjugate with maleimide chemistry for improved homogeneity.¹⁰⁰

2.6. Early ADCs

Initial attempts involved using antibody-toxin conjugates using toxins such as ricin and diphtheria toxin but were unsuccessful due to infusion reactions, development of neutralising antibodies to the exotoxins and vascular leakage.⁵³ One of the first reported cases of an ADC was in 1970 and involved using a diphtheria toxin conjugated to an anti-mumps antibody. Although they found selectivity in monkey-kidney cells, the ADC was not progressed any further.¹⁰¹ The use of murine antibodies as well as proteins as payloads made early ADCs suffer from adverse toxic effects from premature release of the toxin. It wasn't until first generation ADCs were clinically effective.

2.7. First generation ADCs

2.1.7. cBR96

The first breakthrough though began with cBR96 doxorubicin **94**, targeting the Lewis-Y antigen developed by Seattle Genetics (Figure 2.15).¹⁰² It features doxorubicin as the payload with a hydrazone linker and attaches to the antibody through a Michael addition with cysteine and a maleimide. ADCs at this point had moved to using small molecules as the payloads, rather than proteins. In clinical trials it was found to possess significant antitumor properties and regressed large human tumour xenografts in mice and rats.¹⁰² It was also found to have broad and potent antitumor activity in cancers such as lung, breast and colon, with doxorubicin-resistant tumours also affected. Phase I studies had demonstrated a partial response in gastric carcinoma. However, it also suffered significant on-target toxicities not associated with systemic doxorubicin. It was found to cause severe inflammation and ulceration of the gastric mucosa of patients with ulceration. It was later found that there was an unrecognised expression of Lewis-Y antigen on these cells and this affect was dose-limiting.¹⁰³

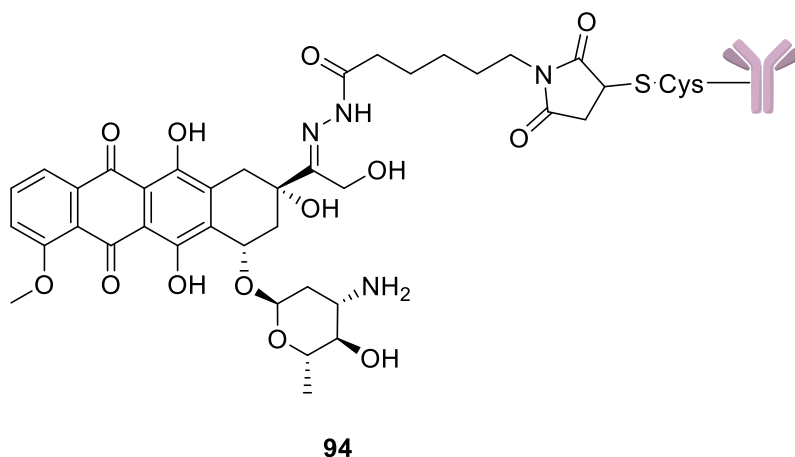


Figure 2.15: Structure of cBR96 doxorubicin, **94**

A randomised phase II study was performed in metastatic breast cancer patients with cBR96 doxorubicin (700 mg/m²) or doxorubicin (75 mg/m²) alone. Results showed the adverse effects of nausea and hematemesis for the ADC but there was a higher tolerability and antitumor potency for doxorubicin.¹⁰⁴ This is a useful evaluation to see if the ADC will surpass the payloads activity with limited systemic toxicity. Despite promising pre-clinical data, the project was abandoned due to the lack of efficacy demonstrated as Seattle Genetics focused on other ADCs in their pipeline with improved efficacy.

Other first generation ADCs showing systemic distribution of the payload include bivatuzumab mertansine **95** (Figure 2.16) which targeted CD44v6 antigen using DM4 for squamous cell carcinoma which caused fatal exfoliate of skin toxicity due to antigen expression in the skin. BAY794620, an ADC which targeted CA9 antigen caused death in two patients due to gastrointestinal toxicity.^{105, 106}

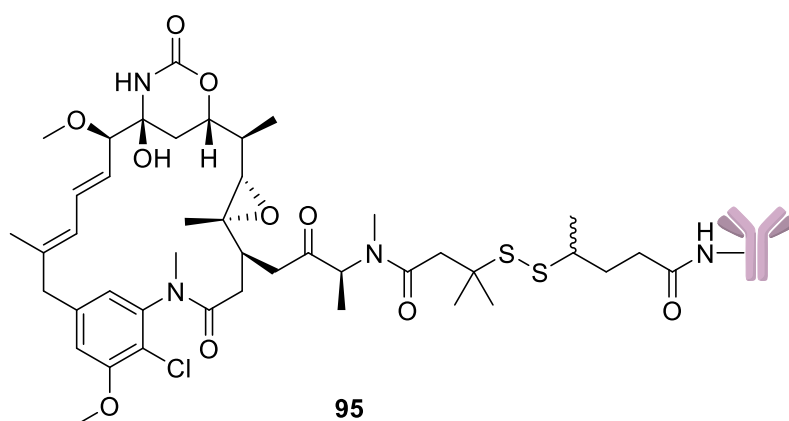


Figure 2.16: Structure of bivatuzumab mertansine, **95**

One of the biggest reasons for these adverse toxicities was due to expression of antigens in normal tissues. Ideally, selected antigens would be selectively expressed in cancer cells over normal cells.⁴⁰ From these early ADCs, it was recognised the importance of useful antigen selection to give confidence in selectivity and their safety profile.

Payloads for these early ADCs were often of relatively low potency, using chemotherapy agents like doxorubicin (IC₅₀ in cell lines around 0.1 uM), 5-FU and methotrexate.¹⁰⁷ Due to the relatively low potency, dosing of the ADCs was high in order to observe efficacy with DARs of up to 8 used. Subsequent ADCs replaced micromolar payloads for more potent (nanomolar to picomolar) payloads in order to decrease the dosing of ADCs. Many ADCs had dose-limiting toxicities and so a better therapeutic window could be achieved with reduced toxicity and an increase in efficacy.⁸⁴

2.2.7. Gemtuzumab ozogamicin

In 2000, the FDA approved by an accelerated-approval process gemtuzumab ozogamicin, Mylotarg, **96** (Figure 2.17). Developed originally by a collaboration between Celltech (now part of UCB) and Wyeth (now part of Pfizer) in 1991, the drug targets CD33 which is expressed in leukemic blast cells and is used in the treatment of acute myeloid leukaemia (AML).¹⁰⁸

CD33 was seen as a good choice of antigen as it was previously seen that an anti-CD33 radio-immunoconjugate was efficiently internalised by CD33+ cells in humans.¹⁰⁹ Due to this evidence of internalisation coupled with its selectivity, this antibody was chosen to use as an antibody conjugate with a derivative of calicheamicin. An average of 2.5 drugs to antibody was used.

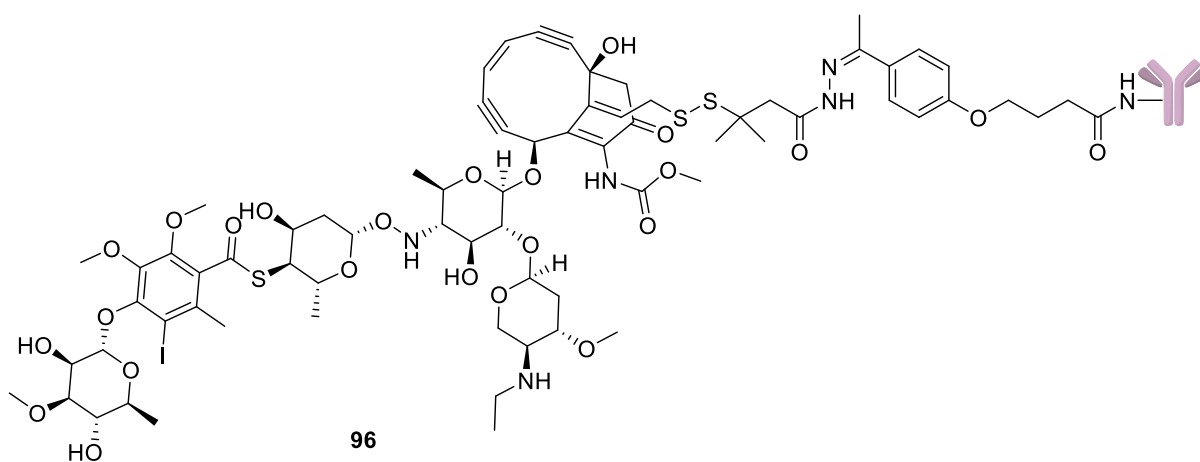


Figure 2.17: Structure of gemtuzumab ozogamicin, **96**

Mylotarg was given accelerated approval for patients aged 60 years and over with CD33+ AML. It was approved based on early clinical studies of monotherapy in AML patients. The results of a post-approval commitment, a randomised phase III study using two different treatment plans, one using daunorubicin, cytarabine and a single dose of Mylotarg, while the other using standard induction therapy of daunorubicin and cytarabine only, showed no improvement in survival with Mylotarg and surprisingly showed an increase in treatment-related mortality in patients.¹¹⁰ Mylotarg was therefore voluntarily removed from the market. However, the mortality rate for the control group was unusually low of 1% compared to 5% of the other Mylotarg group.¹⁰⁹ Mylotarg was required to carry a black box warning due to its risk of hepatic veno-occlusion disease (VOD) in which small veins in the liver can become

obstructed and is an issue before bone marrow transplant.¹¹¹ Its high toxicity as well as increase in mortality rates in patients led to its voluntary removal from the market.

There are several possible explanations for the adverse effects for this drug. The first was the linker used. It was suggested that systemic release of Mylotarg was caused by premature release of the drug by the hydrazone linker. Around 50% of the bound drug is known to release from the linker in 48 h.¹¹² Systemic release of the payload could cause severe adverse effects.

Another reason is concerned with the payload. Calicheamicin is known to cause the bystander effect, facilitated by ADCs and is also susceptible to drug efflux.¹¹³ The reason for this is their high hydrophobicity, which imparts the compound with enhanced cell permeability.⁵⁷

A possible issue arises from problems with the manufacturing processes. Originally, the manufactured drug yielded 50% of unconjugated antibodies in the final drug. The other 50% was heterogeneous in nature with regard to DAR.¹¹⁴ This heterogeneous nature of the drug led to poor efficacy and may have contributed to the premature release of the payload as some would be overloaded rendering them unstable.⁸⁴

From a meta-analysis of subsequent clinical trials, comprising of 3325 total patients, Mylotarg showed no change in complete remission but a significant reduction in risk of relapse and improved 5-year relapse free survival and overall survival in patients with AML was observed.¹¹⁵ Importantly, lower doses of Mylotarg were just as effective as higher doses, which lead to improved tolerability and safety. Gemtuzumab ozogamicin was approved by the FDA in 2017 and studies in other cancers such as APL are still ongoing.¹¹¹

2.3.7. Inotuzumab ozogamicin

Pfizer along with Wyeth and the University of California, Berkeley recently developed a further ADC to this, Inotuzumab Ozogamicin, Besponsa. Besponsa uses the same linker and payload to Mylotarg but targets a different antigen and also carries a black box warning for VOD. Inotuzumab, a humanised IgG4 antibody, targets CD22, which is a specific antigen found in B-acute lymphoblastic leukaemia (B-ALL).¹¹⁶ CD22 has restricted expression on fully mature B cells and has been implicated in adult acute lymphoid leukaemia with patients reportedly showing high expression of CD22 on the cell surface of these cancers.^{117, 118}

Traditional cytotoxic therapy towards non-Hodgkin lymphomas (NHL) include a combination of chemotherapies of cyclophosphamide, vincristine and prednisone without (CVP) or with doxorubicin (CHOP). The antibody rituximab (an anti-CD20 antibody) can be added, (R-

CHOP) and as a continued maintenance drug after chemotherapy. In preclinical data, Besponsa demonstrated superior potency over these methods *in vitro* as well as *in vivo* human B-cell lymphoma xenograft mice models. When used in combination with CVP, there was an increase in efficacy but with CHOP there was an increase in toxicity as well. A dose-dense study with just 2 dosages of Besponsa and CHOP given alternatively were found to reduce this toxicity while retaining efficacy.¹¹⁹ It also showed complete regression in tumour-bearing mice. ALL cell lines were more sensitive to calicheamicin-induced apoptosis compared to NHL and AML rather than needing to fully saturate the CD22 antigens present on the cell, giving rise to the ADCs efficacy. This means that a lower dosage could be used as less ADC is required for efficacy. As a result, it showed potency far below its MTD of 1.8 mg/m². Side effects included loss of platelets, loss of neutrophils, asthenia and nausea.¹²⁰

A phase II study using 49 refractory and relapsed B-ALL patients was conducted. The response rate was 57% from this study with an overall median survival rate of 7.9 months. It was approved in 2017 after further demonstrating superiority over standard chemotherapy.¹²¹ In a Phase III study with 326 patients with CD22 positive B- ALL was conducted. The rate of complete remission for Besponsa was far higher than traditional chemotherapy (80.7% vs 29.4%).¹²²

Despite the initial problems associated with Mylotarg and advances in ADC design with second generation ADCs, the design of first-generation ADCs can still be impactful. This shows the unique nature of ADCs in which certain combinations will work despite concerns.

2.8. Second generation ADCs

Lessons were learnt from the first-generation ADCs, which included the avoidance of premature release of the payload through linkers such as hydrazones and development of more stable cleavable and non-cleavable linkers. Antibody technology had also been improved by moving to humanised antibodies to reduce the clearance and immunogenicity associated with antibodies.

2.1.8. Brentuximab vedotin

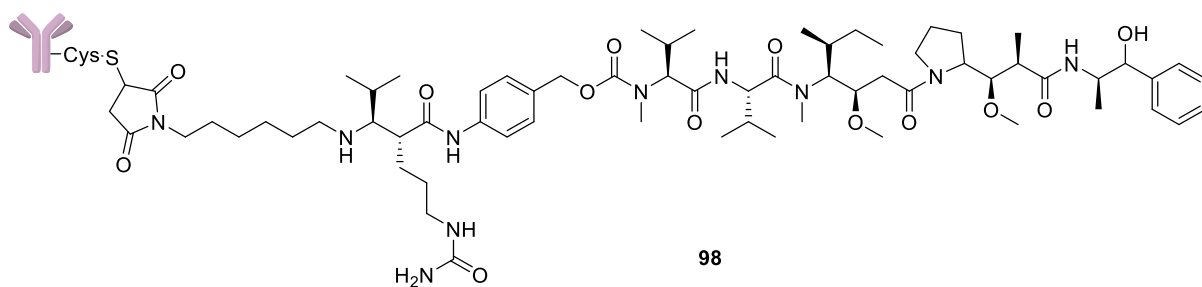


Figure 2.18: Structure of brentuximab vedotin, 97

The second ADC to receive accelerated FDA approval was brentuximab vedotin, Adcetris, 97 (Figure 2.18) in 2011 and was developed by Seattle Genetics. The cost of treatment for this drug is over \$100,000.¹²³ It is used for the treatment of Hodgkin lymphoma and ALCL targets the antigen CD30 which is a prominent marker found in these types of cancers.¹²⁴ The antibody chosen was cAC10 which is a chimeric IgG1 antibody and was used in phase II clinical trials unconjugated showing selectivity.^{125, 126} Limited success was seen with anti-CD30 antibodies such as MDX-060 and SGN-30 (cAC10). They showed partial response in patients with ALCL and Hodgkin lymphoma but were limited. However, it was found that they were well tolerated. Expression of CD30 on healthy cells is very low with some expression on activated T and B cells and CD30 is a tumour necrosis factor receptor superfamily member which induces apoptosis.¹²⁷

The payload used for Adcetris is MMAE. Originally, all 8 sites from the cysteine disulphide bridges found on an antibody were used to generate very uniform conjugated antibodies. However, it was found that a high DAR reduced the therapeutic window due to the heavy loaded antibody having poor pharmacokinetic profile such as high clearance from the increased hydrophobicity generated from the linker and payload.¹²⁸ Antibodies with an average DAR of 4 were produced with primarily two, four and six molecules per mAb.³⁰ As it is conjugated through cysteine, Adcetris uses a maleimide group as its attachment site through a Michael addition. Conjugation to the antibody for brentuximab vedotin resulted in less than 5% of the drug being unconjugated antibody in the final product.

The ADC bound to CD30 with an identical affinity to the unconjugated Ab, (3 nM). *In vitro* the ADC had GI₅₀ of 3-50 pM against CD30-positive Hodgkin Lymphoma and ALCL

tumours. The sensitivity of non-CD30 expressing cells was 1000 times less than those presenting the antigen demonstrating good differentiation between the cell lines.¹²⁹

A further drug has been approved by the FDA in 2019, developed by Genetech® and Roche called polatuzumab vedotin-piiq, Polivy. This targets the CD79b antigen implicated in diffuse large B-cell lymphomas in combination with bendamustine and rituximab. The linker and payload is identical to brentuximab vedotin.¹³⁰

A phase II clinical trial (NCT02257567) which compared Polivy in combination with bendamustine and rituximab against bendamustine and rituximab alone showed an increase in complete response rates from 15% to 40% in people with relapsed or refractory diffuse large B-cell lymphoma (DLBCL). The safety profile of the ADC was good, and patients treated with Polivy lived longer than those who used bendamustine and rituximab alone, demonstrating its efficacy. A phase III clinical trial is currently in progress.

2.2.8. Trastuzumab emtansine

Another second-generation ADC is trastuzumab emtansine **98** (Kadcyla Figure 2.19), which was approved in 2013 by the FDA and was developed by Genetech®, a subsidiary of Roche and the first to be used in solid tumours. Kadcyla targets the HER2 receptor which is overexpressed in around 20% of all breast cancers.¹³¹ The antibody used, trastuzumab (Herceptin) is a humanised anti-HER2 mAb and was already a marketed drug for the treatment of metastatic HER2 positive breast cancers as a first line treatment.¹³² It has a high affinity for HER2 and while normal cells express low levels of HER2, around 20000 receptors, some cancer cells overexpress HER2 (2 million receptors).¹³³ Therefore, selectivity for HER2 positive tumour cells over healthy cells is possible. Although Herceptin in combination with chemotherapy improves time to disease progression and overall survival compared with chemotherapy alone, it is not curative, and patients will eventually relapse. The exact mechanism of resistance to trastuzumab therapy is unknown.²⁴

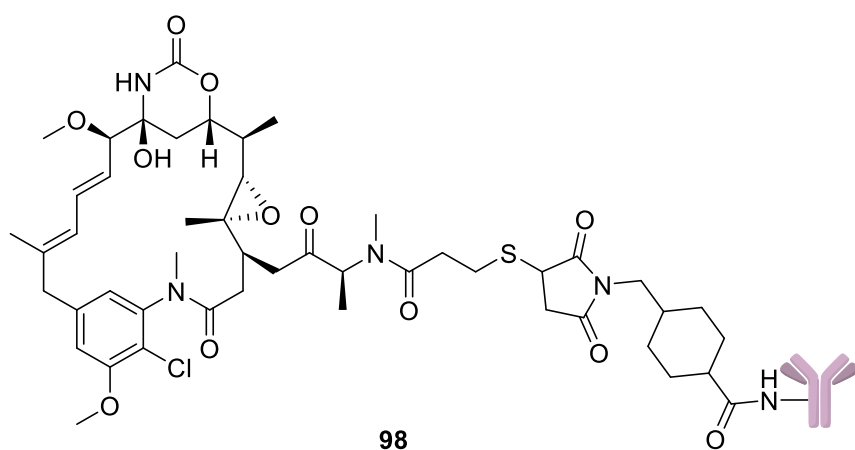


Figure 2.19: Structure of trastuzumab emtansine, **98**

Kadcyla combines this high affinity antibody with the cytotoxic agent DM1 through a stable non-cleavable thioether linker. It is conjugated to the antibody through lysine residues with a DAR of around 3.5 and can last up to 3 days in the blood owing to its plasma stability.^{134, 135} Initially, a reducible disulphide linker was used to attach the payload, but was found to have increased toxicity and lack of efficacy in comparison to the non-cleavable thioether due to its stability.¹³⁶ Most importantly, the drug-linker moiety with the amino acid residue attached retained activity. Another benefit to this non-cleavable linker is that the lysine residue remains with the payload linker after cleavage from the antibody. This positively charged adduct decreases cell permeability and so eliminates any drug diffusing out of the cell eliminating any bystander effect, which is proposed as a reason it has a better safety profile in comparison to the reducible linker. This doesn't interfere with its mechanism of action.¹³⁷

The internalisation process is similar to Herceptin as conjugated trastuzumab is thought to retain its own anticancer mechanism for entering the cell. It is proposed that the mechanism of action for Kadcyla might be independent of the HER2 signalling pathway unlike Herceptin, therefore overcoming several trastuzumab resistance mechanisms.¹³⁴ In preclinical data, Kadcyla was shown to be highly effective at inducing cell death in HER2 positive breast cancer cell lines which were trastuzumab resistant. It was also more potent than trastuzumab alone and caused minimal antiproliferative effect in HER2 normal or negative cell lines demonstrating its selectivity and superiority over current treatments.¹³⁸

In the case of Kadcyla, selecting an antibody already used for treatment was beneficial. However, this is not a requirement for an ADC. For Adcetris, the anti-CD30 antibody only showed modest potency against the target, all that is required of the antibody is to be internalised and deliver the payload to the cell, not to cause the therapeutic effect itself.

2.9. Third generation ADCs

One of the major problems of second-generation ADCs was the heterogeneous in DAR. Third generation ADCs are designed to eliminate this issue. Multiple new ways have been designed to produce homogenous ADCs with uniform DAR, and better conjugation has led to an increase in more drugs being tolerated conjugated to the antibody. Most focus has been on the development of the antibody to give an increase in stability with the attachment to the linker as well as homogeneity.

2.1.9. Vadastuximab talirine

Vadastuximab talirine **99** (Figure 2.20) is being developed targeting CD33 which is expressed on most AML cells. The payload is a PDB dimer, SGD-1882, using a Val-Ala dipeptide linker and is conjugated to the antibody by Michael addition of cysteine with the maleimide functional group. The antibody uses two engineered cysteines on the heavy chain and so tightly controlled DAR is achieved with a near homogeneous average DAR of 2.¹³⁹ It has been developed by Seattle Genetics and a phase I trial had shown the composite remission rate was 70 % in patients with CD33-positive AML with a median age of 75. Despite promising phase 1 results, clinical trials were stopped after a phase III trial showed an increase in the rate of deaths.¹⁴⁰

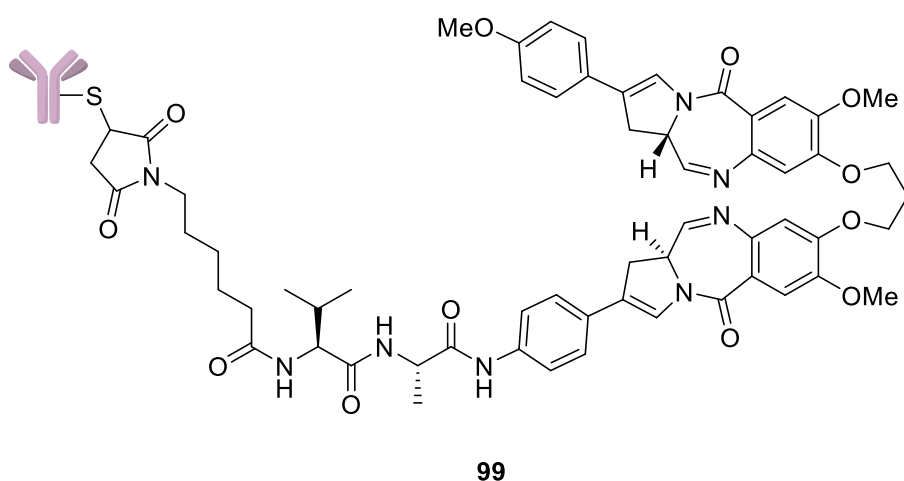


Figure 2.20: Structure of vadastuximab talirine, **99**.

2.2.9. Rovalpituzumab tesirine

Rovalpituzumab tesirine **100** (Figure 2.21), is another third-generation ADC using a PBD dimer as its payload. It uses a Val-Ala cleavable linker with a polyethylene glycol spacer, to

increase hydrophilicity. It targets the protein DLL3, which is expressed on 80% of small-cell lung cancer patient tumours.¹⁴¹

During a phase I trial as third line treatment in recurrent small-cell lung cancer, it was noted that the ADC was well tolerated, and overall survival was found to be 4-6 months. The study was limited as it did not have an active comparator in its exploratory trial design.¹⁴¹ It showed promising data that DLL3 was a clinically relevant target. However, subsequent trials were unsuccessful and so the drug was terminated. Phase II data showed that the objective response rate was just 16% and a phase III trial showed lack of survival benefits for patients.^{142, 143}

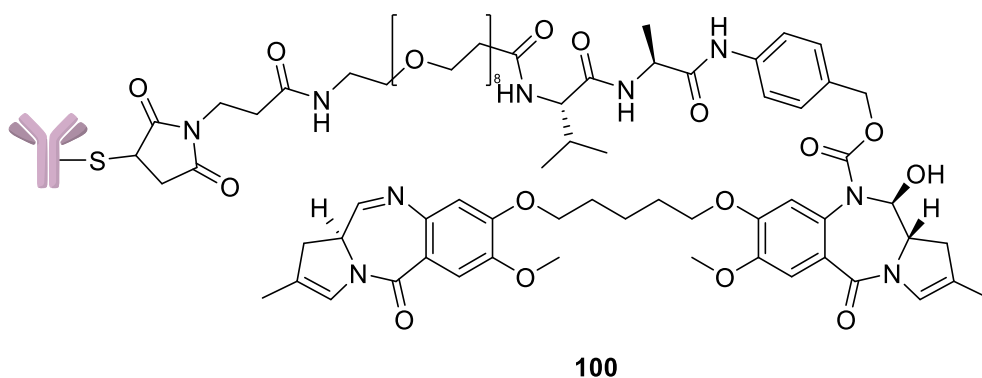


Figure 2.21: Structure of Rovalpituzumab tesirine, **100**

2.3.9. Sacituzumab Govitecan

Sacituzumab Govitecan targets Trop2 using a humanised anti-Trop2 antibody, hRS7 and is conjugated to an active metabolite of irinotecan, SN-38. Trop2 is a glycoprotein that is overexpressed in many cancers and has differential expression in some normal tissues.¹⁴⁴

Irinotecan is a marketed drug for colon and small cell lung cancer and is a prodrug of SN-38. It works as a topoisomerase I inhibitor, which leads to synthetic lethality. Synthetic lethality occurs when two or more genes form a combination of deficiencies that leads to cell death.¹⁴⁵

101 incorporates an acid labile carbonate as its payload release, which can be linked to the payload with a PEG linker for solubility and an imidazole.

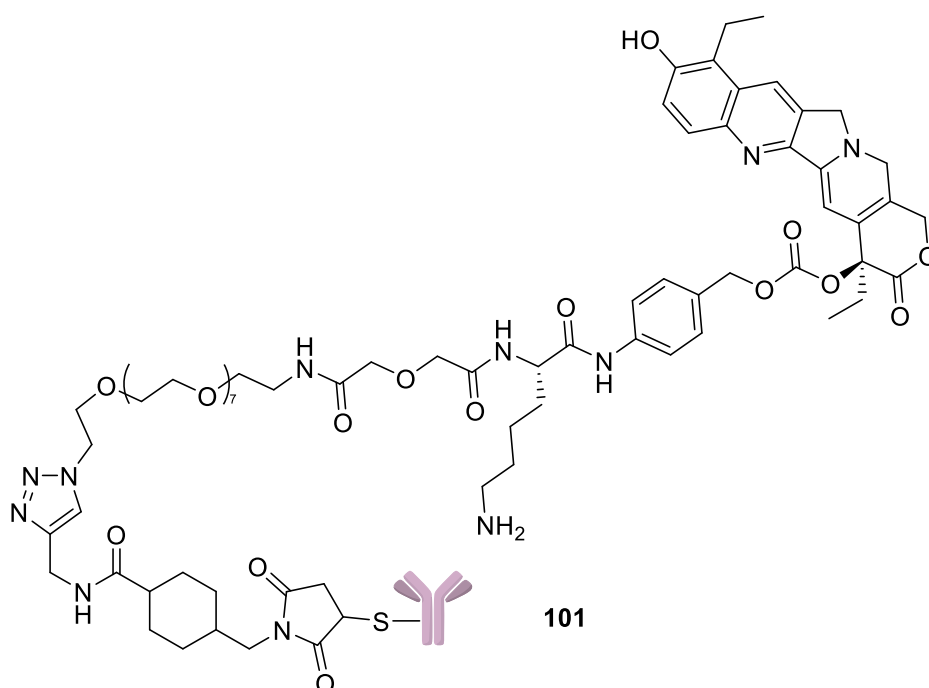


Figure 2.22: Structure of Sacituzumab Govitecan, 101

A phase 1/2 single group, multicentre trial for refractory metastatic triple-negative breast cancer has been completed for Sacituzumab govitecan.¹⁴⁶ Patients had been heavily pretreated, with a median of 3 previous therapies received. The response rate in this trial was 33%, with a clinical benefit rate of 45%. Four deaths did occur during treatment and the most common adverse side effect was myelotoxic effects. Even so, it has demonstrated a durable objective response in patients who have been heavily pretreated before, giving these patients more chance of survival. Sacituzumab govitecan had sought accelerated approval but was refused on manufacturing and control matters grounds.

Sacituzumab govitecan is currently undergoing several clinical trials for metastatic solid tumours (NCT03964727) and breast cancer brain metastasis (NCT03995706) amongst others.

2.4.9. Multi-drug resistance proteins

The increase in multi drug resistance (MDR) proteins as a resistance mechanism can cause problems for payloads. For example, many of the payloads like calicheamicin, aurastatins and maytansines are well-known substrates for the efflux transporter P-gp, which actively pumps the drug out of the cell. This overexpression of efflux transporters can lead to MDR cancers. Mylotarg for example, is less effective in AML patients with high expression of MDR.

MDR1 can efflux hydrophobic compounds more efficiently than hydrophilic ones and so using hydrophilic linkers such as *N*-hydroxysuccinimydyl-4-(2-pyridyldithio)-2-sulfobutane (Sulfo-SPDB) **102** and mal-PEG4-*N*-hydroxysuccinimide **103** have been developed as seen

with Rovalpituzumab tesirine previously.¹⁴⁷ Reducing the hydrophobicity of homogenous ADCs also improves their pharmacokinetic profile. This has been seen with the DM1 payload.²⁹ Incorporation of a hydrophilic linker into the ADC led to the bypassing of MDR1 in MDR1- expressing cells in xenograft models and so efflux was mitigated. Non-cleavable linkers are also more effective against MDR1 as payloads released from the linker are more sensitive to MDR1-expressing cells.¹⁴⁸ One reason is due to the charged nature of the residue amino acid of the antibody which can reduce efflux and cell permeability.

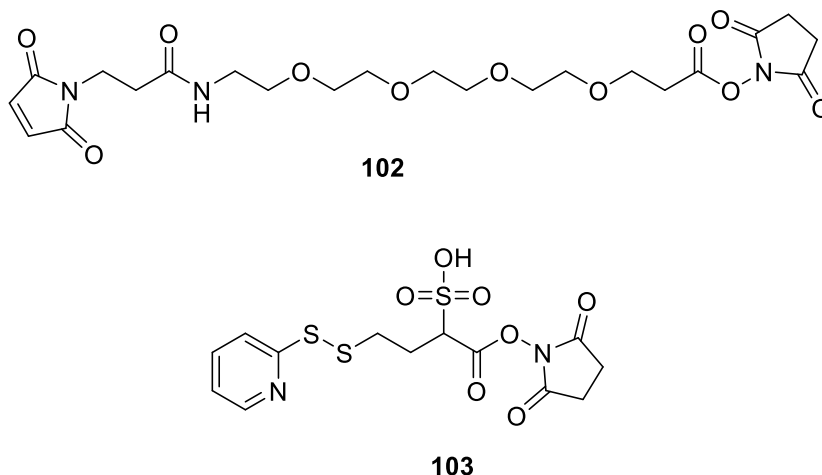


Figure 2.23: Structures of Sulfo-SPDB, **50**, and mal-PEG4-N-hydroxysuccinimide, **51**

2.5.9. Biparatopic antibodies

There has been interest in bivalent biparatopic antibodies which consist of two different binding sites that can crosslink one antigen to another on the same arm of the antibody. There has been development of an antibody MEDI4276, with two distinct non-overlapping epitopes of HER2, the same targets as trastuzumab and pertuzumab, and induces receptor clustering on the tumour cell surface. When conjugated with **58**, a tubulysin derivative developed by AstraZeneca and Medimmune, the ADC showed superior antitumour activity compared to ado-trastuzumab emtansine. This crosslinking of HER2 to form these receptor clusters has been indicated in increasing internalisation rates and lysosomal degradation allowing for more efficient release of the payload.¹⁴⁹ It is currently undergoing a Phase I/II study with in adults with select HER2-expressing advanced solid tumours (NCT02576548).

Much focus recently has been on the development and manufacturing of the antibodies, which has improved dramatically in the last couple of decades due to better technologies being developed. This allows for better stability and reduced clearance, which were issues with earlier generations of ADCs. Allowing for conjugations without compromising stability

through different conjugation methods means more uniform DARs can be generated resulting in an increase in plasma stability, decreasing systemic release of the payload. This has also allowed for an increase in DARs and more recent ADCs have been developed with a greater number of payloads per antibody.

Linker technology has also improved from the first-generation ADCs with more plasma stable linkers. Hydrophilic linkers have been developed, opening up more options for payloads as previous hydrophobic payloads can now be considered with a higher DAR.

Despite most payloads used in ADC development being tubulin binders, more ADCs are now using different payloads. One of the biggest issues with payloads is their complexity, which means analogues can be difficult to synthesise, leading to high costs. It might be possible to use structurally simpler molecules as payloads with different mechanism of action to payloads commonly used. Kadcyla costs around \$90,000 per treatment. More than half of that is for the cost of the antibody, but some of the cost is made up from the payload.⁴⁰

Chapter 3: Aims and objectives

The aim of this project is to evaluate the use of small molecule cytotoxic compounds to be used as a payload incorporated into an ADC while maintaining potency in cancer cells. Proof of concept of ADCs is already well known in the literature, with many ADCs in clinical trials and in development focusing on synthetically challenging molecules such as natural products and the use of the same class of compounds, which could lead to resistance issues due to the same single mechanism of action being exploited. Accessing small molecules in the use of ADCs and retaining potency would allow a greater range of compounds to be considered in the use of ADCs but this has not been reported so far.

The first step in achieving this aim is to identify which small molecules would be suitable to be used as a payload for an ADC. This would be achieved by analysing the NCI database of known compounds to identify synthetically viable cytotoxic agents which would have suitable potencies across a range of different cell backgrounds to have confidence in general cytotoxicity. A variety of different compounds will be identified to allow for flexibility and choice. This was done prior to the project starting by Mike Waring and Alfred Rabow, which is described in more detail in the next chapter.

Once a suitable number of compounds have been selected, work will be done to synthesis several of these compounds and also any related analogues which might be required to help tune potency/pharmacokinetic profile or to be modified for a handle to allow for conjugation with an antibody. Initial work will focus on a couple of the selected compounds to allow time for the final molecules to be synthesised. They will be prioritised based on their literature precedence (well established SARs) and ease of synthesis.

A linker would be required to conjugate the warhead to the antibody. Picking the right linker would be key in helping with the right properties required for an ADC. The linker will be chosen based on its robustness and its proof of concept in ADCs based on literature examples. Synthesis of the linker would be done in parallel with the target molecules.

Once the target molecules are synthesised, they will need to be tested to validate their potencies. They will be tested in cell cytotoxicity assays to evaluate this. The warheads will then need to be coupled to the desired linkers before being conjugated to the antibody. Mass spec will be used to evaluate the conjugation method before the ADCs will then be tested in cell assays to assess their potencies.

Chapter 4: Identifying suitable cytotoxic warheads

4.1. Current problems with cytotoxic warheads

ADCs developed so far have focused on using natural product cytotoxic payloads. The complexity of the payloads has contributed to the growing cost of developing an ADC due to the challenging and demanding synthesis or extraction and isolation of the drug and has also limited the scope for their optimisation. The cost of goods for both Kadcyra and Adcetris is expensive (around \$100,000 for both) and so reducing the amount associated with the payload would be beneficial in lowering the price of treatment.¹²³ It would be advantageous to develop payloads with greater simplicity and easier synthesis, as it would allow the synthesis of different analogues more easily and make optimisation of the linkers easier.

Another issue with current payloads used in the development of ADCs is their overlap in biological mechanisms and consist mostly of the antimetabolic aurastatins and maytansinoids. This is true for the ADCs on the market as well as many in clinical trials, for example, the warhead ozogamicin is used in 2 of the 5 currently approved ADCs with the other 3 using antimetabolic agents. Payloads with different modes of action would potentially circumvent resistance issues.

4.2. Screening the NCI database

Identification of suitable payloads requires the selection of compounds with potent anticancer activity across a wide range of cell lines. An analysis of the NCI database was carried out by Professor Mike Waring and Dr. Alfred Rabow (unpublished results) to assess suitable warheads which could be used. The panel consists of >33,000 compounds screened against a panel of 60 cancer cell lines called the NCI-60 with some extended cell lines that can be used as well. They are an array of different cancers including leukaemia, melanoma and cancers of the lung, colon, brain, ovary. The main concept was to identify compounds with broad activity across the board so were not just having activity on similar types of cell lines as well as having suitable potencies. It was also important to select compounds which had differing profiles as this would help minimise selecting warheads with similar modes of action.

The compounds were characterised within a 2D, self-organising matrix based on their differing activity profiles across the panel.¹⁵⁰ Therefore, compounds that are in different positions within the loci, should have different modes of action, as they affect different cell lines. From the 33,000 compounds, only those with a pGI₅₀ ≥ 9 in at least 16 cell lines were selected. 16 cell lines was considered enough for determining the broad activity of the compounds. This resulted in a set of 165 compounds, which can be visualised within the

matrix (Figure 4.1). 7 compounds were then identified as possible ADC payloads based on structural simplicity and position in the matrix.

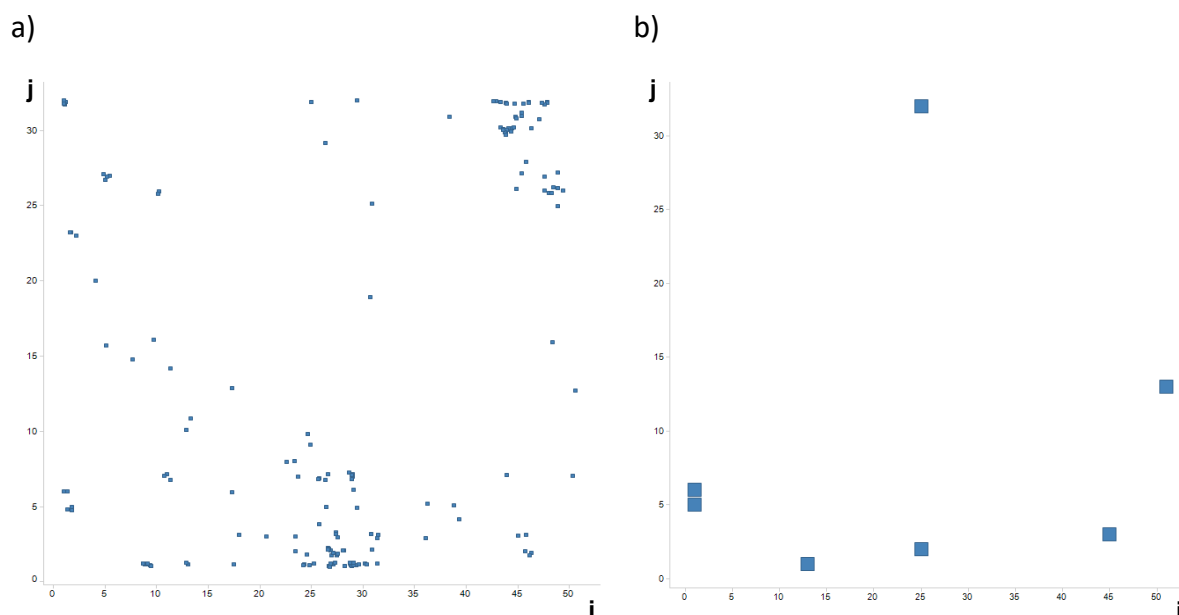


Figure 4.1 a) Location of drugs showing pGI50 values of >9 against at least 16 cell lines within the 2-dimensional matrix, designated by arbitrary coordinates (i,j) b) Location of the selected 7 compounds within the matrix.

From the map, the seven selected compounds are well spaced around the matrix, giving confidence that those selected have different modes of action. The localisation of the tubulin binders was apparent with taxanes NSC664404 and NSC759850 found at locus coordinates of 44,31 and the Vinca alkaloid found at 46,31. This area of the matrix was avoided as tubulin binders are already prominent in ADCs with similar modes of action and so omitting these could lead to more novel structures for ADCs. Interestingly, one of the selected compounds, a quinolone, is also a tubulin binder but is shifted from the other tubulin binders, indicating that they may have different pharmacology to traditional tubulin targeting agents.¹⁵¹

4.3. Selected cytotoxic drugs

4.1.3. Overview of selected warheads

The selected warheads shown in Figure 4.2, may not possess desirable properties for small drug molecules, such as nitro groups and acridines associated with toxicity, boronic acids and metal chelators. However, for ADCs, these functionalities would be of little issue due to the targeted nature. These compounds are structurally simple compared to the payloads seen in the marketed ADCs and those in development.

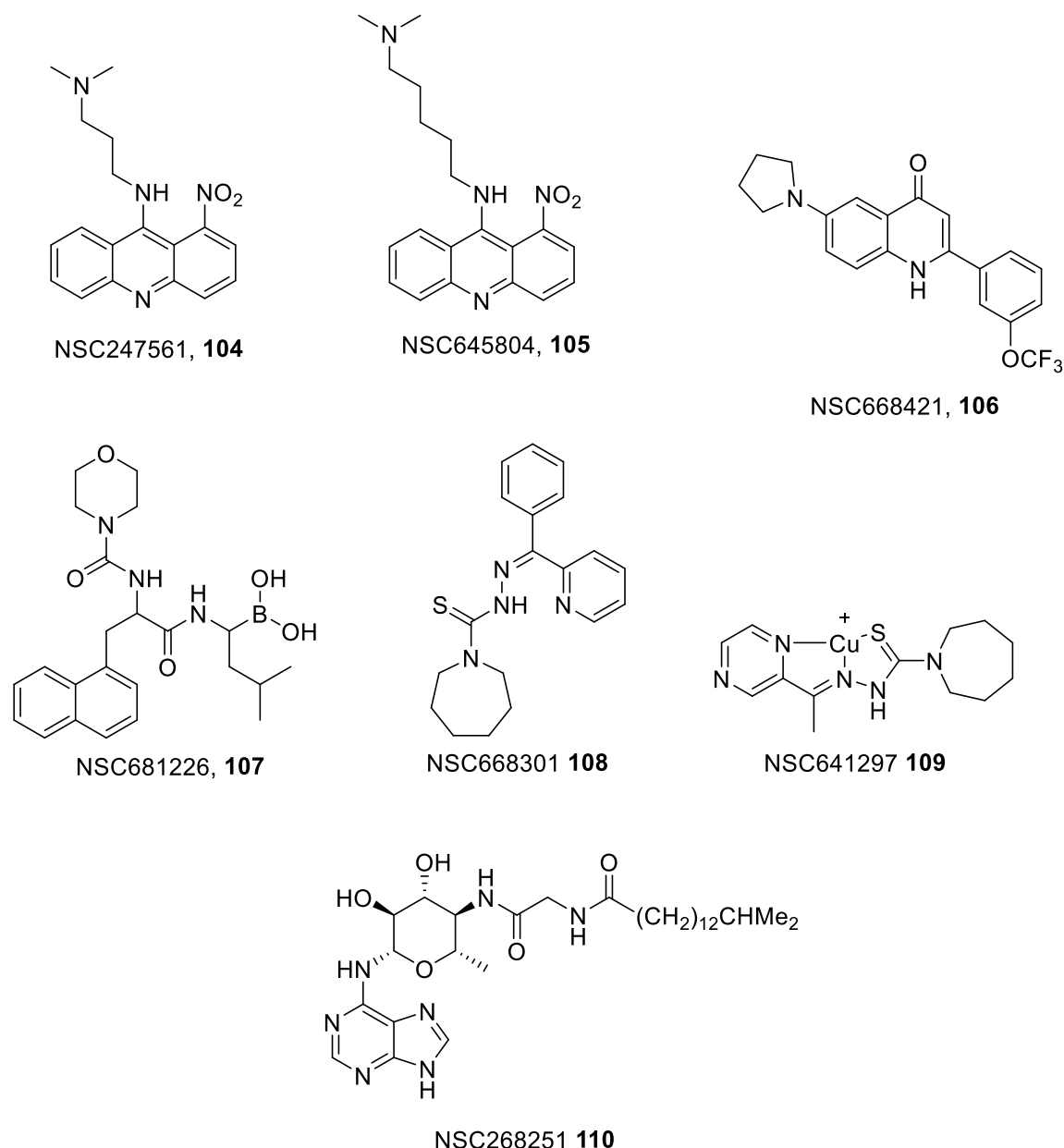


Figure 4.2: The seven selected compounds from analysis of the NCI database

4.2.3. Nitroacridines

Nitracrine, also known as Ledakrin **104** is an antineoplastic drug, which entered into clinical testing but was subsequently stopped due to side effects such as severe nausea and vomiting.¹⁵² It is a member of the 1-nitroacridine family and its modes of action are complex, and are yet to be fully elucidated, but they are known to have cytostatic and antitumour activity and inhibit macromolecular biosynthesis. They can also intercalate with DNA forming DNA-adducts binding covalently with complimentary base pairs and DNA interstrand crosslinks leading to inhibition of RNA synthesis and can induce the unwinding of supercoiled DNA.^{153, 154} Varying the alkyl length chain can have a subtle impact on its activity. Increasing the chain length by 2 carbon atoms can lead to significant differences in

the cell profile, with a shift in their location in the map, from 45,3 to 13,1. Figure 4.3 highlights this as there are differences in activity on the same cell lines but they both demonstrated broad activity across panel. Both compounds exhibited good activity across half the cell lines indicating good cell cytotoxicity with pGI₅₀ values of 9 for **104** and 8.8 for **105** (Table 4.1).

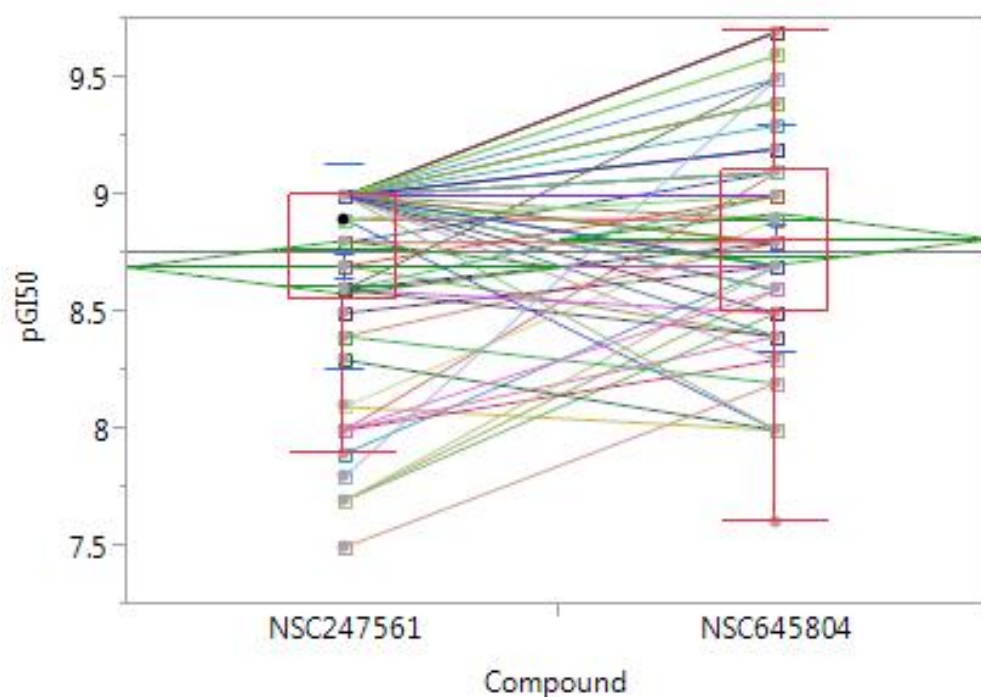


Figure 4.3: Comparison of pGI₅₀ values across the cell lines for the two compounds **104** and **105**, lines connect the same cell line showing differentiated activity between the 2 compounds.

Nitroacridines contain a nitro group, which is not a common functional group in small molecule drugs but is essential for activity in this compound. Under bioreduction, the nitro group is reduced to the highly reactive nitrosoarene and hydroxylamine.¹⁵⁵ Nitracine was found to have selectivity towards hypoxic cells in Chinese hamster ovary cells and is proposed to have an inherent selectivity towards hypoxia cells due to its activation through bioreduction which would occur more rapidly in a hypoxic environment.¹⁵⁶

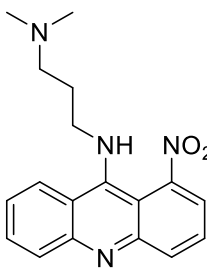
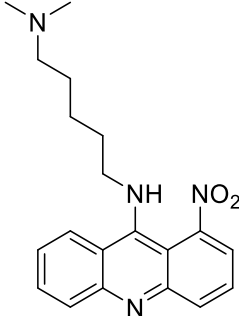
NSC number	NSC247561	NSC645804
Structure		
Locus (I,J)	45,3	13,1
pGIval16	9.0	9.1
pGIval32	9.0	8.8
pGIval64	7.8	8.0

Table 4.1: GI₅₀ values for the two nitroacridines and their position within the matrix. pGIval is defined as the average pGI₅₀ across their most potent cell lines over a set number of cells.

It has been shown through published SARs that the desmethyl analogue of Nitracrine is still active and replacement of a methyl group would allow a site for attachment of a cleavable or non-cleavable linker with confidence that potency could be retained.¹⁵⁶

The two initial targets selected were a desmethyl analogue of nitracrine, **113** and a methylamine derivative, **112** which is the most potent out of the group. SARs data shows that both are active with IC₅₀s of 34 and 3.8 nM respectively (Table 4.2).¹⁵⁷ A methyl group is required for potency as the aniline **111** has significantly less potency compared to the methylated analogue **112**.

Compound number	R	Growth inhibition
		IC ₅₀ , nM
105	(CH ₂) ₃ NMe ₂	26.3 ± 26.3
106	(CH ₂) ₅ NMe ₂	15.5 ± 1.0
111	H	3600 ± 1000
112	CH ₃	3.8
113	(CH ₂) ₃ NHMe	34 ± 7

Table 4.2: SAR data around substituted ring. Using Chinese hamster ovary cell line AA8.

Examples of using the amine as an attachment site for a cleavable or non-cleavable linker are shown in Figure 4.4. For **114**, the use of a carbamate would allow the payload to be released as the free amine. However, compound **115** would need to retain its potency as an amide with the linker still attached and therefore would need to be tested to evaluate its use as a payload. Other payloads have retained potency in this way such as the maytansinoids but it is not known if this would be the case for smaller molecules and so would need to be evaluated.

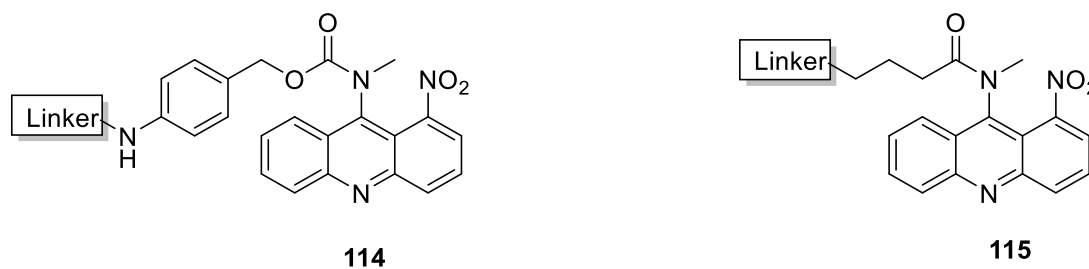


Figure 4.4: Structures of nitroacridines with sites for linker attachment for cleavable and non-cleavable linkers.

4.3.3. Quinolones

2-Phenyl-4-quinolones are thought to interact with tubulin at the colchicine site and inhibit tubulin polymerisation.¹⁵⁸ As tubulin binders, they would appear to be similar to previously reported ADCs such as the aurastatins and maytansinoids. Many of the tubulin binders are complex natural products, in contrast quinolones are relatively simple in their structures. They are shifted considerably in their location in the matrix compared to other tubulin binders (25,2 compared to 46,31) suggesting they may have a different mode of action and a different resistance profile.

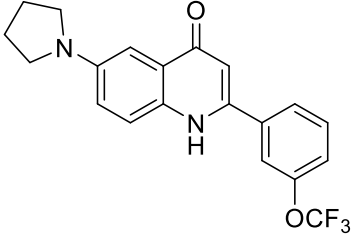
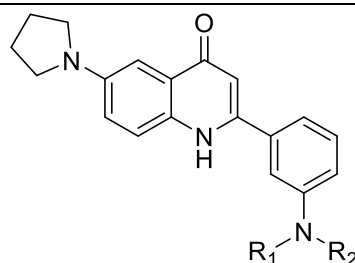
NSC compound	NSC668421
Structure	
Locus (I,J)	25,2
pGIval16	9.9
pGIval32	9.5
pGIval64	6.0

Table 4.3: GI₅₀ values for the quinolone and its position within the matrix

For quinolone **106**, inhibition of tubulin polymerisation was found to be $0.72 \pm 0.2 \mu\text{M}$. Out of the 7 selected compounds, it had the highest pGI_{50} across 16 and 32 cell lines but its activity against 64 cell lines was diminished in comparison to other compounds (Table 4.3). The pyrrolidine substituent appears to be important for potency. However, changes at the 3'-position seem to be well tolerated and alkylated aniline substituents have been synthesised and tested showed excellent potencies in several cell lines (Table 4.4) with weak inhibition of the normal cell line Detroit 551.¹⁵⁹ The disconnect between the IC_{50} values coupled with the different position in the loci to other tubulin binders questions their use as tubulin inhibitors despite inhibition of tubulin polymerisation reported in the literature.¹⁶⁰ Further validation of the mechanism of action of the quinolones may be required but it is clear that they are cytotoxic and could be of use as a payload in the development of ADCs.



Compound	R ¹	R ²	IC ₅₀ (μM)			
			HL-60	HEP3B	H460	Detroit 551
116	H	CH ₃	0.006	0.021	0.035	>10
117	H	CH ₂ CH ₃	0.005	0.020	0.020	>10
118	CH ₃	CH ₃	0.005	0.015	0.013	>1

Table 4.4: IC_{50} values from *in vitro* cytotoxicity testing of amine alkylated quinolone analogues. Cell lines include human promyelocytic leukaemia (HL-60), human hepatoma (Hep3B), human lung cancer (H460), and embryonic skin fibroblast cell line (Detroit 551).

The aniline would be an ideal site for attachment of a linker with confidence that potency could be retained. Another option for an attachment site would be the amine in the quinolone system, which would allow for various analogues on the pendant phenyl ring to be used (Figure 4.5). It is not known if attachment here with a non-cleavable linker would reduce potency, it would need to be established.

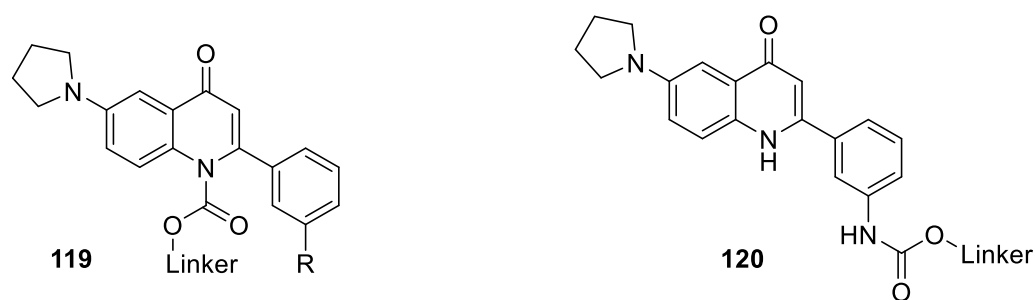


Figure 4.5: Structures of proposed quinolones with attachment sites for linkers, one through the quinolone amine and another through an aniline substituent on the pendant phenyl ring.

4.4.3. Thiosemicarbazones

Thiosemicarbazones are metal chelators and are known to sequester iron and other metals. They were originally developed for the treatment of iron overload diseases such as β -thalassemia major and are known to have broad medicinal properties, having been implicated as antimalarial and anti-HIV agents.^{161, 162} They were also identified to have anti-tumour activity.¹⁶³ This is because they can inhibit Fe-containing enzymes such as ribonucleotide reductase by sequestering the iron, inactivating the enzyme. This enzyme is required to catalyse the rate-limiting step of DNA synthesis and can also interfere with molecules involved in cell cycle control, like cyclin D1 and p21, which can cause cell death. Tumour cells also express higher levels of transferrin receptor 1 which allows the cell to uptake Fe from the serum and so sequestering iron can help stop proliferation, inhibiting tumour growth.¹⁶⁴

Activity of thiosemicarbazones is also dependant on redox-cycling of their Fe complexes. In the reduced form of Fe^{II} , the complex can react with molecular oxygen. This can lead to the generation of reactive oxygen species, which can damage essential biomolecules such as DNA and enzymes within cells, leading to apoptosis.¹⁶³ They are also known to show activity in cells resistant to current chemotherapy agents making them attractive targets.¹⁶⁵ This class of compound are quite lipophilic which may cause an issue with stability if used as part of an ADC. This would need to be tested.

As well as chelation to iron, they have also been shown to chelate with copper and the resulting complexes have also shown antiproliferative effects. The copper complexes can react with molecular oxygen and redox active species to induce a redox-cycle between mono and divalent oxidation states of the complex. It is suggested that the formation of both metal complexes is critical to cytotoxicity compared to the uncomplexed thiosemicarbazone.¹⁶⁶

It is unlikely that sequestering Iron and Copper alone would lead to an anticancer effect but when thiosemicarbazones have already been complexed before treatment with cancer cells,

they are more active than their uncomplexed counter-parts in inhibition of DNA synthesis and cell destruction. *Adv. Enzyme Regul.*,1977, 15 117.

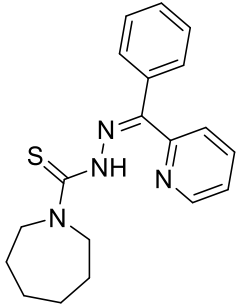
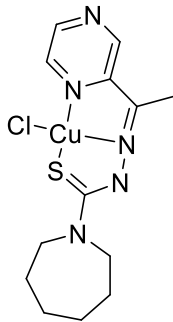
NSC number	NSC668301	NSC641297
Structure		
Locus (I,J)	1,6	1,5
pGIval16	9.0	9.0
pGIval32	7.7	8.6
pGIval64	5.8	6.9

Table 4.5: GI₅₀ values for the two thiosemicarbazones and their position within the matrix

Both copper salts and free thiosemicarbazones have been shown to be active. From the NCI database, the copper complex **109** (Figure 4.2) is more active against a broader range of cells as indicated by the increased pGI₅₀ values in 32 and 64 cell lines compared to the free ligand **110** (Table 4.5). The key pharmacophore is the inclusion of the pyridyl ring with the thiosemicarbazone to allow coordination with the metal. The thiosemicarbazones and their metal complexes are localised together in the matrix with similar coordinates, indicating similar cell profile and pharmacology.

SARs have shown that changes to the amine group are well tolerated and potency can be retained.¹⁶⁷ The phenyl ring can also be removed but does impact potency. Therefore, attachment for the linker will be initially attempted on an amine as seen in **121** (Figure 4.6). The primary amine **122** shows micromolar potency (4.66 μM in SK-N-MC Neuroepithelioma cells) and therefore would not be an ideal choice for a warhead but alkylation of the amine would be possible and methylated analogues have given good potencies.¹⁶⁷

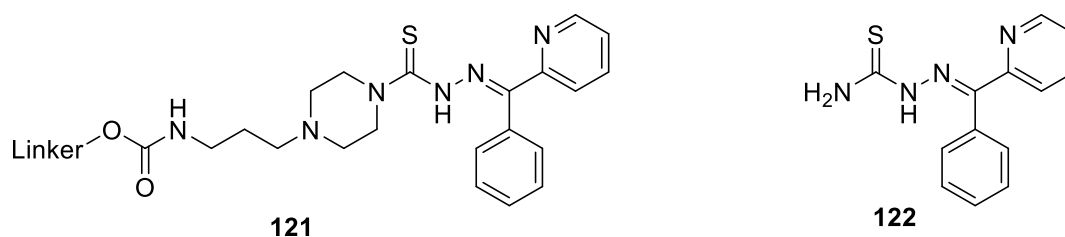


Figure 4.6: Proposed attachment site for linker with thiosemicarbazone and structure of thiosemicarbazone 19.

Analysis of the NCI database has identified 7 suitable warheads which are structurally simple and less complex than those used in for the development of ADCs. These compounds showed broad activity over multiple cell lines giving confidence of general cytotoxicity and were well dispersed in the matrix, suggesting each class of compounds had different modes of action with differing pharmacology. This would help minimise resistance issues in the future, with some of the targets identified having activity in chemotherapy resistant cell lines. Due to the structural simplicity, linker optimisation should be easier as different analogues could be generated more easily.

Out of the 7 compounds, 3 were chosen to be initially explored, the nitroacridines, quinolones and thiosemicarbazones with each having different modes of action to each other. SARs of these compounds showed tolerability around certain groups, giving confidence that analogues with attachment points could be synthesised and retaining potency, allowing for the attachment of linkers.

Chapter 5: Nitroacridine series

5.1. Resynthesis plan for nitroacridines



Figure 5.1: Structure of nitroacridine warheads selected for synthesis, *N*-methyl-1-nitroacridin-9-amine, **113** and *N*¹-methyl-*N*³-(1-nitroacridin-9-yl)propane-1,3-diamine, **114**

The first selected series to be synthesised were the nitroacridines. *N*-methyl-1-nitroacridin-9-amine, **112** and *N*¹-methyl-*N*³-(1-nitroacridin-9-yl)propane-1,3-diamine, **113** (Figure 5.1), were chosen as analogues of the original NCI hits due to their good potencies (3.8 and 34 nM respectively in CHO cell lines) and could be made in 3 or 4 steps. These analogues possess a secondary amine a handle to allow the attachment of a linker group.

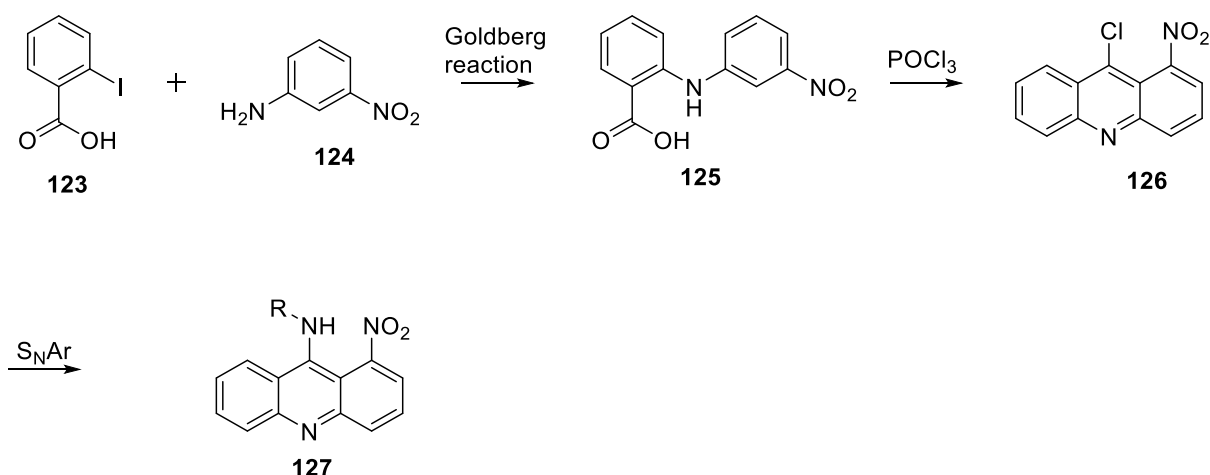


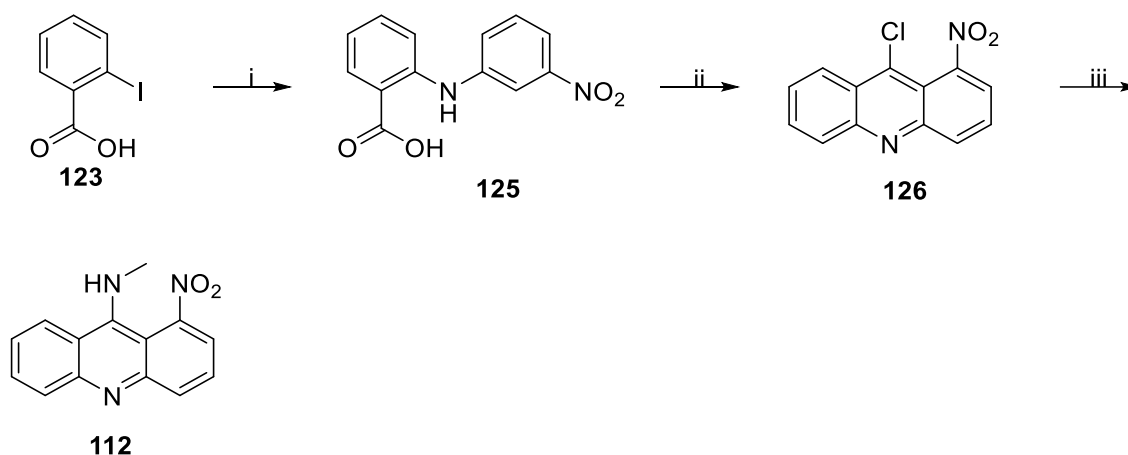
Figure 5.2: Synthetic strategy towards the amino nitroacridines

The synthesis of the nitroacridines was adapted from the synthetic route reported by Denny *et al.*, (Figure 5.2)¹⁵⁶. The first step synthesising *N*-phenylanthranilic acid, **125** was not reported in the original papers but there was literature precedent for this step, and involved the Goldberg reaction, a variant of the Ullmann condensation reaction. This involves the use of a copper catalyst and base under heating at high temperatures to couple an aryl amine with a halogen, normally an iodo group. This is then followed by a cyclisation with POCl₃, forming an acid chloride *in situ* then ring closing with an electrophilic aromatic substitution and

aromatisation of the ring. and subsequent chlorination and finally a S_NAr reaction with an amine.

5.1.1. Synthesis optimisation of 2-((3-nitrophenyl)amino)benzoic acid **125**

The optimised route for the synthesis of **112** is shown in Scheme 5.1. The first step was a coupling reaction between 2-iodobenzoic acid and 3-nitroaniline with a copper catalyst.



Scheme 5.1: Route for the synthesis of *N*-methyl-1-nitroacridin-9-amine, **112**. *Reagents and Conditions*: i) 3-nitroaniline, CuI, Na₂CO₃, DMF, reflux, 69%; ii) POCl₃, 140 °C, 42%; iii) 2M methylamine in THF, Et₃N, THF, reflux, 54%.

A starting point was an environmentally friendly method reported in the literature for the conversion of 2-iodobenzoic acid, **123** to *N*-phenylanthranilic acids and could be done in water under reflux using copper (II) acetate with NaOAc as the base.¹⁶⁸ This would be beneficial in a scale up as a cheap and green solvent would help reduce costs. The reaction was very poorly yielding at 10%, less than stated in the paper, 19%. Initially these reactions were carried out in the microwave at 120 °C but it was found that conventional heating improved yields. There were two postulated issues, the aqueous solubility of the starting materials and the unreactive nature of the nitroaniline. The dependence of reactivity of the aniline was demonstrated in the paper. where electron donating substituents gave far higher yields and using aniline itself gave 95% yield. The reaction proceeded slowly and would be left for 24 hours, with full conversion not seen and leaving the reaction longer did not increase the conversion. Extra addition of catalyst did lead to increased conversion either.

3-nitroaniline, **124** has poor aqueous solubility which impacted its reactivity as the compound was not in solution. In an attempt to address the solubility issue, different solvents were tested (Table 5.1). DMF was first tried as this method has been reported by Nishihama *et al.* in the total synthesis of megistophyllin I using electron rich anilines but using the electron poor 3-

nitroaniline gave a 15% yield¹⁶⁹, suggesting solubility might not be playing a vital role. Acetonitrile was also tried and improved the yield to 23%.

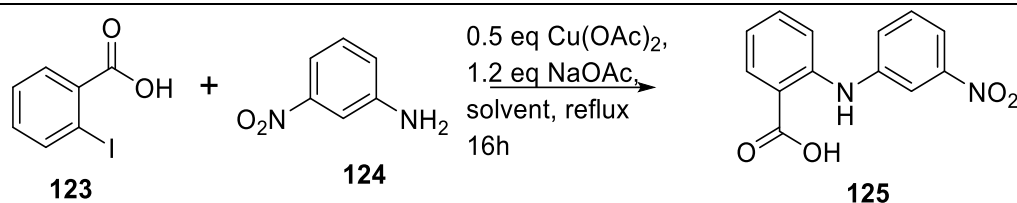
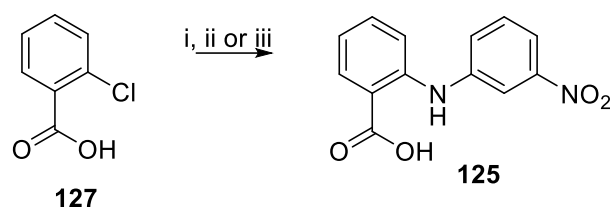
	
Solvent	Yield, %
H ₂ O	10
DMF	15
MeCN	23
H ₂ O:EtOH, 50:50	20
H ₂ O:THF, 50:50	33
H ₂ O:MeCN, 50:50	60
H ₂ O:MeCN 66:33	34

Table 5.1: Different solvent systems used for Ullmann condensation. All reactions done on the same scale using 100 mg, 0.4 mmol of **123**.

The use of acetonitrile and DMF did improve the solubility of 3-nitroaniline but decreased the solubility of copper acetate. A mixture of water miscible organic solvents along with water were trialled in order to maximise the solubility of the reagents, starting with 50:50 mixtures of each solvent. The yields did increase with the mixtures going from 10% in water up to 33% with water and THF. Water and acetonitrile improved the yield significantly to 60% but adjusting the ratio of water and acetonitrile decreased the yield. This reaction did have reproducibility issues with yields ranging from 30-60%.

After 2-iodobenzoic acid had been fully consumed, the mixture was acidified with 6 M HCl to a pH of 2. This caused the product to precipitate, while 3-nitroaniline would stay in solution. After filtration, it was found that the product needed purification to remove copper containing impurities. For small scale, purification by flash column chromatography proved effective but for larger scales this was difficult as the product streaked, eluting with impurities. Activated charcoal was added to a solution of the crude product and filtered to help remove the copper impurities. This was partially successful, but some impurities remained. It was also passed through an ISOLUTE® Si-Thiol metal scavenger and was successful but was not feasible as scale up.



Scheme 5.2: Synthesis of 2-((3-nitrophenyl)amino)benzoic acid, **125**. *Reagents and Conditions:* i) 3-nitroaniline, KOH, DMF, reflux, 16h, no product observed; ii) 3-nitroaniline, K₂CO₃, Cu, IPA, reflux, 16h, no product observed; iii) 3-nitroaniline, K₂CO₃, Cu, Cu₂O, diglyme, reflux, 16h, 34%.

Low yields and slow reaction times led to additional methods being explored for the synthesis of **125**. Scheme 5.2 shows multiple conditions reported in the literature for this conversion. Reaction of 2-chlorobenzoic acid with 3-nitroaniline in the presence of potassium hydroxide in DMF was carried out. Reported yields were 39% but no reaction occurred in our hands.¹⁷⁰ Other groups have reported success with the addition of copper powder and copper (II) oxide. This method gave low yields in comparison (34%).¹⁷¹ Goldberg's original paper also included the synthesis of **125** using just Cu powder but attempts to replicate this failed.¹⁷²

It was later found that switching the catalyst to copper iodide and sodium carbonate as the base improved yields. A low catalyst loading of 3% was sufficient to give a 38% yield but increasing the loading to 0.5 equivalents was optimum along with using 1 equivalent of base gave a significantly improved yield of 69% and shortened the reaction time. The yield was more robust and reproducible than the previous method. These conditions are commonly used in Goldberg reactions but were not reported for this conversion.¹⁷³

Carrying through the copper impurities after this step was found to not have an impact on the cyclisation reaction and so overall yields were improved as the cyclised compound was more easily separated from these impurities. Optimisation of this step was successful, starting with a yield of 10% and significantly being improved to 69%.

5.2.1. Synthesis of 9-chloro-1-nitroacridine, **126**

Compound **125** could be then cyclised and chlorinated in the same step using an excess of POCl₃, acting as the solvent at 140 °C. The reaction proceeds firstly *via* an acid chloride, which is cyclised under an electrophilic aromatic substitution. Once the acridone is formed, the ketone is converted to a chloro group and aromatisation of the system drives the reaction to completion.

Due to free rotation around the amine bonds during the initial cyclisation operation, a mixture of regioisomers were formed as the nitro group could lie in either the 1 or 3 position. Denny

had reported a mixture of 75% 1-nitro and 25% 3-nitro but upon reaction, a roughly 1:1 mixture was consistently observed.

Separation of these regioisomers was difficult as their R_f in many solvent systems were identical. Various solvent systems in normal phase conditions were tried but failed to separate the isomers. From LC-MS analysis, there was splitting between the peaks with some overlap and suggested it might be possible to separate the isomers under reverse phase conditions. The use of MeOH or acetonitrile with water in both acidic and basic conditions were tried but limited separation was seen and there were solubility issues with these solvents. The compound was poorly soluble in aqueous and many organic solvents, ascribed to the suggested high lattice energy and pi stacking, implied by its high melting point ($>250\text{ }^\circ\text{C}$). Ultimately the solvent system chosen was THF and H_2O . The compound had the highest solubility in THF for water miscible solvents. Initially acidic conditions were used with addition of 0.1% formic acid but due to the acid-sensitive nature of the compound, addition of 0.1% ammonia to the solvent system was used. Although separation was possible under flash column chromatography, there was overlap in the compounds eluting and so complete separation was not possible. Separation was better on smaller scales, longer gradients and bigger sized columns used. It was also found that purification of the crude with 100% DCM eluted the mixture of compounds cleanly and this improved the separation through reverse phase.

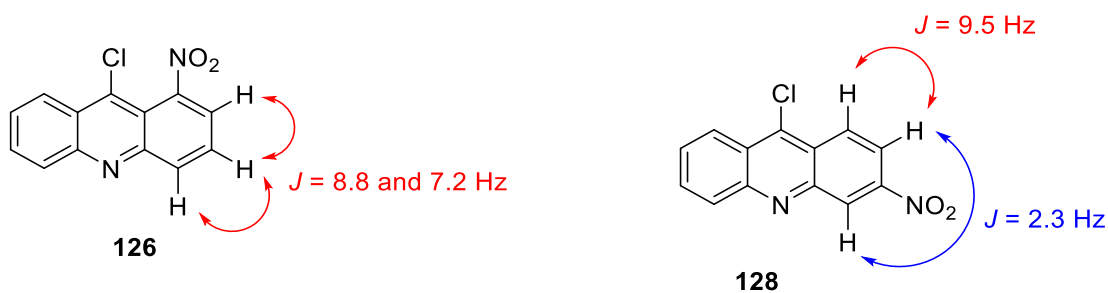
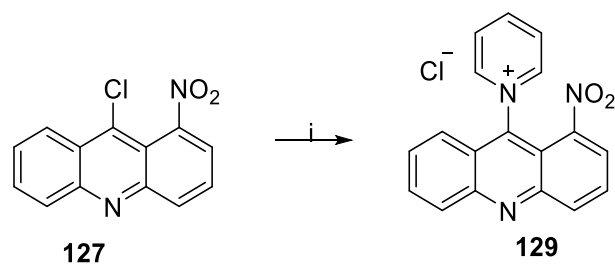


Figure 5.3: Proton-proton coupling values for the chloronitroacridine systems.

The desired isomer was confirmed through ^1H 1D and COSY NMR of both isomers. For **126**, the splitting pattern in the 3 position proton was a doublet of doublets with J values of 8.8 and 7.2 Hz, consistent with proton-proton coupling of 3 contiguous aromatic protons. For **128**, the 2-position proton was also a doublet of doublets but with J values of 9.5 and 2.3 Hz, indicating one proton was ortho and the other meta to the proton in the 2 position (Figure 5.3).



Scheme 5.3: Reported formation of pyridinium salt. *Reagents and Conditions:* i) pyridine, reflux¹⁵⁶.

For large scales, it was reported that using fractional crystallisation by forming a pyridinium complex could separate the isomers by crystallisation of the undesired isomer (Scheme 5.3).¹⁵⁶ The difference in solubility of the isomers could be exploited and so the less soluble isomer could be filtered off leaving pure product in the filtrate. The chloro group could then be reinstalled by reacting with POCl₃ or the pyridinium salt could be reacted directly with an amine but it was found that this gave lower purity products. Unfortunately, no compound crystallised out and when evaporating the solvent slowly, both isomers precipitated together. As a result, flash column chromatography was used in future to purify future compounds.

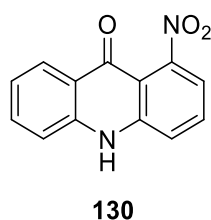


Figure 5.4: Structure of 1-nitroacridin-9-one **130**, an intermediate in the POCl₃ cyclisation reaction and is the hydrolysed product from 9-chloro-1-nitroacridine.

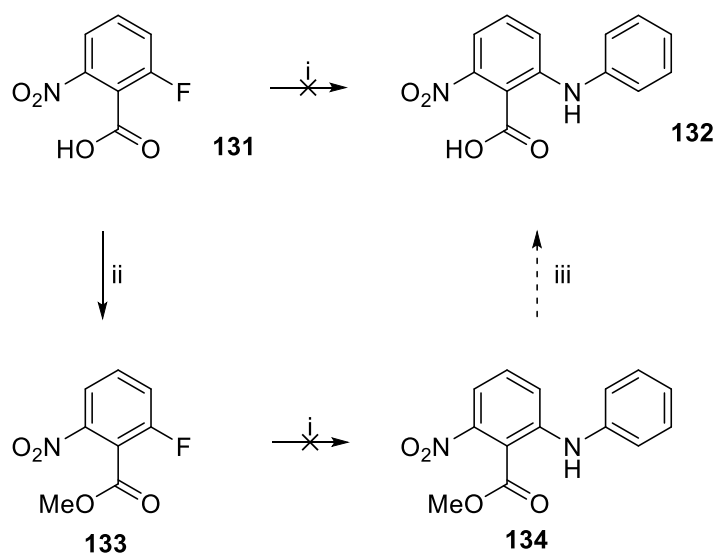
During the work-up and purification stage, a byproduct was observed with a mass of 240 which correlated with the intermediate acridone, **130** (Figure 5.1). The reaction had gone to completion and acridone was only observed after the reaction was worked up. Chloro-nitroacridines are known to undergo acid hydrolysis to form the acridone and the rate of hydrolysis depends on the substituents and the pH.¹⁷⁴ 9-chloro-nitroacridine is susceptible to hydrolysis and left in air would undergo hydrolysis over time. The work up for this reaction involved washing out the excess POCl₃ with petrol and the residue which remained was neutralised with ammonium hydroxide at 0 °C. Switching to bases such as 2M NaOH increased the amount of acridone obtained. Upon neutralisation, the extraction of the compound was carried out as soon as possible as this mitigated the hydrolysis of the acridine to the acridone. One issue with this work up is that the product was not soluble in water and so it was difficult to neutralise the entirety of the residue, therefore dissolving with DCM and

washing with the basic aqueous layer was performed. After reverse phase chromatography, the fractions were concentrated *in vacuo* immediately.

A mixture of the regioisomers was also carried through to the next step so see if addition of a more polar group might help separate the isomers more easily. This had the opposite affect with the peaks more closely overlapping by LC-MS analysis and TLC.

5.3.1. Synthesis of 2-nitro-6-(phenylamino)benzoic acid, **132**

We considered that a better solution to the regioisomer problem was to fix the nitro group onto the same phenyl ring as the carboxylic acid and ensure that cyclisation of 2-nitro-6-(phenylamino)benzoic acid **132** would lead to the desired isomer only due to both ortho positions on the pendant phenyl ring now being equivalent.

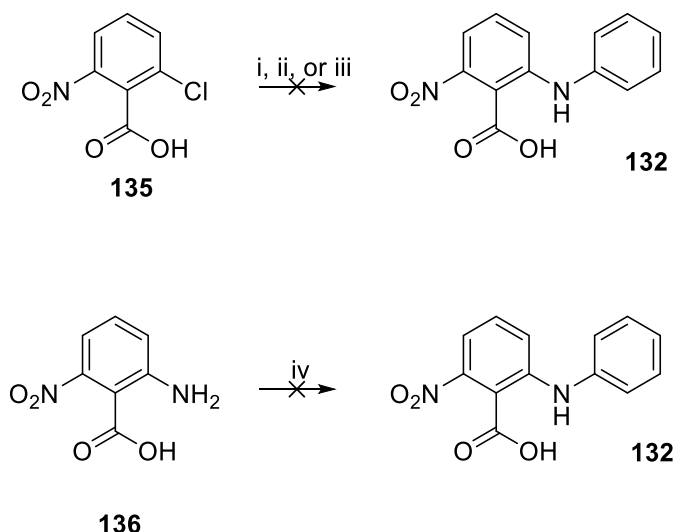


Scheme 5.4: Synthetic strategy to the synthesis of precursor **132**. *Reagents and Conditions:* i) Aniline, TFE, MW 120 °C; ii) Iodomethane, K_2CO_3 , DMF, 0 °C-RT, 78%; iii) LiOH, MeOH

One approach was using 2-fluoro-6-nitrobenzoic acid, **131** in a S_NAr reaction (Scheme 5.4), with aniline. The reaction did not work, and it was suggested a formation of zwitterion might be hindering the reactivity of the aniline. Therefore, the methyl ester, **133** was synthesised from the benzoic acid **131** using iodomethane with potassium carbonate in a good yield of 78% but the subsequent reaction with aniline gave no product. The solvent was switched from THF to TFE and also done under microwave irradiation but again no product was observed.

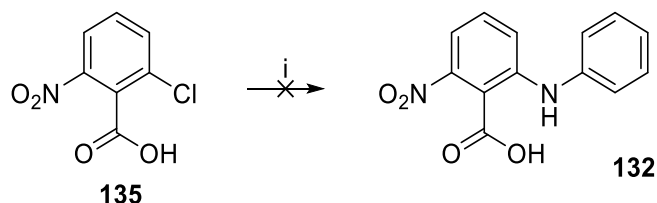
The next method attempted was the Goldberg reaction using copper iodide or copper acetate as the catalyst which had previously worked in generating compound **125** but these reactions failed to give product (Scheme 5.5). Availability of starting materials was an issue with no

iodo or bromo analogue commercially available. These would be more reactive than the chloro analogue in this reaction. Reported literature showed copper oxide with 2-chloro-6-nitrobenzoic acid, **135** could be used with aniline.¹⁷⁵ The paper did not state the exact conditions so previous conditions were used. TLC analysis of the reaction showed many spots and LC-MS analysis did not show a correct mass. In the same paper, it was suggested that switching the partners around could also work to using a nitroaminobenzoic acid, **136** with bromobenzene, but this also did not yield desired product.



Scheme 5.5: Synthetic routes to biaryl amine **132**. *Reagents and Conditions:* i) aniline, CuI, NaCO₃, DMF reflux, 6h; ii) aniline, CuOAc, NaOAc, H₂O:MeCN (1:1), reflux, 6h; iii) aniline, CuO, K₂CO₃, DMF, reflux, 6h; v) bromobenzene, CuO, K₂CO₃, DMF, reflux, 6h.

Buchwald-Hartwig cross coupling was attempted on **135** using Pd(*t*-Bu₃P)₂ as a catalyst with NaOBu^t as a base (Scheme 5.6). However, this reaction yielded no product and only starting material was observed.



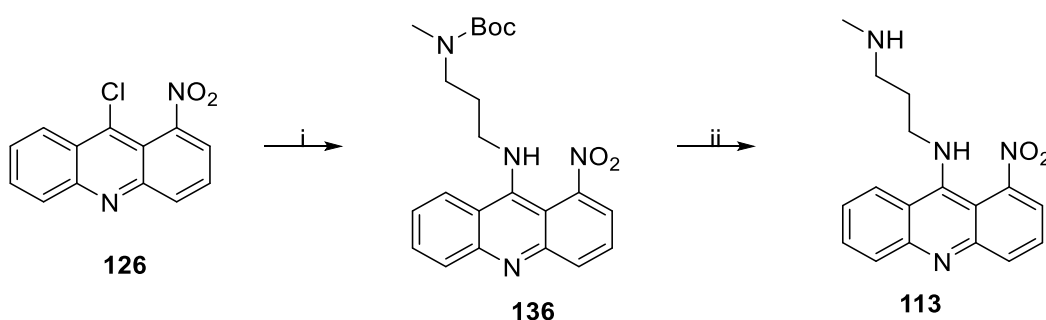
Scheme 5.6: Synthetic route to biaryl amine **132**. *Reagents and Conditions:* i) aniline, Pd(*t*-Bu₃P)₂, NaOBu^t, dioxane, reflux, 16h.

Attempts to synthesise **132** to give one regioisomer exclusively were not successful, suggesting these systems do not readily undergo coupling.

5.4.1. Synthesis of amino-nitroacridines

The original synthesis to generate N-methyl-1-nitroacridine **112** used phenol, producing a melt and reacting with the desired amine.¹⁵⁶ Phenol was not a desired solvent to use due to its associated toxicity and so the solvent was switched to THF. 2M MeNH₂ in THF was reacted with 9-chloro-1-nitroacridine under reflux in a S_NAr reaction (Scheme 5.1). The reaction did proceed but was slow and did not go to completion with only 2 equivalents of methylamine used. It was found that more equivalents were needed to push the reaction. Full conversion was not seen despite attempts to push the reaction with a maximum yield of 54% obtained. Hydrolysis was also seen in this step, which is why the reaction was stopped before all the starting material had converted.

Analogue **113** was also generated (Scheme 5.7), using *tert*-butyl (3-aminopropyl)(methyl)carbamate, **138** as the starting material. The yield for this reaction was better, giving a good yield of 84% and the reaction went to completion.

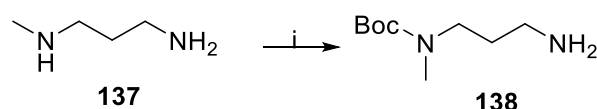


Scheme 5.7: Synthetic route for 1,3-propanediamine nitroacridine, **113** from 9-chloro-1-nitroacridine. *Reagents and Conditions*: i) *tert*-butyl (3-aminopropyl)(methyl)carbamate, Et₃N, THF, reflux, 3h, 84%; ii) 10% TFA in DCM, RT, 3h 91%.

For the deprotection of the Boc group, a non-acidic method was attempted first. TBAF refluxed in THF was tried as this is known to deprotect carbamates¹⁷⁶ but no reaction was observed. Neat TFA was attempted and although the deprotection was successful, the reaction profile was messy with multiple peaks observed on TLC. 10% TFA in DCM worked well and gave desired product only. In the work up it was crucial to neutralise the residue left after concentrating *in vacuo* quickly in order to minimise the exposure to an acid aqueous solution as it was found that left as a residue exposed to air, hydrolysis would occur. Extraction of the compound required multiple washings of the neutral aqueous layer with DCM but adding base such as sodium bicarbonate did cause the product to partition into the organic layer.

The basic nature of the compound made purification difficult, during normal phase chromatography the product would stick to the column and require flushing, giving poor separation. Switching to a NH silica column greatly improved separation and ease of purification, allowing for a yield of 91% to be obtained.

5.2. Synthesis of *N*¹-methylpropane-1,3-diamine, **138**

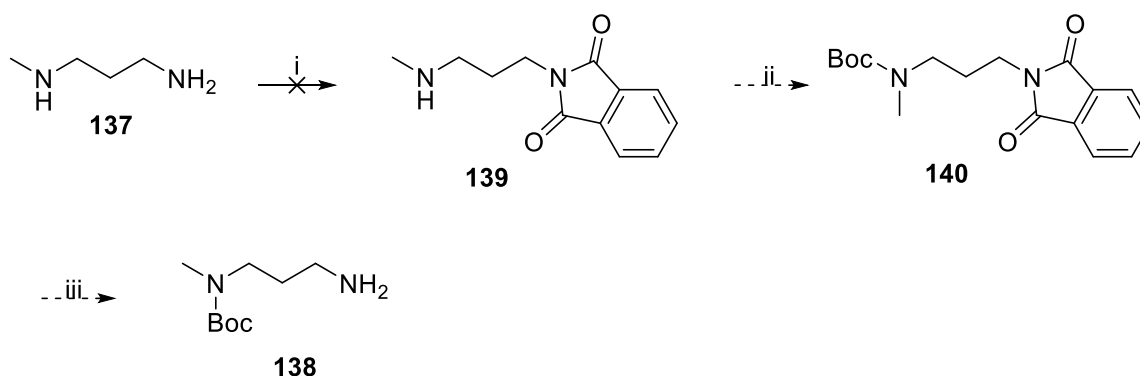


Scheme 5.8: Boc protection of *N*¹-methylpropane-1,3-diamine. *Reagents and Conditions:* i) Boc_2O , MeOH, 0 °C-RT, 2h, 33%.

One of the downsides to this analogue is the expensive starting material tert-butyl (3-aminopropyl)(methyl)carbamate **138**, so a high yielding synthesis to generate this compound would be beneficial to reduce the overall cost of synthesising the payload.

Starting from *N*¹-methylpropane-1,3-diamine **137**, the secondary amine could be Boc protected using Boc_2O under acidic conditions reported from the literature in yields of 23-43%.^{177, 178} The secondary amine should be more nucleophilic, allowing for selective protection. The reaction was tried with a catalytic amount of HCl but yielded very little product that was not isolated with a messy reaction profile. Without the addition of HCl, the reaction worked better giving three spots on TLC. These spots correlated to a mixture of di-Boc protected amine, mono-Boc protected amine and also unreacted starting material. Due to the polarity of these compounds, purification was difficult. However, using 10% ammonia in methanol did help in separation on TLC, with the product having a R_f of 0.2 and this translated well on flash column chromatography. The product was confirmed to have the Boc protection on the secondary amine by the confirmation of the NH_2 peak and no visible NH peak in ^1H NMR. The other biproducts were also analysed by NMR, confirming a di-Boc protection and starting material. The time for the reaction was kept to 3 hours as any longer would have led to decreased yields due to the increase of di-Boc protected product. The yield was only at 36% which is comparable to that in the literature with the addition of HCl but could be done on a large scale using relatively cheap materials.

This reaction was quite wasteful due to the mixture of compounds generated, with much of it starting material, giving a poor yield. Other methods were explored to see if this could be improved upon.



Scheme 5.9: Proposed synthetic route to the starting material, **139**. *Reagents and Conditions:* i) phthalic anhydride, H₂O, reflux; ii) Boc₂O, MeOH, RT; iii) N₂H₄, EtOH, reflux

It was known that 1,3-diaminopropane could react with phthalic anhydride to protect the primary amine selectively¹⁷⁹ but the major product observed in this reaction had a mass of 236 seen by LC-MS analysis, which correlated to the ring opened compound **141** (Figure 5.5). Cyclisation of this compound with catalytic amounts of *p*-toluenesulfonic acid under reflux in MeCN did not work and no desired product was obtained.

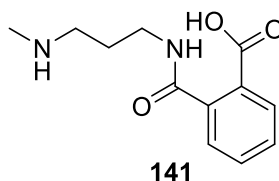
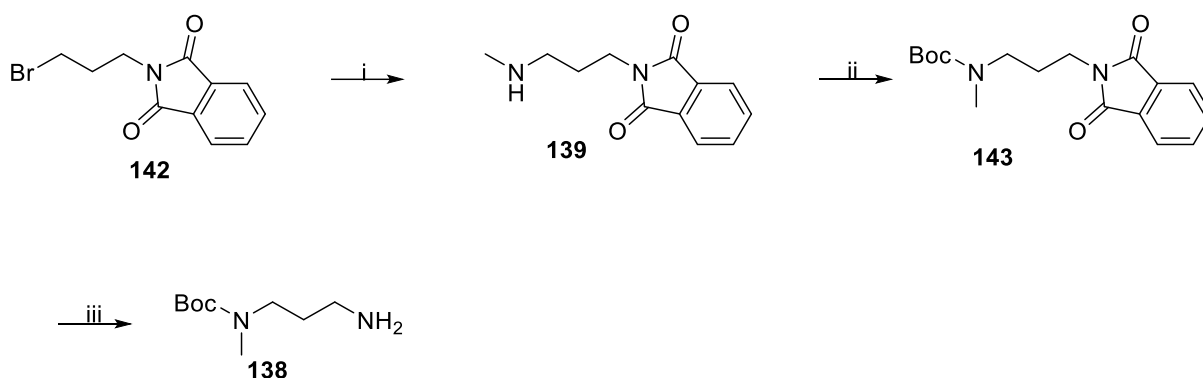


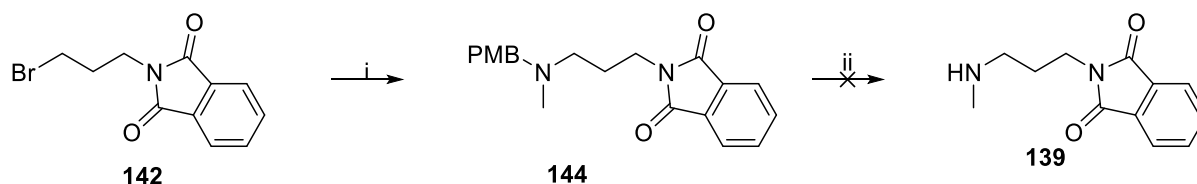
Figure 5.5: Ring opened phthalimide **142** observed.

It was thought that instead of attempting to protect the diamine, initially starting with a protected amine and functionalising a group to add a second amine to the molecule could bypass this problem. (Scheme 5.10).



Scheme 5.10: Synthetic route to the starting material, **139** *Reagents and Conditions:* i) 2M MeNH₂ in THF, Cs₂CO₃, MeCN, reflux, 6h, 39%; ii) Boc₂O, MeOH, RT, 5h, 84% iii) N₂H₄, EtOH, reflux, 4h, 62%.

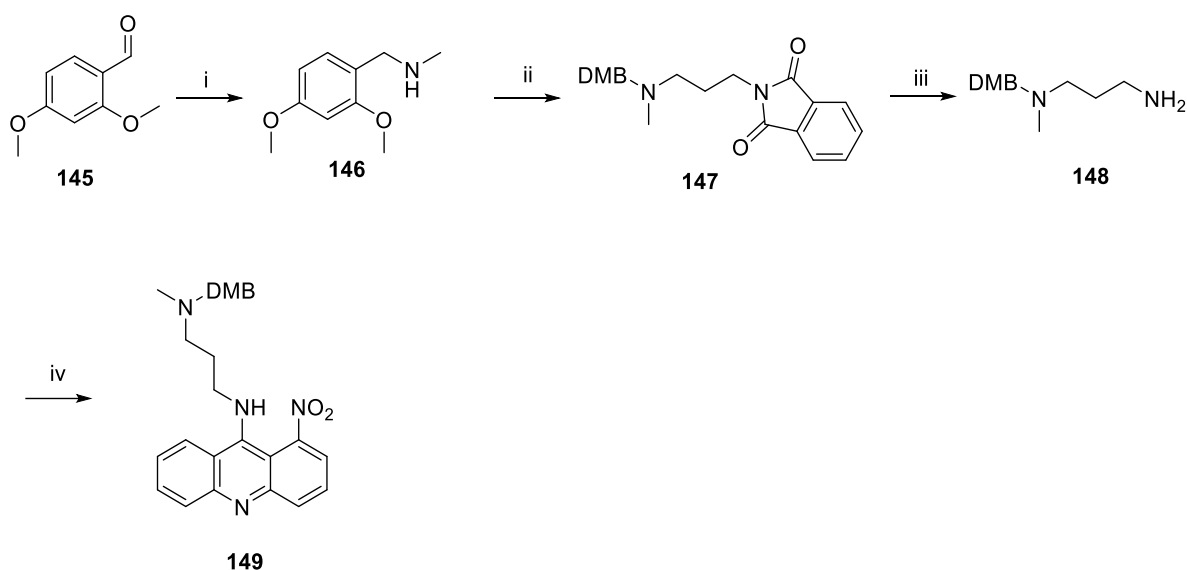
Commercially available 3-bromopropylphthalimide, **142** was reacted with methylamine in an S_N2 reaction. As well as displacing the bromo group, there was also evidence that methylamine was ring opening the phthalimide ring as seen previously, resulting in low yields for this reaction, 34-45%. It has been reported that methylamine can be used deprotect a phthalimide group and is nucleophilic enough to ring open the phthalimide.¹⁸⁰ Enough product, **139** was obtained to carry through and Boc protect the amine to give **143** followed by removal of the phthalimide protecting group with hydrazine. Although the starting material was successfully synthesised, the overall yield was far worse than that of Boc protecting N¹-methylpropane-1,3-diamine.



Scheme 5.11: Synthetic route to the phthalimide protected diamine **139**. *Reagents and Conditions:* i) *N*-(4-methoxybenzyl)-*N*-methylamine Cs₂CO₃, MeCN, reflux 6h, 82%; ii) 10% TFA in DCM, RT, 16h or DDQ, DCM, RT, 5h.

To prevent ring opening by methylamine it was decided that a protected methylamine might be less prone to attacking the phthalimide group and stop side reactions occurring. PMB amine which is commercially available was initially tried and was successful affording **144**, giving a significantly increased yield of 82% with no uncyclised product seen. At this point, conditions were tried to remove the PMB group before reacting with 9-chloro-1-nitroacridine, **126** to ensure deprotection would be possible. The first method attempted was 10% TFA in DCM but no deprotection had occurred. Using harsher conditions of TFA neat under reflux was also tried but failed to remove the PMB group. DDQ was also tried but analysis of the

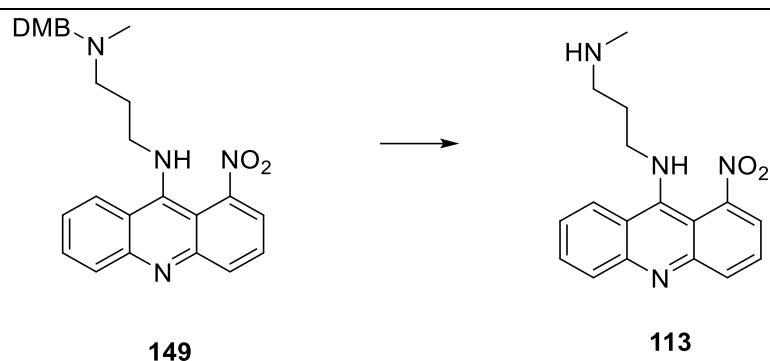
reaction mixture was difficult with multiple spots on TLC. No starting material or product was recovered. Hydrogenation was not tried because this would affect nitroacridine and reduce the nitro group.



Scheme 5.12: Synthetic route to DMB protected aminonitroacridine, **149**. *Reagents and Conditions:* i) 2M MeNH₂ in MeOH, EtOH, MgSO₄, reflux then NaBH₄, RT, 45% ii) 3-bromopropylphthalimide, Cs₂CO₃, MeCN, reflux, 74%; iii) Hydrazine hydrate, EtOH, reflux; iv) 9-chloro-1-nitroacridine, **127**, Et₃N, THF, reflux, 76% over two steps .

Since PMB might be tricky to remove from the nitroacridine, focus switched to DMB group, which is more labile towards acidic deprotection. To synthesise the DMB amine, a condensation between **145** and methylamine was tried. The imine formation was not high yielding with around 50% of product formed by LC-MS. Attempts to increase the degree of imine formation were tried such as adding molecular sieves or magnesium sulfate to the reaction. It was hoped this would remove water from the reaction and allow the reaction to proceed. Changing the solvent to toluene and using a Dean-Stark method was also tried. Different solvents such as THF and DMF were used as well but this also failed to increase the conversion. With the imine formation complete, sodium borohydride was added to reduce the imine to the amine to get desired product **146**. The solvent was removed *in vacuo* and was purified by flash column chromatography without a work-up with good separation giving a yield of 45%. The DMB protected methylamine was reacted with 3-bromopropylphthalimide to give compound **147** in a good yield of 74%. The phthalimide group was removed with hydrazine with the side product filtered off to give **148** before being reacted with 9-chloro-nitroacridine resulting in compound **149** in a yield of 76% over two steps. Deprotection was not carried out until after reacting with 9-chloro-1-nitroacridine as it was predicted the DMB could be removed more easily in the final step. Removal of the DMB initially proved

challenging and multiple conditions were attempted (Table 5.2). Ceric ammonium nitrate, CAN, was tried for oxidative deprotection but no product was seen.¹⁸¹ Previous conditions used for the removal of PMB were tried such as DDQ and TFA. The reaction with DDQ gave multiple spots by TLC with a messy reaction profile.¹⁸² TFA in DCM also did not work, and increasing the amount of TFA had no effect with starting material still observed. Harsher conditions were tried once again. TFA neat under reflux gave no product but using the microwave at 120 °C did remove the DMB group giving the product in 57% yield. As seen previously with Boc deprotection for **114**, this did lead to the formation of degradation products associated with the nitroacridine ring. The harsher conditions also caused a messier reaction profile and so a lower yield than expected was observed.



Conditions	Temperature	Reaction Time	Comments
10% TFA in DCM	RT	16h	No reaction
TFA neat	RT	16h	No reaction
TFA neat	Reflux	5h	No reaction
TFA neat	120 °C with microwave irradiation	2h	Product isolated in 57% yield
DDQ in DCM	Reflux	6h	Messy reaction profile and no product observed
CAN in MeCN/H ₂ O, 1:1	RT	16h	No product observed

Table 5.2: Conditions used for the deprotection of DMB protected amine.

Attempts were made to synthesise starting material **138** in high yield. It was found that reacting diamine **137** with Boc₂O was the highest yielding method despite the reaction not being efficient.

5.3. Biological testing of compound 114

A Sulfurhodamine B (SRB) assay was used to conduct *in vitro* cytotoxicity studies. This involves using the dye SRB which binds stoichiometrically to protein components of cells under mild acidic conditions which then dissociate under basic conditions. As it binds stoichiometrically, the amount of dye extracted is directly proportionate to the cell mass. Use of MCF-7 cells in conjunction with SRB assay is well known and an effective means for testing. MCF-7 cells were used as they are a robust cell line and HER2 presenting cells which would be useful in future testing with an ADC.

Compound **113** was tested in an SRB assay on MCF-7 cells and the GI_{50} was found to be 6.2 ± 1.4 nM (Figure 5.6). This was less potent than the original hit from the NCI database which had a pGI_{50} of 9 against MCF-7 cells. Although not sub-nM as desired, the compound is potent. Due to the possibility of needing more potent payloads, attempts to increase the potency of this series was explored.

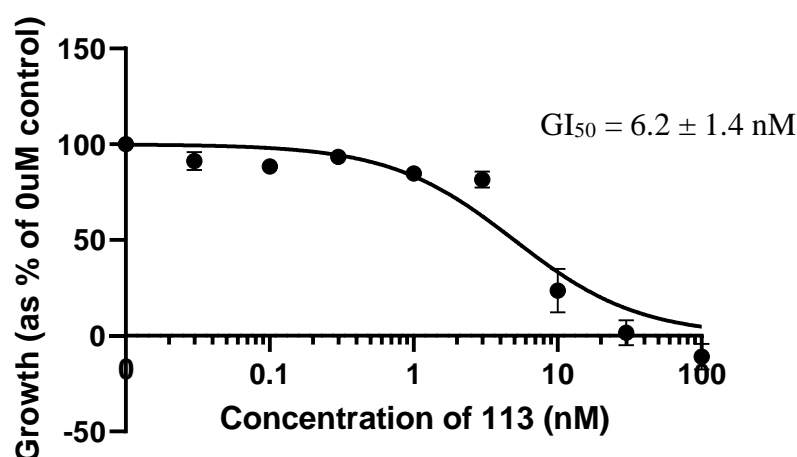


Figure 5.6: Cytotoxicity of the nitroacridine **113** evaluated on MCF-7 breast cancer cell line after 72 h, $n = 2$ (10 repetitions per replicate), error calculated from mean values.

5.4. Nitroacridine dimers

5.1.4. Synthesis of nitroacridine dimers

As nitroacridines are DNA intercalators, it is often seen that dimerization can increase potency in this type of inhibitor. To synthesise these dimers, diamines were reacted with chloronitroacridine. Different symmetrical diamines were used as well as spermidine which would allow for a handle to attach to a linker (Figure 5.7).¹⁸³

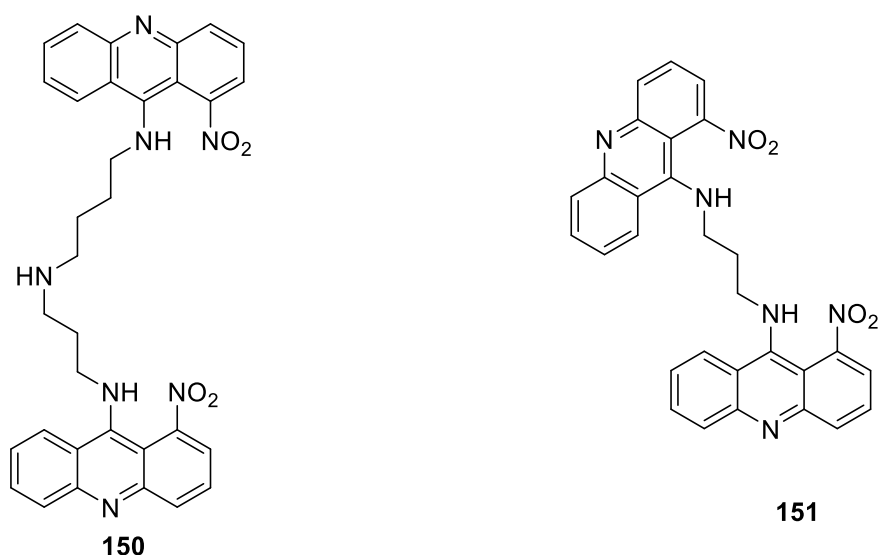
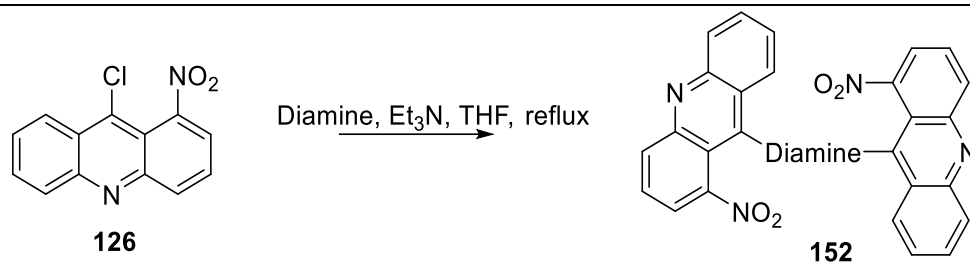


Figure 5.7: Structure of the dimer targets with a spermidine and propyl diamine linker.

An array of different diamine linkers were tried (Table 5.3). Ethylene diamine was unsuccessful, but it was postulated that the rings would be too close together and could sterically clash. Increasing the linker chain to 3 and 4 did yield product in yields 56% and 45% respectively. Other diamines tried were trans 2,4 dicyclohexyl and p-xylylenediamine. p-xylylenediamine gave poor yields and the resulting product was difficult to purify. The compound lost purity over time, degrading. The 1,4-diaminobutane linker was filtered to give pure compound **154**. However, the other linkers could not be purified in the same way. To obtain clean product, flash column chromatography was used followed by reverse phase in THF and H₂O in neutral conditions. Spermidine was also tried as it would allow for a handle for a linker. However, no reaction occurred but this may be due to the starting material not being pure. Analysis of this starting material showed degradation.



Entry	Diamine linker	Reaction time	Yield, %
1	Ethylenediamine, 153	16h	0
2	1,3-diaminopropane, 151	6h	56%
3	1,4-diaminobutane, 154	6h	45%
4	Trans-1,4-diaminocyclohexane, 155	16h	41%
5	p-xylylenediamine, 156	16h	34%
6	Spermidine, 150	16h	0

Table 5.3: Range of diamine linkers trialled to synthesise dimers

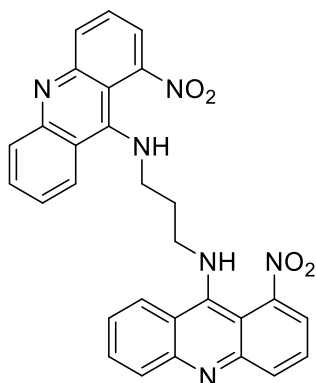
5.2.4. Biological testing of nitroacridine targets

The potencies of the tested compounds were around 3-fold less than that of the parent compound. Adjusting the alkyl length did not really change the potency but adding a sterically hindered cyclohexyl group was 2-fold less potent than the flexible alkyl chains. The p-xylylenediamine was considerably less potent than the others tested. This could be due to being sterically hindered, not allowing enough flexibility for DNA intercalation. This might be due to degradation of the compound prior to testing or because of decreased solubility. One reason for the overall reduction in potency may be due to the poor aqueous solubility of these compounds and thus might be a problem in the cell assay. The mode of action for these series of compounds is complex and although dimerization may increase binding by DNA intercalation, it might reduce the activity of the compound overall.

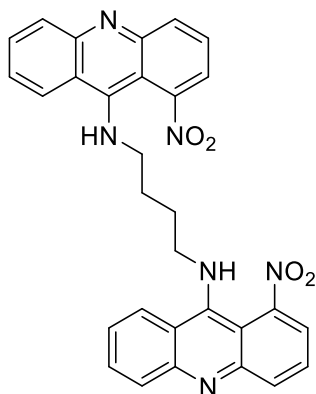
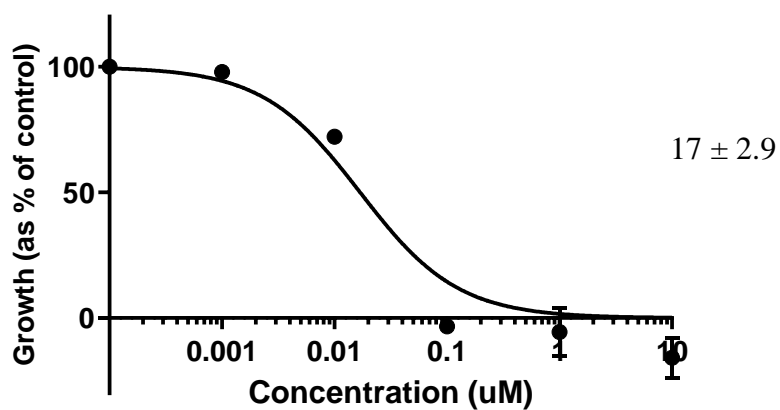
Diamine linker

Cell assay

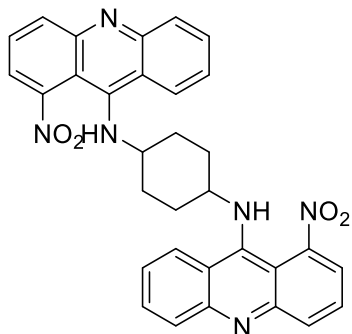
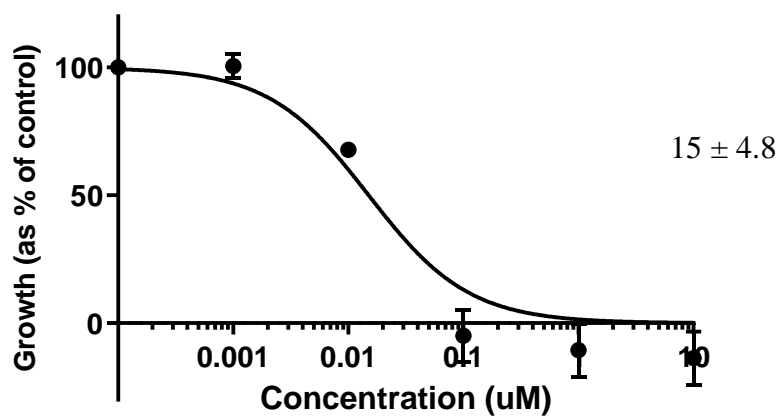
GI₅₀, nM



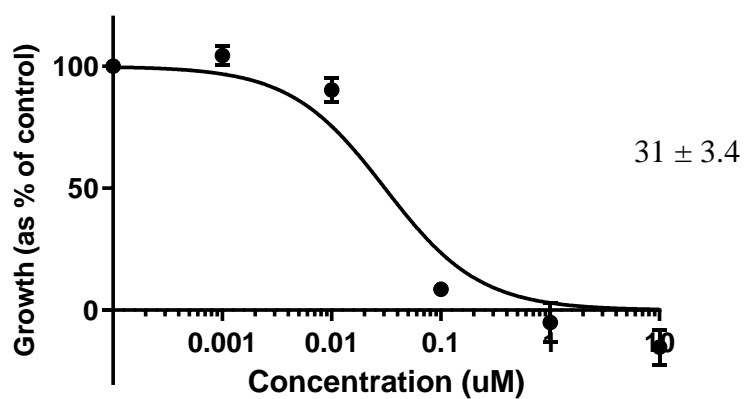
151



154



155



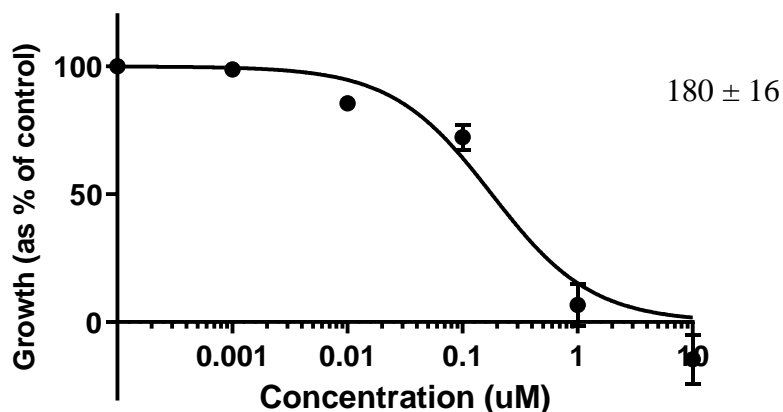
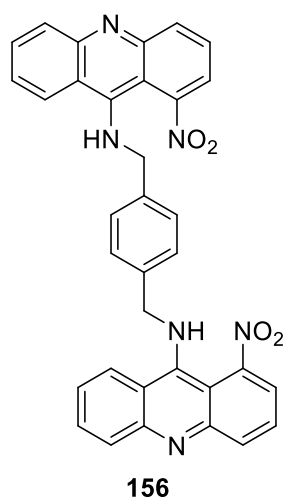


Table 5.4: Cytotoxicity data for the nitroacridine dimers evaluated on MCF-7 cell line after 72 h, n = 2 (10 repetitions per replicate), error calculated from mean values.

The resynthesis of the nitroacridines has been carried out successfully, with improved conditions compared to the original synthesis due to optimisations carried out. Despite only a short synthesis, the reactions were not high yielding and had associated issues such as the formation of regioisomers in a 50:50 ratio. Optimisation of the first step were successful in significantly increasing the yield which could be done on large scale. Attempts to have both nitro and carboxylic acid onto the same pendant phenyl ring to form the biaryl amine to yield only one isomer were attempted but were unsuccessful owing to the unreactive nature of these systems.

The biological evaluation of compound **113** was carried out and was found to be potent at 6 nM in MCF-7 cell lines. This is not the sub-nM that was expected from the NCI database but is comparable to literature values. Dimers of the nitroacridines were synthesised in order to increase potency as DNA intercalators. However, biological testing of the dimers revealed they were less potent than the parent compound. This could be due to solubility issues or that dimerization reduces the activity of the class of compounds.

Chapter 6: Quinolone series

The second warhead to be investigated was the 2-phenyl-4-quinolone. Extensive SARs of this series have given confidence that analogues with linker attachment sites would be tolerated.¹⁶⁰

The two targets include the quinolone hit **1** from the NCI database as well as the aniline derivative **157** (Figure 6.1). The aniline compound has not been tested for activity so would need to be checked to ensure activity was retained.

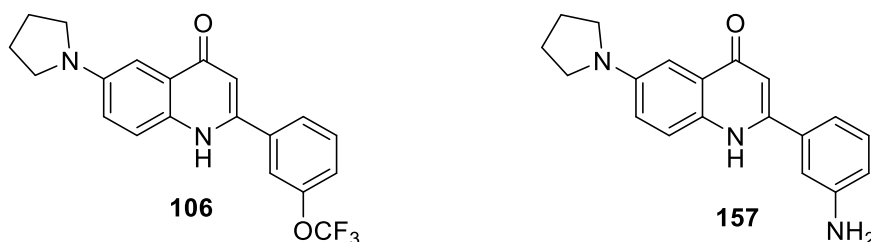
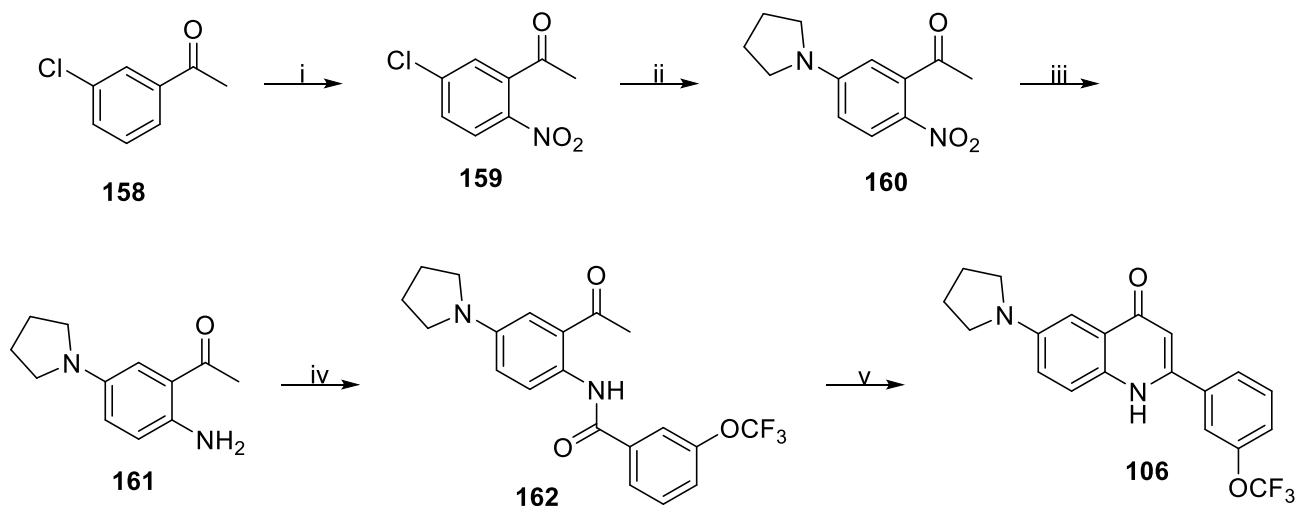


Figure 6.1: Structures of 2-phenyl-4-quinolone targets.

6.1. Resynthesis of quinolone



Scheme 6.1: Resynthesis route to quinolone. *Reagents and Conditions:* i) HNO_3 , H_2SO_4 , -20°C , 5h 73%; ii) pyrrolidine, K_2CO_3 , DMF, reflux 16h, 79%; iii) 10% Pd/C, H_2 , DCM, MeOH, RT, 18h, quant.; iv) 3-(trifluoromethoxy)benzoyl chloride, Et_3N , THF, RT, 3h, 74%; v) $t\text{-BuOK}$, $t\text{-BuOH}$, reflux, 5h, 35%.

The resynthesis of the 2-phenyl-4-quinolones began by incorporating the routes reported in the literature (Scheme 6.1).¹⁶⁰

The first step in the resynthesis was nitration of 3'-chloroacetophenone, **158** using sulphuric acid and fuming nitric acid, giving **159** in a yield of 73%. The use of fuming acid was essential as switching to 60-70% nitric acid gave no reaction with complete recovery of starting material. The reaction profile of this reaction contained multiple species by TLC analysis, but the product was isolated by flash column chromatography. Due to the high, lipophilic nature of the compound, a solvent system of DCM in petroleum ether was used. Separation was not ideal as the product streaked on the column, thus eluting with impurities in later fractions. Impure fractions were discarded, impacting the yield.

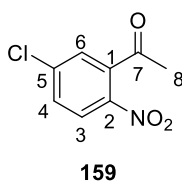


Figure 6.2: Numbered structure of **159**

The position of the nitro group was confirmed based on the coupling patterns in the ^1H NMR spectrum, as H-4 shows a doublet of doublet with J values of 2.1 and 8.7 Hz, indicative of J_{ortho} and J_{meta} and H-3 is a doublet suggesting it has gone ortho to this position. This was corroborated using HMBC, which showed as correlation between the carbonyl carbon and to only one aryl proton was seen.

The regiochemistry was ascribed to the predominant directing effect of the chloro-substituent. Halogens are ortho-para directing and exhibit both inductive and resonance effects. Through the resonance effect, the halogen can donate electrons into the ring, increasing electron density in the ortho and para positions activating these positions to electrophilic attack. However, the inductive effect removes electron density from all positions in the ring due to the electronegativity of the halogen. As the para position is furthest to the halogen, it feels this effect weakest and so less electron density is removed compared to other positions. Based on this, the para position should have the greatest electron density, so more likely to undergo electrophilic attack of the nitronium ion. The effects of the ketone group are less impactful compared to the halogen.

With the nitro in place para to the chloro group, the compound can undergo an $\text{S}_{\text{N}}\text{Ar}$ reaction with pyrrolidine to give **160**. The reaction worked well with full conversion of the starting material by LC-MS analysis. A precipitate was formed upon pouring on to ice, which could then be filtered. Filtration was very slow due to the sludge like precipitate that formed and

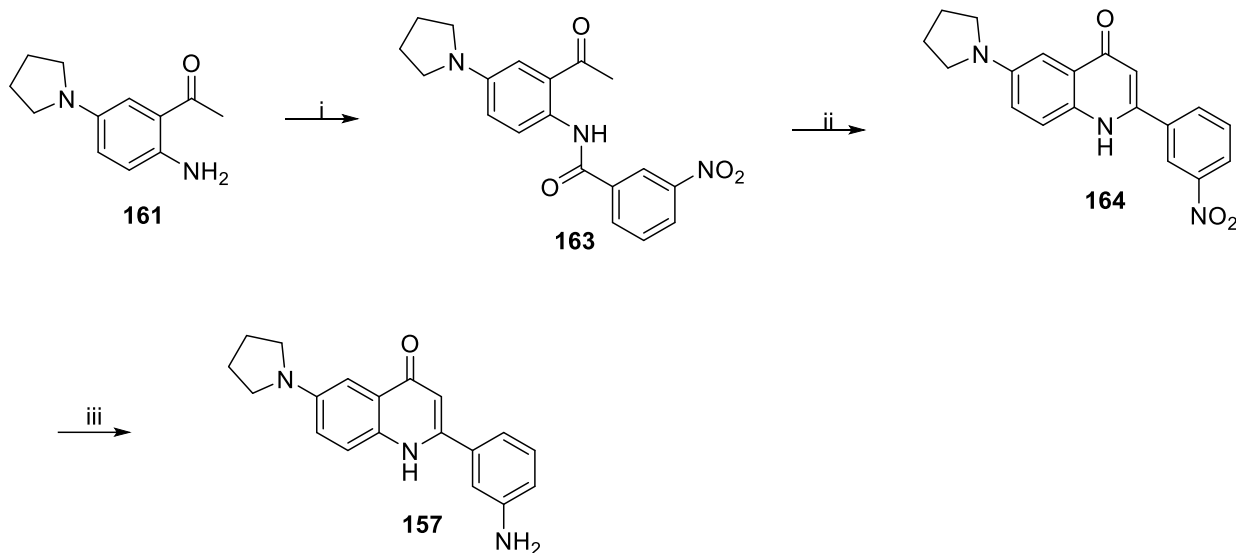
needed to be dried in a vacuum oven before purification was possible. As with the previous step, this compound streaked on silica due to a non-polar solvent system needed for flash column chromatography. An impurity would often elute with the product in later reactions. Purification was not essential at this stage and the impurities could be carried through without interfering with subsequent steps.

The nitro group was reduced *via* hydrogenation using the H-Cube™ flow system in quantitative yield to afford **161**. While this worked for small scales, on larger scales this caused issues such as leaching of the palladium catalyst into the product. This was due to the high viscosity of the solution, at larger scales, which was not compatible with this method. For larger scales, 10% Pd/C with a hydrogen balloon was used instead, which still obtained quantitative yields but required longer reaction times. Using pure starting material led to an orange solid. In solution, it was observed that the aniline product blackened over time, with the NMR showing a reduction in the integral for the NH₂ peak. The aniline was therefore used straight away in the next step, suggesting it is prone to air oxidation.

The amide **162** could be formed through reaction of the aniline **161** with a benzoyl chloride, e.g., 3-trifluoromethoxy benzoyl chloride and 3-nitro benzoyl chloride were used. Poor solubility of these intermediates led to problems on a large scale. Filtration of the product was the method of isolation reported in the literature, but not all product could be collected this way as some remained in solution. Extraction and purification by flash column chromatography was difficult due to limited solubility in solvents, including DCM. In general, 3-nitrobenzoyl chloride produced lower yields compared to 3-trifluoromethoxy benzoyl chloride due to the decrease in solubility, causing issues with chromatography (65% for 3-nitrobenzoyl chloride compared to 74% using 3-trifluoromethoxy benzoyl chloride).

Cyclisation of these compounds was achieved with two different methods, potassium *tert*-butoxide in *tert*-butanol or sodium hydroxide in dioxane under reflux. For the synthesis of **106**, the use of *tert*-butoxide in *tert*-butanol led to comparatively higher yields than using sodium hydroxide, although the reaction was low yielding in general. Monitoring of the reaction showed full consumption of the starting material and LC-MS analysis showed product as the major peak but also smaller peaks. The product was poured into a 10% NH₄Cl solution and then filtered to obtain the crude product. Purification of the final compound was challenging as the filtered precipitate contained impurities. Due to the low solubility of the product, recrystallisation was tried using hot ethanol as the solvent. Although the product would not fully dissolve, the impurities did go into solution and after slowly cooling to room temperature, the solid was filtered. TLC analysis showed impurities had remained but were

significantly reduced and separable from the product. Flash column chromatography was successful and clean fractions were obtained giving a yield of 35%. The yield was low to maximise purity but product from impure fractions could also be used in subsequent reactions with no impact.

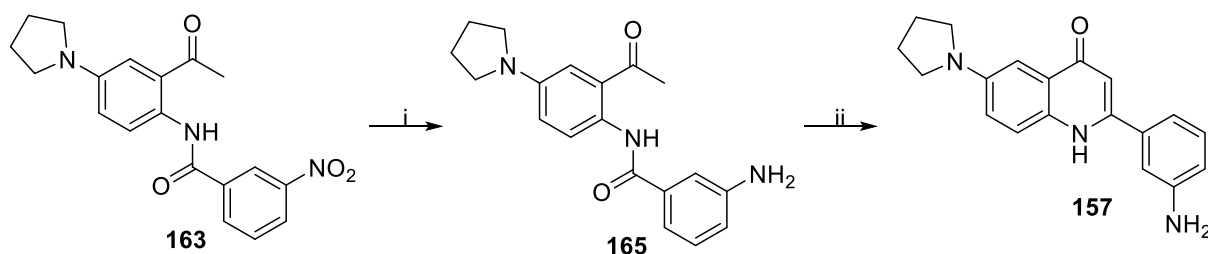


Scheme 6.2: Synthetic route to the formation of quinolone **157**. *Reagents and Conditions:* i) 3-nitrobenzoyl chloride, Et₃N, THF, 18h, 43%; ii) NaOH, dioxane, reflux, 4h; iii) H₂, 10% Pd/C, DCM, MeOH, RT, 6h, 26% over two steps.

The synthesis of **157** was started from **161**. The benzoyl chloride was switched to 3-nitrobenzoyl chloride to give **163** in 43% yield. **163** proved difficult to purify as the compound was not very soluble and so often coeluted with impurities on a column.

For aniline **157**, the best method for cyclisation was using sodium hydroxide in dioxane (Scheme 6.2). The sodium hydroxide was ground to a fine powder before use to give maximum yields. The resulting intermediate **164** was isolated by filtration after precipitation in ice cold water. The crude was washed with copious amounts of water and methanol to remove excess sodium hydroxide that had not fully dissolved and impurities. Attempts to purify and isolate the intermediate proved unsuccessful, with a workup yielding limited product due to the insolubility of the product and its impurities. Instead, the crude was carried through and was reduced using 10% Pd/C in H₂ atmosphere. The resulting product had increased solubility and so after removal of palladium catalyst, was purified by flash column chromatography. As with the trifluoromethoxy, impurities would also elute with the compound, but enough pure fractions were collected. The purification was less successful than with **107**, affording 26% yield over two steps.

The low yield was typical for analogues of this type.¹⁵⁹ Literature examples of anilines included alkylated anilines that have been prepared by reduction of the nitro group first, then alkylation followed by cyclisation, giving yields between 20-30%. This method was assessed to see if the yield could be improved.



Scheme 6.3: Alternate synthetic scheme for synthesis of compound **157**. *Reagents and Conditions:* i) H₂, 10% Pd/C, DCM, MeOH, RT, 6h, 70%; ii) NaOH, dioxane, reflux, 4h, 21%.

Compound **165** was prepared initially by a colleague Charlotte Rayburn. Two new products were formed in the reduction of the nitro group to the aniline. The nitro group was reduced successfully but another product, **168** was observed in which reduction of both the nitro and ketone had occurred (Figure 6.3). The product was afforded with 70% yield while **168** was obtained with 13% yield. Cyclisation of **166** proceeded, with a yield of 21% but the overall yield was lower than the previous method was abandoned for larger scale.

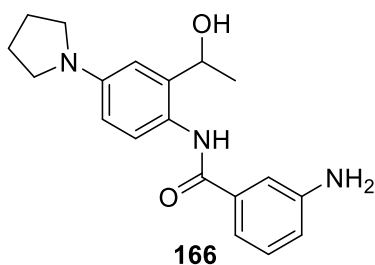


Figure 6.3: Structure of reduction side product, **166**

6.2. Biological testing of quinolones

Compound **157** was tested against MCF-7 cells in an SRB assay (Figure 6.4). The GI₅₀ was found to be 62 ± 0.9 nM which was less potent than what was expected with a sharp drop in growth of the cell line, suggesting no dose dependency. This could suggest that the aniline has a loss a potency compared to other analogues and therefore may need mono alkylating as these analogues have improved potency in cell assays.

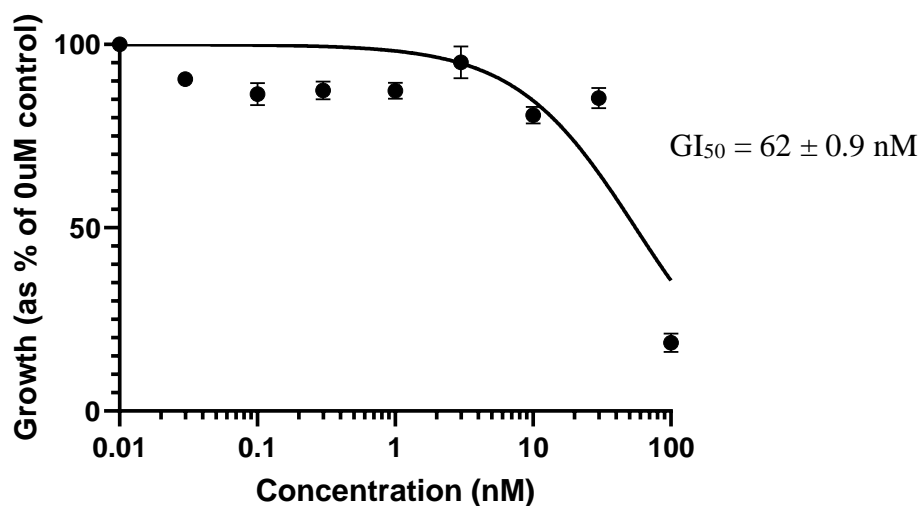


Figure 6.4: Cytotoxicity of quinolone **159** evaluated on MCF-7 breast cancer cell line after 72 h. $n = 2$ (10 repetitions per replicate), error calculated from mean values.

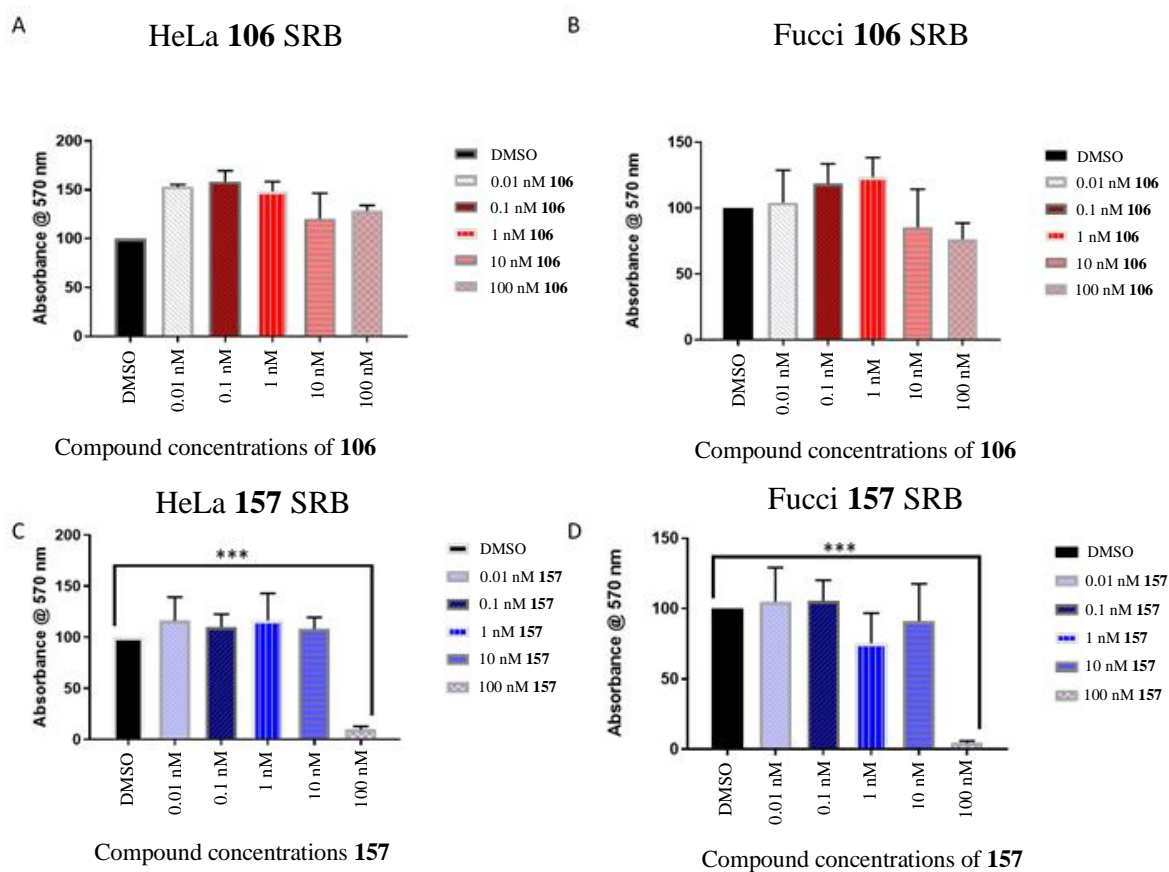


Figure 6.5: SRB proliferation assay results. A/B: compound **106** shows a slight effect on either cell line. C/D: compound **157** has significant activity on cell proliferation at 100 nM in both cell lines. All graphs were normalised to DMSO at 100%.

Both compounds **106** and **157** underwent further biological testing in collaboration with Dr Lisa Prendergast. It was found that HeLa Kyoto alpha-tubulin/GFP mCherry Histone 2B (HeLa GFP-Tubulin) and Fucci U2OS cell lines were significantly less sensitive to **106** compared to **157**, which showed significant cell proliferation at 100 nM (Figure 6.5). No activity was seen at 10 nM as in the MCF-7 cell line.

An interesting difference in these compounds was the effect of spindle width in treated metaphase cells compared to a DMSO control. Compound **106** significantly reduced spindle width at both 10 and 1 nM concentrations. Compound **157** on the other hand, slightly increased spindle width at 10 nM, suggesting a different mode of action between the compounds (Figure 6.6).

Compound **157** also caused similar effects to nocodazole with poor spindle formation and arresting of cells in mitosis in HeLa GFP-tubulin cells, suggesting it may have similar mode of action to other antimitotic agents, whereas for **106** this was not observed. Both compounds showed significant mitotic catastrophe. This might suggest that the compound might be more potent than the SRB assay had originally suggested. Given the nature of the SRB assay, it could misinterpret a cell undergoing delayed cell death as a healthy cell and so the apparent activity of the tubulin binder would be lower than its true value. The cell assays were run over 72 h, but a longer assay may be needed to check. There is also a drop between mechanistic and antiproliferative IC_{50} s which is often reported for tubulin agents. For example, taccalonolide A, a microtubule stabilising agent, is significantly less potent in cell assays than initiating microtubule bundling.¹⁸⁴

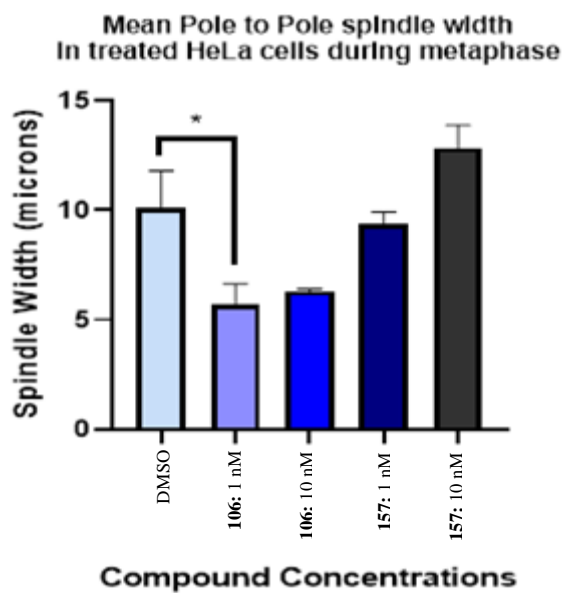
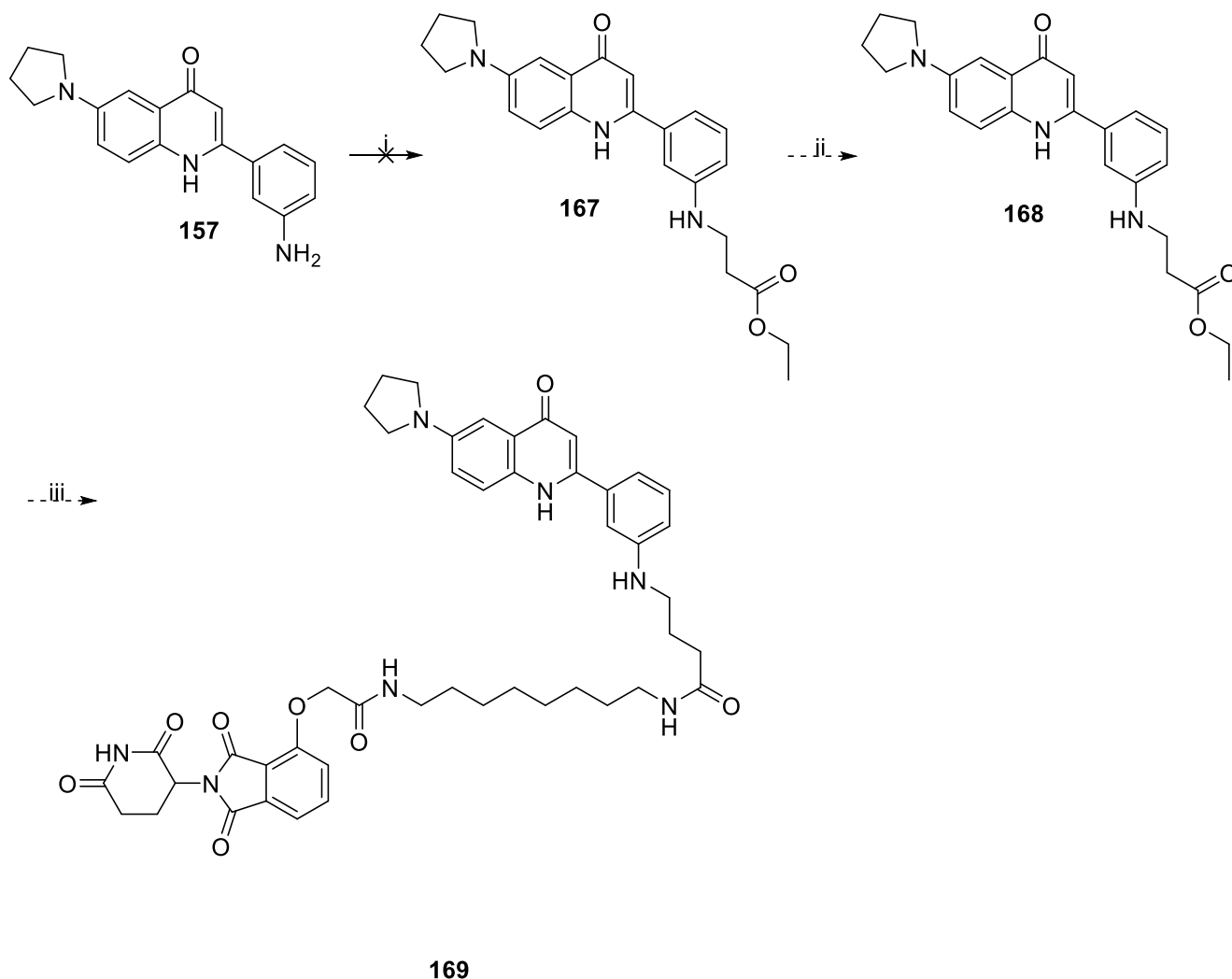


Figure 6.6: Measurements of Spindle width using ImageJ. **106** shows significant decrease in spindle growth compared to DMSO. **157** at 10 nM displays an increase in spindle width at 10 nM suggesting higher concentrations may create wider spindle.

6.3. Design of PROTAC with 2-phenyl-4-quinolone, 157



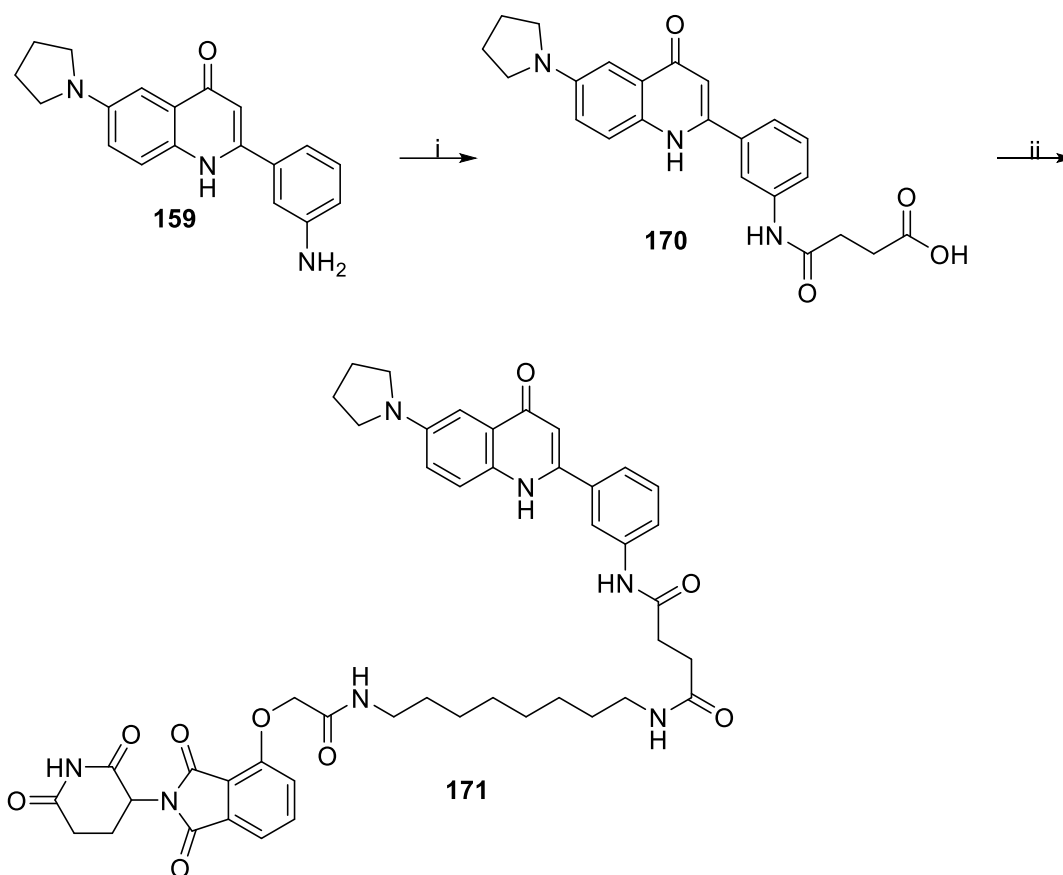
Scheme 6.4: Proposed synthetic route to PROTAC **169**. *Reagents and Conditions:* i) ethyl-3-bromopropionate, Cs_2CO_3 , DMF, reflux; ii) NaOH (aq) in MeOH, RT; iii) EDC.HCl, DMAP, cereblon ligand, THF, RT.

To address the reduced potency of this warhead, a PROTAC (proteolysis targeting chimera) approach was undertaken.¹⁸⁵ It would be interesting to use a tubulin binder combined with a cereblon ligand. PROTACs work by inducing selective proteolysis in proteins by recruitment of the E3 ubiquitin ligase to the selected protein, causing ubiquitination and degradation. The cereblon ligand targets the E3 ubiquitin ligase while the quinolone can target tubulin. It is hoped that this approach could result in the degradation of tubulin. Because PROTACs can act catalytically, full target occupancy would no longer be required, meaning that a less potent compound could be used as an ADC warhead.

The cereblon ligand was prepared by Daniel Fernandez Lopez. To couple the amines, ethyl-3-bromopropionate was used, which was subsequently hydrolysed to allow for an amide

coupling. This method has been used with other projects within the group (Scheme 6.4). Reacting ethyl-3-bromopropionate with compound **157** afforded no product.

An alternative method was ring opening of succinic anhydride followed by an amide coupling. Without the presence of base, no product was formed but addition of DIPEA led to the formation of product **170**, with a yield of 88%. The cereblon linker was then added through an amide coupling with EDC giving **171** in a low yield of 17%. The low yield was due in part to purification issues, which required semi-preparative HPLC. The PROTAC has yet to undergo biological testing.



Scheme 6.5: Synthetic route to PROTAC **171**. *Reagents and Conditions:* i) succinic anhydride, DIPEA, DMF, RT, 16h, 88%; ii) cereblon ligand, EDC.HCl, DIPEA, DMAP, DMF, RT, 18h, 17%.

The 2-phenyl-4-quinolones were successfully resynthesized. The aniline, which contained a handle for conjugation was tested in an SRB assay, giving a GI₅₀ of 62 nM. This analogue was less potent than the literature value for other quinolones. However, it was suggested that the aniline may have broader activity as HeLa and Fucci cells were more sensitive to this compound than the trifluoromethoxy analogue. The modes of action were also explored,

indicating the quinolones cause significant spindle disruption and compounds **106** and **157** have subtle differences in their activity, most noticeably their effects on spindle width. A method of synthesising a PROTAC of the quinolone was performed in the hypothesis that this may negate the lower potency of the parent analogue.

Chapter 7: Thiosemicarbazone series

The last series of warheads explored were the thiosemicarbazones. Out of the seven compounds that were identified from the NCI database, they had the lowest pGI₅₀ values across the multiple cell lines, but literature values of this series are potent with sub-10 nM potencies for selected analogues in SK-N-MC cell lines. SARs around the amine substituent are limited and so groups that allow for an attachment site needed to be explored and tested to confirm their activity. The selected analogues that were to be synthesised include an alkyl primary amine, a piperazine, and a phenyl piperazine (Figure 7.1).

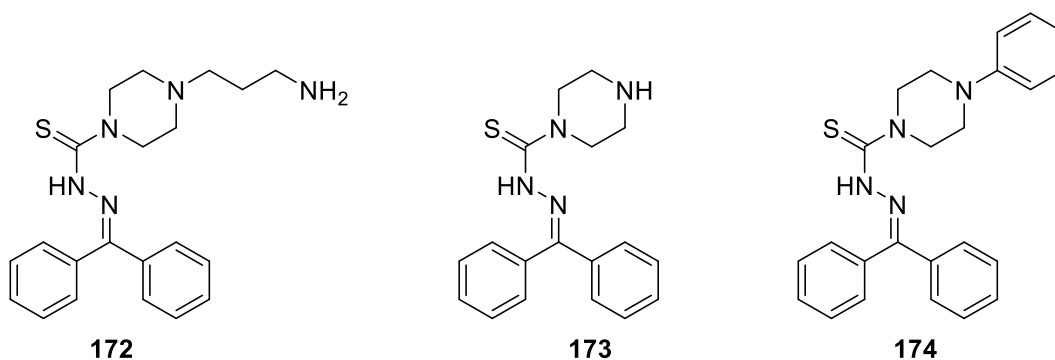
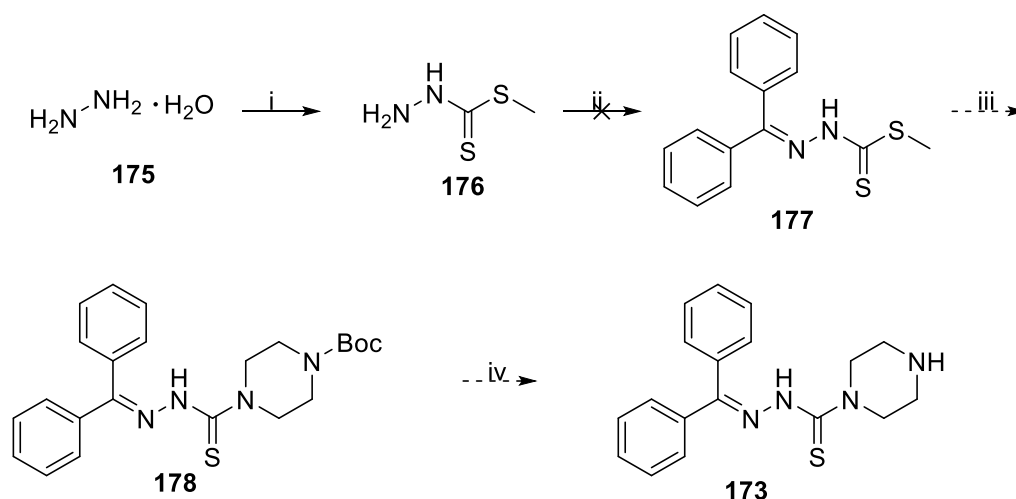


Figure 7.1: Structures of thiosemicarbazone targets

7.1. Synthesis of *N'*-(diphenylmethylene)piperazine-1-carbothiohydrazide, 173

The first step in the proposed synthetic route (Scheme 7.1) involves the use of hydrazine **175** with carbon disulphide followed by iodomethane to form the methyl hydrazinecarbodithioate **176**. This key intermediate can then undergo an imine formation with benzophenone followed by displacement of methyl mercaptan with the desired amine.

As discussed in chapter 2, the first analogues that were to be synthesised would have the pyridyl ring replaced with a phenyl ring to allow for the chemistry to be established, using readily available chemicals.



Scheme 7.1: Proposed synthetic route to thiosemicarbazones. *Reagents and Conditions:* i) KOH, CS₂, MeI, IPA, H₂O, 0 °C, 3h, 56%; ii) Benzophenone, EtOH, reflux, 5h; iii) 1-Boc-piperazine, EtOH, reflux, 6h; iv) TFA/DCM, RT, 3h.

7.1.1. Synthesis of methyl hydrazinecarbodithioate

The formation of methyl hydrazinecarbodithioate was carried out by first reacting hydrazine monohydrate with potassium hydroxide as reported by Klayman *et al.*¹⁸⁶ Then slowly, carbon disulphide was added slowly at 0 °C to give a yellow precipitate, which is consistent with the formation of the potassium thiolate salt. Addition of iodomethane to the precipitate gradually turned it white. This was filtered and recrystallized from DCM giving the product in a 56% yield. The recrystallised product was reported to be colourless prisms; however, a white powder was obtained. Analysis of this intermediate was challenging owing to its poor solubility and lack of diagnostic NMR signals. The product had limited solubility in CDCl₃, making NMR analysis difficult in this solvent. Switching to DMSO-*d*₆, NMR analysis was achieved but showed broad peaks with no CH₃ peak present, but this could possibly be occluded by the solvent peak. ¹³C NMR was attempted but a sufficiently concentrated sample could not be obtained. The IR data matched that of the reported peaks with a C=S absorbance at 1510 cm⁻¹ and N-H stretches at 3313 and 3205 giving some confidence that the compound was synthesised. The melting point was also consistent with literature at 82-86 °C. With partial evidence that the reaction had worked, the intermediate was carried through.

Conversion of benzophenone to the hydrazone was undertaken with intermediate **176** in IPA under reflux but the low solubilities of these starting materials were observed. After three hours, LC-MS analysis of the reaction mixture showed a mass of 361 had formed along with benzophenone still present. It was thought that compound **179** might have formed (Figure 7.2) as it is consistent with this mass. The isolation of this side product was not achieved as it could not be isolated from the crude material.

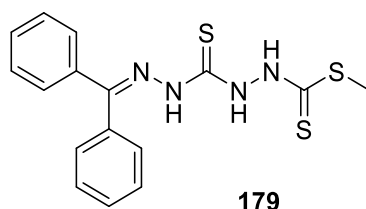
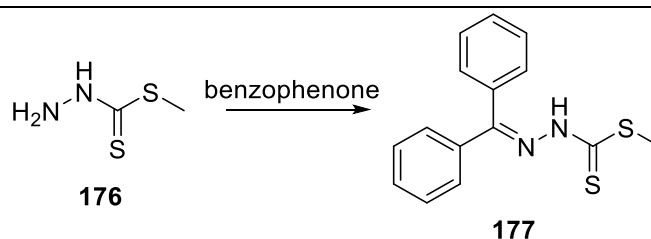


Figure 7.2: Suggested structure for mass peak of 361.

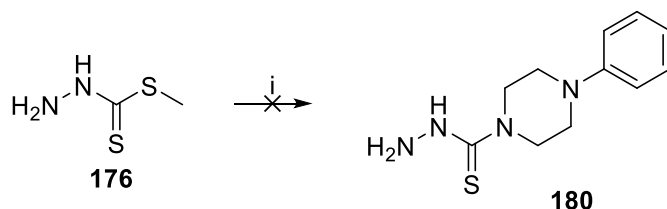
To address solubility problems of both compounds, multiple solvents were investigated (Table 7.1). Catalytic acids such as acetic acid and p-toluenesulfonic acid were added to help aid in imine formation but this made no difference to the reaction. In all the conditions, the major peak observed in LC-MS analysis was benzophenone with a small peak with a mass of 361. The only exception was DMF, where there was a colour change to a green solution and multiple spots were visible by TLC. It is possible that DMF was reacting with the intermediate as no product was formed and the benzophenone starting material was still present.



Entry	Conditions	Comments
1	IPA, reflux, 16h	No product formed
2	IPA, cat. AcOH, reflux, 16h	No product formed
3	IPA, cat TsOH, reflux, 16h	No product formed
4	THF, reflux, 16h	No product formed
5	THF, cat. AcOH, reflux, 16h	No product formed
6	DMF, reflux, 16h	Reaction turned green in colour and multiple spots on TLC
7	Toluene, 16h	No reaction, benzophenone insoluble
8	MeCN, reflux, 16h	No product formed
9	EtOH, reflux, 16h	No product formed
10	MeOH, reflux, cat. AcOH, 16h	No product formed

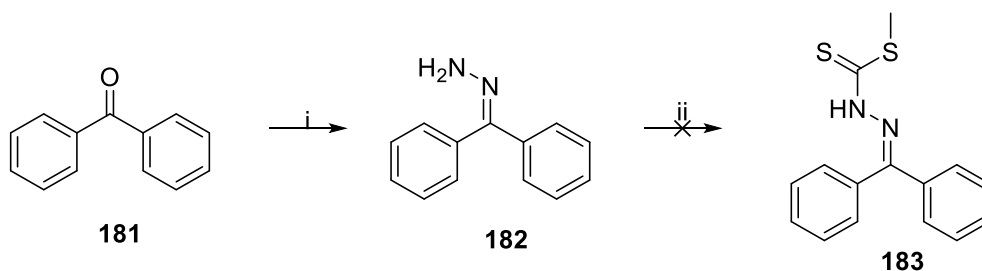
Table 7.1: Solvent screen for the formation of hydrazone with **176** and benzophenone

As the hydrazone formation was not working, attention switched to the displacement of the methyl thioester with an amine first (Scheme 7.2). Attempts were made with both 1-Boc-piperazine and 1-phenyl-piperazine where the reactions were refluxed in EtOH and left for over 16 hours. No effervescence of methyl mercaptan was seen and TLC analysis showed no new spot with starting material present in both cases.



Scheme 7.2: Formation of carbothiohydrazide. *Reagents and Conditions:* i) 1-phenyl piperazine, EtOH, reflux, 6h.

Due to the unreactive nature of key intermediate **176**, a different strategy was developed. Starting with benzophenone, **181** a hydrazone could be formed, **182** which could then be reacted with CS₂ and iodomethane to form compound **183** (Scheme 7.3).



Scheme 7.3: Synthesis towards methyl 2-(diphenylmethylene)hydrazine-1-carbodithioate, **183**. *Reagents and Conditions:* Hydrazone monohydrate, EtOH, cat. AcOH, reflux, 6h 46%; ii) KOH, CS₂, MeI, IPA, H₂O, 0 °C, 3h.

Imine formation was achieved after 3 hours heating in IPA at reflux, with 50% conversion of the ketone to hydrazone **182**. The reaction was left for longer but did not proceed any further. It was thought that the addition of magnesium sulfate or molecular sieves might assist dehydration and favour the imine formation, but neither was effective. Addition of cat. AcOH did increase the rate of reaction but did not lead to increase conversion or overall yield. The hydrazone was isolated in a yield of 46% after purification by flash column chromatography. The benzophenone hydrazone was then reacted with potassium hydroxide followed by addition of CS₂. TLC analysis of the reaction mixture indicated that the starting material had

not been consumed. Compound **182** had poor solubility in IPA and water at low temperatures and so to increase solubility, water was removed as a solvent and Et₃N was added as a base in place of KOH as reported by Berg for the synthesis of *N*-isothiocyanatoimines.¹⁸⁷ Although there was increased solubility of the benzophenone hydrazone, these changes did not produce any product. A mass of 301 was identified by LC-MS analysis which could correlate to compound **184**, with dimethylation occurring (Figure 7.3).

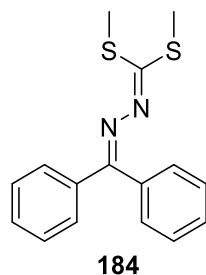
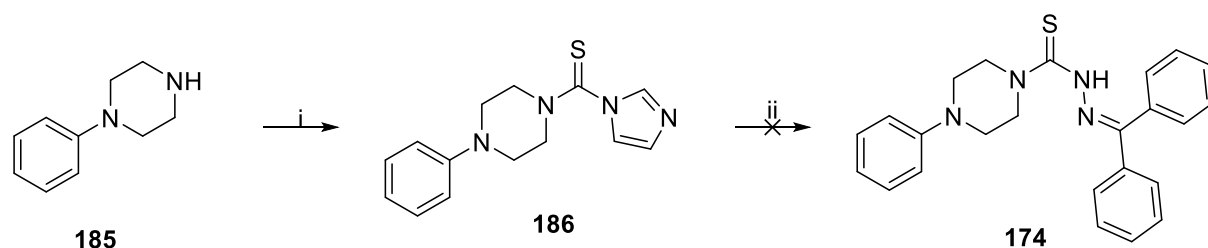


Figure 7.3: Structure of side product in the reaction of benzophenone hydrazone and CS₂ and MeI.

Two peaks at 2.42 and 2.11 ppm each integrating to 3 along with the 10 aromatic C-H peaks were observed and an absence of NH protons in the proton NMR of the isolated compound. This may be expected as the thioethers are not equivalent to each other, which has been reported in the literature.¹⁸⁸ Also seen in the LC-MS was the same mass peak of 361. This observation would not be consistent with the previous reaction as no intermediate **2** is available and so would not be possible to form. This product was reacted with 1-Boc piperazine as displacement of methyl mercaptan would still be possible but yielded no product.



Scheme 7.4: Synthesis towards thiosemicarbazone. *Reagents and Conditions:* TCDI, THF, RT, 5h, 63%; ii) Benzophenone hydrazone, TFA/TFE, 120 °C, 6h.

The key step involving addition of the amine to CS₂ to form the thiocarbonyl was proving difficult and so a different approach was undertaken to install the thiocarbonyl. Using thiocarbonyl diimidazole (TCDI), **186** was synthesised successfully with one equivalent of 1-phenyl piperazine used (Scheme 7.4). After 3 hours, LC-MS analysis showed only mono-

substitution with full conversion of starting material and purification of the compound was achieved by flash column chromatography in a yield of 63%. Benzophenone hydrazone was then reacted with **186** in the microwave at 120 °C in TFA/TFE, but upon monitoring the reaction by LC-MS analysis, a mass peak of 434 was seen corresponding to disubstitution of the benzophenone hydrazone, **187** with no desired product present (Figure 7.4).

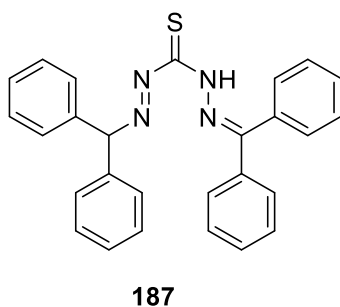
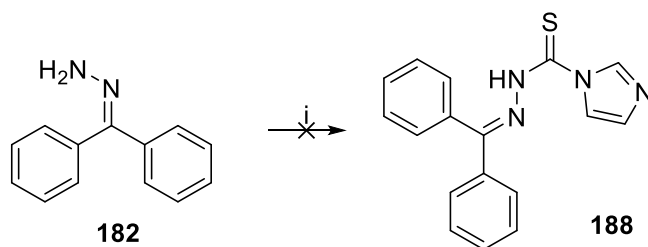


Figure 7.4: Structure of side product **187**

This was confirmed by NMR after isolation of the product. Adding fewer equivalents of benzophenone hydrazone did not help, with a mixture of starting material and disubstitution present in the reaction. The reaction was repeated using lower temperatures starting at RT to decrease the rate of reaction. No reaction occurred at RT and gradually raising the temperature also did not affect the reaction. At reflux, disubstitution was seen. It was found that the reaction only proceeded at the harsher conditions and mono-substituted product could not be isolated.

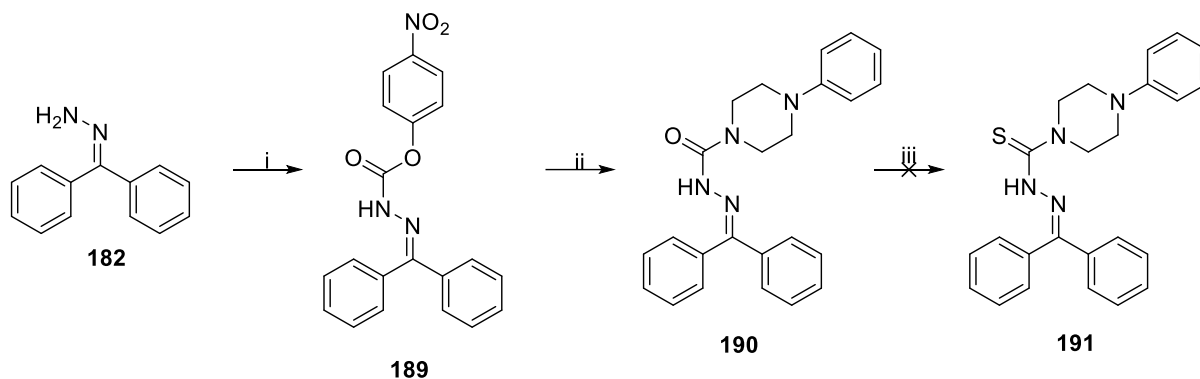
Polanski *et al.* had reported the use of hydrazine to displace the second imidazole group.¹⁸⁹ Reaction of **186** with hydrazine resulted in product with a white powder obtained in a yield of 64%. However, attempts to form the hydrazone from **186** by reaction with benzophenone failed with no product forming.

Addition of benzophenone hydrazone **182** to TCDI was also investigated but suffered the same problems with double addition occurring, as the reaction did not proceed at RT unlike with 1-phenylpiperazine (Scheme 7.5).



Scheme 7.5: Synthetic route to thiohydrazide. Reagents and Conditions: i) TCDI, THF, RT, 6h.

Formation of a semicarbazone followed by conversion to the thiosemicarbazone was also explored. This would allow the use of more commercially available compounds to allow the synthesis of a semicarbazone.



Scheme 7.6: Synthetic route to thiosemicarbazone. *Reagents and Conditions:* i) 4-nitrophenyl chloroformate, DCM, RT, 5h, 75%; ii) 1-phenylpiperazine, DIPEA, DCM, RT, 3h, 84%; iii) Lawesson's reagent, THF, reflux, 16h.

Sabatino *et al* have used benzophenone hydrazones for aza peptide synthesis, *via* carbamate intermediates akin to **189** (Scheme 7.6). The reaction with 4-nitrophenyl chloroformate and benzophenone hydrazone was successful in generating **189** in a good yield of 75%. The compound was isolated cleanly with no double addition observed. Compound **189** was reacted further with 1-phenylpiperazine to give semicarbazone **190** in a good yield of 84%. For the conversion of the carbonyl to the thiocarbonyl, **191**, Lawesson's reagent was used at 100 °C in THF under microwave irradiation. The reaction mixture was monitored but although the starting material was being consumed, no product was forming. The crude NMR was complex with no indication of product and multiple spots were visible with TLC. The reaction was repeated at RT, but no conversion was seen. Heating the reaction to reflux led to the same issues as using the MW.

West, *et al.* have reported the synthesis of thiosemicarbazones through the starting material 4-phenylthiosemicarbazide as another method for the synthesis of thiosemicarbazones.¹⁹⁰ However, this would have to be synthesised through the key step involving CS₂ which had already proven to be problematic and so has not been attempted.

Attempts to synthesise semithiocarbazone targets were tried but were unsuccessful. A number of strategies were employed, starting with the key reaction of forming the thiocarbonyl with CS₂. As this key reaction was unsuccessful, different strategies were used including the use of TCDI and 4-nitrophenyl chloroformate given further time. The next steps would involve

replacing the benzophenone with 2-benzoylpyridine to see if any difference is noted between the reactivity in the imine formation and would more closely match that of the reported literature. At this stage of the project, this work was paused in order to focus on the other warheads, with more promising results.

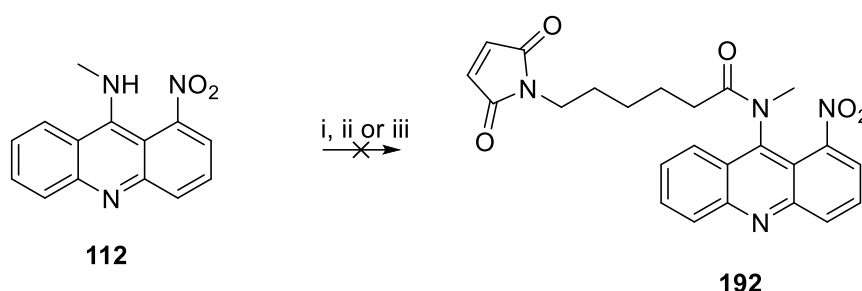
Chapter 8: Preparation of payloads

8.1. Non-Cleavable linkers

The advantage of a non-cleavable linker over a cleavable one is their apparent improved stability in plasma, which reduces the risk of systemic release of the warhead in the body. This could be useful where plasma stability is an issue.

Synthesis of the non-cleavable warheads was initially attempted with an amide coupling reaction between 6-maleimidohexanoic acid and the warhead amine, for example **192**.

EDC.HCl was the first amide coupling reagent that was tried for this reaction, however the amide coupling was not as straight forward as anticipated for some of the targets.

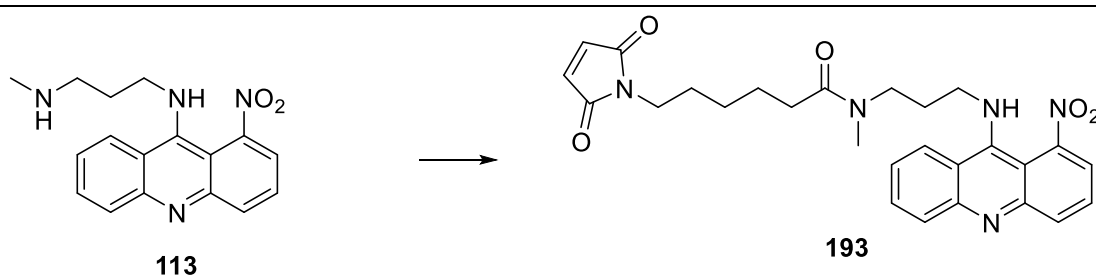


Scheme 8.1: Attempted amide formation to product **191** using various conditions. Reagents and conditions: i) EDC.HCl, DMAP, 6-maleimidohexanoic acid, THF, RT, 16h; ii) HATU, DMAP, 6-maleimidohexanoic acid, 16h; iii) 6-maleimidohexanoic acid, oxalyl chloride, DMF, THF, RT, 6h.

In the case of compound **112** there was no reaction with EDC.HCl, with just starting material recovered. Other amide coupling conditions were explored. Firstly, HATU was tried but was not successful, with starting material still visible by LC-MS analysis. The more reactive acid chloride derivative of 6-maleimidohexanoic acid was synthesised using oxalyl chloride with catalytic amount of DMF and used *in situ*. However, this procedure also failed, and no product was observed. Further to this, along with starting material recovered, hydrolysed nitroacridone was observed. An explanation for the low reactivity of **112** could be from the electron withdrawing nature of the nitroacridone ring itself, lowering the reactivity of the 2° amine sufficiently to be unreactive.

Attention switched to the warhead **113**. Owing to the more reactive nature of **113**, which contains a more nucleophilic amine, uncoupled from the aromatic system, the reaction with 6-maleimidohexyl chloride was successful, giving the desired product in a good yield of 78%. Conversion from the LC-MS showed complete conversion of starting material to product, but on work up and purification, there was evidence that one of the by-products was the hydrolysed nitroacridone as seen previously.

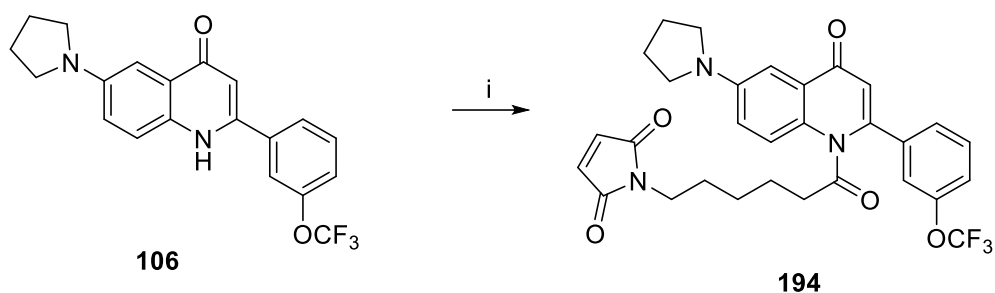
Therefore, other methods were explored (Table 8.1). Using EDC.HCl was surprisingly low yielding, less so was using the succinimide ester approach, which gave 22% product which was a much milder but less reactive approach. The reaction with HATU was roughly equivalent to using an acyl chloride and was used in preference due to the less harsh conditions.



Conditions	Yield
i) 6-maleimidohexanoic acid, oxalyl chloride, DMF, THF, RT, 6h	78%
6-maleimidohexanoic acid, EDC.HCl, DMAP, THF, RT, 16h	36%
6-Maleimidohexanoic acid <i>N</i> -succinimidyl ester, DIPEA, THF, RT, 16h	22%
6-maleimidohexanoic acid, HATU, DMAP, THF, RT, 16h	74%

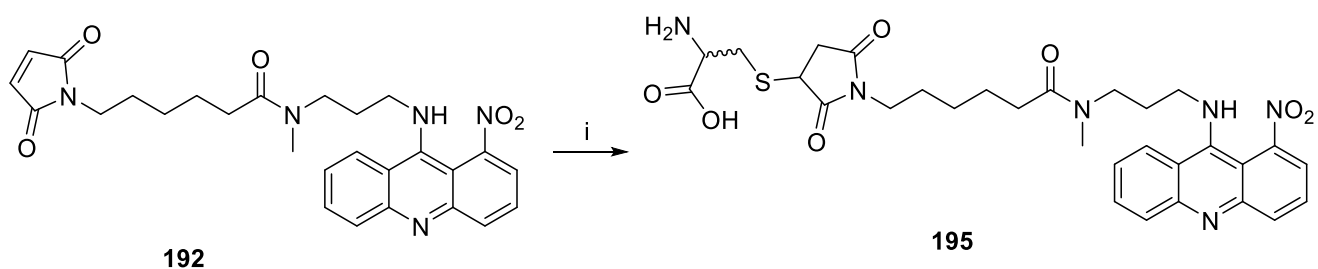
Table 8.1: Conditions and yields for the amide formation of **193** with 6-maleimidohexanoic acid.

For the 2-phenyl-4-quinolone, the trifluoromethoxy quinolone, **107** was selected as the first warhead as this was the compound identified from the NCI database. This also had the same problems as compound **112** previously, with no reaction with HATU. However, using the more reactive partner of 6-maleimidohexyl chloride was successful despite a low yield of 44% (Scheme 8.2). The work-up involved an acid and base wash which might have reduced the yield, with concerns of its stability. There is an argument between whether there is N or O alkylation. It was decided that alkylation did go on the amine due to the significant shift in the NMR of the vinyl proton. 2d NMR experiments such as HMBC also seemed to corroborate this.



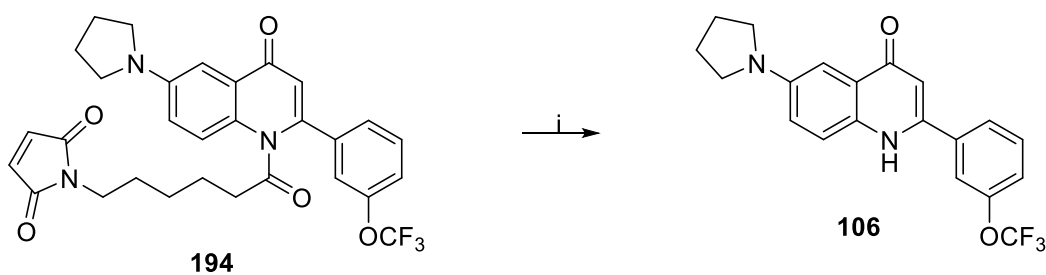
Scheme 8.2: Synthesis of non-cleavable quinolone linker; *Reagents and Conditions*: i) 6-maleimidohexanoic acid, oxalyl chloride, DMF, THF, RT, 18h, 44%.

In the cell, compound **194** would be released from the ADC after being broken down by catabolism with a single cysteine from the antibody still attached to the non-cleavable linker. Therefore, it might be useful to test this compound as this would be the active drug in the cell.



Scheme 8.3: 1,4-Michael addition of L-cysteine with maleimide group of non-cleavable linker **192**. *Reagents and Conditions*: i) L-cysteine, DABCO, DMF, RT, 6h, 52%.

For the 1,4 Michael addition to take place, the non-cleavable linker warheads were reacted with cysteine and DABCO. Initially, the non-cleavable nitroacridine, **192**, was used. This underwent conjugate addition with L-cysteine to afford **195** with a yield of 52%. Purification of the product proved challenging. The best separation was observed under normal phase conditions, however, the compound did not run smoothly on silica, as seen on TLC, requiring 10% ammonia in methanol for the desired compound to be eluted. A mixture of diastereomers was obtained but further purification was not necessary for biological testing as a mixture would be expected in the cell.



Scheme 8.4: 1,4-Michael addition of L-cysteine with maleimide group of non-cleavable linker **193** giving back the parent quinolone **107**. Reagents and Conditions: i) L-cysteine, DABCO, DMF, RT.

The reaction between **194** and L-cysteine was unsuccessful and instead of product being observed, the parent warhead, **106** was recovered instead, suggesting that the amide bond was hydrolysing in the reaction (Scheme 8.4).

To assess the stability of the compound, it was subjected to varying pH buffers (4, 7 and 10) and observed by NMR in a DMSO-*d*₆/D₂O system.

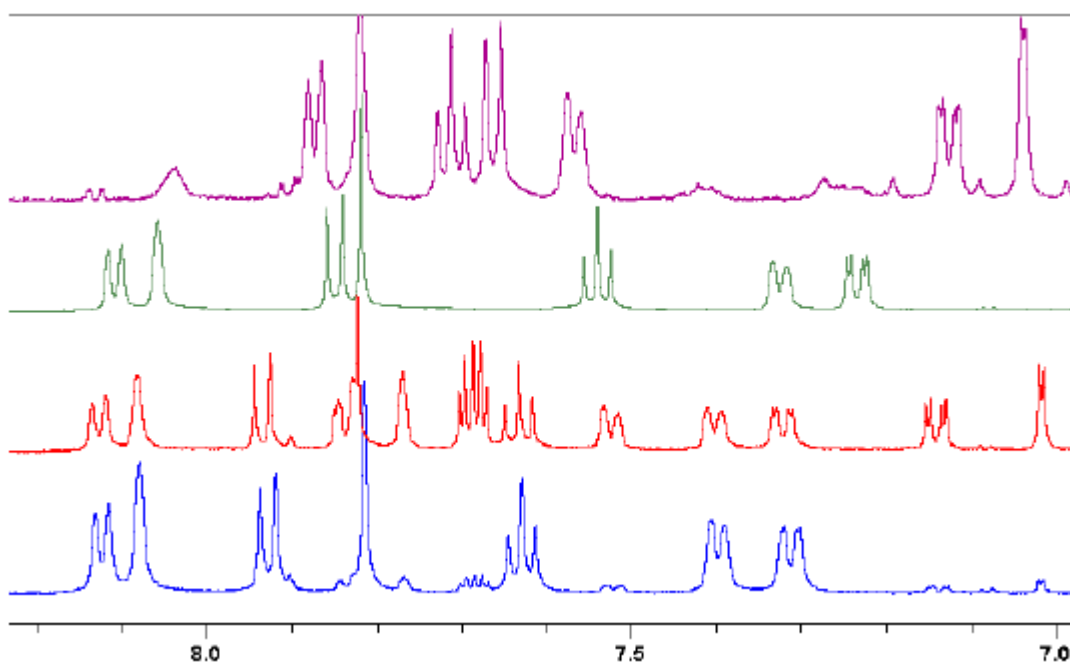


Figure 8.1: NMR comparison of aromatic regions of **194** at pH 4, blue – after 30 minutes, red – after 2 weeks, green – starting material, purple – parent quinolone.

For acidic conditions, at pH 4, hydrolysis was observed to be slow, and after two weeks, a 50:50 mixture of the quinolone and non-cleavable linked warhead was seen by NMR (Figure 8.1).

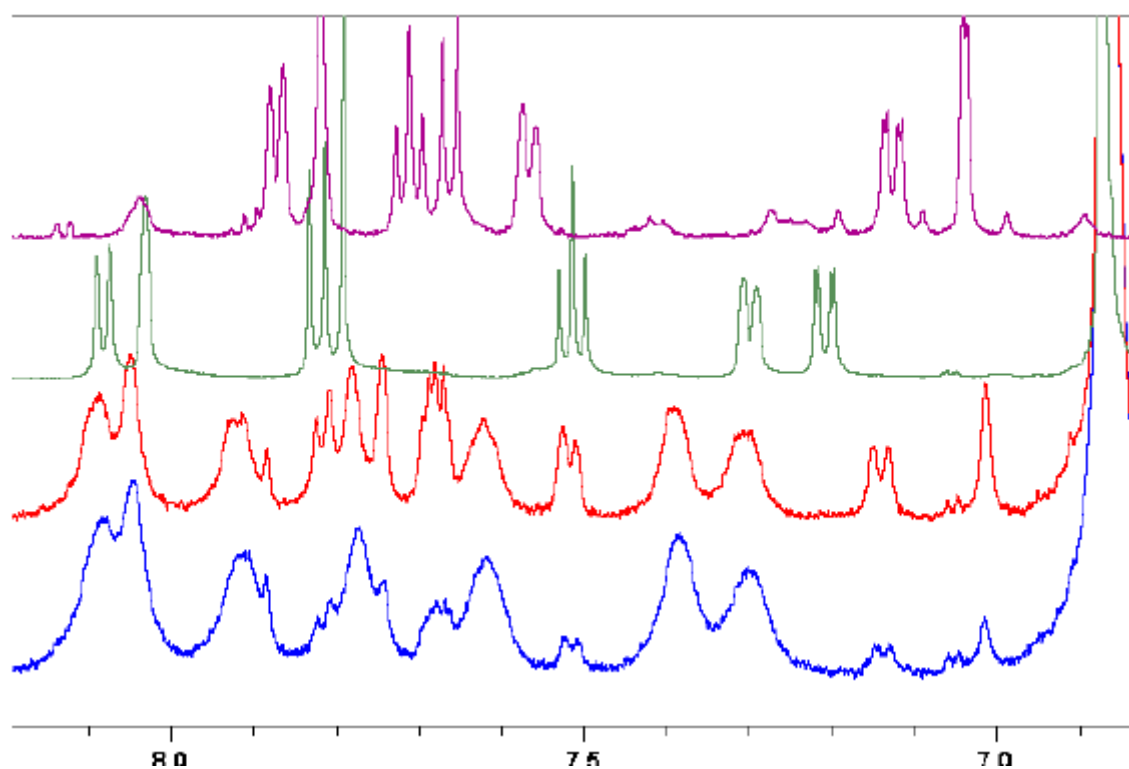


Figure 8.2: NMR comparison of aromatic regions of **194** at pH 7, blue – after 30 minutes, red – after 2 weeks, green – starting material, purple – parent quinolone.

At pH 7, the rate of hydrolysis was faster than that of pH4, and after two weeks, the ratio had also reached a 50:50 mixture, the same as the acidic buffer. Broader peaks were also observed, suggesting proton exchange was seen in this buffer solution.

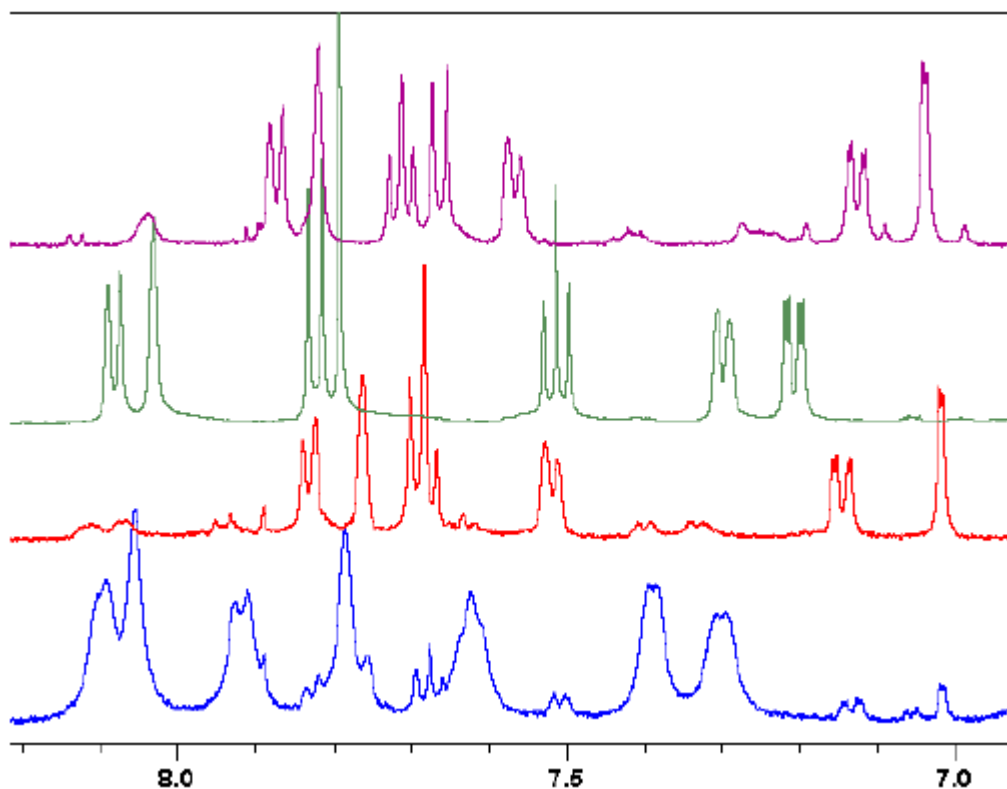
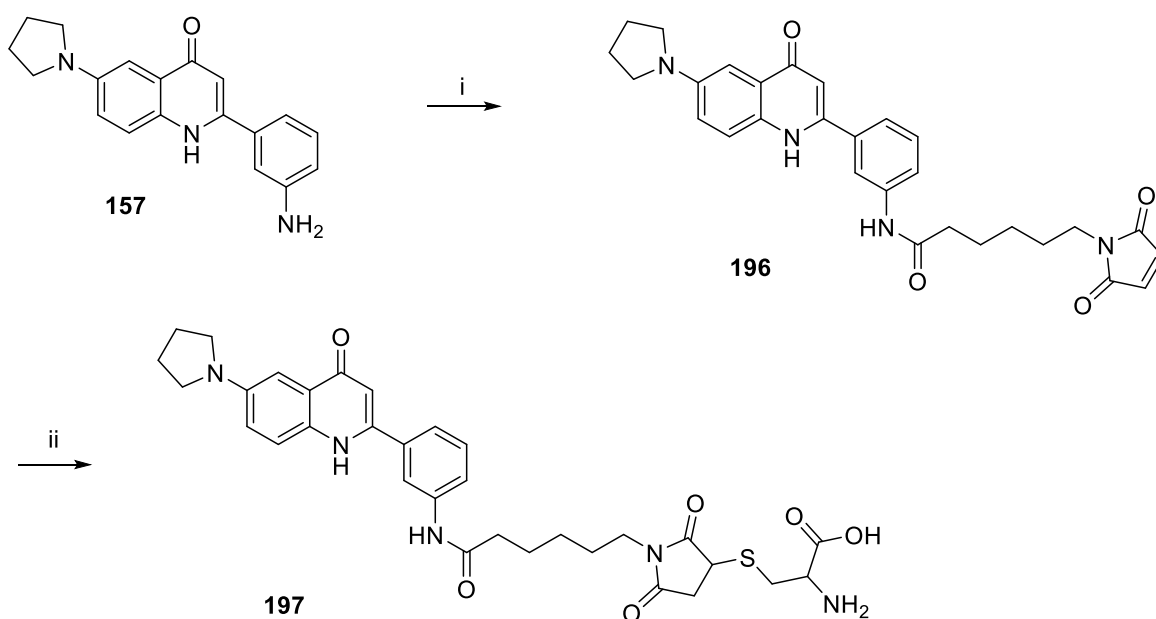


Figure 8.3: NMR comparison of aromatic regions of **194** at pH 10, blue – after 30 minutes, red – after 2 weeks, green – starting material, purple – parent quinolone.

However, at pH 10, hydrolysis of the amide was more rapid. Although initial hydrolysis after 30 minutes was similar to the previous two pH ranges, after two weeks there was near full conversion to the parent compound, indicating that basic conditions were pushing the hydrolysis to completion.



Scheme 8.5: Synthesis of cysteine derivative. Reagents and Conditions: i) HATU, 6-maleimido-hexanoic acid, Et₃N, DMF, RT, 18 h, 68%; ii) L-cysteine, DABCO, DMF, RT, 6h, 52%.

Due to the instability of this amide bond, attention switched to the aniline derivative **157** synthesised previously, which would allow a better handle for attachment of the non-cleavable and cleavable linker and allow for a more stable amide bond, with the aniline also being more reactive. HATU conditions were used for the amide formation previously used for the nitroacridine series (Scheme 8.5). These conditions were tried by Charlotte Rayburn and worked well but a mass ion corresponding to double acylation was observed in the LC-MS. This compound, **198** was also isolated and confirmed by NMR by the loss of the NH peak (Figure 8.4).

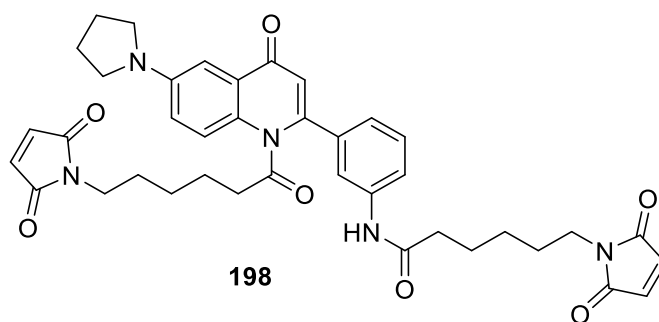


Figure 8.4: Structure of quinolone of double addition with 6-maleimido-hexanoic acid.

Given the proposed instability of the amide bond, the compound was redissolved in DCM and washed several times with 1M NaOH which was successful in cleaving one of the amide

bonds. The NMR showed both NHs, confirming addition was on the aniline. Including a basic wash in the work up helped in obtained more desired product.

Reacting on further with L-cysteine proved successful, giving adduct **196** with a yield of 56% using the same conditions as before with a mixture of diastereoisomers.

8.2. Synthesis of amino acid backbone

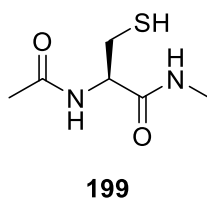
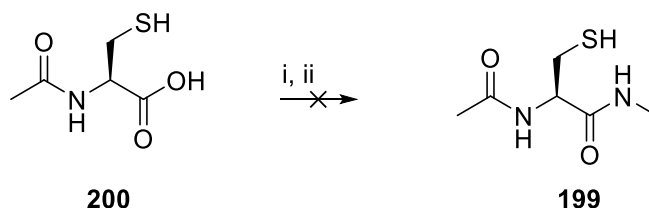


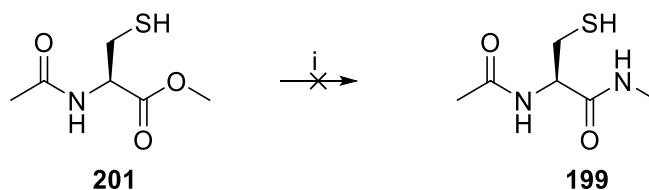
Figure 8.5: Structure of mimic for protein back bone **199**.

In order to better mimic the protein back bone for the conjugation, **199** was selected as a target to use for the 1,4 Michael addition.



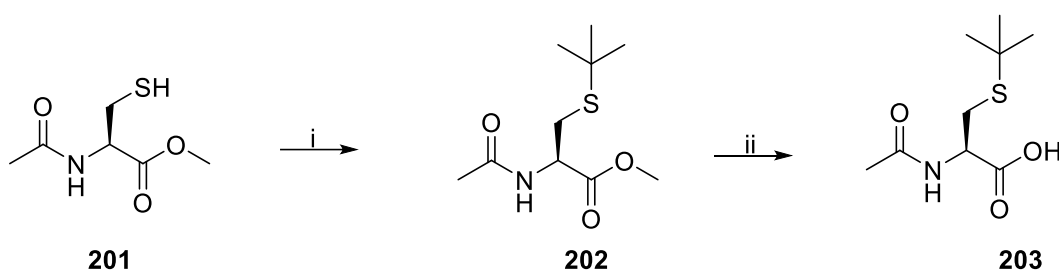
Scheme 8.6: Proposed synthetic route to **198**. Reagents and conditions: i) NMM, pivaloyl chloride, DMF/THF, RT, 16h; ii) MeNH₂.HCl, Et₃N, H₂O, RT, 6h.

Starting from *N*-acetyl- L-cysteine, **200** (Scheme 8.6), the acid was then activated using pivaloyl chloride *in situ* forming the mixed anhydride and then reacted with methylamine hydrochloride in an attempt to convert the acid to the methyl amide. However, this reaction did not work and upon work up, the NMR did not show product despite literature precedence.¹⁹¹



Scheme 8.7: Aminolysis of protected L-cysteine. Reagents and Conditions: i) 2M MeNH₂ in MeOH, MeOH, reflux, 5h.

Attempts were made to form the methyl amide from the *N*-acetyl protected cysteine methyl ester **201** as seen in the literature (Scheme 8.7).¹⁹² Instead of methylamine hydrochloride being used, this was switched with 2M MeNH₂ in MeOH. Upon reaction with *N*-Acetyl L-cysteine methyl ester at reflux, two spots were observed by TLC, and LC-MS gave the mass as 353 which correlates to the dimer of the starting material, but no desired product was observed. TLC of the starting material also gave the same two spots, compound **200** and the disulfide dimer. The reaction was heated to reflux in a sealed microwave vial to see if this would push the reaction, but no reaction occurred. A new route was determined which protected the thiol and may allow the use of amide coupling reagents without the thiol interacting (Scheme 8.8).



Scheme 8.8: Synthetic route to protect thiol with *tert*-butyl group. Reagents and Conditions: i) TFA, *t*-BuOH, RT, 4h, 87%; ii) 1M NaOH, MeOH, 5h, 60%.

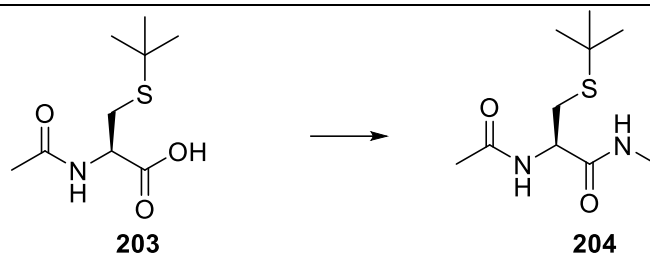
Starting from *N*-acetyl-L-cysteine methyl ester, **201**, the thiol was protected as a thioether using *t*-BuOH and TFA affording the product **202** in a yield of 87% (Scheme 8.8). This was chosen due to its relative ease of removal.

Once the thiol was protected, the ester was reacted with the conditions previously tried with refluxing with 2M MeNH₂ with the free thiol. However, these reactions did not lead to the product and so the ester was then hydrolysed using 1 M NaOH in MeOH giving a yield of 60% to allow amide coupling conditions to be attempted (Scheme 8.8). The low yield for the hydrolysis was ascribed to the high aqueous solubility of compound **203**, which had to be extracted out of the aqueous layer with 10% IPA in ethyl acetate. Once the carboxylic acid was obtained, several different amide conditions were attempted (Table 8.2).

Forming an acid chloride of the cysteine derivative with oxalyl chloride and reacting with methylamine did not yield product. It showed a complex crude NMR profile, with no indication of starting material or product present.

Another attempt using HATU with Et₃N with 2M MeNH₂ proved interesting and the crude NMR showed peaks correlating to product and starting material. Excess of methylamine was needed as using one or two equivalents was not sufficient in the completion of the reaction.

This was also the case for EDC.HCl. However, separation of product and starting material proved tricky and purification was not pursued.



Reagents

Result

i) Oxalyl chloride, DMF, THF, 2h; ii) Et ₃ N, 2M methylamine in THF, THF, RT, 6h	No reaction – crude NMR shows no product or starting material
HATU, Et ₃ N, 2M methylamine in THF, THF, RT, 16h	Crude NMR shows mixture correlating to S.M and product
EDC.HCl, DMAP, 2M methylamine in THF, THF, RT, 16h	Crude NMR shows mixture correlating to S.M and product
B(OCH ₂ CF ₃) ₃ , 2M methylamine in THF, MeCN, reflux, 18h	Crude NMR shows product only

Table 8.2: Conditions attempted for amide coupling of protected L-cysteine with methylamine.

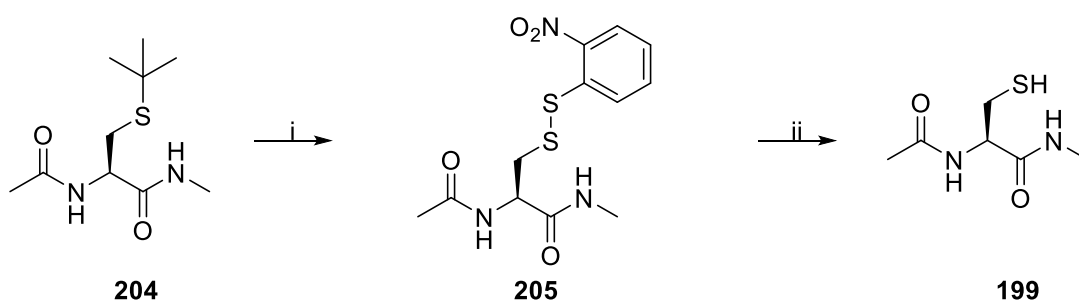
A fourth option was utilised instead. This involved using a borate catalyst reported by Sheppard *et al.*¹⁹³ The catalyst was commercially available and allowed for direct amidation with amino acids; methylamine was not reported as an example however. This reaction gave a cleaner reaction profile and the product did not need to be purified after workup as the borate catalyst was washed out giving a modest yield of 69%.

Once the methyl amide was in place, the *t*-butyl could be removed (Table 8.3). Initially, common acidic conditions were tried such as TFA in DCM and TFA neat, which is commonly used in the deprotection of *t*-butyl thioethers (Table 8.3). Refluxing in TFA led to degradation of the starting material. Unfortunately, as this was not successful, other methods were explored. Another method which has been used is the use of *p*-toluenesulfonic acid, but this degraded the product, giving a complex crude NMR profile. 85% H₃PO₄ has been used to remove the *t*-butyl group from ethers but this failed to work in the case of the thioether.¹⁹⁴

Reagents	Result
50% TFA in DCM, 16h	No reaction – S.M recovered
TFA neat, 16h	No reaction – S.M recovered
TsOH.H ₂ O, toluene, reflux, 6h	S.M degraded
85% H ₃ PO ₄ , THF, RT, 6h	No reaction – S.M recovered

Table 8.3: Deprotection conditions attempted for removal of *tert*-butyl group.

There were multiple papers in the literature suggesting the conversion of the *t*-butyl thioether into a disulphide using sulfenyl chlorides, creating an unsymmetrical disulfide bridge. It was hoped that reduction of a disulphide bond to the free thiol would be easier than from the *t*-butyl thioether. Variations in the disulphide bridge partner were seen but the first substitution tried was with 2-nitrosulphenyl chloride which gave the product **205** in a yield of 49%.¹⁹⁵ Following on, reduction of the disulphide bridge was initially tried with NaBH₄.¹⁹⁶ However, in this case it did not afford any product and no starting material was recovered, with the reaction profile too messy.



Scheme 8.9: Conversion of *t*-butyl group to disulphide bridge and subsequent reduction of bridge. Reagents and conditions: i) 2-nitrosulphenyl chloride, acetic acid, RT, 6h, 49%; ii) PPh₃, H₂O, THF, RT, 4h, 19%.

Different reducing agents were therefore used. Use of triphenylphosphine in a H₂O/THF system did prove successful but gave a yield of just 19%. The low yield was mainly due to a

difficult work up and purification. The other issue was the byproduct which was the dimerization of the compound, which could not be avoided. This could be overcome by reduction *in situ* then followed by a Michael addition with the maleimide functional group. It was also trialled with the more aqueous soluble TCEP and slightly improved the yield to 24%. The purification was simpler owing to an aqueous wash in the work up removing most of the TCEP.

Upon scale up however, the amide coupling reaction using the borate catalyst failed, giving erratic yields on repeat. Despite using the exact same conditions and concentrations, the reaction did not prove to be successful and coupled with low yields was consequently not used, with L-cysteine being in its place.

Future attempts would be direct amidation between unprotected L-cysteine and methylamine and different alternative disulphide bridging partners.

8.3. Biological evaluation of non-cleavable linkers

The non-cleavable linkers and their cysteine derivatives were tested in an SRB assay on MCF-7 cells (Table 8.4). The potency of all the compounds were found to be poor. For the cysteine conjugated compounds, this can be explained by the zwitterion present with the cysteine. High molecular weight charged compounds can have difficulties crossing the cell membrane and so a reduced activity from this is not unexpected. For compounds **192** and **195**, cell permeability could be a factor and thus resulting in poor activity. The modification with a sterically demanding maleimide linker could also be affecting the warhead's ability to kill cells, preventing its mechanism of action, leading to no activity seen.

Compound **206** was synthesised by acetylating amine **113** and was also tested in the same assay (Scheme 8.10). The acetamide **208** was found to be active with a GI₅₀ of 28 ± 1.2 nM. This is less potent than the parent compound **114** (6 ± 1.4 nM) but demonstrates that small modifications of the amine do not lead to significant potency loss or cell permeability.

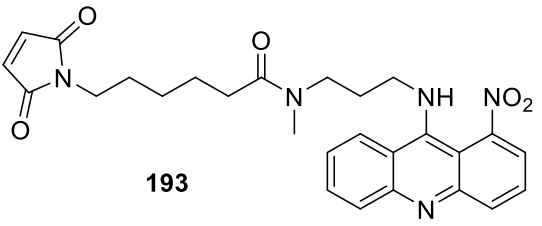
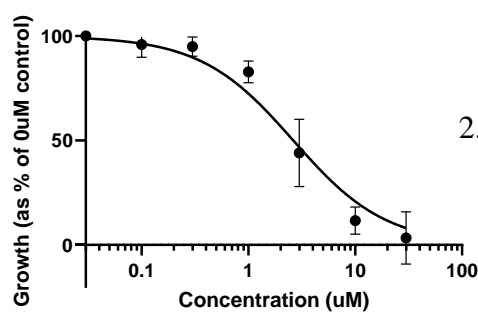
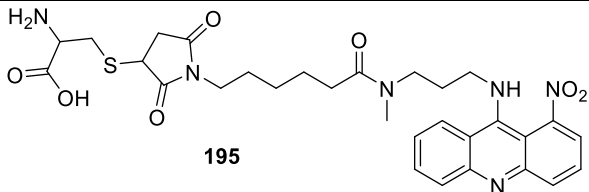
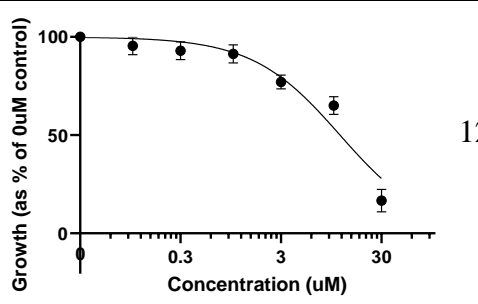
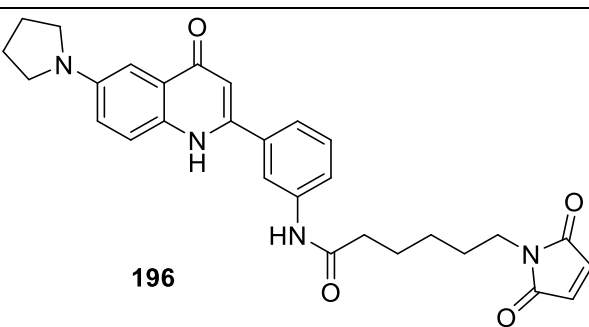
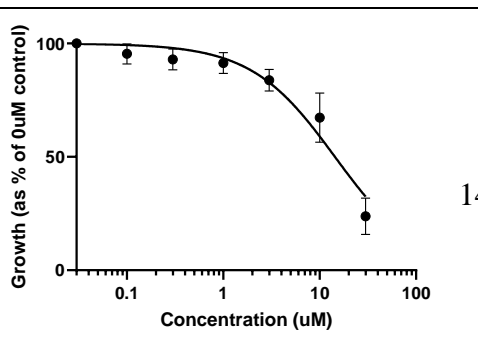
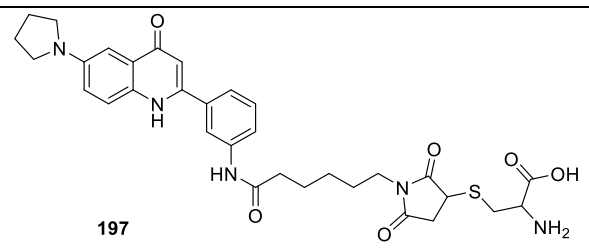
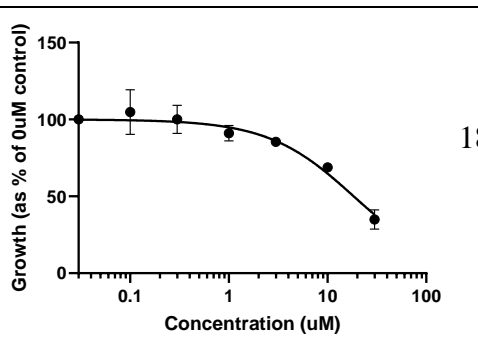
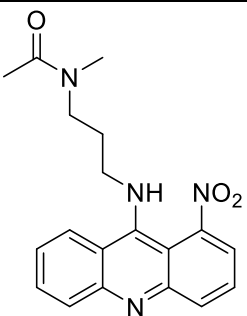
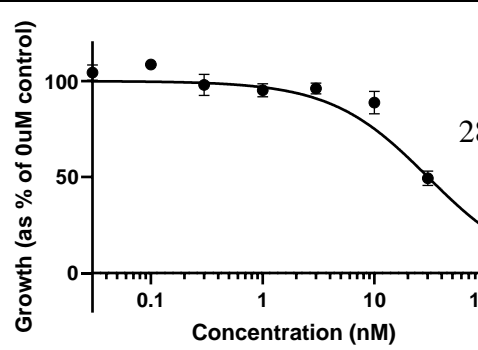
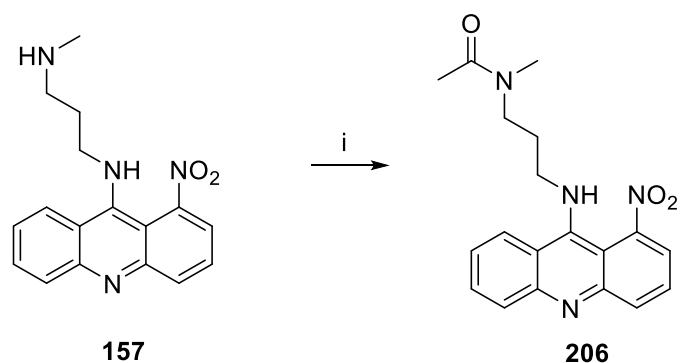
Compound	Cell assay	GI ₅₀
 <p data-bbox="391 369 438 414">193</p>		$2.6 \pm 0.5 \mu\text{M}$
 <p data-bbox="446 694 494 739">195</p>		$12.7 \pm 0.4 \mu\text{M}$
 <p data-bbox="375 1142 422 1187">196</p>		$14.1 \pm 2.4 \mu\text{M}$
 <p data-bbox="343 1444 391 1489">197</p>		$18.2 \pm 0.6 \mu\text{M}$
 <p data-bbox="670 1792 718 1836">206</p>		$28 \pm 1.2 \text{ nM}$

Table 8.4: Cytotoxicity data for non-cleavable linkers and cysteine derivatives as well as acetylated nitroacridine evaluated on MCF-7 cell line after 72 h, n = 2 (10 repetitions per replicate), error calculated from mean values.



Scheme 8.10: Synthesis of acetamide . *Reagents and Conditions:* i) Acetic anhydride, K_2CO_3 , DMF, 4 h, 44%.

8.4. Cleavable linkers

As discussed previously, a dipeptide cleavable linker was chosen which would exploit the use of proteases found in the cell to cleave and release the warhead (Figure 8.6). This linker would allow release of the nitroacridine in the cell.

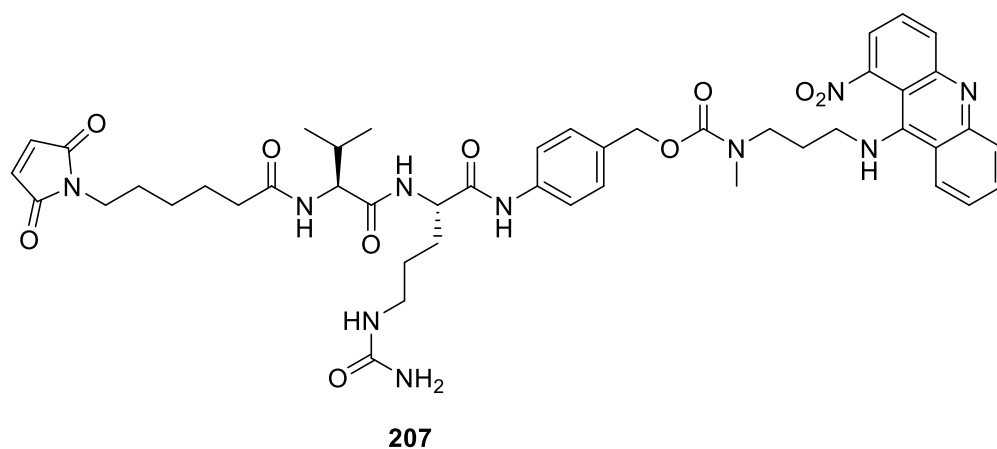
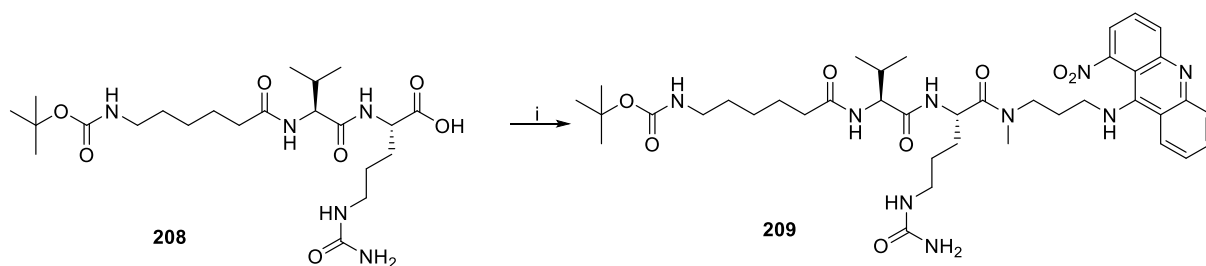


Figure 8.6: An example of a cleavable linker nitroacridine target, **207**.

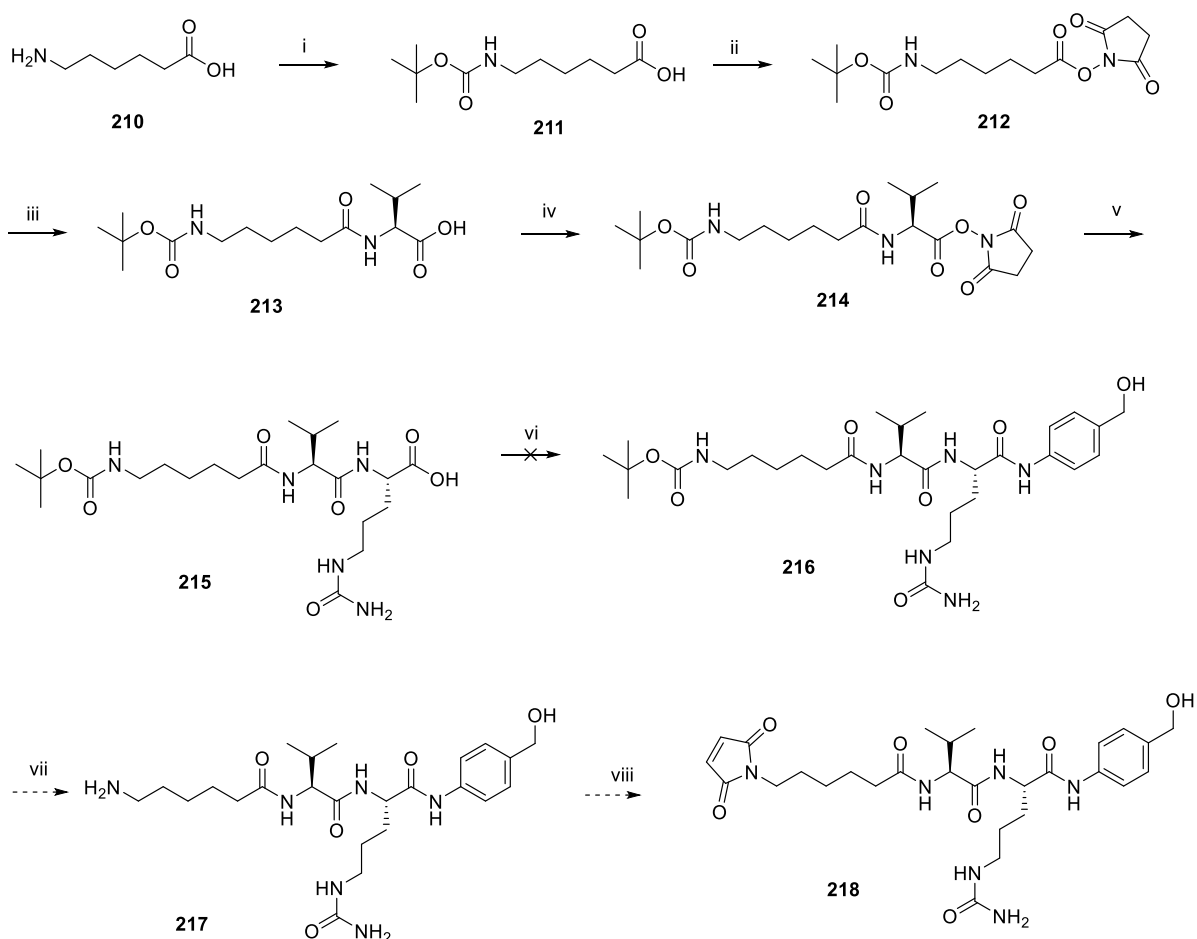
Another reason for this choice of route was to enable the synthesis of a linker without the immolative PAB-OH in place (Scheme 8.11). This would be to determine the necessity of the immolative spacer and whether it was needed as the relative size of the warhead compared to the linker was not large, unlike the natural products that are often used. This would be done after **207** was synthesised and evaluated.



Scheme 8.11: Proposed synthesis of cleavable linker without PAB spacer in place. Reagents and conditions: i) EEDQ, **157**, DCM, MeOH.

The first proposed route is shown in Scheme 8.12 employing peptide chemistry in which carboxylic acids are activated to the succinimide esters for mild and effective amide coupling with amines to avoid any epimerisation.¹⁹⁷ The maleimide group would be installed at the end of the synthesis to ensure that no side products could form from addition to the Michael acceptor.

Starting with commercially available 6-aminohexanoic acid **210**, the amine was protected with the Boc protecting group using Boc_2O with DMAP in DCM at 0 °C. This proceeded in an excellent yield of 88% and required no further purification after work-up. Activation of the carboxylic acid using *N*-hydroxysuccinimide also proceeded well using DCC in DCM to form the ester **212**. Removing the biproduct DCU was problematic. The reaction mixture could initially be filtered to remove the white precipitate formed in the reaction and purification could be achieved by exploiting this insolubility of DCU and so the filtrate was concentrated *in vacuo*, redissolved in the minimum amount of DCM, cooled to 0 °C and filtered again. This was repeated several times. However, some of the impurities still remained and were visible in the NMR. It was not necessary to completely eliminate this impurity and so could be used in the next step.



Scheme 8.12: Initial route to cleavable linker **218**. Reagents and Conditions: i) Boc_2O , DMAP, DCM, RT, 88%; ii) *N*-hydroxysuccinimide, DCC, DCM, 91%; iii) L-valine, NaHCO_3 , DME: H_2O , RT, 73%; iv) *N*-hydroxysuccinimide, DCC, DCM, RT, 88%; v) L-citrulline, NaHCO_3 , DME: H_2O , RT, 65%; vi) EEDQ, 4-aminobenzyl alcohol, THF; vii) TFA/DCM; viii) acetic acid, maleic anhydride.

The next step involved forming the amide bond using L-valine with a base, in this case NaHCO_3 . A polar solvent system of DME and water was used to allow for solubility of both organic and aqueous soluble components. A weak acid, 15% citric acid, was used to quench the reaction. Extraction of **213** did cause initial problems due to the polarity of the product and so stayed in the aqueous phase even once the aqueous phase was neutralised. To combat this, 10% IPA in EtOAc was used, which allowed the product to be extracted. Again, no further purification was carried out, but some small impurities did remain from the NMR. The same process was again used to attach L-citrulline, by first activation of L-valine as the *N*-hydroxysuccinimide, **214** and then reacting on with L-citrulline to give **215**.

For the amide coupling of 4-aminobenzyl alcohol with the dipeptide chain **215**, EEDQ was chosen due to its literature precedent for this reaction.¹⁹⁸ This is because it is known to reduce racemisation in comparison with other amide coupling agents. It does not require a tertiary

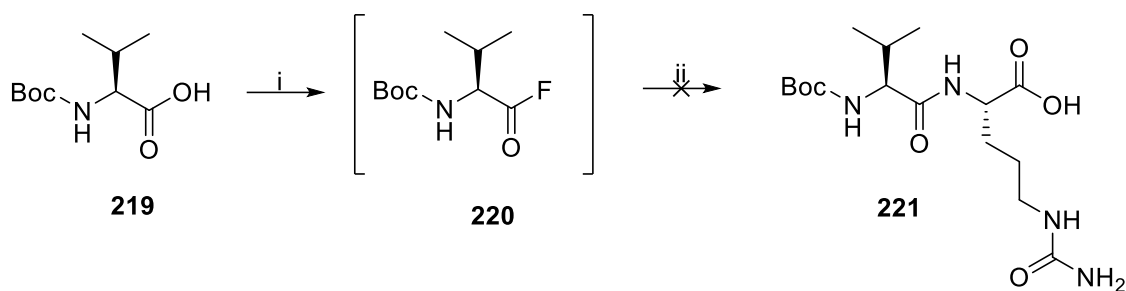
base and although the anhydride is formed relatively slowly, it is consumed quickly, reducing the propensity for racemisation in this step.

The resulting crude product, **216** from this step showed many spots on TLC, and the crude NMR appeared complex. Upon purification, TLC analysis showed one spot but the NMR was again complex, indicating unusual splitting patterns for the peaks suggesting two similar compounds. One explanation could be rotamers due to the steric hindrance of the amine. A VT NMR was undertaken to examine this possibility. Despite going upwards to a final temperature of 125 °C, the peaks showed no sign of coalescing and so the idea of rotamers was discounted.

Another possibility was epimerisation. From a HPLC analysis of the compound, two closely running peaks were identified. These were attempted to be separated through semi-preparative HPLC. Due to the presence of the Boc group, separation was poor and was removed before proceeding using 10% TFA in DCM. In running the method to increase separation of the compounds, further peaks running very closely were found as well, indicating multiple different compounds. After purification, NMR spectra of each peak were assessed. The NMR showed no difference from before purification and the HPLC analysis showed multiple peaks. This suggested that the compound was unstable and was decomposing.

Due to the failure of this route, new routes were considered. One change was to remove the alkyl chain and instead use commercially available 6-maleimidohexanoic acid instead, involving an amide coupling reaction with L-valine. Another suggested change was the coupling between L-valine and L-citrulline by using an acyl fluoride. This mild method would allow the coupling to happen in one pot and should not lead to epimerisation of the compound. As previously mentioned, it would be beneficial to add the maleimide group last and so the dipeptide was synthesised first.

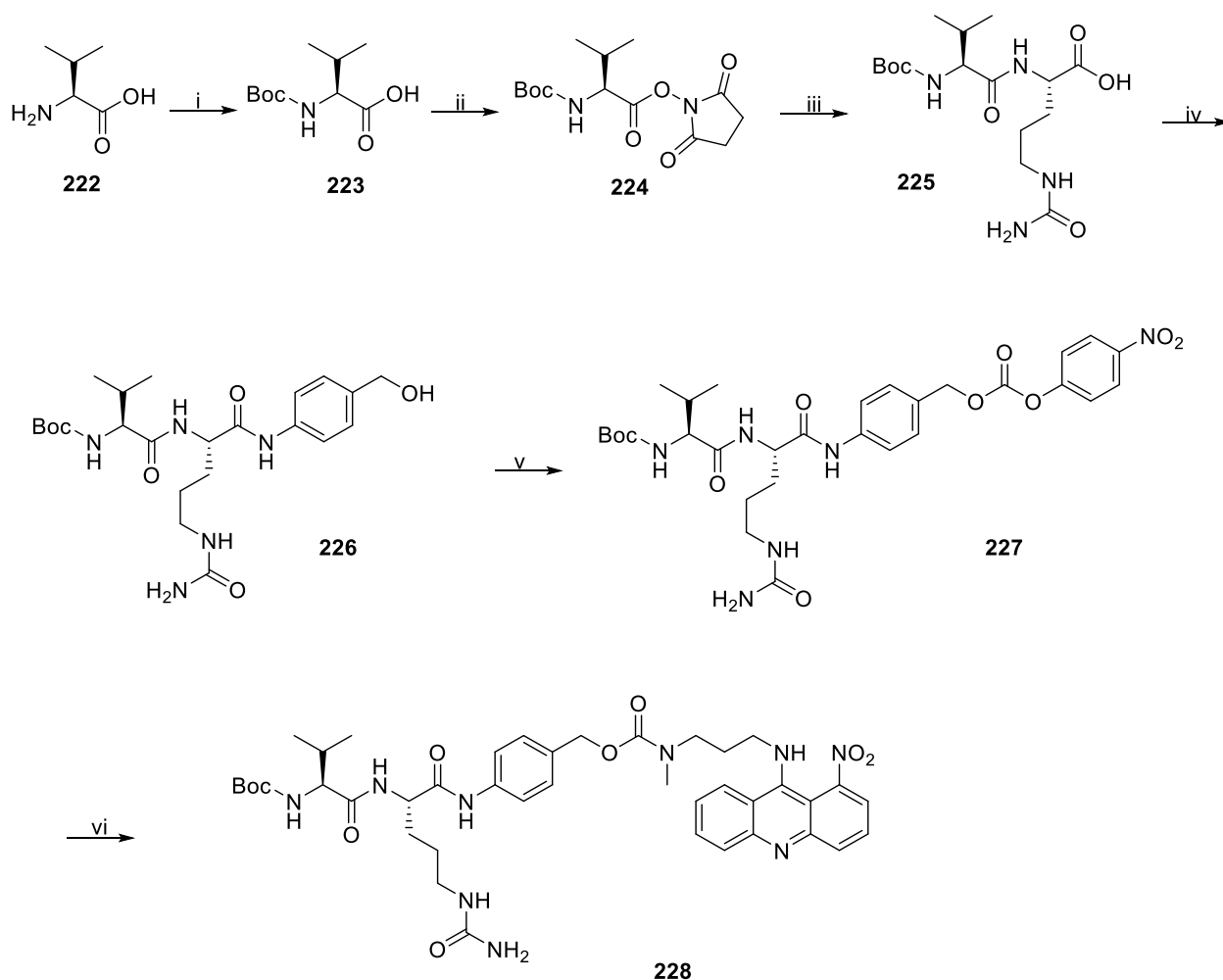
Boc-protected L-valine, **219** was treated with cyanuric fluoride with pyridine in DCM to fluorinate the acid to give intermediate **220** (Scheme 8.13).¹⁹⁹ Although **220** was not isolated, a crude IR was performed to check whether the reaction had worked, and a stretch at 1860 cm^{-1} was observed, consistent with the presence of an acyl fluoride. No product, **221** was seen however after L-citrulline was added. The methyl ester L-citrulline was also used in the reaction but this also yielded no product.



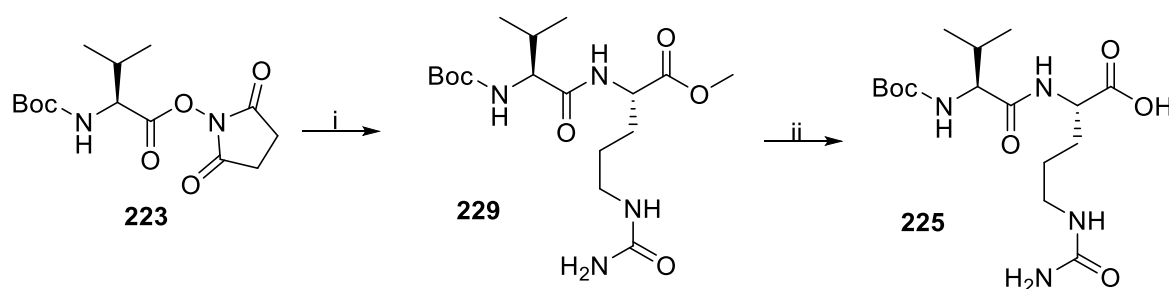
Scheme 8.13: Formation of acyl fluoride and addition of L-citrulline. Reagents and conditions: cyanuric fluoride, pyridine, DCM; ii) L-citrulline, NaHCO₃, THF

A final proposed route was used as seen with the previous route and reported in the literature²⁰⁰; activation of L-valine with succinimide ester was attempted and gave a crude yield of 96% (Scheme 8.14) affording **224**. In this case, L-citrulline methyl ester was initially used. The proved successful as the coupling partner affording **229** in a good yield of 97%. Deprotection of the methyl ester with sodium hydroxide again proved difficult but repeated washing of the aqueous layer with 10% IPA in EtOAc gave **225** in a good yield of 84%. This amide coupling was also tried with unprotected L-citrulline and also worked giving **225** in a yield of 76%. The reaction was quenched with 15% citric acid and extracted with 10% IPA in EtOAc and proved successful, thus eliminating an extra step and could be used directly in the next step.

The reaction with 4-aminobenzyl alcohol and the dipeptide **225** with EEDQ did not proceed as smoothly as anticipated. One of the issues with this reaction was solubility, hence the need for a multi solvent system. The reaction often produced a sticky gum in the reaction mixture which did not dissolve easily. The reaction was also wrapped in tin foil to exclude light as EEDQ is light sensitive. The purity of the starting material could also have affected the yields and cause issues with the solubility but attempts at purification of dipeptide **225** led to poor recovery and yields so was used directly in the next step.



Scheme 8.14: Synthetic route to the cleavable linked warhead. Reagents and conditions: i) Boc_2O , NaOH, THF, 0 °C – RT, 4 h, 94% ii) *N*-hydroxysuccinimide, DCC, THF, 0 °C – RT, 15 h, 107%; iii) L-citrulline, NaHCO_3 , DME, THF, H_2O , RT, 16 h, 89%; iv) 4-aminobenzyl alcohol, EEDQ, MeOH, DCM, RT, 34%; v) 4-nitrophenyl chloroformate, pyridine, THF, RT, 5 h, 26%; vi) HOBt, DIPEA, **113**, DMF, RT, 16h, 67%.



Scheme 8.15: Alternative route to acid **225** through the methyl ester. Reagents and Conditions: i) L-citrulline methyl ester, NaHCO_3 , DME, THF, H_2O , RT, 18 h, 74% ii) NaOH, MeOH, RT, 6h, 38%.

The work up was equally challenging as it was hard to extract the product, which was not as soluble in the extracting solvents and after purification gave a low yield of 38% of **226**. To avoid this problem, it was decided to put the crude reaction mixture straight onto Isolute® and purified by chromatography directly. However, this decreased the separation of the product as

the crude product had multiple impurities and the yield only modestly improved to 67%. Despite the fact that LC-MS indicated that starting material had been fully consumed and product was seen, purification had a significant impact on the yield.

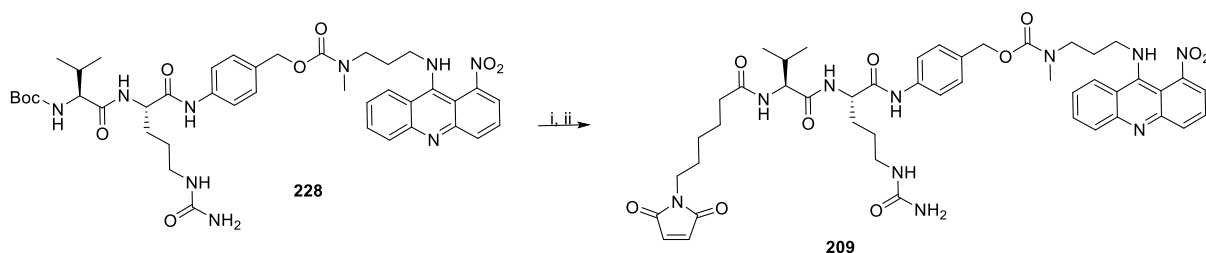
At this point, other amide coupling reagents were assessed including EDC.HCl and HATU. On a small scale they both gave good yields in comparison with EEDQ (78% and 69% respectively) but this did not translate into a larger scale with poorer yields obtained than that with EEDQ and were as consequence not used. Interestingly, no racemisation was observed during this step, and so EEDQ would not necessarily need to be used to avoid this problem.

Once the PAB-OH was in place, **226**, the next task was to create the carbamate linker. This could be achieved using various agents such as CDI or phosgene. However, literature precedence had dictated the use of chloroformates in order to form a carbonate, allowing for a mild method. Initially, the reaction was carried out in an excess of pyridine, but LC-MS of the reaction mixture showed that conversion was slow and had stalled mid-way through the reaction. Therefore, more nitrophenyl chloroformate was added sequentially until the starting material had been consumed. Repeating the reaction using an excess of the chloroformate did not lead to complete conversion. Also, changing the amount of pyridine for fewer equivalents in DCM was also tried. Although this did not necessarily improve the conversion, it meant less pyridine was needed overall.

The product, **227** was initially quenched with 15% citric acid and worked up, however, this led to very poor yields. Instead, concentrating the solution, and columning directly did improve yields, but not significantly (up to 65%). **227** itself was stable under nitrogen and under column chromatography conditions so was not degrading quickly. However, the conditions used for the column used upwards of 5% MeOH as eluent and this could potentially react with the carbonate.

The warhead **113** could then be coupled to the peptide with the installation of the maleimido group was done last, as to prevent epimerisation as seen before. Initially the nitroacridine warhead **113** was used and was coupled using HOBt. The reaction worked well with starting material being consumed, and the excess warhead was recovered. However, isolating **228** proved challenging. Purification in normal phase conditions cleaned up the product to a degree but TLC showed multiple impurities remained. A further reverse phase column, using THF and H₂O under neutral conditions were used, and although by TLC was impure, NMR showed enough purity to continue with the synthesis.

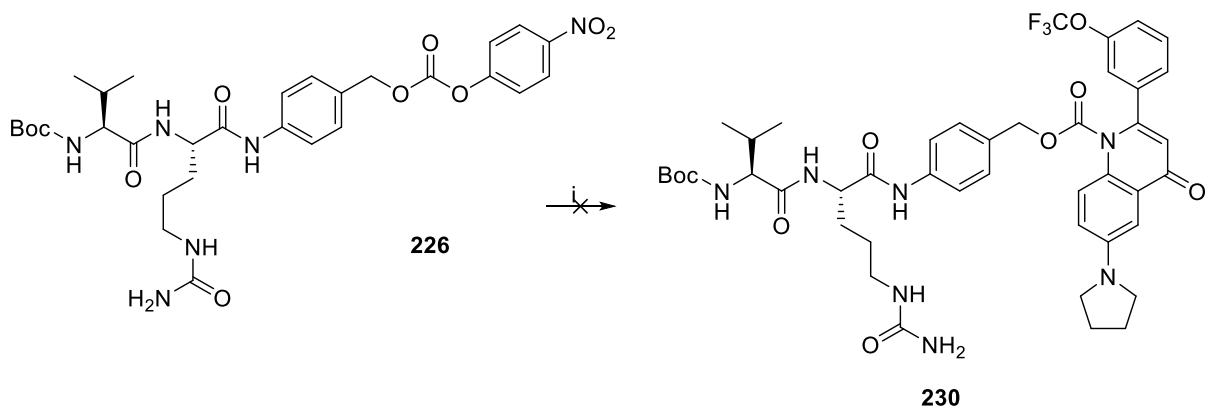
Removing the Boc group was the next step. This was done with 10% TFA in DCM and from TLC, it was hard to tell whether the reaction had gone to completion or not as the R_f of the starting material and product were unusually close (Scheme 8.16). It was also noted on LC-MS that often the peak corresponding to starting material showed a mass corresponding to the loss of Boc, presumably occurring in the mass spectrometer but there was a slight difference in retention times.



Scheme 8.16: Synthetic route to nitroacridine cleavable linker. *Reagents and Conditions:* i) 10% TFA in DCM, RT, 26%; ii) HATU, DIPEA, DMF, RT.

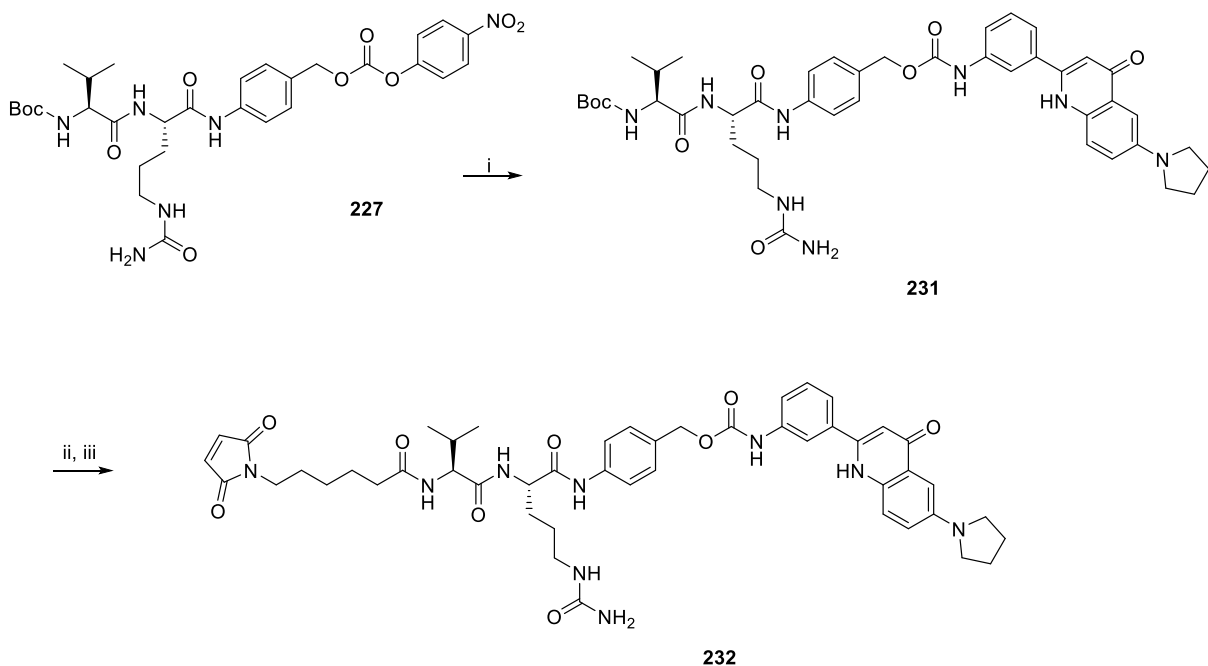
Once the amine deprotection had gone to completion, the solvent was removed, the crude was dissolved in DMF, quenched with excess DIPEA and 6-maleimidosuccinimide ester was added. From LC-MS, some product had formed but there were also several impurities. Once the starting material had been consumed, the reaction was worked up. Purification proved challenging and after various unsuccessful procedures it was decided that purification through semi-preparative HPLC would be most effective. No product was isolated from this method though.

An alternative method was also attempted. This involved the use of HATU with 6-maleimidohexanoic acid instead of the succinimide ester. After 16 hours, the starting material had been consumed, and there were mass peaks for the product present. The reaction did not seem to form epimers and had a better reaction profile than the previous step with a yield of 52% and was used subsequently as no semi-prep HPLC was needed.



Scheme 8.17: Attempted synthesis of **230**. *Reagents and Conditions:* i) HOBt, DIPEA, **157**, DMF, RT, 16h.

Attempts at reacting **106** with **226** failed and gave back starting material. As noted previously, the reactivity of the quinolone nitrogen is electron deficient, leading to low nucleophilicity and concerns about hydrolytic stability of the product. For the aniline, **157** this reaction worked modestly with a yield of 64%, to give **231** (Scheme 8.18). Like before, the Boc group was deprotected before the maleimide was installed with HATU, giving **232** in a good yield of 56%.



Scheme 8.18: Synthetic route to cleavable linked quinolone **232**. *Reagents and Conditions:* i) HOBt, DIPEA, **157**, DMF, RT, 16h, 64%; ii) 10% TFA in DCM, RT, 26%; iii) HATU, DIPEA, DMF, RT, 56%.

However, the purification was again problematic, and a combination of normal phase and reverse phase procedures needed to be utilised. For the purposes of conjugations, the product did not need to be 100% pure but needed to be clear of any reactive compounds such as

residual 6-maleimidohexanoic acid or any similar functional groups that could interfere with the conjugation process. These intermediates were ready to be conjugated to the antibody.

8.5. Urea Linker

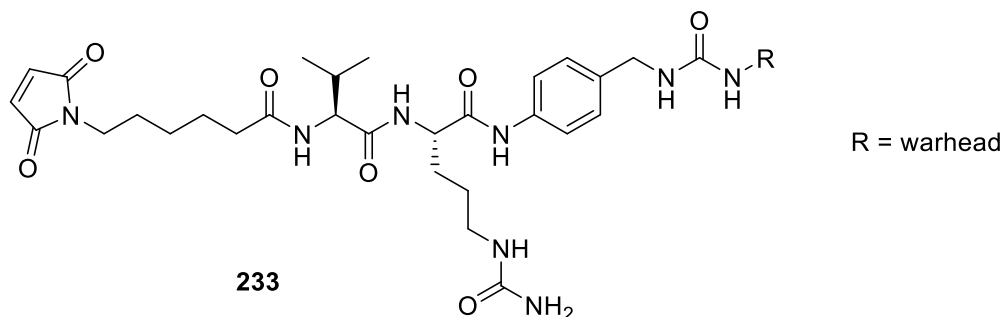
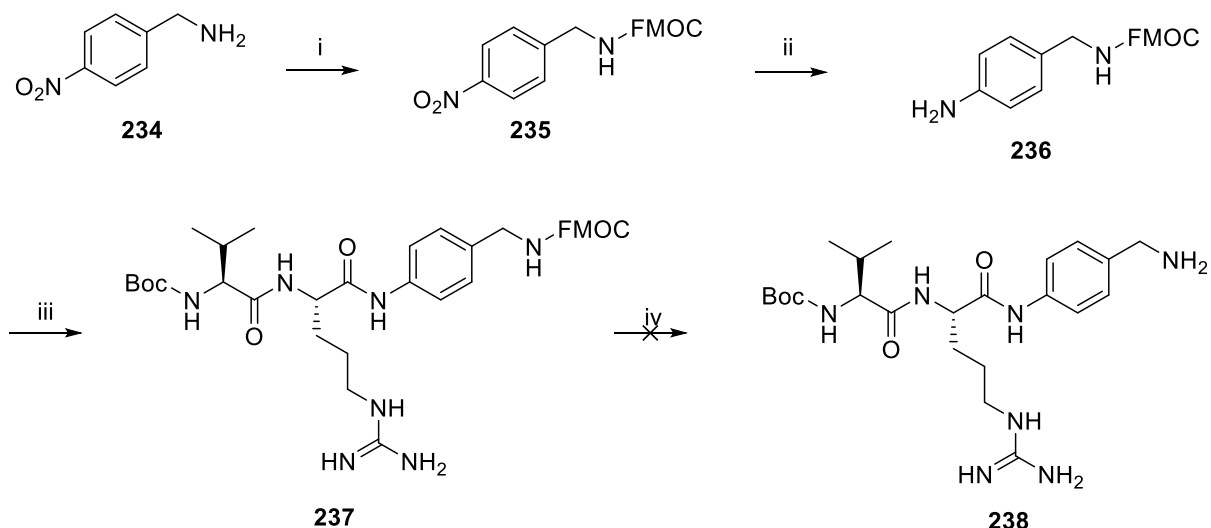


Figure 8.7: A urea cleavable linker

Due to the apparent instability of compound **106** with the previous linkers, a urea derivative was proposed (Figure 8.7) as this might lead to a more stable linker. It would also be interesting to note any differences in the release mechanism. To generate the urea linker, protecting groups would need to be used (Scheme 8.19). An Fmoc protecting group was chosen due to its established use in peptide chemistry and orthogonality to the Boc protecting group on the dipeptide. It would also be orthogonal to the nitro group and not be removed under hydrogenation conditions which would be used to reduce the nitro to the aniline.



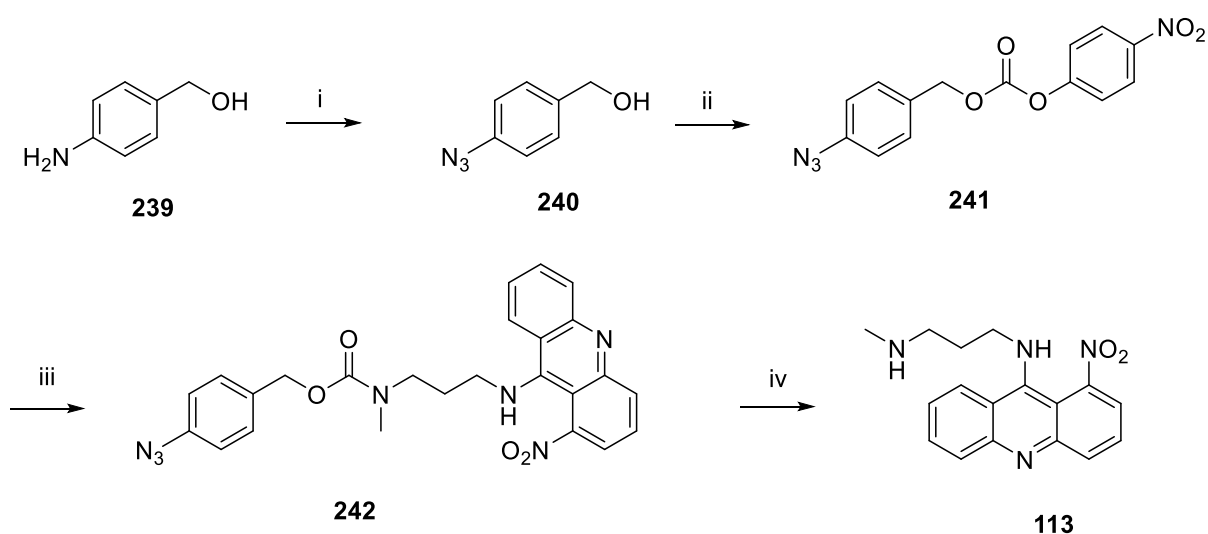
Scheme 8.19: Attempted synthesis of urea linker. Reagents and conditions: i) Fmoc chloride, DIPEA, DCM, RT, 6h, 44%; ii) H₂, 10% Pd/C, DCM, MeOH, RT, 16h, 72%; iii) EEDQ, **225**, DCM, MeOH, RT, 16h, 49%; iv) 20% piperidine in DMF, RT.

4-Nitrobenzyl amine, **234**, was reacted with Fmoc chloride and was completed in 6 hours to give the Fmoc protected amine, **235** in modest yield of 44%. The nitro group was then reduced using 10% Pd/C with H₂ gas to the amine **236** in a yield of 72%. The LC-MS showed 100%

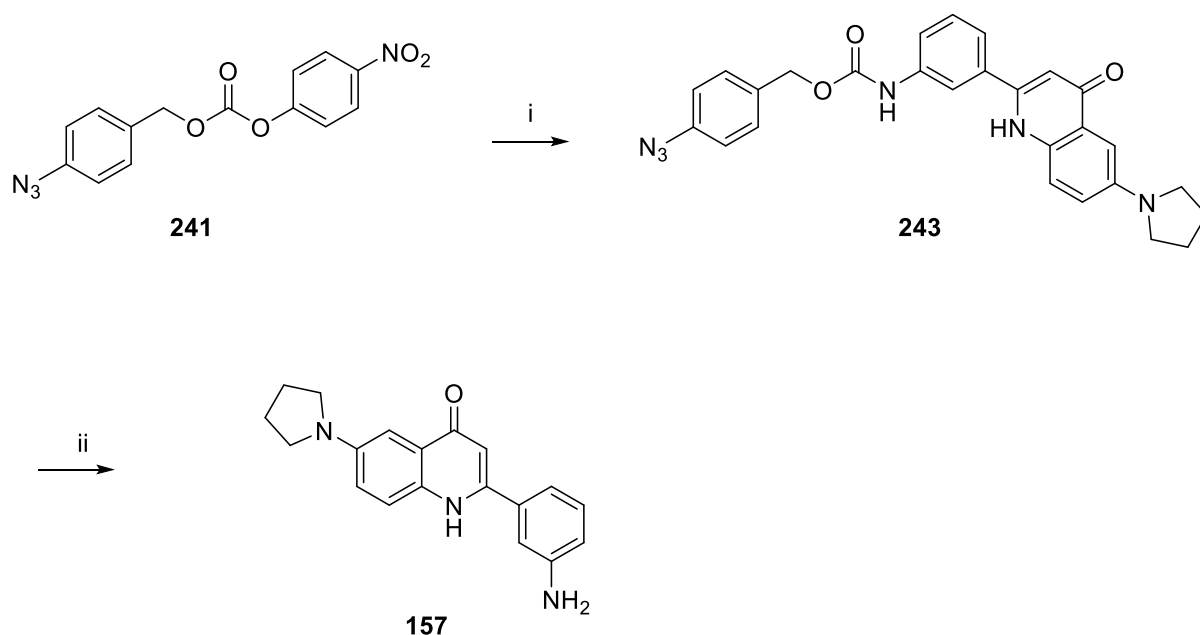
conversion to the product, but due to the insolubility of the product, some was lost on filtration through Celite® despite repeated flushing. **236** was then reacted with **225** to give **237** in a yield of 49%. The compound proved challenging to purify as it was insoluble and so some product was lost through flash column chromatography. The removal of the Fmoc group failed with 20% piperidine. The compound did not go into solution and only starting material was seen. This work was paused due to priority shifted away from using compound **106**.

8.6. Model System for Release Mechanism

To confirm that the immolative linker would release the warhead, a model system was studied. The synthesis of the model system would employ an azide to be reduced to the aniline, which would initiate the release of the warhead (Scheme 8.20).



Scheme 8.20: Route for the model system. *Reagents and Conditions:* i) Sodium nitrite, 6 M HCl, H₂O, 0 ° to RT, 5 h, 69%; ii) 4-nitrophenyl chloroformate, pyridine, THF, RT, 6 h, 46%; iii) **113**, Et₃N, DMF, RT, 16 h, 65%; iv) TCEP.HCl, H₂O, THF, RT, 1h, 30%.



Scheme 8.21: Route for the model system. *Reagents and Conditions:* i) **157**, Et₃N, DMF, RT, 16 h, 46%; ii) TCEP.HCl, H₂O, THF, RT, 1h, 98%.

Starting with 4-aminobenzyl alcohol, **239**, the benzenediazonium ion was formed by reacting with sodium nitrite under strong acidic conditions, (6 M HCl), at 0 °C.²⁰¹ The intermediate was then immediately reacted with sodium azide *in situ* to form the azide **240** in a good yield of 69%, which was filtered from the reaction. Once the azide was in place, a similar reaction with 4-nitrophenyl chloroformate was undertaken as seen previously for the peptide linker. Like before, the reaction did not proceed as straightforwardly as expected, with excess 4-nitrophenyl chloroformate needing to be added to give the product, **241**, but did give a good a yield of 80%.

It should be noted that the azide products were not stable long term, even under N₂ and would turn brown. TLC analysis had shown that degradation was likely, with the formation of multiple spots, but the product could be purified by chromatography. On scale up, the carbonate products were used immediately to avoid this.

Displacement of the 4-nitrophenyl group was successful with both **113** and **157** warhead (yields of 65% for **113** and 46% for **157** respectively). It was tried with the trifluoromethoxy quinolone but had failed to react.

The resulting azide with the warhead in place was reduced using a Staudinger reduction with TCEP.HCl as a mild reagent in the presence of water. In both cases from the LC-MS, the starting material had been consumed. For the quinolone, the warhead mass was seen in the LC-MS but for the nitroacridine, the hydrolysed product was the major peak seen. The

reaction mixtures were worked up and purified to recover the warhead. Surprisingly for the nitroacridine, the warhead was also recovered along with the hydrolysed nitroacridone. The quinolone was recovered successfully.

It is unclear whether the conditions affected the hydrolysis of the nitroacridine due to the use of a hydrochloride salt of TCEP, with the reaction mixture being slightly acidic. Future studies of this would need to be done using a buffer solution or replacement of TCEP.HCl with another reducing reagent such as triphenylphosphine.

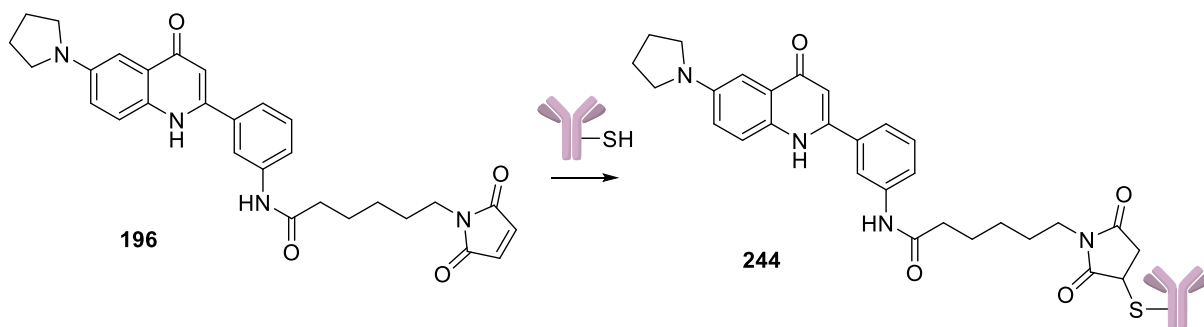
Chapter 9: Conjugations to the Antibody

With the cleavable and non-cleavable linkers synthesised, they could be conjugated to an antibody. The antibody chosen was trastuzumab owing to its robustness and gold standard in testing ADCs.

In order to conjugate to the antibody, the disulphide bridges of the antibody need to be reduced. This can be done with mild reducing agents such as TCEP.HCl. For these conjugations, a DAR of 4 was chosen as this is the classically accepted DAR.

The antibodies were incubated with 2.5 equivalents of TCEP to ensure an average DAR of 4.²⁰² After 1 hour, the antibodies were treated with either the cleavable or non-cleavable linkers with 4 equivalents used. After a further 1 hour, the antibodies were quenched with cysteine. To purify the ADCs, they were concentrated using Amicon® centrifugal filters which allowed small molecules to pass through but retained the protein. This also allowed a buffer exchange from PBS pH 7.2, 1mM EDTA to ultrapure water. After repeated centrifuging, the antibodies were then passed through a zeba™ spin desalting column. This caused some issues as the antibody stuck to the column and needed flushing. This was checked by using a NanoDrop UV spectrometer which showed no concentration of Ab was present until after flushing.

The resulting conjugated antibodies were analysed by HRMS using the intact antibody. Some of the ADCs were treated with DTT to reduce the antibody to its light chain and heavy chain parts. These were also analysed on HRMS. Unfortunately, for most of these conjugates, the expected mass was not observed in the mass spectrum. The conjugations were repeated but gave the same result. Intact antibody was not seen even for trastuzumab, but the light chains were identified with a mass of 23439.8 (Figure 9.1). The non-cleavable ADC **244** did show the correct mass, with a difference of 499 observed with the light chains, suggesting the conjugation was successful (Scheme 9.1 and Figure 9.2).



Scheme 9.1: General scheme for the conjugation of non-cleavable linker **196** to **244**

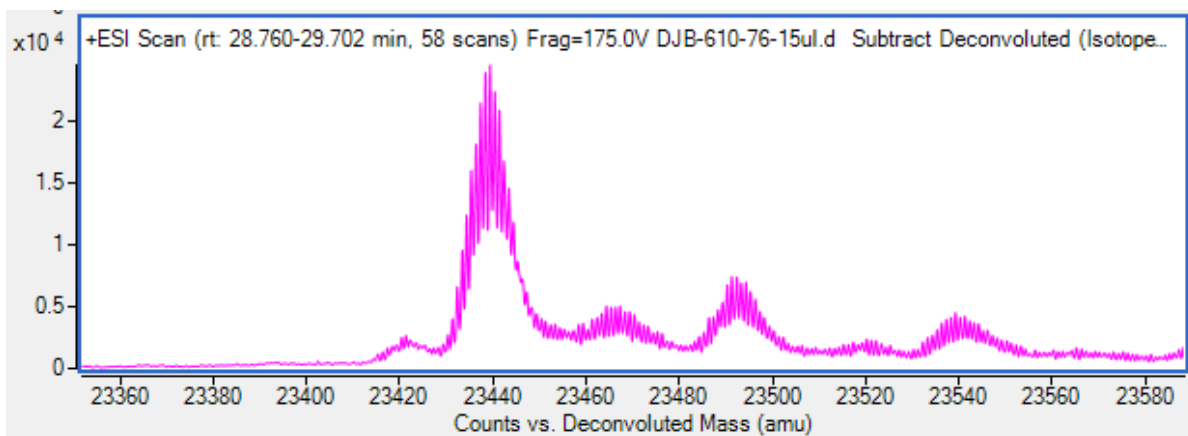


Figure 9.1: ESI+ deconvoluted mass spectrometry data of trastuzumab at mass 23439.8.

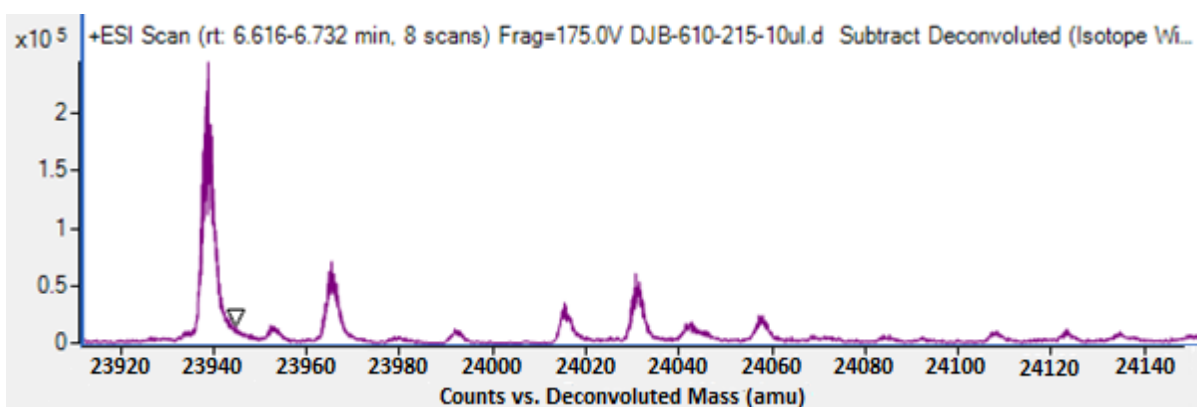


Figure 9.2: ESI+ deconvoluted mass spectrometry data of conjugate of **244**, showing mass at 23938.8.

A common way to check for DAR is using UV. However, both payloads are UV active at the same wavelength of the Ab, at 220 cm^{-1} and so the results were not accurate.

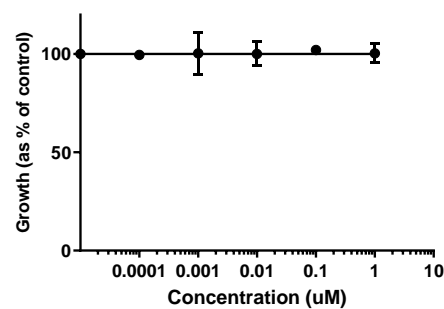
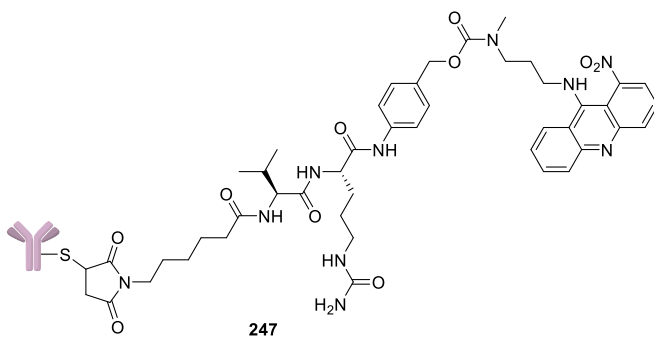
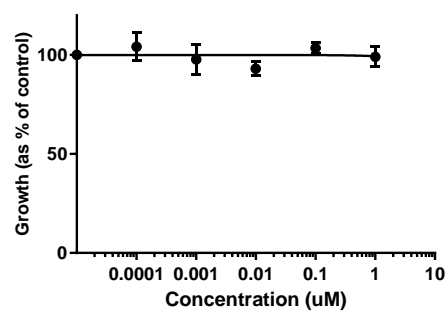
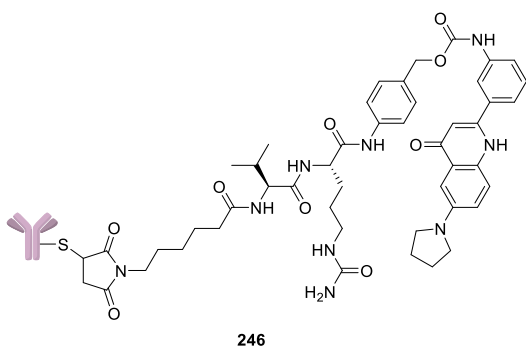
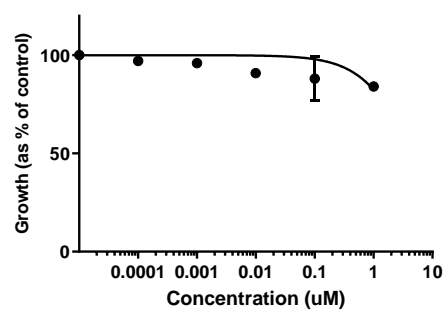
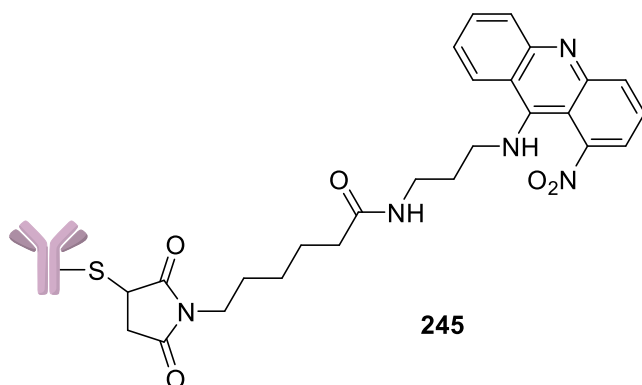
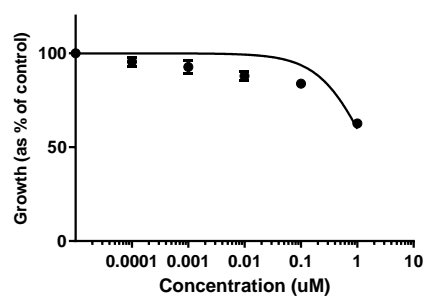
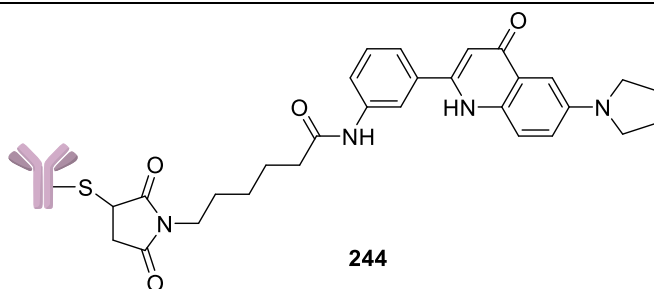
All the conjugated antibodies were submitted for testing in an SRB assay with MCF-7 cells. The results showed that none of the conjugates were active against this cell line. Interestingly, Herceptin did not show activity in this cell assay either.

There could be several reasons for a lack of activity. One could be the antibody is not active in this cell line, even though MCF-7 is HER2 positive. This could be checked by trying a different cell line such as SKBR3 cells. The antibody itself might not be of high purity since clear analysis of the antibody was not possible. Therefore, a new source of antibody might be needed.

With the linker themselves, it could also be down to their stability. The nitroacridines are prone to hydrolysis so under conjugation conditions, they might hydrolyse back to the nitroacridine, released from the linker which is why no mass was seen for these linkers compared to the quinolone. This would not explain why Herceptin was inactive.

The ADCs would need to be checked alongside other known ADCs, which have demonstrated activity already to confirm that the ADCs have no activity and checked against other cell lines.

ADC

Cell assay data – concentrations in μM 

Herceptin

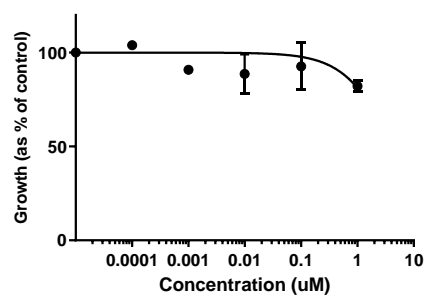


Table 9.1 :Cytotoxicity data for the nitroacridine dimers evaluated on MCF-7 cell line after 72 h, n = 2 (10 repetitions per replicate), error calculated from mean values. Herceptin is shown as a comparison, it is not cytotoxic.

Chapter 10: Conclusions and Future work

Antibody-drug conjugates are a therapeutic class of drugs which can selectively deliver a potent cytotoxic payload to a targeted cell. Their proof of concept has been confirmed with five ADCs FDA approved. ADCs are made up of 3 main components; the antibody, the linker and the warhead. The antibody's selectivity and specificity towards its target is essential and picking the correct target is critical as there needs to be a differential in the number of antigens between normal cells and cancer cells. The optimisation of the linker is important as it can play a pivotal role in the properties of the drug as well as for bioconjugations. Often the linker has labile bonds that can be cleaved inside the cell such as the cathepsin B sensitive dipeptide. The warheads are often drugs which have failed clinical trials due to adverse toxicities and possess sub-nM cytotoxicity. Often, natural products are selected such as the aurastatins and maytansinoids. These are synthetically challenging and complex, which can increase the cost of goods for an ADC where the cost is already high. Optimisation of these compounds is more demanding as analogues are synthetically difficult to make. There are also resistance issues in payloads as most common warheads share similar MoA.

To identify suitable warheads, an analysis of the NCI database was conducted. Seven compounds were identified which had differing cell profiles suggesting a difference in their MoA. They were also picked for their broad activity across over 60 cell lines and their structural simplicity. Three of these compounds have been explored, the nitroacridines, the quinolones and the thiosemicarbazones (Figure 10.1).

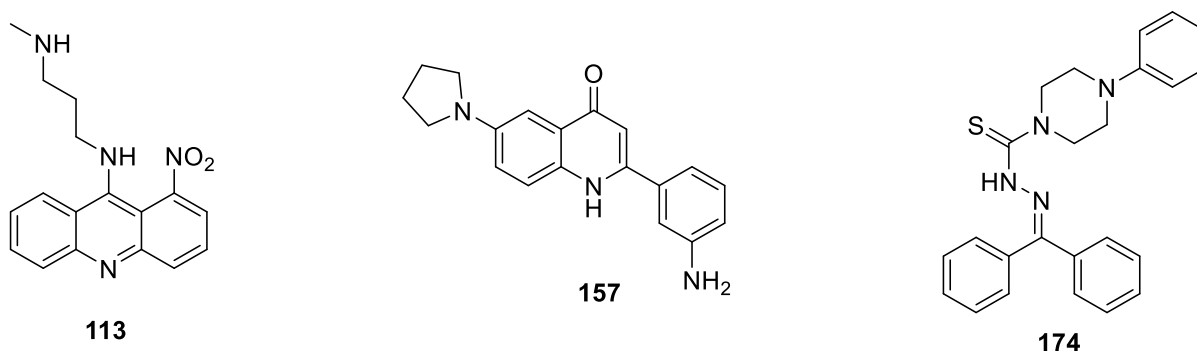


Figure 10.1: Compound series identified by screening the NCI database, nitroacridine **113**, quinolone **157** and thiosemicarbazone **174**.

Firstly, the optimisation of the warheads was conducted. The nitroacridine **113** was successfully resynthesised and attempts at optimisation of the route to improve the overall yield were unsuccessful.

The quinolone **157** was synthesised after the original hit **106** had stability problems.

The synthesis of the thiosemicarbazones was attempted but the synthesis was not successful. Different routes were explored but the project was stopped to focus on other aspects of the project.

Both warheads, **113** and **157**, were tested in SRB cell assays. **113** had a potency of 6 ± 1.4 nM which was less than seen from the NCI database. This could be due to a different cell assay. The warhead still demonstrated good potency. **157** was less active, with a GI_{50} of 62 ± 1.2 nM. Further biological evaluations were carried out with **157** and **106** which suggested that they might be more potent than they seem. This is because they can cause mitotic catastrophe which leads to delayed cell death, and so the cell assay might have been too short to visualise this. Both quinolones also showed subtle differences to each other in respect to their MoA. For example, quinolone **106** causes spindle width to decrease as opposed to **159** which has the opposite effect.

With the warheads synthesised, they were coupled to non-cleavable and cleavable linkers. The non-cleavable linkers were tested in the SRB assay to see if they had any potency. The failure of the assay might be because these compounds are not cell permeable, losing all activity. Acetylation of the nitroacridine retained potency, suggesting cell permeability is more likely as the nitroacridine does not lose all activity. Attempts were made to make a mimic like backbone from an antibody but was unsuccessful.

The release mechanism was also checked by synthesising compound **242**. Reduction of the azide causes a spontaneous cleavage, releasing the warhead. The warhead was successfully recovered, giving confidence that in the cell the warhead will be released.

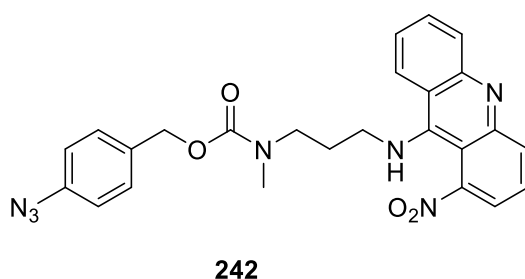


Figure 10.2: Structure of model system with nitroacridine

The cleavable and non-cleavable linkers were conjugated to trastuzumab. Analysis of the ADCs through mass spec showed that the non-cleavable quinolone linker had successfully conjugated with the mass difference seen. It is unclear as to why the other linkers have not bound or can't be seen through mass spec. MCF7 cells were then treated with these ADCs but no activity was seen. MCF-7 are HER2 presenting cells so should be susceptible to treatment with Herceptin. However, no activity was observed with Herceptin either.

Future work will need to be focused on optimising the ADCs. Firstly, the ADCs need to be checked on other cell lines to ensure that it is not the specific cell line or experiment, but the ADCs themselves. They should be tested alongside ADCs known to have activity so a direct comparison can be made. This might mean optimisation of the linker would be needed. This could involve swapping the dipeptide linker for another cleavable linker such as the β -glucuronides. Also, a fresh batch of antibodies should be tried to ensure no aggregation has occurred with the antibody, causing inactivity of the antibody.

Chapter 11: Experimental and Analysis

9.1 Safety

All procedures were carried out in line with the School of Natural and Environmental Sciences Safety Policy. COSHH risk assessments were completed before starting any practical work.

9.2 Solvents and Reagents

Chemicals were purchased from Sigma-Aldrich, Alfa Aesar, Fluorochem and Apollo Scientific and used without further purification. SureSeal™ or AcroSeal™ bottles of anhydrous solvents were purchased from Sigma-Aldrich or Acros, respectively. Deuterated solvents used for the determination of NMR spectra were purchased from Sigma-Aldrich and Cambridge Isotope Laboratories, Inc.

9.3 Chromatography and Equipment

Purifications by column chromatography were carried out using a Biotage SP4 automated flash system with UV monitoring at 298 nm and collection at 254 nm, or a Biotage Isolera automated flash system. Grace Resolv pre-packed flash cartridges were used in most cases for normal phase separations. Reveleris pre-packed NH silica cartridges and Reveleris C-18 silica cartridges were also used where stated.

Semi-preparative HPLC purifications were carried out by Dr. Suzannah Harnor, and Dr. Lauren Molyneux using an Agilent 1200 HPLC system with a binary pump, autosampler, fraction collector and diode array detector, controlled by Agilent ChemStation software.

Where stated, reactions were carried out under microwave irradiation in sealed microwave vials with the use of a Biotage Initiator Sixty with a robotic sample bed. Reactions were irradiated at 2.45 GHz, and were able to reach temperatures between 60 and 250 °C. Heating was at a rate of 2-5 °C/s and the pressure was able to reach 20 bar.

9.4 Analytical Techniques

Melting points were measured using a Stuart Scientific SMP3 apparatus. FTIR spectra were measured using an Agilent Cary 630 FTIR as a neat sample. UV spectra were recorded on a Hitachi U-2800A spectrophotometer and were performed in EtOH or MeOH. HRMS were provided by the ESPRC National Mass Spectrometry Service, University of Wales, Swansea. Or alternatively, HRMS analyses were conducted in house using an Agilent 6550 iFunnel QTOF LCMS with an Agilent 1260 infinity UPLC system. The sample was eluted on Acquity

UPLC BEH C-18 (1.7 μm , 2.1 x 50 mm) with a flow rate of 0.7 mL/min, and run at a gradient of 1.2 min 5-95% MeCN (0.1% formic acid) in water (0.1% formic acid).

LCMS analyses were conducted using a Waters Acquity UPLC system with PDA and ELSD. When a 2 min gradient was used, the sample was eluted on Acquity UPLC BEH C-18, 1.7 μm , 2.1 x 50mm, with a flow rate of 0.6 mL/min using 5-95% MeCN (0.1% formic acid). Analytical purity of compounds which were biologically tested was determined using Waters XTerra RP18, 5 μm (4.6 x 150 mm) column at 1 mL/min using either MeCN and water (0.1% ammonia) or MeCN and water (0.1% formic acid) with a gradient of 5-100% over 15 min, and were required to meet the purity criteria of >95% as a single peak under each gradient.

^1H -NMR spectra were obtained using a Bruker Avance III 500 spectrometer using a frequency of 500 MHz. ^{13}C and ^{19}F -NMR spectra were acquired using the Bruker Avance III 500 spectrometer operating at a frequency of 125 MHz, and 470 MHz, respectively. The abbreviations for spin multiplicity are as follows: s = singlet; d = doublet; t = triplet; q = quartet, p = pentet, sext = sextet, sept = septet and m = multiplet. Combinations of these abbreviations are employed to describe more complex splitting patterns (e.g. dd = doublet of doublets) and where broadening of the peak is observed, spin multiplicity is accompanied by the prefix br = broad. There are some occasions where there was not enough material isolated or remaining to ensure a ^{13}C -NMR where all the carbons could be visualised. Where this is the case, it is referenced in the text.

11.1. Conjugations

For a classically conjugated ADC with DAR 4, 1 equivalent of trastuzumab was reduced using 2.5 equivalents of TCEP in PBS pH 7.2, 1 mM EDTA for 1 h at 37 °C. Then, 4 equivalents of cleavable or non-cleavable linkers in DMSO were incubated with the antibody for 1 h at 37 °C in PBS pH 7.2, 1 mM EDTA to give a 10% v/v DMSO solution. After 1 h, the reaction was quenched with 16 equivalents of cysteine and left for a further 1 h. The ADCs were purified by concentrating the solution using an amicon® Ultra-0.5 mL Centrifugal filter 10 KDa. Using the filters, the ADCs were washed with ultrapure water, enabling a buffer exchange. After washing 3 x with ultrapure water, the residual solution was passed through a Zeba™ spin desalting column, eluting the ADCs in ultrapure water, ready for analysis.

11.2. SRB assay

The colorimetric sulphorhodamine B assay was used in order to measure cell proliferation. Harvested cells are centrifuged at 1000 rpm for 5 mins. The pellet is resuspended in 10 mL of RPMI 1640 with L-glutamine growth medium. The cells are then counted using a

Haemocytometer to ensure cell density is adequate. The cells are diluted with Trypsin 1-X (Trypsin 5 mL mixed with 45 mL PBS). 0.1 mL of medium was added to the outer rows and columns of two 96 well plate. Day 0 plate (plate 1) was seeded with 80 μ L of cells each in 10 wells while the growth inhibition plate (plate 2), 80 μ L of cells was added to 60 wells (6 x 10). The plates were incubated at 37 °C overnight. The first ten wells in plate 2 are used as a control and 20 μ L of a 1% DMSO concentration, plus media was added. Up to 5 different compounds could be tested and for each compound, 20 μ L was added to each well on a row (x 10). The drugged cells were incubated at 37 °C for 72 hours. Plate 1 was fixed at Day 1 using 25 μ L of ice cold 50% (wt/v) TCA solution to each well and leave for 1 hour at 4 °C. The plates were then washed with tap water 4-5 times and shaken to remove excess water and dried at 60 °C for 3 hours. Stored at 4 °C until needed. After 72 hours, plate 2 was fixed in the same manner as just described. Plates were stained using 100 μ L of 0.4% SRB solution and left for 30 mins. Dye is removed and plate is rinsed with 1% acetic acid, five times. Dried at 60 °C before 100 μ L of 10 mM Tris pH 10.5 is added to each well and shaken gently for 20 mins. Absorbance is read at 570 nm using FluoStar Omega Plate reader. Data was analysed using Prism software, mean value across the 10 wells are used to generate data point. Experiment was repeated for each compound tested.

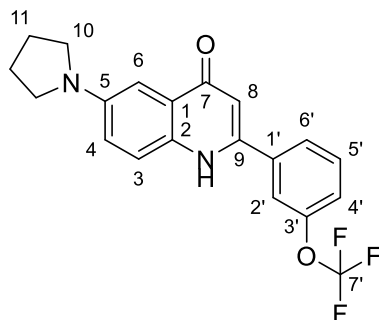
11.3. Compound Data

11.1.3. General Procedures

General Procedure A – S_NAr on 9-chloro-1-nitroacridine

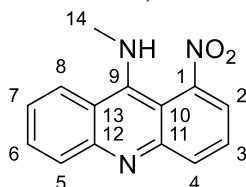
Amine (2 eq) was added to a solution of 9-chloro-1-nitroacridine **127** (1 eq) in THF (3 mL/mmol) followed by Et₃N (2 eq). The reaction was heated to reflux for 16 h before the solvent was removed *in vacuo*. The crude material was purified by flash column chromatography.

Synthesis of 6-(pyrrolidin-1-yl)-2-(3-(trifluoromethoxy)phenyl)quinolin-4(1H)-one, 106



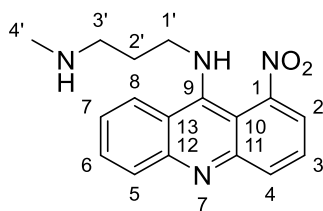
To a solution of N-(2-acetyl-4-(pyrrolidin-1-yl)phenyl)-3-(trifluoromethoxy)benzamide **164** (248 mg, 0.63 mmol) dissolved in *tert*-butanol (6.6 ml) was added potassium *tert*-butoxide (284 mg, 2.53 mmol). The reaction was heated to 70 °C and left for 5h. The reaction was left to cool to room temperature before water (10 ml) was added. The product was extracted with DCM (3 x 10 ml) and the combined organic layers were dried over MgSO₄, filtered and concentrated *in vacuo*. The crude product purified by flash column chromatography (silica; 0-10% MeOH in DCM) to afford a yellow solid (68 mg, 0.19 mmol, 30%); *R_f* 0.45 (10% MeOH in DCM); m.p. 301.6-312.9 °C; UV λ_{\max} (EtOH/nm) 272.0, 291.2, 400.0; IR $\nu_{\max}/\text{cm}^{-1}$ 3245 (NH), 1576 (C=O); ¹H-NMR (500 MHz, DMSO-*d*₆) δ_{H} 2.01-2.03 (4H, m, H-11), 3.29-3.31 (4H, m, H-10), 6.29 (1H, s, H-8), 7.03-7.05 (1H, m, H-3), 7.12-7.14 (1H, m, H-2'), 7.54-7.56 (1H, m, H-4'), 7.66-7.68 (1H, m, H-4), 7.71 (1H, t, *J* = 8.0 Hz, H-5'), 7.81-7.82 (1H, m, H-6), 7.87-7.89 (1H, m, H-6'), 11.56 (1H, s, NH); ¹³C-NMR (125 MHz, DMSO-*d*₆) δ_{C} 25.1 (C-11), 48.6 (C-10) (Not all visualized); ¹⁹F-NMR (470 MHz, DMSO-*d*₆) δ_{F} -56.6; LRMS (ES⁺) *m/z* 374.0 [M+H]⁺; HRMS failed to detect mass. Data consistent with literature values, lit. m.p. 280-282 °C (decomposition).¹⁶⁰

Synthesis of *N*-methyl-1-nitroacridin-9-amine, 112



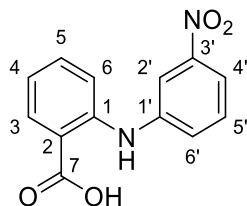
To a stirred solution of 9-chloro-1-nitroacridine (142 mg, 0.55 mmol) in THF (2 mL) was added Et₃N (0.38 ml, 2.75 mmol) and methylamine (2M in THF) (1.38 mL, 2.75 mmol) and heated to reflux. The reaction was left for 5 hours before cooled to RT, diluted with H₂O (10 mL) and extracted into DCM (3 x 10 mL). The combined organic extracts were washed with brine (10 mL), dried over MgSO₄, filtered and concentrated *in vacuo* before purified by flash column chromatography (silica; 30-60% EtOAc in petroleum ether) to afford a red oil (76 mg, 0.29 mmol, 54%); *R_f* 0.16 (60% EtOAc in petroleum ether); UV λ_{\max} (EtOH/nm) 221.0, 275.2, 399.8; IR $\nu_{\max}/\text{cm}^{-1}$ 3070 (NH), 1521 (N=O), 1333 (N=O); ¹H-NMR (500 MHz, DMSO- *d*₆) δ_{H} 7.34-7.36 (1H, m, H-7), 7.46-7.49 (1H, m, H-6), 7.60 (1H, d, *J* = 8.2 Hz, H-5), 7.75-7.77 (1H, m, H-3), 7.80-7.87 (2H, m, H-4, H-8), 8.05-8.08 (1H, m, H-2) 12.27 (1H, s, NH); ¹³C-NMR (125 MHz, DMSO- *d*₆) δ_{C} 53.4 (C-14), 116.9 (C-5), 118.8 (C-6), 122.6 (C-4), 129.7 (C-3), 130.2 (C-2), 131.4 (C-11), 148.9 (C-1) (C-10, C-12, C-13 not visualised); LRMS (ES⁺) *m/z* 254.1 [M+H]⁺; HRMS failed to detect mass. Data consistent with literature values.¹⁵⁶

***N*¹-methyl-*N*³-(1-nitroacridin-9-yl)propane-1,3-diamine, 113**



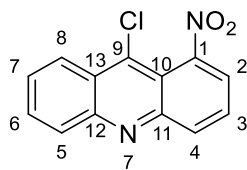
To *tert*-butyl methyl (3-((1-nitroacridin-9-yl)amino)propyl)carbamate (300 mg, 0.76 mmol) was added 10% TFA in DCM (5 mL) at 0 °C. The temperature was allowed to warm to RT and was stirred for 3 hours after which the reaction mixture was concentrated *in vacuo*, and the residue was neutralised with a saturated solution of NaHCO₃ (30 mL) and extracted in DCM (5 x 30 mL). The combined organic layers were washed with NaHCO₃ (2 x 20 mL), then brine (30 mL) and then dried over MgSO₄ and concentrated *in vacuo* to give a red oil. The product was purified by amine column chromatography (NH₂-silica; 0-10% MeOH in DCM) to afford the title compound (214 mg, 0.69 mmol, 91%) as a red oil. *R*_f 0.23 (10% MeOH in DCM); UV λ_{max} (EtOH/nm) 222.2, 277.6; IR ν_{max} /cm⁻¹ 3262 (N-H), 3184 (N-H), 1526 (N=O); ¹H NMR (500 MHz, , DMSO-*d*₆) δ_H 1.83-1.88 (2H, m, H-2'), 2.57 (3H, s, H-4'), 2.99-3.02 (2H, m, H-1') 3.43 (1H, br s, NHCH₃), 3.73-3.77 (2H, m, H-3'), 7.10 (1H, t, *J* = 7.6 Hz, H-7), 7.26-7.30 (1H, m, H-6), 7.34 (1H, d, *J* = 8.2 Hz, H-5), 7.40-7.44 (1H, m, H-3) 7.49-7.53 (2H, m, H-4, H-8) 7.81 (1H, d, *J* = 8.0 Hz, H-2), 11.06 (1H, s, NH-Ar); ¹³C NMR (125 MHz, CDCl₃) δ_C 31.2 (C-2'), 35.6 (C-4'), 50.0 (C-3'), 50.9 (C-1'), 116.3 (C-5), 116.6 (C-13), 129.0 (C-6), 130.2 (C-4), 131.5 (C-3), 141.2 (C-2), 149.6 (C-11), 150.3 (C-1), (C-10, C-8, C-7, C-12 and C-9 not visualised); LRMS (ES⁺) *m/z* 311.3 [M+H]⁺; HRMS *m/z* calculated for C₁₇H₁₉N₄O₂ [M+H]⁺ 311.1987 found 311.1969. Data consistent with literature values.¹⁵⁶

Synthesis of 2-((3-nitrophenyl)amino)benzoic acid, 125



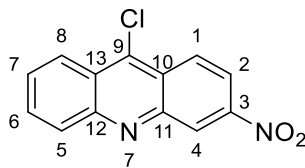
To a solution of 2-iodobenzoic acid (5.0 g, 20 mmol) in DMF (50 mL) was added 3-nitroaniline (5.6 g, 40 mmol), Na_2CO_3 (21 mg, 0.2 mmol), and copper iodide (118 mg, 0.6 mmol). The reaction mixture was stirred under reflux for 6 hours. The solution was cooled to RT before 6 M HCl (30 mL) was added and the solution was left overnight to form a precipitate which was collected and washed with H_2O . The crude product was purified by flash column chromatography (silica; 60-80% DCM in petroleum ether) to give a yellow solid (3.6 g, 14 mmol, 69%). R_f 0.27 (60% EtOAc in petroleum ether); m.p. 204.8-206.7 °C; UV λ_{max} (EtOH/nm) 207.8, 228.4, 339.2; IR $\nu_{\text{max}}/\text{cm}^{-1}$ 3309 (NH), 2852 (OH), 1665 (C=O), 1521 (N=O), 1336 (N=O); $^1\text{H-NMR}$ (500 MHz, CDCl_3) δ_{H} 6.92-6.95 (1H, m, H-4), 7.35-7.37 (1H, m, H-5'), 7.47-7.53 (2H, m, H-5, H-4'), 7.56-7.58 (1H, m, H-3), 7.92-7.94 (1H, m, H-6'), 8.10 – 8.12 (1H, m, H-2'), 8.15-8.16 (1H, m, H-6), 10.2 (1H, s, NH), 13.29 (1H, s, OH); ^{13}C NMR (125 MHz, CDCl_3) δ_{C} 114.5 (C-2), 115.7 (C-2), 117.8 (C-6'), 119.2 (C-6), 127.2 (C-4), 128.1 (C-3'), 130.2 (C-5'), 132.0 (C-3), 133.5 (C-5), 135.4 (C-6'), 141.9 (C-1), 142.2 (C-1') 173.2 (C-7); LRMS (ES+) m/z 258.0 $[\text{M}+\text{H}]^+$; HRMS $[\text{M}+\text{H}]^+$ ($\text{C}_{13}\text{H}_{11}\text{N}_2\text{O}_4$), calcd 258.0147 found 258.0136. Analytical data consistent with literature values, lit. m.p. 220 °C.²⁰³

Synthesis of 9-chloro-1-nitroacridine, 126



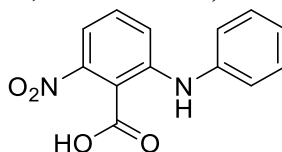
To 2-((3-nitrophenyl)amino)benzoic acid (1.0 g, 3.9 mmol) was added POCl_3 (7.2 mL, 78 mmol) and the mixture was heated to 140 °C and stirred for 1 h. The reaction mixture was cooled to RT and petroleum ether was added (20 mL) and stirred for 30 mins followed by no stirring for 30 mins. The solution was decanted off to leave a residue which was quenched with ice and quickly neutralized with 28% NH_4OH solution. The reaction mixture was extracted into DCM (3 x 100 mL). The combined organic extracts were dried over MgSO_4 , filtered and concentrated *in vacuo*. The crude material was purified by flash column chromatography (silica; 100% DCM) followed by reverse phase flash column (C-18; 20-60% THF (0.1% NH_3) in water (0.1% NH_3)) to give a yellow solid (391 mg, 1.51 mmol, 39%); R_f 0.59 (100% DCM); m.p. 154-156 °C; λ_{max} (EtOH/nm) 212.8, 249.2, 362.4; IR ν_{max} / cm^{-1} 1519 (N=O), 1356 (N=O); $^1\text{H-NMR}$ (500 MHz, $\text{DMSO-}d_6$) δ_{H} 7.89 (1H, m, H-6), 7.97 (1H, dd, $J = 7.2, 8.8$ Hz, H-3) 8.04 (1H, m, H-7), 8.25 (2H, m, H-4 and H-8), 8.45 (2H, m, H-2 and H-5); $^{13}\text{C NMR}$ (125 MHz, $\text{DMSO-}d_6$) δ_{C} 115.3 (C-10), 124.6 (C-13), 129.6 (C-8), 130.0 (C-7), 130.1 (C-5), 133.1 (C-6), 134.6 (C-4), 137.4 (C-3), 146.5 (C-2), 148.3 (C-9), 149.1 (C-1) (C-11, C-12 not visualised); LRMS (ES^+) m/z 259.1 [$\text{M}^{(35}\text{Cl})+\text{H}$] $^+$, 261.1 [$\text{M}^{(37}\text{Cl})+\text{H}$] $^+$; HRMS m/z calculated for $\text{C}_{13}\text{H}_8\text{ClN}_2\text{O}_2$ [$\text{M}^{(35}\text{Cl})+\text{H}$] $^+$ 259.0269 found 259.0274. Data consistent with literature values, lit m.p. 150-151 °C.¹⁵⁶

9-chloro-3-nitroacridine, **128**



Compound **129** was prepared using the same procedure as described for **127**, to afford the desired product (198 mg, 0.77 mmol, 20%) as a yellow solid. R_f 0.59 (100% DCM); m.p. 207-210 °C; UV λ_{max} (EtOH/nm) 364.6, 347.0, 295.2, 238.8; IR ν_{max} / cm^{-1} 1309 (N=O), 1343 (N=O); 1H NMR (500 MHz, DMSO- d_6) δ_H 7.95 (1H, ddd, $J = 1.4, 6.6, 8.8$ Hz, H-7), 8.08 (1H, ddd, $J = 1.4, 6.6, 8.8$ Hz, H-6), 8.33 (1H, dd, $J = 1.4, 8.8$ Hz, H-5), 8.45 (1H, dd $J = 2.3, 9.5$ Hz, H-2), 8.50 (1H, dd, $J = 1.4, 8.8$ Hz, H-8), 8.67 (1H, d, $J = 9.5$ Hz, H-1) 9.04 (1H, d, $J = 2.3$ Hz, H-4); LRMS (ES $^+$) m/z 259.1 [$M(^{35}Cl)+H$] $^+$, 261.1 [$M(^{37}Cl)+H$] $^+$; HRMS m/z calculated for $C_{13}H_8ClN_2O_2$ [$M(^{35}Cl)+H$] $^+$ 259.0269 found 259.0257. Data consistent with literature values, lit m.p. 214-216 °C.¹⁵⁶

Synthesis of 2-nitro-6-(phenylamino)benzoic acid, 132



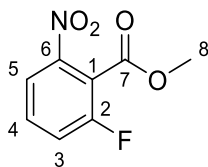
Synthesis of 2-nitro-6-(phenylamino)benzoic acid, was attempted in several ways as outlined below.

a) To a solution of 2-chloro-6-nitrobenzoic acid (50 mg, 0.25 mmol) in DMF (2 mL) was added aniline (46 HRMS m/z calculated for $C_{13}H_7ClN_2O_2$ [$M(^{35}Cl)+H$] $^+$ 259.0269 found 259.0257.), CuI (1.9 mg, 0.01 mmol) and $NaHCO_3$ (1 mg, 0.01 mmol). The reaction mixture was heated to reflux and left for 16 hours. Reaction abandoned as no product was observed by LC-MS.

b) To a solution of 2-chloro-6-nitrobenzoic acid (50 mg, 0.25 mmol) in 1,4-dioxane (2 mL) was added aniline (46 μ L, 0.5 mmol), $NaOBu^t$ (48 mg, 0.5 mmol) and $Pd(t-Bu_3P)_2$ (15 mg, 0.03 mmol). The reaction was heated to reflux and left for 16 hours. Reaction abandoned as no product was observed by LC-MS.

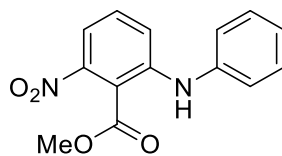
c) To a solution of 2-amino-6-nitrobenzoic acid (50 mg, 0.27 mmol) in DMF (2 mL) was added bromobenzene (57 μ L, 0.54 mmol) followed by CuO (22 mg, 0.27 mmol) and K_2CO_3 (75 mg, 0.54 mmol). The reaction was heated to reflux and left for 16 hours. Reaction abandoned as no product was observed by LC-MS.

Synthesis of Methyl 2-fluoro-6-nitrobenzoate, 133



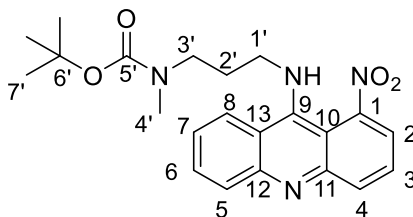
To a stirred solution of 2-fluoro-6-nitrobenzoic acid (5.0 g, 27 mmol) in DMF (50 mL), was added potassium carbonate (7.5 g, 54 mmol). The reaction was cooled to 0 °C in an ice bath for 10 minutes before iodomethane (1.8 mL, 29 mmol) was added slowly. The solution was warmed to RT and stirred overnight for 16 hours. Ether (50 mL) was added and the reaction mixture was filtered through Celite® and then concentrated *in vacuo*. A saturated solution of NH₄Cl (50 mL) was added and the product was extracted into EtOAc (3 x 50 mL). The organic layers were combined, washed with H₂O (2 x 30 mL) and brine (30 mL) before being dried over MgSO₄, filtered, concentrated *in vacuo* to obtain an orange crystalline solid (4.2 g, 21 mmol, 78%). *R_f* 0.81 (60% EtOAc in petroleum ether); m.p. 59.4-62.1 °C; UV λ_{max} (EtOH/nm) 204.2, 254.0; IR $\nu_{\text{max}}/\text{cm}^{-1}$ 1673 (C=O); ¹H-NMR (500 MHz, DMSO-*d*₆) δ_{H} 3.84 (3H, s, H-8), 7.54-7.55 (1H, m, H-3), 7.62 (1H, dt, *J* = 8.2, 7.8 Hz, H-4), 7.91 (1H, d, *J* = 8.2 Hz, H-5); ¹³C-NMR (125 MHz, DMSO-*d*₆) δ_{C} 54.2 (C-8), 117.6 (C-1), 123.2 (C-5), 124.7 (C-3), 133.7 (C-4), 157.8 (C-2), 159.7 (C-6), 162.6 (C7); ¹⁹F-NMR (470 MHz, DMSO-*d*₆) δ_{F} -113.9; LRMS (ES⁺) *m/z* 213.2 [M+H]⁺. HRMS *m/z* calculated for C₈H₇FNO₄ [M+H]⁺ 200.0314 found 200.0319. Data consistent with literature values, lit m.p. 60-61 °C. ²⁰⁴

Synthesis of methyl 2-nitro-6-(phenylamino)benzoate, 134



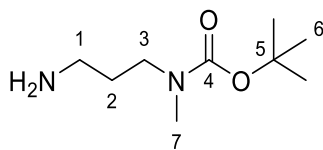
To a microwave vial containing methyl 2-fluoro-6-nitrobenzoate (50 mg, 0.18 mmol) in TFE (2 mL) was added aniline (35 μ L, 0.36 mmol). The reaction mixture was heated in the microwave at 120 $^{\circ}$ C for 2 hours. Reaction abandoned as no product was seen by LC-MS.

Synthesis of *Tert*-butyl methyl(3-((1-nitroacridin-9-yl)amino)propyl)carbamate, 136



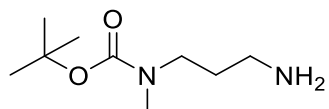
To a stirred solution of 9-chloro-1-nitroacridine (400 mg, 1.55 mmol) in THF (10 mL) was added Et₃N (648 μL, 4.65 mmol) followed by *tert*-butyl (3-aminopropyl)(methyl)carbamate (874 mg, 4.65 mmol). The reaction mixture was heated to reflux and was allowed to stir for 3 h to give a red solution. The solution was allowed to cool to RT and concentrated *in vacuo*. The crude product was redissolved in DCM (10 mL) and then washed with a saturated solution of NaHCO₃ (10 mL) followed by H₂O (10 mL). The organic layer was dried over MgSO₄, filtered and concentrated *in vacuo* to give a crude oil. The product was purified by flash column chromatography (silica; 0-10% MeOH in DCM) to give the title compound as a red oil (535 mg, 1.3 mmol, 84%). *R*_f 0.2 (5% MeOH in DCM); UV λ_{max} (EtOH/nm) 221.6, 278.6 and 387.4; IR ν_{max}/cm⁻¹ 3278 (br N-H), 1661 (C=O); ¹H-NMR (500 MHz, DMSO- *d*₆) δ_H 1.32-1.38 (9H, m, H-7), 1.72 (2H, br s, H-2'), 2.73 (3H, br s, H-4'), 3.24 (2H, t, J = 6.8 Hz, H-1'), 3.65 (2H, t, J = 6.1 Hz, H-3'), 7.08 (1H, t, J = 7.6 Hz, H-7), 7.27-7.31 (2H, m, H-5, H-6), 7.36 (1H, d, J = 8.3 Hz, H-3), 7.49-7.51 (2H, m, H-4, H-8), 7.79 (1H, br s, H-2); ¹³C NMR (125 MHz, DMSO- *d*₆) δ_C 28.5 (C-4'), 31.2 (C-2'), 34.5 (C-7'), 36.2 (C-1'), 47.1 (C-3') 78.6 (C-6'), 114.5 (C-10), 116.3 (C-5), 116.5 (C-13), 118.5 (C-8), 120.2 (C-7), 129.0 (C-6), 130.2 (C-4), 131.5 (C-3), 141.1, 141.2 (C-2, C-12), 149.7 (C-11), 150.2 (C-1), 150.2 (C-5'), 162.8 (C-9); LRMS (ES⁺) *m/z* 411.3 [M+H]⁺; HRMS *m/z* calculated for C₂₂H₂₇H₄O₄ [M+H]⁺ 411.2027 found 411.2040.

Synthesis of *tert*-butyl (3-aminopropyl)(methyl)carbamate, 138



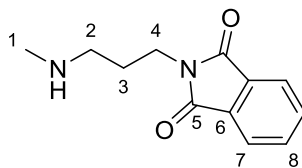
To a stirring solution of *N*-methyl-1,3-diaminopropane (3.9 mL, 37 mmol) in MeOH (100 mL) at 0 °C was added Boc₂O (8.1 g, 37 mmol). The solution was warmed to RT and stirred for 2 h before the solvent was removed *in vacuo*. The crude mixture was redissolved in DCM (50 mL), washed with a saturated solution of NaHCO₃ (50 mL), H₂O (50 mL) and brine (50 mL). The organic phase was dried over MgSO₄, filtered and concentrated *in vacuo*. The crude mixture was purified by flash column chromatography (silica; 0-20% MeOH in DCM (10% NH₃)) to give a colourless oil (2.23 g, 12.2 mmol, 33%). *R_f* 0.15 (20% MeOH in DCM (10% NH₃)); IR $\nu_{\max}/\text{cm}^{-1}$ 3364 (NH), 1670 (C=O); ¹H NMR (500 MHz, CDCl₃) δ_{H} 1.39 (9H, s, H-6), 1.55-1.58 (2H, m, H-2), 1.84 (2H, br, H-2), 2.62-2.64 (2H, m, H-1), 2.77 (3H, s, H-7), 3.22-3.23 (2H, m, H-3); ¹³C NMR (125 MHz, CDCl₃) δ_{C} 25.6 (C-2), 29.4 (C-6), 35.4 (C-7), 40.1 (C-1), 44.3 (C-3), 74.6 (C-5), 161.3 (C-4). LRMS (ES⁺) *m/z* 188.9 [M+H]⁺; HRMS failed to detect mass. Data consistent with literature values.^{179, 205}

Synthesis of *tert*-butyl (3-aminopropyl)(methyl)carbamate, 138



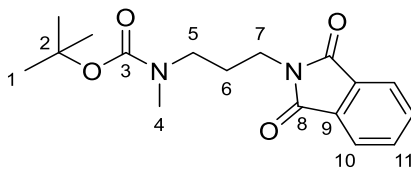
To a solution of *tert*-butyl (3-(1,3-dioxoisindolin-2-yl)propyl)(methyl)carbamate (154 mg, 0.82 mmol) in MeOH (5 mL) was added hydrazine hydrate monohydrate (79 μ L 1.64 mmol) and heated to reflux. After 4 hours, the reaction mixture was cooled to RT and the precipitate formed was filtered off. The filtrate was concentrated to dryness *in vacuo* and diluted with H₂O (10 mL). It was extracted with EtOAc (3 x 10 mL) and the combined organic layers were dried over MgSO₄, filtered and concentrated *in vacuo* to give a colourless oil (96 mg, 0.51 mmol, 62%). See above for data.

Synthesis of 2-(3-(methylamino)propyl)isoindoline-1,3-dione, 139



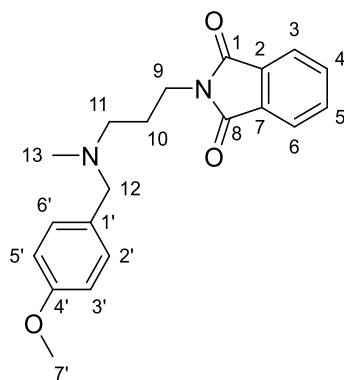
To a solution of 3-bromopropylphthalimide (1.0 g, 3.7 mmol) in MeCN (30 mL) was added Methylamine (2M in THF, 9.3 mL, 19 mmol) and Cs₂CO₃ (2.4 g, 7.5 mmol) and the reaction mixture was heated to reflux and left to stir for 6 hours. After cooling to RT, the reaction mixture was extracted into EtOAc (3 x 30 mL) and the combined organic fractions were dried over MgSO₄, filtered and concentrated *in vacuo*. The crude product was purified by flash column chromatography (silica; 0-10% MeOH in DCM) to afford a white solid (417 mg 1.45 mmol, 39%). *R_f* 0.16 (10% MeOH in DCM); m.p. 190-194 °C; UV λ_{max} (MeOH/nm) 271.8; IR ν_{max}/cm⁻¹ 3391 (NH), 3056 (NH), 1667 (C=O); ¹H NMR (500 MHz CDCl₃) δ_H 1.20 (1H, br s, NH), 1.68-1.71 (2H, m, H-3), 2.64 (3H, s, H-1), 2.71-2.75 (2H, H-2), 3.84-3.87 (2H, m, H-3), 7.70-7.84 (4H, m, H-7, H-8); ¹³C NMR (125 MHz, CDCl₃) δ_C 28.6 (C-3), 35.8 (C-1), 47.1 (C-2), 56.2 (C-4), 118.9 (C-7), 129.8 (C-8), 131.1 (C-6), 165.4 (C-5); LRMS (ES+) *m/z* 219.3 [M+H]⁺; HRMS *m/z* calculated for C₁₂H₁₅N₂O₂ [M+H]⁺ 219.1078 found 219.1089. Data consistent with literature values, lit m.p. 204-206 °C.¹⁷⁹

Synthesis of *tert*-butyl (3-(1,3-dioxoisindolin-2-yl)propyl)(methyl)carbamate, 143



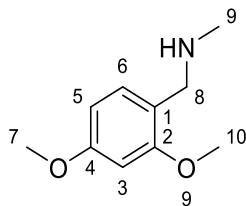
To a solution of 2-(3-(methylamino)propyl)isoindoline-1,3-dione (200 mg, 0.92 mmol) in MeOH (10 mL) at 0 °C was added Boc₂O (400 mg, 1.83 mmol). The reaction mixture was warmed to RT and stirred for 5 hours before concentrating *in vacuo*. The compound was redissolved in DCM (10 mL), washed with 1M HCl (10 mL) and H₂O (10 mL), dried over MgSO₄, filtered and concentrated *in vacuo* to obtain a white solid (245 mg, 0.77 mmol, 84%). *R_f* 0.32 (10% MeOH in DCM); m.p. 78-82 °C; UV λ_{max} (MeOH/nm) 272.4; IR ν_{max}/cm⁻¹ 3086, 1661 (C=O); ¹H NMR (500 MHz CDCl₃) δ_H 1.25 (9H, s, H-1), 1.88-1.91 (2H, m, H-6), 3.10 (3H, s, H-4), 3.41-3.43 (2H, m, H-5), 3.75-3.80 (2H, m, H-7), 7.70-7.84 (4H, m, H-10, H-11); ¹³C NMR (125 MHz, CDCl₃) δ_C 25.3 (C-6), 29.4 (C-1) 36.2 (C-4), 48.3 (C-5), 56.1 (C-7), 80.4 (C-2), 119.0 (C-10), 129.7 (C-9), 131.2 (C-11), 165.5 (C-5); LRMS (ES⁺) *m/z* 319.4 [M+H]⁺; HRMS *m/z* calculated for C₁₇H₂₃N₂O₄ [M+H]⁺ 319.1654 found 319.1641. Data consistent with literature values, lit m.p. 74-76 °C.¹⁷⁹

Synthesis of 2-(3-((4-methoxybenzyl)(methyl)amino)propyl)isoindoline-1,3-dione, 144



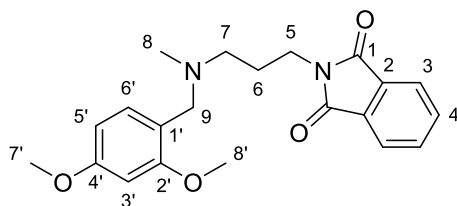
To a solution of 3-bromopropylphthalimide (250 mg, 0.93 mmol) in MeCN (10 mL) was added *N*-(4-methoxybenzyl)-*N*-methylamine (422 μ L, 2.80 mmol) and Cs_2CO_3 (909 mg, 2.79 mmol) and the reaction mixture was heated to reflux and left to stir for 6 hours. After cooling to RT, the reaction mixture was extracted into EtOAc (3 x 10 mL) and the combined organic fractions were dried over MgSO_4 , filtered and concentrated *in vacuo*. The crude product was purified by flash column chromatography (silica; 0-10% MeOH in DCM) to afford a white solid (261 mg, 0.77 mmol, 82%). R_f 0.55 (10% MeOH in DCM); m.p. 145-149 $^\circ\text{C}$; UV λ_{max} (MeOH/nm) 265.4, 224.9; IR $\nu_{\text{max}}/\text{cm}^{-1}$ 3056 (NH), 1667 (C=O); ^1H NMR (500 MHz CDCl_3) δ_{H} 1.88-1.90 (2H, m, H-10), 2.40 (3H, s, H-13), 2.61 (t, $J = 7.1$ Hz, H-11) 3.72 (2H, s, H-12), 3.83 (3H, s, H-7') 3.95-4.00 (2H, t, $J = 7.1$ Hz, H-9), 7.01 (2H, t, $J = 7.6$ Hz, H-3 and 5') 7.21 (2H, t, $J = 7.6$ Hz, H-1' and 2'), 7.74-7.76 (2H, m, H-3 and 6) 7.84-7.86 (2H, m, H-3 and 6); ^{13}C NMR (125 MHz, CDCl_3) δ_{C} 25.5 (C-10), 39.8 (C-13), 55.8, 55.9 (C9 and 10), 118.3 (C-2', C5'), 121.5 (C-3, C-6), 132.5 (C-2', C-6'), 166.1 (C-1) (C-2, C-7 C-1' and C-4' not visualised); LRMS (ES+) m/z 339.4 $[\text{M}+\text{H}]^+$; HRMS m/z calculated for $\text{C}_{20}\text{H}_{23}\text{N}_2\text{O}_3$ $[\text{M}+\text{H}]^+$ 339.1164 found 339.1183.

Synthesis of 1-(2,4-dimethoxyphenyl)-*N*-methylmethanamine, 146



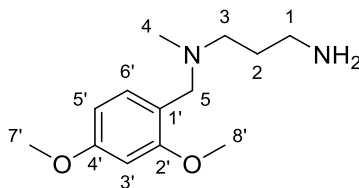
To a solution of 2,4-dimethoxybenzaldehyde (1.0 g, 6.0 mmol) in EtOH (20 mL) was added MeNH₂ (2M in MeOH, 9 mL, 18 mmol). MgSO₄ was added to the reaction and was refluxed for 16 hours. The solution was cooled to RT, filtered and at 0 °C, NaBH₄ (454 mg, 12 mmol) was added. The reaction mixture was warmed to RT and left to stir for 3 hours. The solvent was concentrated *in vacuo* and the residue redissolved in EtOAc (10 mL). The organic layer was washed with H₂O (10 mL), dried over MgSO₄, filtered and concentrated *in vacuo* to give a white product (489 mg, 2.70 mmol, 45%) *R_f* 0.27 (10% MeOH in DCM); m.p. 81-86 °C; UV λ_{max} (MeOH/nm) 275.1; IR ν_{max}/cm⁻¹ 3420 (NH), 3004 (NH); ¹H NMR (500 MHz CDCl₃) δ_H 2.36 (3H, s, H-9), 3.54 (2H, s, C-8), 3.76 (3H, s, H-10), 3.78 (3H, s, H-7), 6.45-6.48 (2H, m, C-4, C-5), 7.14-7.15 (1H, m, H-6); ¹³C NMR (125 MHz, CDCl₃) δ_C 34.8 (C-9), 49.4 (C-8), 56.2 (C-10), 56.3 (C-7), 101.6 (C-3), 109.5 (C-5), 118.4 (C-1), 131.1 (C-6), 157.1 (C-2 and C-4). LRMS (ES⁺) *m/z* 182.4 [M+H]⁺; HRMS *m/z* calculated for C₁₀H₁₆NO₂ [M+H]⁺ 182.1347 found 182.1361. Data consistent with literature values.²⁰⁶

**Synthesis of 2-(3-((2,4-dimethoxybenzyl)(methyl)amino)propyl)isoindoline-1,3-dione,
147**



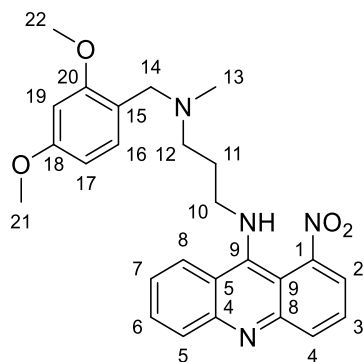
To a solution of 3-bromopropylphthalimide (110 mg, 0.4 mmol) in MeCN (10 mL) was added 1-(2,4-dimethoxyphenyl)-*N*-methylmethanamine, **148** (150 mg, 0.83 mmol) and Cs₂CO₃ (811 mg, 2.49 mmol) and the reaction mixture was heated to reflux and left to stir for 6 hours. After cooling to RT, the reaction mixture was extracted into EtOAc (3 x 10 mL) and the combined organic fractions were dried over MgSO₄, filtered and concentrated *in vacuo*. The crude product was purified by flash column chromatography (silica; 20-50% EtOAc in petroleum ether) to afford a white solid (112 mg 0.30 mmol, 74%). *R_f* 0.45 (50% EtOAc in petroleum ether); m.p. 1140-155 °C; UV λ_{max} (MeOH/nm) 276.8; IR ν_{max}/cm⁻¹ 3056 (NH), 1667 (C=O); ¹H NMR (500 MHz CDCl₃) δ_H 2.36 (3H, s, H-9), 3.54 (2H, s, C-8), 3.76 (3H, s, H-10), 3.78 (3H, s, H-7), 6.45-6.48 (2H, m, C-4, C-5), 7.14-7.15 (1H, m, H-6); ¹³C NMR (125 MHz, CDCl₃) δ_C 34.8 (C-9), 49.4 (C-8), 56.2 (C-10), 56.3 (C-7), 101.6 (C-3), 109.5 (C-5), 118.4 (C-1), 131.1 (C-6), 157.1 (C-2 and C-4). LRMS (ES⁺) *m/z* 182.4 [M+H]⁺; HRMS *m/z* calculated for C₂₁H₂₅N₂O₄ [M+H]⁺ 369.1422 found 369.1436.

Synthesis of *N*¹-(2,4-dimethoxybenzyl)-*N*¹-methylpropane-1,3-diamine, 148



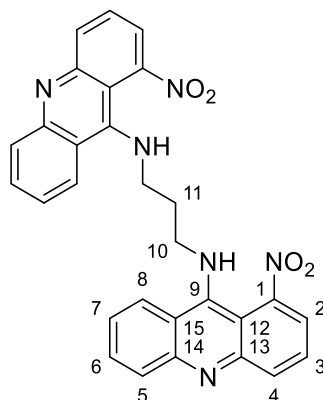
To a solution of 2-(3-((2,4-dimethoxybenzyl)(methyl)amino)propyl)isoindoline-1,3-dione (70 mg, 0.19 mmol) in MeOH (5 mL) was added hydrazine hydrate monohydrate (14 μ L 0.29 mmol) and heated to reflux. After 4 hours, the reaction mixture was cooled to RT and the precipitate formed was filtered off. The filtrate was concentrated to dryness *in vacuo* and diluted with H₂O (10 mL). It was extracted with EtOAc (3 x 10 mL) and the combined organic layers were dried over MgSO₄, filtered and concentrated *in vacuo* to give a white solid (40.7 mg, 0.17 mmol, 90%). *R_f* 0.40 (10% MeOH in DCM); m.p. 65-71 °C; UV λ_{max} (MeOH/nm) 261.1; IR $\nu_{\text{max}}/\text{cm}^{-1}$ 3374 (NH), 3074 (NH); ¹H NMR (500 MHz CDCl₃) δ_{H} 1.90-1.92 (2H, m, H-2), 2.36 (3H, s, H-4), 2.42-2.44 (2H, m, H-3), 2.48-2.52 (2H, m, H-1), 2.87 (2H, br, NH₂), 3.60 (2H, s, H-5), 3.67 (3H, s, H-8'), 3.71 (3H, s, H-7'), 7.01-7.05 (2H, m, H-3' and H-5'), 7.41-7.43 (1H, m, H-6') ¹³C NMR (125 MHz, CDCl₃) δ_{C} 23.4 (C-2), 39.1 (C-1), 41.1 (C-4), 55.2, 55.3, 55.5 (C-3, C-7', C-8') 102.3 (C-3'), 107.1 (C-5') 131.5 (C-5') (C-1', C-2 and C-4' are not visualised); LRMS (ES⁺) *m/z* 239.6 [M+H]⁺; HRMS *m/z* calculated for C₁₃H₂₃N₂O₂ [M+H]⁺ 239.1756 found 239.1744.

***N*^l-(2,4-dimethoxybenzyl)-*N*¹-methyl-*N*³-(1-nitroacridin-9-yl)propane-1,3-diamine, 149**



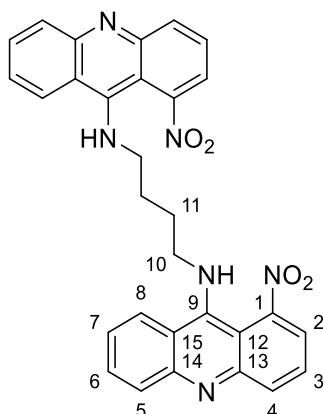
To a solution of 9-chloro-1-nitroacridine (50 mg, 0.19 mmol) in THF (5 mL) was added Et₃N (81 μL, 0.58 mmol) and *N*^l-(2,4-dimethoxybenzyl)-*N*¹-methylpropane-1,3-diamine, (40 mg, 0.17 mmol). The reaction was heated to reflux for 6 hours before cooling to RT. The solvent was concentrated *in vacuo* and purified on flash column chromatography (silica; 0-10% MeOH in DCM) to give a yellow solid (66 mg, 0.14 mmol, 84%) *R*_f 0.65 (10% MeOH in DCM); m.p. 214-218 °C; UV λ_{max} (MeOH/nm) 271.8; IR ν_{max}/cm⁻¹ 3289 (NH), ;¹H NMR (500 MHz CDCl₃) δ_H 1.76-1.80 (2H, m, H-11), 2.15 (3H, s, H-13), 2.39-2.42 (2H, m, H-12), 3.23-3.26 (2H, m H-10), 3.64 (2H, s, H-14), 3.71 (3H, s, H-21), 3.84 (3H, s, H-22), 6.74 (1H, br, NH)7.02-7.06 (2H, m, H-17, H-19), 7.21-7.23 (1H, m, -16), 7.48-7.56 (2H, m, H-7, H-6), 7.80-7.89 (3H, m, H-5, H2, H-8,, 8.14-8.16 (1H, m, H-2).¹³C NMR (125 MHz, CDCl₃) δ_C 28.4 (C-11), 4.08 (C-13), 55.9, 56.1 (C-21, C-22), 57.2 (C-14), 102-7 (C-16), 110.1 (C-17), 120.4 (C-5), 126.7 (C-7), 130.8 (C-4), 135.4 (C-7). (Tertiary carbons not visualised); LRMS (ES+) *m/z* 461.7 [M+H]⁺; HRMS *m/z* calculated for C₂₆H₂₉N₄O₄ [M+H]⁺ 461.2571 found 461.2559.

Synthesis of *N*¹,*N*³-bis(1-nitroacridin-9-yl)propane-1,3-diamine, 151



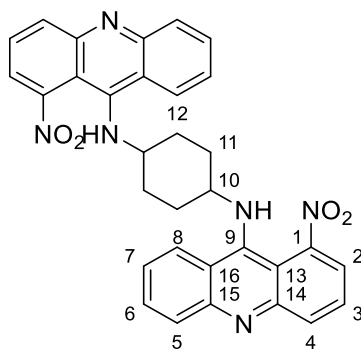
Synthesised according to general procedure A, using 9-chloro-1-nitroacridine (50 mg, 0.19 mmol), Et₃N (79 μ L, 0.57 mmol), 1,3-propanediamine (32 μ L, 0.38 mmol) in THF (0.57 mL). The crude material was purified by flash column chromatography (silica; 0-10% MeOH in DCM) followed by reverse phase flash column chromatography (C-18; 5-95% THF in H₂O) to give a red oil (55 mg, 0.11 mmol, 56%). *R*_f 0.20 (10% MeOH in DCM); λ_{max} (MeOH/nm) 224.8, 270.6; IR $\nu_{\text{max}}/\text{cm}^{-1}$ 3310 (NH) ¹H NMR (500 MHz CDCl₃) δ_{H} 1.80 (2H, dd, *J* = 5.5 Hz, H-11), 3.16-3.18 (4H, m, H-10), 7.39-7.46 (6H, m, H-5, H-6, H-7), 7.71-7.76 (4H, m, H-3) 8.11-8.13 (2H, m, H-8) 8.19-8.22 (2H, m, H-2), 2.39-2.42 (2H, m, H-12), 3.23-3.26 (2H, m, H-10), 3.64 (2H, s, H-14), 3.71 (3H, s, H-21), 3.84 (3H, s, H-22), 6.74 (1H, br, NH) 7.02-7.06 (2H, m, H-17, H-19), 7.21-7.23 (1H, m, H-16), 7.48-7.56 (2H, m, H-7, H-6), 7.80-7.89 (3H, m, H-5, H-2, H-8), 8.14-8.16 (2H, m, H-2). ¹³C NMR (125 MHz, CDCl₃) δ_{C} 28.5 (C-11), 42.5 (C-10), 120.4 (C-5), 125.1 (C-7) 130.7 (H-6, 136.8 (C-4), (Tertiary carbons not visualised); LRMS (ES⁺) *m/z* 519.8 [M+H]⁺; HRMS *m/z* calculated for C₂₉H₂₃N₆O₄ [M+H]⁺ 519.1743 found 519.1726.

Synthesis of N¹,N⁴-bis(1-nitroacridin-9-yl)butane-1,4-diamine, 154



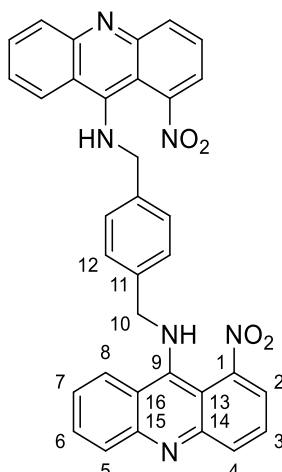
Synthesised according to general procedure A, using 9-chloro-1-nitroacridine (50 mg, 0.19 mmol), Et₃N (79 μ L, 0.57 mmol), 1,4-butanediamine (38 μ L, 0.38 mmol) in THF (0.57 mL). The crude material was purified by flash column chromatography (silica; 0-10% MeOH in DCM) followed by reverse phase flash column chromatography (C-18; 5-95% THF in H₂O) to give a yellow oil (45 mg, 0.09 mmol, 45%). R_f 0.25 (10% MeOH in DCM); λ_{max} (MeOH/nm) 222.8, 264.6; IR ν_{max}/cm^{-1} 3323 (NH)¹H NMR (500 MHz CDCl₃) δ_H 1.61-1.65 (4H, m, H-11), 3.24-3.29 (4H, m, H-10), 7.42-7.45 (2H, m, H-7), 7.66-7.74 (6H, m, H-5, H-6, H-3) 8.08-8.11 (2H, m, H-8), 8.17-8.21 (2H, m, H-2); ¹³C NMR (125 MHz, CDCl₃) δ_C 27.3 (C-11), 48.6 (C-10), 120.3 (C-5), 125.3 (C-7) 130.4 (C-6), 137.0 (C-4), (Tertiary carbons not visualised); LRMS (ES⁺) m/z 533.1 [M+H]⁺; HRMS m/z calculated for C₃₀H₂₅N₆O₄ [M+H]⁺ 533.1932 found 533.1946.

Synthesis of N^1,N^4 -bis(1-nitroacridin-9-yl)cyclohexane-1,4-diamine, 155



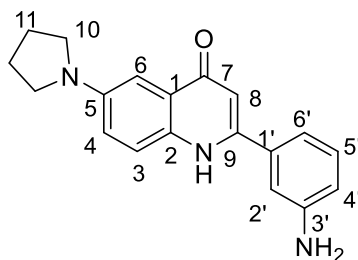
Synthesised according to general procedure A, using 9-chloro-1-nitroacridine (50 mg, 0.19 mmol), Et_3N (79 μL , 0.57 mmol), trans-1,4-diaminocyclohexane (43 mg, 0.38 mmol) in THF (0.57 mL). The crude material was purified by flash column chromatography (silica; 0-10% MeOH in DCM) followed by reverse phase flash column chromatography (C-18; 5-95% THF in H_2O) to give an orange oil (44 mg, 0.08 mmol, 41%). R_f 0.30 (10% MeOH in DCM); λ_{max} (MeOH/nm) 223.4, 271.6; IR $\nu_{\text{max}}/\text{cm}^{-1}$ 3314 (NH); ^1H NMR (500 MHz CDCl_3) δ_{H} 1.44-1.56 (8H, m, H-11, H-12), 2.61-2.64 (2H, H-10), 5.4 (1H, br, NH), 7.43-7.49 (2H, m, H-7), 7.58-7.62 (2H, m, H-6), 7.71-7.75 (4H, m, H-5, H-3), 8.08-8.11 (4H, m, H-8, H-4), 8.24-8.28 (2H, m, H-2); ^{13}C NMR (125 MHz, CDCl_3) δ_{C} 24.9 (C-11, C-12), 55.8 (C-10), 120.4 (C-5), 125.6 (C-7) 125.9 (C-6), 136.4 (C-4), (Tertiary carbons not visualised); LRMS (ES+) m/z 559.6 $[\text{M}+\text{H}]^+$; HRMS m/z calculated for $\text{C}_{32}\text{H}_{27}\text{N}_6\text{O}_4$ $[\text{M}+\text{H}]^+$ 559.2175 found 559.2167.

Synthesis of *N,N'*-(1,4-phenylenebis(methylene))bis(1-nitroacridin-9-amine), 156



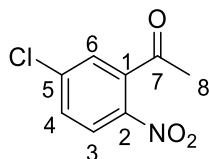
Synthesised according to general procedure A, using 9-chloro-1-nitroacridine (50 mg, 0.19 mmol), Et₃N (79 μ L, 0.57 mmol), *m*-xylylenediamine (50 μ L, 0.38 mmol) in THF (0.57 mL). The crude material was purified by flash column chromatography (silica; 0-10% MeOH in DCM) followed by reverse phase flash column chromatography (C-18; 5-95% THF in H₂O) to give a brown oil (38 mg, 0.06 mmol, 34%). R_f 0.61 (10% MeOH in DCM); λ_{max} (MeOH/nm) 226.7, 278.9; IR ν_{max}/cm^{-1} 3327 (NH); ¹H NMR (500 MHz CDCl₃) δ_H 4.36 (4H, s, H-10), 7.29 (4H, s, H-12) 7.42-7.45 (2H, m, H-7), 7.60-7.63 (2H, m, H-6), 7.73-7.78 (4H, m, H-5, H-3), 8.03-8.07 (4H, m, H-8, H-4), 8.23-8.28 (2H, m, H-2); ¹³C NMR (125 MHz, CDCl₃) δ_C 47.8 (C-10), 120.9 (C-5), 124.8 (C-7), 125.9 (H-6), 127.6 (C12) 136.4 (C-4), 136.8 (C-11) (Tertiary carbons not visualised); LRMS (ES+) m/z 581.6 [M+H]⁺; HRMS m/z calculated for C₂₉H₂₃N₆O₄ [M+H]⁺ 581.1914 found 581.1926.

2-(3-aminophenyl)-6-(pyrrolidin-1-yl)quinolin-4(1H)-one, 157



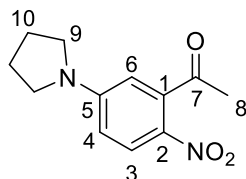
To a stirred solution of 2-(3-nitrophenyl)-6-(pyrrolidin-1-yl)quinolin-4(1H)-one (253 mg, 0.76 mmol) in DCM (5 mL) and MeOH (55 mL) was added 10% Pd/C (9 mg, 0.08 mmol) and put under a H₂ atmosphere. The reaction mixture was stirred at rt for 6 h before passing through Celite®. The filtrate was concentrated *in vacuo* to afford a yellow solid. Purification was achieved by flash column chromatography (silica; 0-5% MeOH in DCM) to afford the desired compound (45 mg, 0.15 mmol, 26% over two steps) as a yellow solid. *R_f* 0.16 (5% MeOH in DCM); m.p. 338-343 °C; UV λ_{max} (EtOH/nm) 282.6, 398.0; IR ν_{max} /cm⁻¹ 3471 (NH), 3369 (NH), 1571 (C=O); ¹H NMR (500 MHz, DMSO-*d*₆) δ_{H} 1.98-2.01 (4H, m, H-11), 3.29-3.31 (4H, m, H-10), 5.40 (2H, br s, NH₂), 6.09 (1H, s, H-8), 6.71 (1H, d, *J* = 7.8 Hz, H-4'), 6.88 (1H, d, *J* = 7.1 Hz, H-2'), 6.92-6.93 (1H, m, H-3), 7.01 (1H, d, *J* = 2.8 Hz, H-4), 7.07 (1H, dd, *J* = 2.8, 8.9 Hz, H-6), 7.17-7.19 (1H, m, H-5'), 7.65 (1H, d, *J* = 8.9 Hz, H-6'), 11.50 (1H, br s, NH); ¹³C NMR: (125 MHz, DMSO-*d*₆) δ_{C} : 25.5 (C-11), 48.8 (C-10), 103.1 (C-8), 105.3 (C-2'), 112.6 (C-6), 114.9 (C-4'), 115.9 (C-3), 119.1 (C-6'), 120.2 (C-4), 128.6 (C-1), 129.9 (C-5'), 132.3 (C-1'), 144.8 (C-9), 149.6 (C-3'), 176.6 (C-7) (C-2 and C-5 not visualized); LRMS (ES⁺) *m/z* 306.3 [M+H]⁺; HRMS [M+H]⁺ (C₁₉H₂₀N₃O) calcd 306.1601 found 306.1622. Data consistent with literature values.¹⁵⁹

Synthesis of 1-(5-chloro-2-nitrophenyl)ethan-1-one, 159



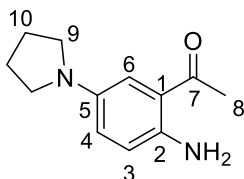
To fuming HNO_3 (2.6 mL, 61 mmol) at $-20\text{ }^\circ\text{C}$ was slowly added dropwise H_2SO_4 (0.4 mL, 7.0 mmol). The reaction mixture was allowed to stir for 15 min before 3-chloroacetophenone (0.6 mL, 4.8 mmol) was added dropwise under vigorous stirring over 15 minutes. The reaction mixture was warmed to $-10\text{ }^\circ\text{C}$ stirred for 5 h. After this time the reaction mixture was quenched with H_2O (50 mL) and stirred for a further 1 h before extracted into DCM (75 mL). The combined organic layers were washed with H_2O (5 x 100 mL), dried over MgSO_4 and concentrated *in vacuo*. The crude product was purified by flash column chromatography (silica; 50-100% DCM in petroleum ether) to give the desired product as a white solid (656 mg, 3.20 mmol, 66%). R_f 0.28 (50% petrol in DCM); m.p. $56\text{-}60\text{ }^\circ\text{C}$; UV λ_{max} (EtOH/nm) 270.8; IR $\nu_{\text{max}}/\text{cm}^{-1}$ 1694 (C=O), 1541 (N=O), 1357 (N=O); ^1H NMR (500 MHz, CDCl_3) δ_{H} 2.56 (3H, s, H-8), 7.39 (1H, d $J = 2.1$ Hz, H-6), 7.57 (1H, dd, $J = 2.1, 8.7$ Hz, H-4), 8.09 (1H, d, $J = 8.7$ Hz, H-3); ^{13}C NMR (125 MHz, CDCl_3) δ_{C} 30.2 (C-8), 125.9 (C-3), 127.4 (C-6), 130.5 (C-4), 139.6 (C-1), 141.2 (C-5), 143.8 (C-2), 198.2 (C-7); LRMS (ES^+) m/z 200.0 $[\text{M}+\text{H}]^+$. HRMS failed to detect mass. Data consistent with literature values, lit m.p. $60\text{-}62\text{ }^\circ\text{C}$.²⁰⁷

Synthesis of 1-(2-nitro-5-(pyrrolidin-1-yl)phenyl)ethan-1-one, 160



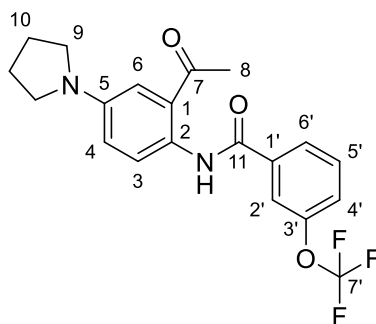
To a stirred solution of 1-(5-chloro-2-nitrophenyl)ethan-1-one (656 mg, 3.28 mmol) in DMF (3 mL) was added pyrrolidine (582 mg, 8.2 mmol) and K_2CO_3 (1.81 g, 13.1 mmol). The reaction mixture was heated to 140 °C and stirred overnight. The reaction mixture was poured onto ice and filtered to afford the crude product which was purified by flash column chromatography (silica; 50-100% DCM in petroleum ether) to afford the title compound as a yellow solid (675 mg, 2.88 mmol, 88%). R_f 0.15 (80% petrol in DCM); m.p. 124-127 °C; UV λ_{max} (EtOH/nm) 399.6; IR ν_{max}/cm^{-1} 1699 (C=O), 1596 (N=O), 1389 (N=O); 1H NMR (500 MHz, $CDCl_3$) δ_H 2.07-2.09 (4H, m, H-10), 2.49 (3H, s, H-8), 3.38-3.41 (4H, m, H-9), 6.22 (1H, $J = 2.4$ Hz, H-6), 6.48 (1H, dd, $J = 2.4, 8.9$ Hz, H-4), 8.05 (1H, d, $J = 8.9$ Hz, H-3); ^{13}C NMR (125 MHz, $CDCl_3$) δ_C 25.5 (C-10), 30.7 (C-8), 48.1 (C-9), 108.0 (C-6), 111.2 (C-4), 127.5 (C-3), 132.7 (C-2), 142.3 (C-1), 151.7 (C-5), 201.8 (C-7); LRMS (ES^+) m/z 235.4 $[M+H]^+$. HRMS m/z calculated for $C_{12}H_{15}N_2O_3$ $[M+H]^+$ 235.2570 found 235.2543. Data consistent with literature values, lit m.p. 119-121 °C.¹⁶⁰

1-(2-amino-5-(pyrrolidin-1-yl)phenyl)ethan-1-one, 161



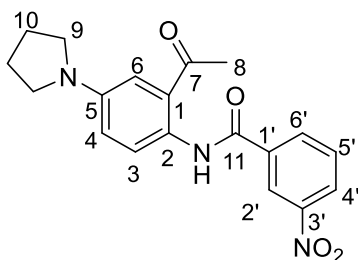
To a stirred solution of 1-(2-nitro-5-(pyrrolidin-1-yl)phenyl)ethan-1-one (417 mg, 1.78 mmol) in DCM (5 mL) and MeOH (5 mL) was added 10% Pd/C (20 mg, 0.18 mmol) under a H₂ atmosphere. The reaction mixture was stirred at RT for 18 h. The reaction mixture was passed over Celite® and the filtrate was concentrated *in vacuo* to afford the desired product (358 mg, 1.75 mmol, 99%) as an orange solid *R_f* 0.23 (50% petrol in DCM); m.p. 86-89 °C; UV λ_{max} (EtOH/nm) 241.2; IR $\nu_{\text{max}}/\text{cm}^{-1}$ 3401 (N-H), 1646 (C=O); ¹H NMR (500 MHz, CDCl₃) δ_{H} 2.00 (d, *J* = 6.2 Hz, H-10), 2.57 (3H, s, H-8), 3.23 (4H, d, *J* = 6.2 Hz, H-9), 5.69 (2H, s, NH₂), 6.64 (1H, d, *J* = 8.8 Hz, H-3), 6.77 (1H, dd, *J* = 2.7, 8.8 Hz, C-4), 6.85 (1H, d, *J* = 2.7 Hz, H-6); ¹³C NMR (125 MHz, CDCl₃) δ_{C} 25.3 (C-10), 28.2 (C-8) 48.9 (C-9), 113.5 (C-1), 118.8 (C-6), 119.3 (C-3), 121.3 (C-4), 139.8 (C-2), 142.0 (C-5), 201.0 (C-7); LRMS (ES⁺) *m/z* 205.4 [M+H]⁺. HRMS *m/z* calculated for C₁₂H₁₇N₂O [M+H]⁺ 205.3418 found 205.3426. Data consistent with literature values.¹⁶⁰

Synthesis of N-(2-acetyl-4-(pyrrolidin-1-yl)phenyl)-3-(trifluoromethoxy)benzamide, 162



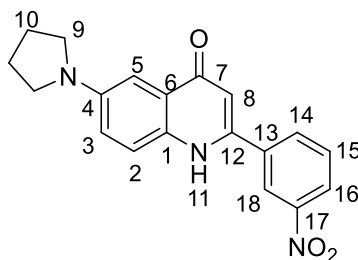
To a stirred solution of 1-(2-amino-5-(pyrrolidin-1-yl)phenyl)ethan-1-one (261 mg, 1.3 mmol) in THF (4 ml) was added Et₃N (0.7 ml, 4.7 mmol) and the solution was cooled to 0 °C before 3-(Trifluoromethoxy)benzoyl chloride (0.3 ml, 1.6 mmol) was added slowly over 5 minutes. The solution was stirred for 30 minutes before warmed to RT and stirred for a further 3 hours. The reaction mixture was concentrated *in vacuo*, redissolved in DCM (30 mL) and washed with NaHCO₃ (3 x 30 mL), then brine (30 mL), dried over MgSO₄ and concentrated *in vacuo* to give a brown solid. The crude product was purified by flash chromatography (silica; 0-10% MeOH in DCM) to afford an orange solid (395 mg, 1.0 mmol 79%); *R_f* 0.86 (10% MeOH in DCM); m.p. 146.5-147.7 °C; UV λ_{max} (EtOH/nm) 202.0, 247.4, 329.6, 400.0; IR ν_{max}/cm⁻¹ 3268 (NH), 1673 (C=O), 1587 (C=O); ¹H-NMR (500 MHz, DMSO-*d*₆) δ_H 1.97-1.99 (4H, m, H-10), 2.63 (3H, s, H-8), 3.30-3.32 (4H, m, H-9), 6.84 (1H, dd, *J* = 9.0, 2.8 Hz, H-2'), 7.00 (1H, d, *J* = 8.4 Hz, H-4), 7.62 (1H, s, H-6), 7.71-7.72 (1H, m, H-4'), 7.87-7.89 (1H, m, H-6'), 7.70-8.00 (1H, m, H-5'), 8.10-8.11 (1H, m, H-3), 11.54 (1H, s, NH); ¹³C-NMR (125 MHz, DMSO-*d*₆) δ_C 23.2 (H-10) 25.5 (H-8), 48.0 (H-9), 118.3 (C-6), 119.2 (C-2'), 122.2(C-7'), 126.7 (C-4), 127.4 (C-4'), 129.6 (C-6'), 130.1 (C-3), 131.5 (C-1) 132.1 (C-2), 133.7 (C-5'), 138.1 (C-1'), 145.6 (C-5), 163.4 (C-11), 201.3 (C-7) (C-3' not visualized); ¹⁹F-NMR (470 MHz, DMSO-*d*₆) δ_F -55.8; LRMS (ES⁺) *m/z* 393.1 [M+H]⁺; HRMS [M+H]⁺ (C₂₀H₂₀F₃N₂O₃) calcd 393.1241 found 393.1271. Data consistent with literature values.¹⁶⁰

***N*-(2-acetyl-4-(pyrrolidin-1-yl)phenyl)-3-nitrobenzamide, 163**



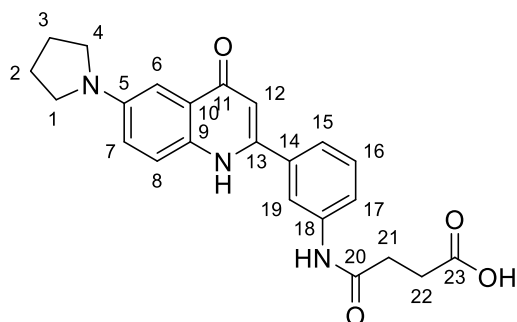
To a stirred solution of 1-(2-amino-5-(pyrrolidin-1-yl)phenyl)ethan-1-one (358 mg, 1.75 mmol) in THF (15 mL) under N₂ was added Et₃N (1.22 mL, 8.75 mmol) at 0 °C. To this was added portion wise 3-nitrobenzoyl chloride (971 mg, 5.25 mmol). The reaction mixture was allowed to stir for 30 min, before warmed to RT and stirred for 18 h. After this time the reaction mixture was concentrated *in vacuo*, redissolved in DCM and washed with NaHCO₃ (3 x 30 mL), then brine (30 mL), dried over MgSO₄ and concentrated *in vacuo* to give a brown solid. Purification was achieved by flash column chromatography (silica; 0-10% MeOH in DCM) to give the title compound (267 mg, 0.756 mmol, 43%) as a red solid. *R*_f 0.22 (100% DCM); m.p. 216-219 °C; UV λ_{max} (EtOH/nm) 328.0, 247.6; IR ν_{max}/cm⁻¹ 3216 (N-H), 1670 (C=O), 1590 (C=O), 1525 (N=O), 1339 (N=O); ¹H NMR (500 MHz, CDCl₃) δ_H 2.04 (4H, d, *J* = 6.2 Hz, H-10), 2.71 (3H, s, H-8), 3.34 (4H, d, *J* = 6.2 Hz, H-9), 6.87 (1H, dd, *J* = 2.8, 9.1 Hz, H-4), 7.03 (1H, d, *J* = 2.8 Hz, H-6), 7.70 (1H, t, *J* = 8.0 Hz, H-5'), 8.34-8.37 (2H, m, H-6', H-4'), 8.77 (1H, d, *J* = 9.1 Hz, H-3), ¹³C NMR (125 MHz, CDCl₃) δ_C 25.5 (C-10), 28.5(C-8), 47.8 (C-9), 113.3 (C-6), 118.4 (C-4), 122.4 (C-3), 122.8 (C-2'), 123.4 (C-1), 124.1 (C-2), 125.9 (C-4'), 129.8 (C-5'), 132.6 (C-6'), 137.3 (C-1'), 144.0 (C-5), 148.5 (C-3'), 162.7 (C-11), 204.0 (C-7); LRMS (ES⁺) *m/z* 354.3 [M+H]⁺; HRMS [M+H]⁺ (C₁₉H₂₀N₂O₄) calcd 354.1448 found 354.1446. Data consistent with literature values, lit m.p. 213-215 °C.¹⁵⁹

2-(3-nitrophenyl)-6-(pyrrolidin-1-yl)quinolin-4(1H)-one, 164



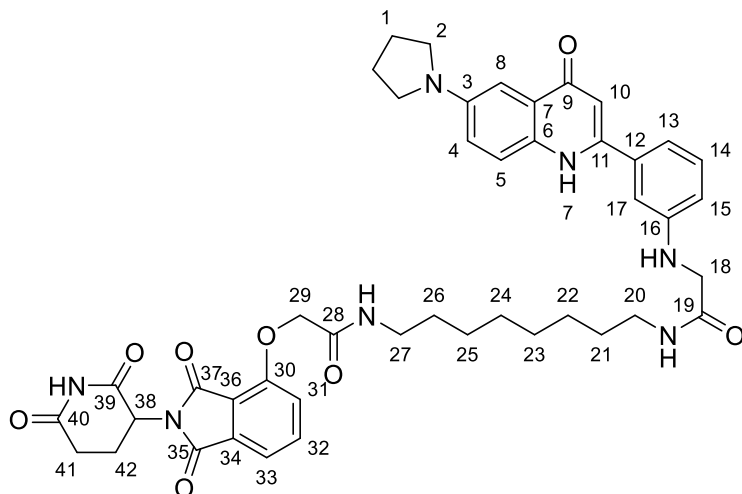
To a stirred solution of N-(2-acetyl-4-(pyrrolidin-1-yl)phenyl)-3-nitrobenzamide (267 mg, 0.756 mmol) in dioxane (10 mL) was added NaOH (454 mg, 11.3 mmol) and heated to reflux. The reaction was left to stir for 4 h before cooling to RT and poured into 10% NH₄Cl solution (100 mL) producing a brown precipitate. The crude was collected and was washed with H₂O (3 x 20 mL). The crude product was used directly in the next step with no purification. Crude characterisation: *R_f* 0.6 (10% MeOH in DCM); m.p. 325-329 °C; IR $\nu_{\text{max}}/\text{cm}^{-1}$ 3257 (N-H), 1592 (C=O), 1531 (N=O), 1341 (N=O); LRMS (ES⁺) *m/z* 336.3 [M+H]⁺.

Synthesis of 4-oxo-4-((3-(4-oxo-6-(pyrrolidin-1-yl)-1,4-dihydroquinolin-2-yl)phenyl)amino)butanoic acid, 170



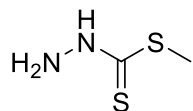
To 2-(3-aminophenyl)-6-(pyrrolidin-1-yl)quinolin-4(1H)-one, 2-(3-aminophenyl)-6-(pyrrolidin-1-yl)quinolin-4(1H)-one (100 mg, 0.33 mmol) in DMF (2 mL) was added DIPEA (114 μ L, 0.66 mmol) and succinic anhydride (33 mg, 0.33 mmol) and left to stir at RT for 16 hours. The solvent was removed *in vacuo* and was purified by reverse phase flash column chromatography (C-18; 5-95% THF in H₂O) to obtain a yellow oil (117 mg, 0.29 mmol, 88%). R_f 0.14 (10% MeOH in DCM); UV λ_{max} (MeOH/nm) 304.2 224.1; IR ν_{max}/cm^{-1} 35013 (COOH); ¹H NMR (500 MHz CDCl₃) δ_H 2.43 (2H, d, J = 6.8 Hz, H-21), 2.51 (2H, d, J = 6.8 Hz, H-22), 3.38-3.42 (4H, m, H-3), 3.46-3.49 (4H, m, H-4), 6.90-6.91 (1H, m, H-13), 6.94 (2H, d, J = 8.2 Hz, H-8), 7.20-7.25 (3H, m, H-6, H-7), 7.38-7.40 (1H, m, H-16), 7.77-7.80 (2H, m, H-16 and H-20), 12.2 (1H, s, COOH); ¹³C NMR (125 MHz, CDCl₃) δ_C 20.4 (C-2), 29.4 (C-21), 29.9 (C-21) 50.4 (C-1, C-4), 97.1 (C-12), 114.1 (C-6, 119.2 (C-8), 121.9 (C-7), 128.7 (C-15), 147.5 (C-1), 171.8 (C-11), 172.2 (C-23), 173.1 (C-20); (Not all carbons visualised) LRMS (ES⁺) m/z 406.3 [M+H]⁺; HRMS m/z calculated for C₂₃H₂₄N₃O₄ [M+H]⁺ 406.5132 found 406.5114.

Synthesis of 2-((2-(2,6-dioxopiperidin-3-yl)-1,3-dioxoisindolin-4-yl)oxy)-N-(8-(2-((3-(4-oxo-6-(pyrrolidin-1-yl)-1,4-dihydroquinolin-2-yl)phenyl)amino)acetamido)octyl)acetamide, 171



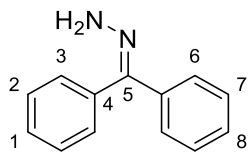
To 4-oxo-4-((3-(4-oxo-6-(pyrrolidin-1-yl)-1,4-dihydroquinolin-2-yl)phenyl)amino)butanoic acid, (100 mg, 0.25 mmol) in DMF (2 mL) was added DIPEA (44 μ L, 0.25 mmol), DMAP (3 mg, 0.03 mmol), EDC.HCl (39 mg, 0.25 mmol) and cereblon ligand (118 mg, 0.25 mmol). The reaction was left overnight and was concentrated *in vacuo*. The crude product was purified by reverse phase flash column chromatography (C-18; 5-95% THF in H₂O) to afford the title compound as a yellow oil (34 mg, 0.04 mmol). R_f 0.27 (10% MeOH in DCM); UV λ_{max} (MeOH/nm) 364.2 206.7; IR ν_{max}/cm^{-1} 1715 1650; ¹H NMR (500 MHz CDCl₃) δ_H 1.22-1.36 (12H, m, H-21 to H-26), 2.11-2.14 (8H, m, H-1, H-41, H-42), 2.78 (2H, m, H-26), 3.35-3.40 (4H, m, H-2), 3.85 (2H, s, H-18), 4.32-4.36 (3H, m, H-29, H-38), 6.88-6.92 (2H, m, H-10, H-17), 6.99-7.09 (5H, m, H-8, H-15, H-4, H-13, H-14), 7.44-7.49 (2H, m, H-31, H-33), 7.88-7.90 (1H, m, H-32), 8.11 (1H, s, NH); ¹³C NMR (125 MHz, CDCl₃) δ_C 20.6 (C-42), 24.8 (C-1), 25.4 (C-22, C25), 28.4 (C-24, C23), 29.1 (C24, C23), 29.3 (C-41), 37.9 (C-20), 28.4 (C-27), 48.6 (C-2), 55.9 (C-18), 61.3 (C-38), 65.4 (C-29), 94.6 (C-10), 113.7 (C-17), 116.2 (C-8, C-15), 118.1 (C-13), 188.4 (C-5), 119.2 (C-4), 169.0 (C-37), 169.8 (C-19). (Can't visualise rest of carbons) LRMS (ES⁺) m/z 804.8 [M+H]⁺; HRMS [M+H]⁺ (C₄₄H₅₀N₇O₈) calcd 804.3452 found 804.3428.

Synthesis of methyl hydrazinecarbodithioate, 176



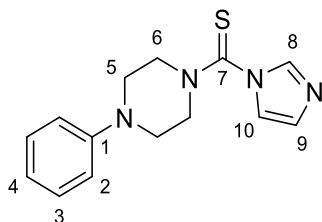
To a solution of KOH (0.56 g, 12 mmol) in H₂O (1 mL) and IPA (0.8 mL) was added dropwise at 0 °C, hydrazine hydrate (0.32 mL, 12 mmol) in water (0.5 mL). Then carbon disulfide (0.60 mL, 0.1 mmol) was added dropwise to the solution over 30 mins. The solution was stirred at 0 °C for 2 h before MeI (0.75 mL, 12 mmol) was added and the reaction was stirred for a further 1 h. The white precipitate was then filtered and washed with cold water to give a white solid (0.82 g, 6.72 mmol, 56%). *R_f* 0.23 (10% MeOH in DCM); m.p. 82-86 °C; UV λ_{\max} (MeOH/nm) 249.4, 321.8; IR $\nu_{\max}/\text{cm}^{-1}$; ¹H NMR (500 MHz DMSO-*d*₆) δ_{H} 3.25 (1H, br, NH₂), 5.24 (1H, br, NH). CH₃ not visualised, occluded by solvent peak. Data consistent with literature, lit m.p. 81-82 °C.²⁰⁸

Synthesis of (diphenylmethylene)hydrazine, 182



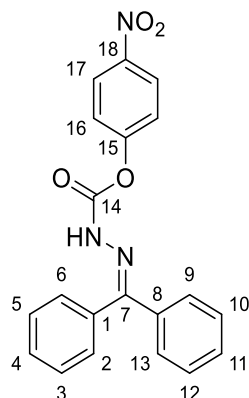
To a solution of benzophenone (1.0 g, 5.5 mmol) in ethanol (20 mL) was added hydrazine monohydrate (0.47 mL, 10 mmol) and cat. AcOH (0.1 mL). The reaction was heated to reflux and stirred for 6 hours. The solvent was removed *in vacuo* and the crude product was purified by flash column chromatography (silica; 0-10% MeOH in DCM) to give a white solid. R_f 0.15 (10% MeOH in DCM); m.p. 94-97 °C; UV λ_{\max} (MeOH/nm) 272.3, 315.8; IR $\nu_{\max}/\text{cm}^{-1}$ 3340 (NH); $^1\text{H NMR}$ (500 MHz CDCl_3) δ_{H} 5.15 (2H, s, NH_2), 7.01-7.06 (5H, m, H-2, H-7, H-8,), 7.21-7.25 (3H, m, H-6, H-1), 7.28-7.32 (2H, m, H-3); $^{13}\text{C NMR}$ (125 MHz, CDCl_3) δ_{C} 126.4 (C-7), 127.9 (C-2), 128.7 (C-1), 128.8 (C-8), 129.0 (C-4) 149.1 (C-5); LRMS (ES^+) m/z 197.3 $[\text{M}+\text{H}]^+$; HRMS m/z calculated for $\text{C}_{13}\text{H}_{13}\text{N}_2$ $[\text{M}+\text{H}]^+$ 197.2103 found 197.2141. Data consistent with literature values, lit m.p. 94-96 °C.²⁰⁹

Synthesis of (1H-imidazol-1-yl)(4-phenylpiperazin-1-yl)methanethione, 186



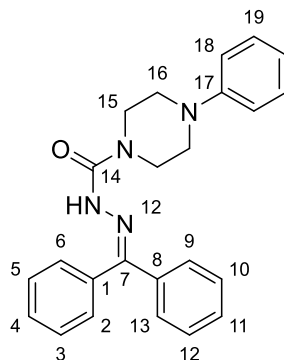
To 1-phenyl-piperazine (100 mg, 0.62 mmol) in THF (5 mL) was added TCDI (122 mg, 0.68 mmol). The reaction was stirred at RT for 5 h. The solvent was removed *in vacuo* and the product was purified by flash column chromatography (silica; 0-10% MeOH in DCM) giving a yellow oil (125 mg, 0.46 mmol, 74%). R_f 0.24 (10% MeOH in DCM); UV λ_{\max} (MeOH/nm) 314.5, 224.1; IR $\nu_{\max}/\text{cm}^{-1}$ 1514 (C=S); ^1H NMR (500 MHz CDCl_3) δ_{H} 3.42-3.44 (4H, m, H-5), 3.46-3.49 (4H, m, H-6), 6.89-6.91 (1H, m, H-4), 6.98 (2H, d, $J = 8.4$ Hz, H-2), 7.18-7.25 (3H, m, H-3, H-9), 7.36-7.40 (1H, m, H-10), 8.11 (1H, s, H-8); ^{13}C NMR (125 MHz, CDCl_3) δ_{C} 50.6 (C-5), 54.9 (C-6), 115.1 (C-2), 118.9 (C-10), 121.9 (C-4), 128.7 (C-3), 128.9 (C-9), 135.4 (C-8), 147.5 (C-1), 170.8 (C-7); LRMS (ES^+) m/z 273.4 $[\text{M}+\text{H}]^+$; HRMS m/z calculated for $\text{C}_{14}\text{H}_{17}\text{N}_4\text{S}$ $[\text{M}+\text{H}]^+$ 273.3941 found 273.3956. Data consistent with literature values.¹⁸⁹

Synthesis of 4-nitrophenyl 2-(diphenylmethylene)hydrazine-1-carboxylate, 189



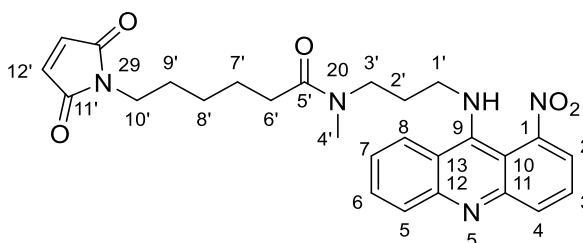
To a solution of (diphenylmethylene)hydrazine (500 mg, 2.55 mmol) in a mixture of DCM (20 mL), THF (10 mL) and pyridine (0.47 mL, 5.61 mmol) at 0 °C stirring was added 4-nitrophenyl chloroformate (1.13 g, 5.61 mmol) and left to stir at room temperature for 5 hours. After the reaction was completed, the yellow solution was concentrated *in vacuo* and purified by flash chromatography (silica; 0-5% MeOH in DCM) to afford a yellow solid (695 mg, 1.91 mmol, 75%). $R_f = 0.35$ (10% MeOH in DCM); m.p. 119-123 °C; UV λ_{\max} (MeOH/nm) 251.3, 205.6; IR $\nu_{\max}/\text{cm}^{-1}$ 3384 (NH₂), 2954 (NH), 2910 (NH), 1630 (C=O), 1607 (C=O); ¹H NMR (500 MHz CDCl₃) δ_{H} 7.21-7.25 (3H, m, H-10, H-11, H-12), 7.48-7.59 (8H, m, H-3, H-4, H-5, H-9, H-13, H-16), 7.88-7.92 (2H, m, H-6, H-2), 8.21-8.24 (2H, m, H-17); ¹³C NMR (125 MHz, CDCl₃) δ_{C} 123.6 (C-16), 126.8 (C-16), 128.4, 128.5 (C-5, C-3, C-10, C-12), 131.1 (C-4, C-11), 133.8 (C-1), 144.6 (C-18), 157.4 (C-7), 158.5 (C-14); LRMS (ES⁺) m/z 362.7 [M+H]⁺; HRMS m/z calculated for C₂₀H₁₆N₃O₄ [M+H]⁺ 362.6147 found 362.6130. Data consistent with literature values.²¹⁰

Synthesis of *N'*-(diphenylmethylene)-4-phenylpiperazine-1-carbohydrazide, 190



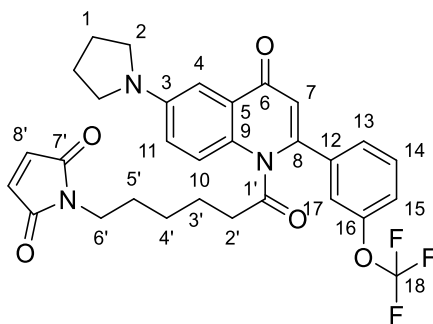
To a solution of 4-nitrophenyl 2-(diphenylmethylene)hydrazine-1-carboxylate (150 mg, 0.42 mmol) in DCM (10 mL) was added DIPEA (220 μ L, 1.26 mmol) and 1-phenylpiperazine (66 μ L 0.42 mmol) and was stirred for 3 h at RT. The reaction mixture was washed with 1M HCl (5 mL), H₂O (5 mL) and brine (5 mL). The organic fraction was dried over MgSO₄, filtered, concentrated in vacuo and purified by flash column chromatography to give a yellow oil (136 mg 0.35 mmol, 83%) $R_f = 0.55$ (10% MeOH in DCM); UV λ_{\max} (MeOH/nm) 260.3, 216.7; IR $\nu_{\max}/\text{cm}^{-1}$ 2957 (NH), 1630 (C=O), 1680 (C=O); ¹H NMR (500 MHz CDCl₃) δ_{H} 3.14-3.16 (4H, m, H-16), 3.41-3.43 (4H, m, C-15) 6.76-6.78 (1H, m, H-20), 6.88-6.90 (2H, m, C-18), 7.15-7.26 (5H, m, H-19, H-10, H-11, H-12) 7.45-7.51 (5H, m, H-4, H-5, H-3), 7.89-7.92 (2H, m, H-6, H-2); ¹³C NMR (125 MHz, CDCl₃) δ_{C} 50.9 (C-15), 52.6 (C-16), 117.4 (C-18), 121.1 (C-20), 130.9 (C-13, C-2) 131.1 (C-9, C-6), 133.1 (C-4), 157.6 (C-7), 158.4 (C-14); LRMS (ES⁺) m/z 385.3 [M+H]⁺; HRMS m/z calculated for C₂₄H₂₅N₄O [M+H]⁺ 385.4716 found 385.4734.

Synthesis of 6-(2,5-dioxo-2,5-dihydro-1H-pyrrol-1-yl)-N-methyl-N-(3-((1-nitroacridin-9-yl)amino)propyl)hexanamide, 193



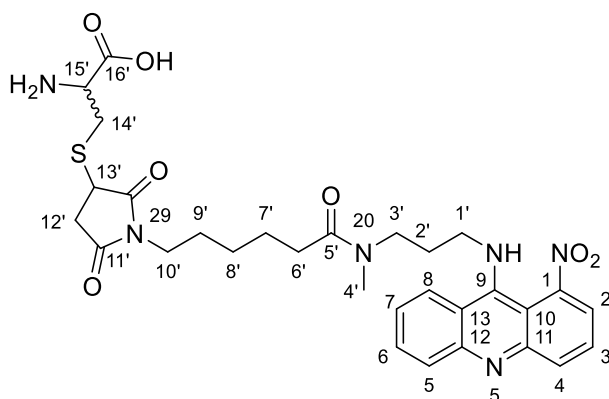
To a stirred solution of N^1 -methyl- N^3 -(1-nitroacridin-9-yl)propane-1,3-diamine (50 mg, 0.16 mmol) in DMF (2 mL) was added 6-maleimidoheptanoic acid (34 mg, 0.16 mmol), HATU (73 mg, 0.19 mmol) and DMAP (1 mg, 0.01 mmol) at 0 °C. The reaction was warmed to RT and stirred for 16 h. The solution was concentrated *in vacuo*, loaded onto Isolute® and purified by flash column chromatography (silica; 0-10% MeOH in DCM) to afford a red oil (61 mg, 0.12 mmol, 74%). *Rf* 0. (5% MeOH in DCM); UV λ_{\max} (EtOH/nm) 221, 278.0; IR $\nu_{\max}/\text{cm}^{-1}$ 3263 (NH), 1700 (CO), 1602 (CO), 1528 (NO); ^1H NMR: (500 MHz, DMSO- d_6) δ_{H} ; 1.08-1.13 (2H, m, H-8'), 1.41-1.46 (2H, m, H-7'), 1.51-1.55 (2H, m, H-9'), 1.71 (2H, br, H-2'), 2.16-2.20 (2H, m, H-6'), 1.99-2.01 (2H, m, H-10), 2.88 (3H, s, H-4'), 3.41-3.44 (2H, m, H-3'), 3.47-3.52 (2H, m, H-1'), 3.72 (1H, br, NH), 6.64 (2H, s, H-12'), 7.01-7.10 (1H, m, H-7), 7.17 (1H, br, H-6), 7.33-7.41 (2H, m, H-3, H-5), 7.51-7.61 (1H, m, H-4), 7.75-7.78 (1H, m, H-8), 8.27-8.30 (1H, m, H-2); ^{13}C NMR: (125 MHz, DMSO- d_6) δ_{C} ; 25.0 (C-7'), 25.4 (C-8'), 26.2 (C-1'), 28.6 (C-9'), 35.4 (C-4'), 37.2 (C-6'), 42.7 (C-10') 48.7 (C-3'), 103.2 (C-10), 118.7 (C-5), 119.7 (C-13), 124.3 (C-8), 125.9 (C-7), 129.8 (C-6), 134.9 (C-12'), 135.4 (C-4), 140.4 (C-2), 171.4, 172.0 (C-5', C-11'), (C-1, C=11, C-12 and C-13 were not visualized); LRMS (ES $^+$) m/z 504.4 [M+H] $^+$; HRMS [M+H] $^+$ (C $_{27}$ H $_{30}$ N $_5$ O $_5$) calculated 504.4891 found 504.4810.

Synthesis of 1-(6-oxo-6-(4-oxo-6-(pyrrolidin-1-yl)-2-(3-(trifluoromethoxy)phenyl)quinolin-1(4H)-yl)hexyl)-1H-pyrrole-2,5-dione, 194



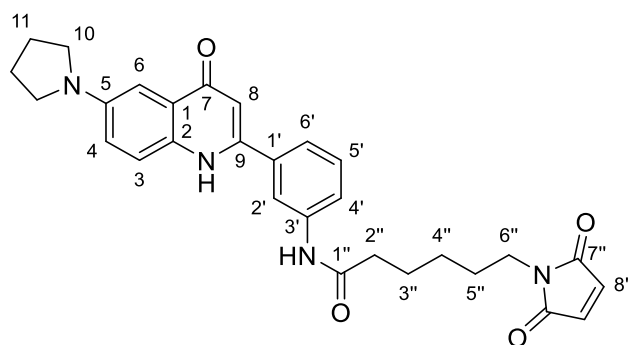
To a solution of 6-maleimidocaproic acid (50 mg, 0.24 mmol) in THF (1 mL) at 0°C was added 1 drop of DMF followed by oxalyl chloride (10 μ L, 0.11 mmol). The solution was stirred for 3 hours at RT and then concentrated *in vacuo* before the crude reaction mixture was redissolved in THF (2 ml) and Et₃N (77 μ L, 0.55 mmol) was added followed by 6-(pyrrolidin-1-yl)-2-(3-(trifluoromethoxy)phenyl)quinolin-4(1H)-one (101 mg, 0.33 mmol). The solution was stirred at 50 °C for 16 hours and then concentrated *in vacuo*. The crude mixture was quenched with water (10 mL) and the product was extracted with DCM (3 x 10 mL). The organic layers were combined, washed with brine (10 mL), dried over MgSO₄, filtered and concentrated *in vacuo*. The crude product was purified by flash column chromatography (silica; 0-10% MeOH in DCM) to afford a brown solid, (48 mg, 0.08 mmol, 35%); R_f = 0.79 (10% MeOH in DCM); m.p. 220-223 °C; UV λ_{max} (EtOH/nm) 213.2, 278.2, 334.8, 397.2; IR ν_{max} /cm⁻¹ 1761 (C=O), 1703 (C=O), 1630 (C=O); ¹H-NMR (500 MHz, CDCl₃) δ_{H} 1.20 (2H, m, H-4'), 1.38-1.44 (4H, m, H-3', H-5'), 2.16-2.18 (4H, m, H-1) 2.40 (2H, t, *J* = 7.5 Hz, H-2'), 3.09-3.12 (4H, m, H-2), 3.25 (2H, t, *J* = 7.2 Hz, H-6'), , 6.59 (2H, s, H-8'), 6.74 (1H, d, *J* = 2.6 Hz, H-7), 6.90-6.92 (2H, m, H-15, H-17), 7.16-7.18 (2H, m, H-4, H-11), 7.69-7.71 (1H, m, H-13), 7.74-7.76 (1H, m, H-14), 7.79-7.80 (1H, m, H-10); ¹³C NMR (125 MHz, CDCl₃) δ_{C} 24.5 (C-1), 25.7 (C-3'), 26.3 (C-4'), 28.3 (C-5'), 30.9 (C-2'), 34.3 (C-6'), 37.5 (C-2), 96.2 (C-7), 110.8 (C-17), 119.6 (C-4), 120.4 (C-14), 120.8 (C-15), 121.6 (C-11), 123.7 (C-13), 125.2 (C-10), 130.0 (C-12), 130.9 (C-9), 134.1 (C-18), 137.4 (C-5), 141.9 (C-8'), 143.7 (C-3), 151.3 (C-8), 152.8 (C-16), 170.8 (C=O), 170.9 (C=O), 179.4 (C=O). ¹⁹F NMR (470 MHz, CDCl₃) -57.5; LRMS (ES⁺) *m/z* 568.2 [M+H]⁺; HRMS failed to detect a mass.

Synthesis of S-(1-(6-(methyl(3-((1-nitroacridin-9-yl)amino)propyl)amino)-6-oxohexyl)-2,5-dioxopyrrolidin-3-yl)cysteine, 195



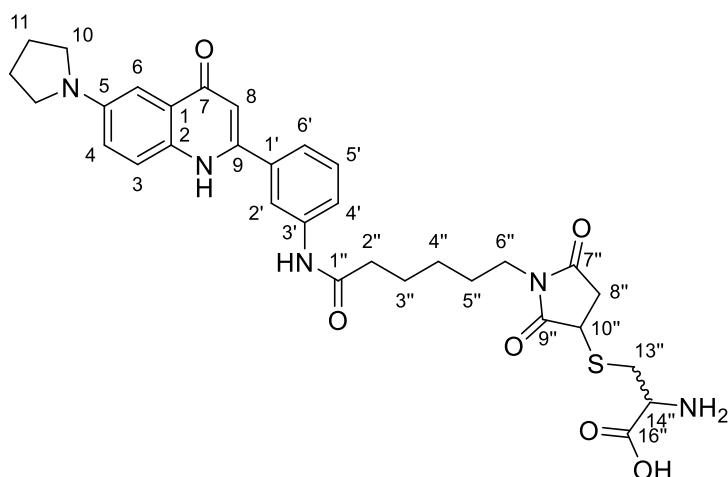
To a solution of 6-(2,5-dioxo-2,5-dihydro-1*H*-pyrrol-1-yl)-*N*-methyl-*N*-(3-((1-nitroacridin-9-yl)amino)propyl)hexanamide (50 mg, 0.1 mmol) in DMF (2 mL) was added L-cysteine (12 mg, 0.1 mmol) and DABCO (1 mg, 0.01 mmol). The reaction mixture was stirred for 6 hours before the solvent was concentrated *in vacuo*. The product was purified by reverse phase flash column chromatography (C-18, 5-95% THF in H₂O) to afford a red solid (31 mg, 0.05 mmol) 52%. *R_f* 0.1 (10% MeOH in DCM); m.p. 180-185 °C; UV λ_{max} (EtOH/nm) 222.0, 245.0, 280.2; IR ν_{max} /cm⁻¹ 3258 (NH), 1603 (CO); ¹H NMR: (500 MHz, DMSO-*d*₆) δ_{H} ; 1.09-1.12 (2H, m, H-8'), 1.42-1.48 (2H, m, H-7'), 1.53-1.57 (2H, m, H-9'), 1.74-1.78 (2H, m, H-2'), 2.16-2.20 (2H, m, H-6'), 2.00-2.02 (2H, m, H-10), 2.85 (3H, s, H-4'), 3.01-3.11 (4H, m, H-12', H-14'), 3.39-3.42 (2H, m, H-3'), 3.45-3.50 (2H, m, H-1'), 3.64-3.68 (1H, m, H-15'), 3.71-3.74 (1H, m, H-13'), 3.88 (1H, br, NH), 7.03-7.10 (1H, m, H-7), 7.16-7.19 (1H, m, H-6), 7.34-7.43 (2H, m, H-3, H-5), 7.51-7.59 (1H, m, H-4), 7.76-7.80 (1H, m, H-8), 8.27-8.30 (1H, m, H-2), 9.14 (2H, s, NH₂), 11.71 (COOH); ¹³C NMR: (125 MHz, DMSO-*d*₆) δ_{C} ; 25.1 (C-7'), 25.4 (C-8'), 26.1 (C-1'), 28.8 (C-9'), 31.7 (C-14'), 34.1 (C-12'), 35.1 (C-4'), 37.6 (C-6'), 42.4 (C-10'), 44.6 (C-13'), 48.8 (C-3'), 56.7 (C-15'), 103.2 (C-10), 118.6 (C-5), 119.6 (C-13), 124.3 (C-8), 126.1 (C-7), 129.7 (C-6), 135.1 (C-4), 140.7 (C-2), 171.6, 171.9, 171.3 (C-5', C-11', C-), (C-1, C=11, C-12 and C-13 were not visualized); LRMS (ES⁺) *m/z* 625.71 [M+H]⁺; HRMS [M+H]⁺ (C₃₀H₃₇N₆O₇S) calculated 625.1601 found 625.1622.

Synthesis of 5-(2,5-dioxocyclopent-3-en-1-yl)-N-(3-(4-oxo-6-(pyrrolidin-1-yl)-1,4-dihydroquinolin-2-yl)phenyl)pentanamide, 196



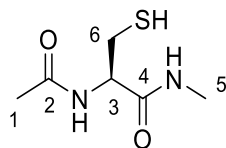
To a stirred solution of 6-(pyrrolidin-1-yl)-2-(3-aminophenyl)-quinolin-4(1*H*)-one (57 mg, 0.19 mmol) in DMF (2 mL) was added 6-maleimidohexanoic acid (40 mg, 0.19 mmol), HATU (87 mg, 0.23 mmol) and DMAP (2 mg, 0.02 mmol) at 0°C. This was left to stir for 10 minutes before warming to room temperature and was left to stir for a further 18 hours. The reaction was quenched using 1 M HCl (5 mL) followed by water (5 mL) and extracted in DCM. The combined organic layers were washed with water (5 mL) followed by brine (5 mL) and a saturated solution of NaHCO₃ (5 mL) before dried over MgSO₄, filtered and concentrated *in vacuo*. The crude compound was purified by flash column chromatography (silica; 0-10% MeOH in DCM) to obtain a yellow oil (65 mg, 0.13 mmol 68% yield). *R*_f 0.3 (5% MeOH in DCM); UV λ_{max} (EtOH/nm) 216.8, 289.2, 397.0; IR ν_{max}/cm⁻¹ 3364 (NH), 3243 (NH), 1695 (C=O); ¹H NMR: (500 MHz, DMSO-*d*₆) δ_H; 1.23-1.26 (2H, m, H-4''), 1.51 (2H, p, *J* = 7.2 Hz, H-3''), 1.60 (2H, p, *J* = 7.2 Hz, H-5''), 1.96-2.00 (4H, m, H-11), 2.31 (2H, t, *J* = 2.5 Hz, H-2''), 3.27-3.30 (4H, m, H-10), 3.39 (2H, t, *J* = 7.1 Hz, H-6''), 6.11 (1H, s, H-8), 6.97 (2H, s, H-8''), 7.00-7.02 (1H, m, H-3), 7.07 (1H, d, *J* = 8.3 Hz, H-4), 7.42-7.45 (2H, m, H-6, H-5'), 7.63 (1H, d, *J* = 7.7 Hz, H-4'), 7.70 (1H, d, *J* = 7.3 Hz, H-2'), 7.98-8.0 (1H, m, H-6'), 10.1 (1H, s, NHCO), 11.55 (1H, s, NH); ¹³C NMR: (125 MHz, DMSO-*d*₆) δ_C; 25.0 (C-3''), 25.5 (C-11), 26.3 (C-4''), 28.3 (C-5''), 36.7 (C-2''), 37.4 (C-6''), 48.1 (C-10), 103.2 (C-5'), 118.2 (C-6), 119.2 (C-2'), 120.2 (C-3), 120.9 (C-2'), 122.3 (C-4'), 129.8 (C-6'), 134.9 (C-8''), 140.3 (C-5), 145.0 (C-3'), 171.5, 171.9 (C-7'', C-1''), 176.82 (C-7) (C-1, C-2, C-9, C-1' were not visualized); LRMS (ES⁺) *m/z* 499.5 [M+H]⁺; HRMS [M+H]⁺ (C₂₉H₃₁N₄O₄) calculated 499.4872 found 499.4813.

Synthesis of S-(2,5-dioxo-1-(6-oxo-6-((3-(4-oxo-6-(pyrrolidin-1-yl)-1,4-dihydroquinolin-2-yl)phenyl)amino)hexyl)pyrrolidin-3-yl)cysteine, 197



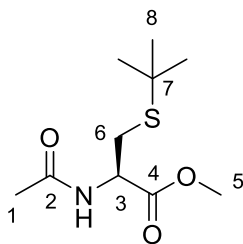
To a solution of 6-(2,5-dioxo-2,5-dihydro-1*H*-pyrrol-1-yl)-*N*-methyl-*N*-(3-((1-nitroacridin-9-yl)amino)propyl)hexanamide (50 mg, 0.1 mmol) in DMF (2 mL) was added L-cysteine (12 mg, 0.1 mmol) and DABCO (1 mg, 0.01 mmol). The reaction mixture was stirred for 6 hours before the solvent was concentrated *in vacuo*. The product was purified by reverse phase flash column chromatography (C-18, 5-95% THF in H₂O) to afford a yellow solid (24 mg, 0.04 mmol, 40%). *R_f* 0.1 (10% MeOH in DCM); m.p. 205-211 °C; UV λ_{max} (EtOH/nm) 252.0, 280.2; IR ν_{max}/cm⁻¹ 3234 (NH), 1613 (CO); ¹H NMR: (500 MHz, DMSO-*d*₆) δ_H; 1.11-1.14 (2H, m, H-4'), 1.52-1.57 (4H, m, H-3'', H-5''), 2.04-2.06 (4H, m, H-11), 2.08-2.11 (2H, m, H-2''), 2.44-2.62 (6H, m, H-6'', H-8'', H-13'') 3.84-3.87 (2H, m, H-10'', H14'') 6.79 (1H, s, H-8), 6.87-6.90 (1H, m, H-3), 6.95-7.0 (2H, m, H-6, H-4), 7.23-7.27 (2H, m, H-5', H-4'), 7.56-7.61 (2H, m, H-6', H-2'), 8.9 (2H, s, NH₂) 12.6 (1H, br, COOH) NMR: (125 MHz, DMSO-*d*₆) δ_C; Carbon NMR too weak LRMS (ES⁺) *m/z* 620.8 [M+H]⁺; HRMS [M+H]⁺ failed to find a mass.

Synthesis of (R)-2-acetamido-3-mercapto-N-methylpropanamide, 199



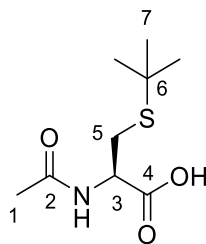
To a solution of (R)-2-acetamido-N-methyl-3-((2-nitrophenyl)disulfaneyl)propanamide (50 mg, 0.15 mmol) in THF (2 mL) and H₂O (0.2 mL) was added TCEP.HCl (132 mg, 0.46 mmol) and the reaction was left to stir for 6 hours at RT. The organic solvent was removed *in vacuo*, diluted with H₂O (10 mL) and was then extracted with 10% IPA in EtOAc (3 x 5 mL). The organic layers were combined, washed with brine (10 mL), dried over MgSO₄, filtered and concentrated *in vacuo*. The crude mixture was purified by flash column chromatography (silica; 0-10% MeOH in DCM) to give a white solid (6.3 mg, 0.04 mmol, 24%). *R_f* 0.75 (10% MeOH in DCM); m.p. 178-182 °C; IR $\nu_{\max}/\text{cm}^{-1}$ 2921 (NH), 2952 (NH), 2520 (SH) 1637 (C=O); ¹H NMR (500 MHz, CDCl₃) δ_{H} 2.04 (3H, s, H-1), 1.84 (3H, s, H-1), 2.85 (3H, d, *J* = 5 Hz, H-5), 3.08-3.18 (2H, m, H-6), 4.72-4.88 (1H, m, H-3), 6.55-6.58 (1H, m, NH), 6.69-6.72 (1H, d, *J* = 8.0 Hz, NH), 7.38-7.41 (1H, m, H-10), 7.70-7.73 (1H, m, H-9), 8.25-8.30 (2H, m, H-8 and H-11). ¹³C NMR (125 MHz, CDCl₃) δ_{C} 23.1 (C-1), 26.3 (C-5), 30.1 (C-6), 43.1 (C-5), 53.3 (C-3), 172.2 (C-2), 174.2 (C-4). LRMS (ES⁺) *m/z* 177.3 [M+H]⁺; HRMS [M+H]⁺ (C₆H₁₃N₂O₂S) calculated 177.5136 found 177.5153. Data consistent with literature values, lit m.p. 192-195 °C.²¹¹

Synthesis of methyl *N*-acetyl-S-(*tert*-butyl)-L-cysteinate, 202



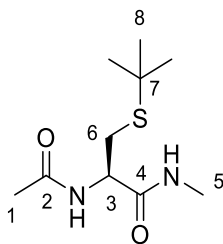
To a solution of *N*-acetyl L-cysteine methyl ester (1.0 g, 1.1 mmol) in TFA (10 mL) was added *tert*-butanol (0.56 mL, 1.06 mmol). The reaction was stirred for 4 hours before being concentrated *in vacuo* and diluted with H₂O (10 mL). The pH was adjusted to 8 with 28% ammonium hydroxide solution and was extracted in EtOAc (3 x 25 mL). The organic layers were combined, dried over MgSO₄, filtered and concentrated *in vacuo* to give a colourless oil (1.18 g, 87%). *R_f* 0.75 (10% MeOH in DCM); m.p. 110-112 °C; IR $\nu_{\max}/\text{cm}^{-1}$ 2962 (NH), 1780 (C=O), 1740 (C=O); ¹H NMR (500 MHz, DMSO-*d*₆) δ 1.27 (9H, s, H-1), 1.85 (3H, s, H-1), 2.73 – 2.88 (2H, m, H-6), 3.64 (2H, s, H-5), 4.37 – 4.48 (1H, m, H-3), 8.38 (1H, d, *J* = 7.8 Hz, NH); ¹³C NMR (125 MHz, DMSO-*d*₆) δ_{C} 22.7 (C-1), 29.8 (C-6), 31.1 (C-8), 42.8 (C-7), 52.5 (C-5), 53.3 (C-3), 169.8 (C-4), 171.7 (C-2). LRMS (ES⁺) *m/z* 234.1 [M+H]⁺; HRMS [M+H]⁺ (C₁₀H₂₀NO₃S) calculated 234.3613 found 234.3631.

Synthesis of *N*-acetyl-*S*-(*tert*-butyl)-*L*-cysteine, 203



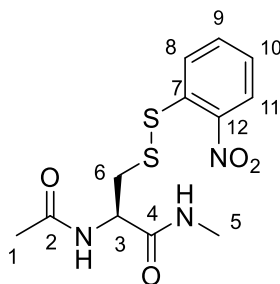
To a solution of methyl *N*-acetyl-*S*-(*tert*-butyl)-*L*-cysteinate (1.18g, 5.05 mmol) in MeOH (30 mL) stirring at 0 °C was added 1 M NaOH (10 mL) and warmed to RT. The reaction was stirred for 5 hours before concentrated *in vacuo* to give an aqueous residue. The pH was adjusted to 5 with 1 M HCl and concentrated *in vacuo*. The crude product was redissolved in H₂O (20 mL) and extracted in EtOAc (3 x 20 mL). The organic layers were combined, dried over MgSO₄, filtered and concentrated in vacuo to give a white solid (669 mg, 60%). *R_f* 0.75 (10% MeOH in DCM); m.p. 164-166 °C; IR $\nu_{\max}/\text{cm}^{-1}$ 3333 (COOH), 2965 (NH), 1704 (C=O), 1637 (C=O); ¹H NMR (500 MHz, DMSO-*d*₆) δ 1.27 (9H, s, H-7), 1.84 (3H, s, H-1), 2.71 – 2.88 (2H, m, H-5), 4.32 – 4.40 (1H, m, H-3), 8.23 (1H, d, *J* = 7.0 Hz, NH); ¹³C NMR (125 MHz, DMSO-*d*₆) δ_{C} 22.6 (C-1), 30.1 (C-5), 31.0 (C-7), 42.4 (C-6), 53.4 (C-3), 172.3 (C-2), 174.2 (C-4). LRMS (ES⁺) *m/z* 220.2 [M+H]⁺; HRMS [M+H]⁺ (C₉H₁₈NO₃S) calculated 220.3798 found 220.3814. Data consistent with literature values, lit m.p. 130 °C.²¹²

Synthesis of (R)-2-acetamido-3-(*tert*-butylthio)-*N*-methylpropanamide, 204



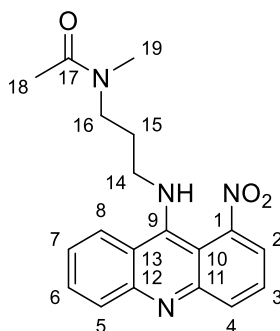
To a solution of *N*-acetyl-*S*-(*tert*-butyl)-*L*-cysteine (640 mg, 2.90 mmol) in MeCN (15 mL) was added $\text{B}(\text{OCH}_2\text{CF}_3)_3$ (1.3 mL, 5.85 mmol) and 2 M methylamine in THF (2.1 mL, 58.5 mmol) and the solution was stirred and refluxed at 80 °C overnight. The solution was concentrated *in vacuo* before being redissolved in DCM. The organic layer was washed with a saturated solution of NaHCO_3 (10 mL) followed by 1 M HCl (10 mL). The organic layer was then dried over MgSO_4 , filtered and concentrated *in vacuo* to give a pale yellow solid (355 mg, 69%). R_f 0.75 (10% MeOH in DCM); m.p. 154-157 °C; IR $\nu_{\text{max}}/\text{cm}^{-1}$ 2935 (NH), 1712 (C=O), 1646 (C=O); ^1H NMR (500 MHz, $\text{DMSO-}d_6$) δ_{H} 1.26 (9H, s, H-8), 1.84 (3H, s, H-1), 2.58 (3H, d, $J = 4.5$ Hz, H-5) 2.61 – 2.82 (2H, m, H-6), 4.28-4.32 (1H, m, H-3), 7.94-7.96 (1H, m, NH), 8.10 (1H, d, $J = 8.0$ Hz, NH); ^{13}C NMR (125 MHz, $\text{DMSO-}d_6$) δ_{C} 23.4 (C-1), 26.1 (C-5), 30.6 (C-6), 31.2 (C-8), 42.5 (C-5), 53.7 (C-3), 172.3 (C-2), 174.2 (C-4). LRMS (ES^+) m/z 233.3 $[\text{M}+\text{H}]^+$; HRMS $[\text{M}+\text{H}]^+$ ($\text{C}_{29}\text{H}_{31}\text{N}_4\text{O}_4$) calculated 233.4106 found 233.4091.

Synthesis of (R)-2-acetamido-N-methyl-3-((2-nitrophenyl)disulfaneyl)propanamide, 205



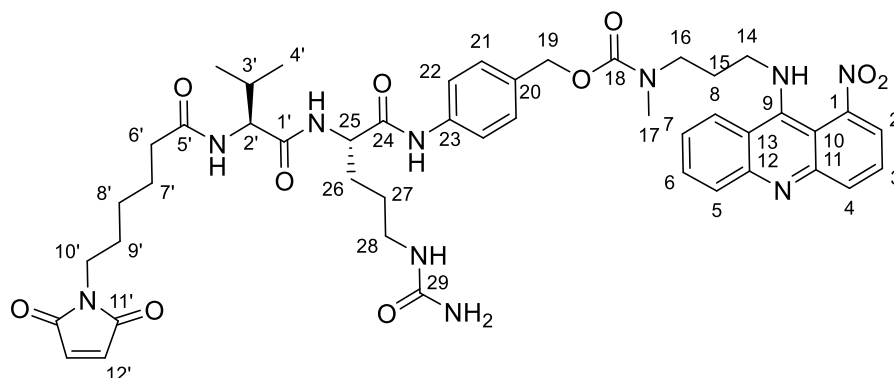
To a solution of (R)-2-acetamido-3-(*tert*-butylthio)-*N*-methylpropanamide (177 mg, 1.0 mmol) in acetic acid (10 mL) stirring was added 2-nitrobenzene sulfenyl chloride (228 mg, 1.2 mmol). After 6 hours the reaction mixture was concentrated *in vacuo* before diluted with H₂O (20 mL) and extracted in EtOAc (3 x 20 mL). The organic washings were combined, dried over MgSO₄, filtered and concentrated *in vacuo*. The crude product was purified by flash column chromatography (silica; 0-10% MeOH in DCM) to afford a yellow solid (162 mg, 49%). *R_f* 0.75 (10% MeOH in DCM); m.p. 187-190 °C; UV λ_{max} (EtOH/nm) 279.1, 224.1; IR $\nu_{\text{max}}/\text{cm}^{-1}$ 2924 (NH), 1716 (C=O), 1654 (C=O); ¹H NMR (500 MHz, CDCl₃) δ 2.04 (3H, s, H-1), 1.84 (3H, s, H-1), 2.85 (3H, d, *J* = 5 Hz, H-5) 3.08-3.18 (2H, m, H-6), 4.72-4.88 (1H, m, H-3), 6.55-6.58 (1H, m, NH), 6.69-6.72 (1H, d, *J* = 8.0 Hz, NH), 7.38-7.41 (1H, m, H-10), 7.70-7.73 (1H, m, H-9), 8.25-8.30 (2H, m, H-8 and H-11). ¹³C NMR (125 MHz, CDCl₃) δ_{C} 23.4 (C-1), 26.4 (C-5), 31.2 (C-6), 54.1 (C-7), 124.3 (C-11) 124.7 (C-10), 128.9 (C-7). 133.3 (C-8), 139.4 (C-9), 145.2 (C-12), 172.4 (C-2), 174.1 (C-4). LRMS (ES⁺) *m/z* 230.1 [M+H]⁺; HRMS failed to detect a mass.

Synthesis of *N*-methyl-*N*-(3-((1-nitroacridin-9-yl)amino)propyl)acetamide, 206



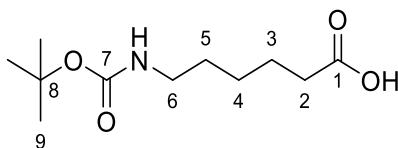
To a solution of nitro (34 mg, 0.11 mmol) in DMF (2 mL) was added K_2CO_3 (15 mg, 0.11 mmol) followed by acetic anhydride (10 μ L, 0.11 mmol). The reaction was stirred for 4 hours until consumption of the starting material and then concentrated *in vacuo*. The residue was dissolved in DCM (10 mL) and washed with H_2O (3 x 10 mL) before being dried over $MgSO_4$, filtered and concentrated *in vacuo*. The crude product was purified by flash column chromatography (silica; 0-20% MeOH in DCM) to give a red oil (17 mg, 0.05 mmol, 44%). *R_f* 0.29 (RP C-18, 50% THF (0.1% NH_3) in H_2O (0.1% NH_3)); UV λ_{max} (EtOH/nm) 261.7, 347.8, 391.2; IR ν_{max}/cm^{-1} 3359 (NH), 1617 (CO), 1527 (NO); 1H NMR: (500 MHz, $DMSO-d_6$) δ_H 1.68-1.78 (2H, m, H-15), 1.93 (3H, s, H-18), 2.88 (3H, s, H-19), 2.94 (1H, s, NH), 3.16-3.19 (2H, m, H-14), 3.24-3.26 (2H, m, H-16), 7.10-7.12 (1H, m, H-7), 7.28-7.33 (2H, m, H-3, H-5), 7.35-7.38 (1H, m, H-6), 7.49-7.54 (2H, m, H-4, H-8), 7.78-7.83 (1H, m, H-2) ^{13}C NMR (125 MHz, $DMSO-d_6$) δ_C ; 19.6 (C-18), 23.4 (C-15), 34.8 (C-19), 40.1 (C-14), 47.4 (C-16), 111.9 (C-10), 115.1 (C-13), 115.3 (C-5), 117.4 (C-13), 118.6 (C-8), 122.0 (C-7), 130.1 (C-6), 130.8 (C-6), 134.8 (C-4), 135.1 (C-3), 140.1, 140.2 (C-2, C-11), 151.3 (C-1), 157.3 (C-9). LRMS (ES^+) m/z 353.4 [$M+H$] $^+$; HRMS [$M+H$] $^+$ ($C_{19}H_{21}N_4O_3$) calculated 353.6147 found 353.6127.

Synthesis of 4-((S)-2-((S)-2-(6-(2,5-dioxo-2,5-dihydro-1H-pyrrol-1-yl)hexanamido)-3-methylbutanamido)-5-ureidopentanamido)benzyl methyl(3-((1-nitroacridin-9-yl)amino)propyl)carbamate, **207**



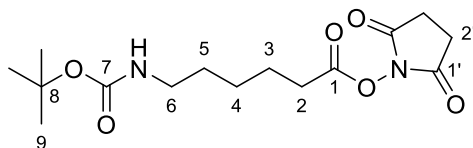
To 4-((S)-2-((S)-2-((tert-butoxycarbonyl)amino)-3-methylbutanamido)-5-ureidopentanamido)benzyl methyl(3-((1-nitroacridin-9-yl)amino)propyl)carbamate **229** (35 mg, 0.04 mmol) was added 10% TFA in DCM (1 mL). The reaction was left at RT for 5 hours. The solvent was removed *in vacuo* and DMF (1 mL) was added. The solution was cooled to 0 °C and DIPEA (87 μ L, 0.5 mmol) was added followed by HATU (30 mg, 0.08 mmol) and 6-maleimido-hexanoic acid (17 mg, 0.08 mmol). The reaction was left to stir for 16 h at RT. The reaction mixture was concentrated *in vacuo* and the crude product was purified by reverse phase column chromatography (C-18; 5-95% THF in H₂O) to give the product as a red oil (13 mg, 0.02 mmol, 50%). *R_f* 0.25 (10% MeOH in DCM); UV λ_{max} (EtOH/nm) 284.0, 242.2 216.3; IR ν_{max} /cm⁻¹ 3334 (NH), 1613, 1649(CO); ¹H NMR: (500 MHz, DMSO-*d*₆) δ_{H} ; 0.98 (6H, dd, *J* = 7.1, 20.4 Hz, H-4'), 1.24-1.28 (4H, m, H-7', H-8'), 1.55-1.61 (4H, m, H-9', H-27), 1.70-1.74 (2H, m, H-26), 2.85-2.89 (1H, m, H-6'), 2.92-2.94 (2H, m, H-16), 3.08-3.10 (2H, m, H-28), 3.15 (3H, s, H-17), 3.18-3.20 (2H, m, H-15) 3.46-3.49 (2H, m, H-10'), 4.15-4.18 (1H, m, H-2'), 4.22-4.25 (1H, m H-25), 4.56 (2H, s, H-19), 7.52-7.58 (3H, m, H-7, H-21), 7.62-7.71 (3H, H-6, H-22), 7.81-7.90 (5H, m, H-12', H-3, H-4, H-5, H-8). 8.16-8.19 (2H, m, H-4, H-8), 8.24-8.26 (1H, m, H-2); ¹³C NMR: (125 MHz, DMSO-*d*₆) δ_{C} ; Carbon sample too weak for ¹³C NMR; LRMS (ES⁺) *m/z* 909.7 [M+H]⁺; HRMS [M+H]⁺ (C₄₆H₅₇N₁₀O₁₀) calculated 909.7423. found 909.7465

Synthesis of 6-((*tert*-butoxycarbonyl)amino)hexanoic acid, 211



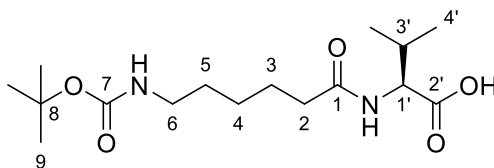
To a solution of 6-aminohexanoic acid (5.0 g, 38 mmol) in 1,4-dioxane:H₂O (40 mL, 2:1) was added 1 M NaOH (20 mL) and cooled to 0 °C. Boc₂O (9.2 g, 42 mmol) was added and the solution was allowed to warm to RT and stirred for 4 hours. The solution was concentrated *in vacuo* and redissolved in water (50 mL). The aqueous layer was washed with EtOAc (30 mL) and the pH of the aqueous layer was adjusted to pH 1. The product was then extracted into EtOAc (3 x 50 mL), dried over MgSO₄, filtered and concentrated *in vacuo* to give a colourless oil which crystallised to a white solid on standing (7.74 g, 88%). *R_f* 0.10 (10% MeOH in DCM); m.p. 41-44 °C; IR $\nu_{\max}/\text{cm}^{-1}$ 3287 (COOH), 3012 (NH), 1710 (C=O); ¹H NMR (500 MHz, DMSO-*d*₆) δ_{H} 1.23 (2H, p, *J* = 7.1 Hz, H-4), 1.33-1.40 (11H, m, H-5, H-9), 1.48 (2H, p, *J* = 7.5 Hz, H-3), 2.18 (2H, t, *J* = 7.5 Hz, H-2) 2.89 (2H, p, *J* = 6.6 Hz, H-6) 6.77 (1H, s, NH), 11.99 (1H, s, COOH); ¹³C NMR (125 MHz, DMSO-*d*₆) δ_{C} 24.7 (C-3), 26.3 (C-4), 28.7 (C-9), 29.7 (C-5), 34.1 (C-2), 55.7 (C-6), 77.8 (C-8), 156.0 (C-7), 174.9 (C-1). LRMS and HRMS failed to detect mass. Data consistent with literature values, lit m.p. 35-37 °C.²¹³

Synthesis of 2,5-dioxopyrrolidin-1-yl 6-((tert-butoxycarbonyl)amino)hexanoate, 212



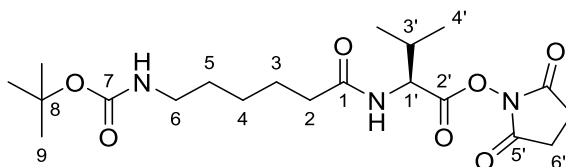
To a stirring solution of 6-((tert-butoxycarbonyl)amino)hexanoic acid (5.0 g, 22 mmol) in THF (40 mL) was added N-hydroxysuccinimide (2.7 g, 24 mmol) and the reaction mixture was cooled to 0 °C before DCC (4.9 g, 24 mmol) was added. The solution was warmed to room temperature and stirred under N₂ for 16 hours. The white precipitate that formed was filtered off and the filtrate was concentrated *in vacuo* to give an oil which was redissolved in DCM (20 mL) and left for 1 hour before being filtered again and concentrated *in vacuo* to give a white solid (6.2 g, 19 mmol, 86%); *R_f* 0.25 (10% MeOH in DCM); m.p. 76-80 °C; IR $\nu_{\max}/\text{cm}^{-1}$ 3017 (NH), 1730 (C=O), 1715 (C=O), 1695 (C=O); ¹H NMR (500 MHz, DMSO-*d*₆) δ_{H} 1.25-1.40 (15H, m, H-3, H-4, H-5, H-9), 2.65 (2H, t, *J* = 7.7 Hz, H-2), 2.81 (4H, s, H-2'), 2.87-2.92 (2H, m, H-6), 6.78 (1H, br, NH); ¹³C NMR (125 MHz, DMSO-*d*₆) δ_{C} 24.4 (C-3), 25.8 (C-2'), 25.9 (C-4), 28.7 (C-9), 29.4 (C-5), 35.0 (C-2), 55.2 (C-6), 77.8 (C-8), 156.0 (C-7), 169.4 (C-1), 170.7 (C-1'). LRMS (ES⁺) *m/z* 329.4 [M+H]⁺; HRMS [M+H]⁺ (C₁₅H₂₅N₂O₆) calculated 329.1729 found 329.1742. Data consistent with literature values, lit m.p. 82-86 °C.²¹⁴

Synthesis of (6-((*tert*-butoxycarbonyl)amino)hexanoyl)-L-valine, 213



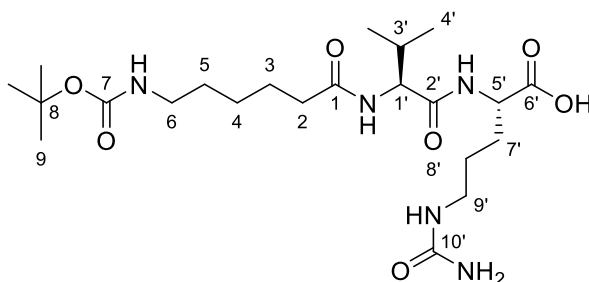
To a solution of 2,5-dioxopyrrolidin-1-yl 6-((*tert*-butoxycarbonyl)amino)hexanoate (6.0 g, 19 mmol) in DME (66 mL) and THF (20 mL) was added L-valine (2.5 g, 21 mmol) and NaHCO_3 (1.8 g, 21 mmol) in water (66 mL) and the reaction mixture was stirred for 16 hours at room temperature before 15% citric acid (75 mL) was added. The solution was extracted with 10% IPA in EtOAc (3 x 70 mL) and the organic layers were combined and washed with water (50 mL) followed by brine (50 mL) before being dried over MgSO_4 , filtered and concentrated *in vacuo* to give a crude yellow solid which was titrated with ether three times to give a white solid (6.2 g, 19 mmol, 95% yield). R_f 0.16 (10% MeOH in DCM); m.p. 74-78 °C; IR $\nu_{\text{max}}/\text{cm}^{-1}$ 3213 (COOH), 3017 (NH), 1715 (C=O), 1695 (C=O), 1676 (COOH); ^1H NMR (500 MHz, $\text{DMSO-}d_6$) δ_{H} 0.87 (6H, dd, $J = 6.9$ and 11.5 Hz, H-4'), 1.21-1.23 (2H, m, H-3) 1.37 (11H, br, H-4, H-9), 1.46-1.49 (2H, m, H-5), 1.99-2.05 (1H, m, H-3') 2.11-2.19 (2H, m H-2), 2.87-2.92 (2H, m, H-6), 4.14 (1H, dd, $J = 5.8$ and 2.6 Hz, H-1'), 6.75 (1H, s, NH), 7.91 (1H, d, $J = 9.0$ Hz, NH), 12.49 (1H, s, COOH); ^{13}C NMR (125 MHz, $\text{DMSO-}d_6$) δ_{C} 18.5 (C-4'), 24.9 (C-3), 25.6 (C-4), 25.7 (C-9), 28.7 (C-5), 33.8 (C-3'), 35.4 (C-2), 57.4 (C-1'), 77.7 (C-8), 156.0 (C-7), 172.9 (C-1), 173.7 (C-2'). LRMS (ES^+) m/z 331.4 $[\text{M}+\text{H}]^+$; HRMS $[\text{M}+\text{H}]^+$ ($\text{C}_{16}\text{H}_{31}\text{N}_2\text{O}_5$) calculated 331.6249 found 331.6271.

Synthesis of 2,5-dioxopyrrolidin-1-yl (6-((*tert*-butoxycarbonyl)amino)hexanoyl)-L-valinate, 214



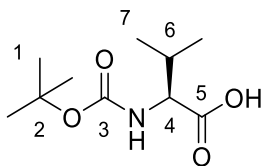
To a stirring solution of 6-((*tert*-butoxycarbonyl)amino)hexanoyl)-L-valine (3.0 g, 9.1 mmol) in THF (30 mL) was added at 0 °C *N*-hydroxysuccinimide (1.2 g, 10.0 mmol) followed by DCC (2.1 g, 10.0 mmol). The solution was warmed to room temperature and stirred under N₂ for 16 hours. The cloudy white precipitate was filtered off and the filtrate was concentrated in vacuo to give an oil which was redissolved in DCM (20 mL) and left for 1 hour before being filtered again and concentrated in vacuo to give a white solid (3.8 g, 8.9 mmol, 98%). *R_f* 0.22 (10% MeOH in DCM); m.p. 88-90 °C; IR $\nu_{\max}/\text{cm}^{-1}$ 3105 (NH), 3024 (NH), 1730 (C=O), 1715 (C=O), 1695 (C=O), 1676 (C=O); ¹H NMR (500 MHz, DMSO-*d*₆) δ_{H} 0.99 (6H, t, *J* = 7.4 Hz, H-4'), 1.20-1.26 (2H, m, H-3) 1.37 (11H, br, H-4, H-9), 1.48-1.51 (2H, m, H-5), 2.16-2.18 (3H, m, H-2, H-3') 2.81 (4H, s, H-6') 2.88 (2H, q, *J* = 6.3 Hz, H-6), 4.57 (1H, dd, *J* = 6.2 and 2.6 Hz, H-1'), 6.75 (1H, s, NH), 8.35 (1H, d, *J* = 6.2 Hz, NH); ¹³C NMR (125 MHz, DMSO-*d*₆) δ_{C} 18.4 (C-4'), 24.9 (C-3), 25.4 (C-6'), 25.6 (C-9) 25.9 (C-5), 28.7 (C-3'), 33.8 (C-2), 35.2 (C-6), 55.8 (C-1'), 77.8 (C-8), 156.0 (C-7), 168.2 (C-5') 170.5 (C-1), 173.2 (C-2'). LRMS (ES⁺) *m/z* 428.5 [M+H]⁺; HRMS [M+H]⁺ (C₂₀H₃₃N₃O₇) calculated 428.7194 found 428.7162.

Synthesis of (13S,16S)-13-isopropyl-2,2-dimethyl-4,11,14-trioxo-16-(3-ureidopropyl)-3-oxa-5,12,15-triazaheptadecan-17-oic acid, 215



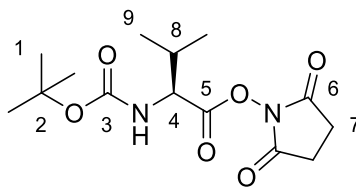
To a solution of 2,5-dioxopyrrolidin-1-yl (6-((tert-butoxycarbonyl)amino)hexanoyl)-L-valinate (3.5 g 8.2 mmol) in DME (40 mL) and THF (15 mL) was added L-citrulline (1.6 g, 9.0 mmol) and NaHCO₃ (1.8 g, 21 mmol) in water (40 mL). The reaction mixture was stirred for 16 hours at room temperature before 15% citric acid (50 mL) was added. The solution was extracted with 10% IPA in EtOAc (3 x 50 mL) and the organic layers were combined, washed with water (40 mL) followed by brine (40 mL) before being dried over MgSO₄, filtered and concentrated *in vacuo* to a yellow solid (3.7 g, 7.6 mmol, 93%). *R_f* 0.13 (10% MeOH in DCM); m.p. 130 – 132 °C; IR $\nu_{\max}/\text{cm}^{-1}$ 3436 (NH₂), 3301 (NH), 3071 (COOH), 2951 (NH), 1723 (C=O), 1704 (C=O), 1635 (C=O), 1610 (C=O); ¹H NMR (500 MHz, DMSO-*d*₆) δ_{H} 0.95 (6H, dd, *J* = 6.8, 17.8 Hz, H-4'), 1.25-1.27 (2H, m, H-3), 1.33-1.43 (13H, m, H-4, H-9, H-8'), 1.46 (2H, m, H-5), 1.52-1.64 (2H, m, H-7'), 2.01-2.08 (3H, m, H-2, H-3'), 2.89-2.96 (4H, m, H-6, H-9'), 3.70-3.75 (1H, m, H-1'), 4.10 (1H, q, *J* = 5.1 Hz, H-5'), 5.42 (2H, s, NH₂), 5.88 (1H, m, NH), 7.01 (1H, d, *J* = 9.3 Hz, NH), 7.67 (1H, s, NH), 7.89 (1H, s, NH), 9.10 (1H, s, COOH); ¹³C NMR (125 MHz, DMSO-*d*₆) δ_{C} 18.3 (C-4'), 21.2 (C-8), 23.4 (C-3), 23.6 (C-4), 28.9 (C-9), 30.6 (C-5), 31.1 (C-7'), 31.6 (C-3'), 36.4 (C-2), 40.9 (C-6), 48.1 (C-9'), 55.2 (C-5'), 61.2 (C-1'), 79.4 (C-8), 159.4 (C-7), 160.1 (C-10') 168.9 (C-2'), 176.1 (C-1), 176.3 (C-6'). LRMS (ES⁺) *m/z* 353.4 [M+H]⁺; HRMS failed to detect mass.

Synthesis of (*tert*-butoxycarbonyl)-L-valine, 223



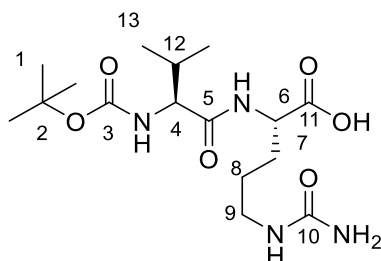
To a solution of L-valine (5.0 g, 43 mmol) in THF (75 mL) and water (38 mL) stirring was added 1 M NaOH (50 mL). The solution was cooled to 0 °C before Boc₂O (10 g, 47 mmol) was added slowly and allowed to warm to RT and stirred for 4 hours. The reaction mixture was concentrated *in vacuo* and diluted with H₂O (50 mL). The aqueous solution was washed with EtOAc (50 mL) before acidified to pH 2 with 2 M HCl. The aqueous layer was extracted with EtOAc (3 x 100 mL) and the combined organic layers were dried over MgSO₄, filtered and concentrated *in vacuo* to give a colourless oil (8.67 g, 40 mmol 94%) *R_f* 0.55 (10% MeOH in DCM); IR $\nu_{\text{max}}/\text{cm}^{-1}$ 3327 (NH), 2968 (COOH), 1688 (C=O); ¹H NMR (500 MHz, DMSO-*d*₆) δ_{H} 0.87 (6H, t, *J* = 7.2 Hz, H-7), 1.39 (9H, s, H-1), 1.97-2.00 (1H, m, H-6), 3.79 (1H, dd, *J* = 6.0, 8.5 Hz, H-4), 6.93 (1H, d, *J* = 8.5 Hz, NH), 12.46 (1H, br, COOH); ¹³C NMR (125 MHz, DMSO-*d*₆) δ_{C} 18.61 and 19.61 (C-7), 28.67 (C-1), 49.05 (C-6), 59.56 (C-4), 78.42 (C-2), 156.23 (C-3), 173.96 (C-5); LRMS (ES⁺) *m/z* 218.2 [M+H]⁺; HRMS [M+H]⁺ (C₁₀H₂₀NO₄) calculated 218.1347 found 218.1470. Data consistent with literature values.²¹⁵

Synthesis of 2,5-dioxopyrrolidin-1-yl (*tert*-butoxycarbonyl)-L-valinate, 224



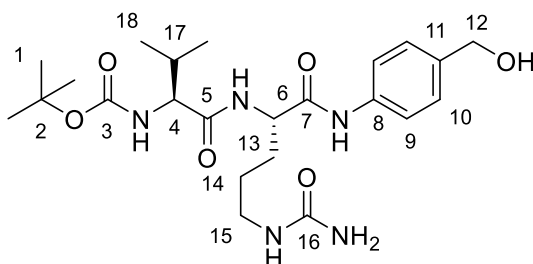
To a solution of (*tert*-butoxycarbonyl)-L-valine (2.24 g, 10.3 mmol) in THF (40 mL) was added *N*-hydroxysuccinimide (1.31 g, 11.4 mmol) followed by DCC (2.35 g, 11.4 mmol) at 0 °C. The reaction was warmed to RT and left to stir for 15 hours. The precipitate that was formed was filtered off and the filtrate was concentrated *in vacuo* before being redissolved in DCM and left to stand for 1 hour. The precipitate was filtered off and the filtrate was concentrated *in vacuo* to give a white powder (3.51 g, 1.1 mmol, 107%). R_f 0.79 (10% MeOH in DCM); m.p. 113-115 °C; IR $\nu_{\max}/\text{cm}^{-1}$ 3318 (NH), 2929 (COOH), 1779 (C=O), 1732 (C=O), 1691 (C=O); ^1H NMR (500 MHz, DMSO- d_6) δ_{H} 0.99 (6H, d, $J = 6.8$ Hz, H-9), 1.40 (9H, s, H-1), 2.11-2.15 (1H, m, H-8), 2.80-2.82 (4H, m, H-7), 4.22 (1H, dd, $J = 6.4, 8.2$ Hz, H-4), 7.60 (1H, d, $J = 8.2$ Hz, NH); ^{13}C NMR (125 MHz, DMSO- d_6) δ 18.6 and 19.0 (C-9), 26.0 (C-1), 33.9 (C-7), 58.4 (C-8), 79.1 (C-2), 156.1 (C-3), 168.4 (C-6), 170.6 (C-5). LRMS (ES $^+$) m/z 315.4 [M+H] $^+$; HRMS [M+H] $^+$ (C $_{14}$ H $_{23}$ N $_2$ O $_6$) calculated 315.4371 found 315.4346. Data consistent with literature values, lit m.p. 123-124 °C.²¹⁶

Synthesis of (S)-2-((S)-2-((tert-butoxycarbonyl)amino)-3-methylbutanamido)-5-ureidopentanoic acid, 225



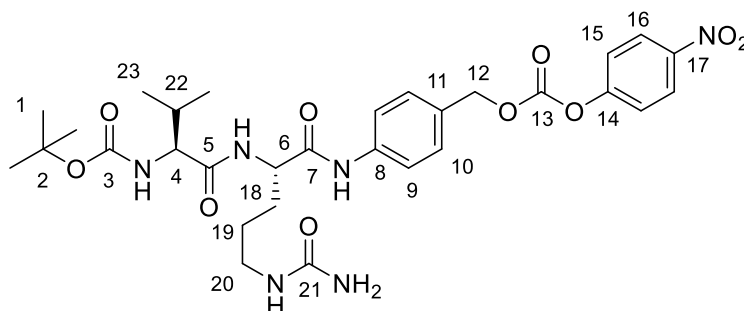
To a solution of L-citrulline (2.82 g, 16.1 mmol) in H₂O (36 mL), DME (36 mL) and THF (9 mL) was added 2,5-dioxopyrrolidin-1-yl (tert-butoxycarbonyl)-L-valinate (4.59 g, 14.6 mmol) followed by NaHCO₃ (1.35 g, 16.1 mmol) and the reaction was stirred for 16 hours before the organic solvents were removed *in vacuo*. To the aqueous residue was added 10% citric acid (75 mL) and was extracted with 10% IPA in EtOAc (3 x 100 mL). The organic extracts were combined and washed with brine before being dried over MgSO₄, filtered and concentrated *in vacuo* to give a white solid (4.08 g, 10.9 mmol, 89%). *R_f* 0.20 (20% MeOH in DCM); IR $\nu_{\max}/\text{cm}^{-1}$ 3444 (NH₂), 3310 (NH), 3087 (COOH), 2964 (NH), 1719 (C=O), 1640 (C=O), 1599 (C=O); m.p. 199.3 – 200.7 °C. ¹H NMR (500 MHz, DMSO-*d*₆) δ_{H} 0.80 (6H, dd, *J* = 6.8, 17.8 Hz, H-13), 1.36 (2H, br, H-8) 1.40 (9H, s, H-1), 1.47-1.64 (2H, m, H-7), 2.01-2.08 (1H, m, H-12), 2.82-2.99 (2H, m, H-9), 3.68-3.73 (1H, m, H-6), 4.13 (1H, q, *J* = 5.4 Hz, H-4), 5.36 (2H, s, NH₂), 5.92 (1H, m, NH), 7.08 (1H, d, *J* = 9.5 Hz, NH) 7.42 (1H, s, COOH); ¹³C NMR (125 MHz, DMSO-*d*₆) δ_{C} 18.2 (C-13), 20.2 (C-8), 28.8 (C-1), 31.1 (C-7), 31.7 (C-12), 49.3 (C-9), 54.7 (C-6), 60.5 (C-4), 78.8 (C-2), 159.1 (C-10), 168.1 (C-3), C-5 and C-11 not visualised. LRMS (ES⁺) *m/z* 375.5 [M+H]⁺; HRMS [M+H]⁺ (C₁₀H₂₀NO₄) calculated 375.6179 found 375.6155. Data consistent with literature values.²¹⁷

Synthesis of *tert*-butyl ((*S*)-1-(((*S*)-1-((4-(hydroxymethyl)phenyl)amino)-1-oxo-5-ureidopentan-2-yl)amino)-3-methyl-1-oxobutan-2-yl)carbamate, 226



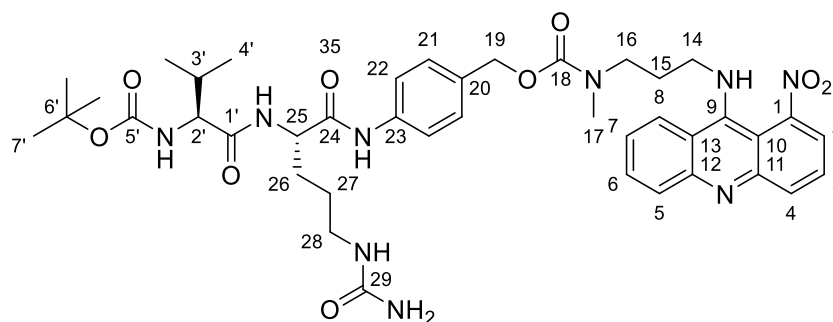
To a solution of (*S*)-2-((*S*)-2-((*tert*-butoxycarbonyl)amino)-3-methylbutanamido)-5-ureidopentanoic acid (1.56 g, 4.17 mmol) in dry DCM (30 mL) and MeOH (15 mL) stirring at RT was added EEDQ (2.06 g, 8.34 mmol) and 4-nitrobenzyl alcohol (616 mg, 5 mmol). The orange solution was stirred overnight in the dark. The reaction mixture was concentrated *in vacuo* and purified by flash column chromatography (silica; 0-10% MeOH in DCM) to afford a white solid (875 mg, 1.83 mmol, 34% yield). R_f 0.49 (10% MeOH in DCM); m.p. 119-123 °C; UV λ_{\max} (MeOH/nm) 247.2, 208.4; IR $\nu_{\max}/\text{cm}^{-1}$ 3286 (NH₂), 3060 (OH), 2964 (NH), 2930 (NH), 1644 (C=O), 1604 (C=O); ¹H NMR (500 MHz, DMSO-*d*₆) δ_{H} 0.84 (6H, m, H-1), 1.20-1.24 (2H, m, H-14), 1.39 (9H, s, H-1), 1.54-1.74 (2H, m, H-13), 1.90-2.00 (1H, m, H-17), 2.90-3.07 (2H, m, H-15), 3.80-3.84 (1H, m, H-6), 4.43 (2H, d, $J = 4.7$ Hz, H-12), 5.10-5.14 (1H, m, H-4), 5.77 (1H, s, NH), 7.23 (2H, d, $J = 8.2$ Hz, H-10), 7.55 (2H, d, $J = 8.2$ Hz, H-9), 10.03 (1H, s, OH); ¹³C NMR (125 MHz, DMSO-*d*₆) δ_{C} 18.9 (C-18), 20.2 (C-14), 27.2 (C-13), 28.8 (C-1), 31.1 (C-17), 49.0 (C-15), 53.1 (C-6), 60.5 (C-4), 63.4 (C-12), 78.8 (C-2), 119.4 (C-9), 127.4 (C-10), 137.9 (C-8 and C-11), 155.9 (C-3), 159.3 (C-16), 171.1 (C-5), 172.1 (C-7); LRMS (ES⁺) m/z 480.6 [M+H]⁺; HRMS [M+H]⁺ (C₂₃H₃₈N₅O₆) calculated 480.2744 found 480.2752. Data consistent with literature values.²¹⁷

Synthesis of *tert*-butyl ((*S*)-3-methyl-1-(((*S*)-1-((4-(((4-nitrophenoxy)carbonyl)oxy)methyl)phenyl)amino)-1-oxo-5-ureidopentan-2-yl)amino)-1-oxobutan-2-yl)carbamate, 227



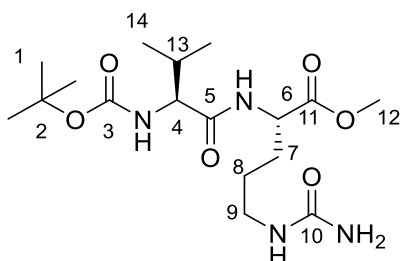
To a solution of *tert*-butyl ((*S*)-1-(((*S*)-1-((4-(hydroxymethyl)phenyl)amino)-1-oxo-5-ureidopentan-2-yl)amino)-3-methyl-1-oxobutan-2-yl)carbamate (875 g, 1.83 mmol) in a mixture of DCM (20 mL), THF (10 mL) and pyridine (0.33 mL, 4.03 mmol) at 0 °C stirring was added 4-nitrophenyl chloroformate (812 mg, 4.03 mmol) and left to stir at room temperature for 5 hours. After the reaction was completed, the yellow solution was concentrated *in vacuo* and purified by flash chromatography (silica; 0-5% MeOH in DCM) to afford a pale yellow solid (303 mg, 0.47 mmol, 26%). $R_f = 0.80$ (10% MeOH in DCM); m.p. 119-123 °C; UV λ_{\max} (MeOH/nm) 251.3, 205.6; IR $\nu_{\max}/\text{cm}^{-1}$ 3384 (NH₂), 2954 (NH), 2910 (NH), 1630 (C=O), 1607 (C=O); ¹H NMR (500 MHz, DMSO-*d*₆) δ_{H} 0.84 (6H, dd, $J = 6.7, 20.6$ Hz, H-23), 1.38 (11H, br, H-1 and H-19), 1.53-1.76 (2H, m, H-18), 1.86-2.03 (1H, m, H-22), 2.87-3.10 (2H, m, H-20), 3.83 (1H, dd, $J = 6.7, 8.9$ Hz, H-4), 4.37-4.48 (1H, m, H-6), 5.24 (2H, s, H-12), 5.41 (2H, s, NH₂), 5.92-6.03 (1H, m, NH), 6.74 (1H, d, $J = 8.9$ Hz, NH), 7.41 (2H, d, $J = 8.5$ Hz, H-10), 7.56 (2H, d, $J = 9.0$ Hz, H-15), 7.64 (2H, d, $J = 8.5$ Hz, H-9), 8.01 (1H, d, $J = 7.5$ Hz, NH), 8.31 (2H, d, $J = 9.0$ Hz, H-16). ¹³C NMR (125 MHz, DMSO-*d*₆) δ_{C} 18.6, 19.7 (C-23), 27.2 (C-19), 28.7 (C-1), 30.0 (C-18), 30.9 (C-22), 38.8 (C-20), 53.5 (C-6), 60.3 (C-4), 70.8 (C-12), 78.6 (C-2), 119.5 (C-9), 123.0 (C-15), 125.8 (C-16), 130.2 (C-11), 130.3 (C-10), 139.8 (C-8) 145.4 (C-17), 152.4 (C=O), 155.8 (C-14), 155.9 (C=O), 159.3 (urea), 171.2 (C=O), 171.9 (C=O). LRMS (ES⁺) m/z 645.8 [M+H]⁺; HRMS [M+H]⁺ (C₃₀H₄₀N₆O₁₀) calculated 645.2841 found 645.2832. Data consistent with literature values.²¹⁷

Synthesis of 4-((S)-2-((S)-2-((tert-butoxycarbonyl)amino)-3-methylbutanamido)-5-ureidopentanamido)benzyl methyl(3-((1-nitroacridin-9-yl)amino)propyl)carbamate, 228



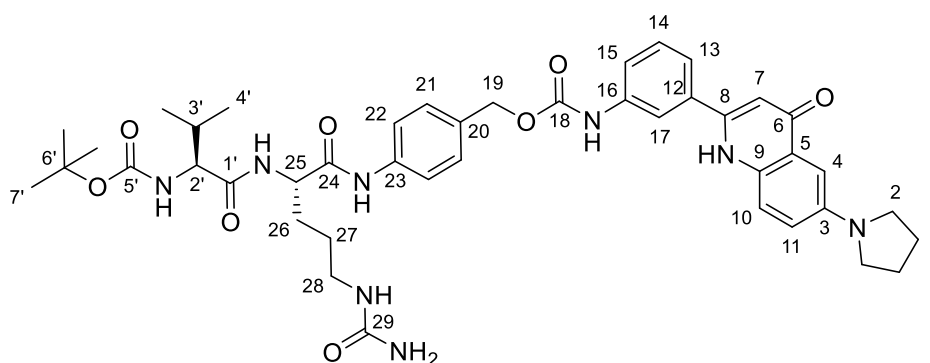
To a solution of tert-butyl ((S)-3-methyl-1-(((S)-1-((4-(((4-nitrophenoxy)carbonyl)oxy)methyl)phenyl)amino)-1-oxo-5-ureidopentan-2-yl)amino)-1-oxobutan-2-yl)carbamate (50 mg, 0.08 mmol) in DMF (2 mL) was added *N*¹-methyl-*N*³-(1-nitroacridin-9-yl)propane-1,3-diamine (25 mg, 0.08 mmol) HOBt (13 mg, 0.1 mmol) and DIPEA (42 μ L, 0.24 mmol). The reaction was stirred at RT for 16 hours. The solvent was removed *in vacuo* and the product was purified directly by flash column chromatography (silica; 0-10% MeOH in DCM) followed by reverse phase column chromatography (C-18; 5-95% THF in H₂O) to afford a red oil (44 mg, 0.05 mmol, 67%). *R*_f 0.35 (10% MeOH in DCM); UV λ_{max} (EtOH/nm) 280.3, 234.2 210.3; IR ν_{max} /cm⁻¹ 3321 (NH), 1680 (C=O), 1649 (C=O), 1634 (C=O); ¹H NMR: (500 MHz, DMSO-*d*₆) δ_{H} ; 0.94 (6H, dd, *J* = 7.1, 20.4 Hz, H-4'), 1.43 (9H, s, H-7'), 1.55-1.58 (2H, m, H-27), 1.70-1.74 (2H, m, H-26), 2.86-2.87 (1H, m, H-3'), 2.93-2.95 (2H, m, H-16), 3.06-3.09 (2H, m, H-28), 3.15 (3H, s, H-17), 3.18-3.20 (2H, m, H-15), 4.22-4.25 (1H, m H-25), 4.59 (2H, s, H-19), 7.52-7.58 (3H, m, H-21, H-7), 7.62-7.71 (3H, H-22, H-6), 7.81-7.90 (4H, m, H-3, H-4, H-5, H-8), 8.24-8.26 (1H, m, H-2) ¹³C NMR: (125 MHz, DMSO-*d*₆) δ_{C} ; Carbon sample too weak for ¹³C NMR. LRMS (ES⁺) *m/z* 816.1 [M+H]⁺; HRMS [M+H]⁺ (C₄₁H₅₃N₉O₉) calculated 816.3158 found 816.3173.

Synthesis of methyl (S)-2-((S)-2-((tert-butoxycarbonyl)amino)-3-methylbutanamido)-5-ureidopentanoate, 229



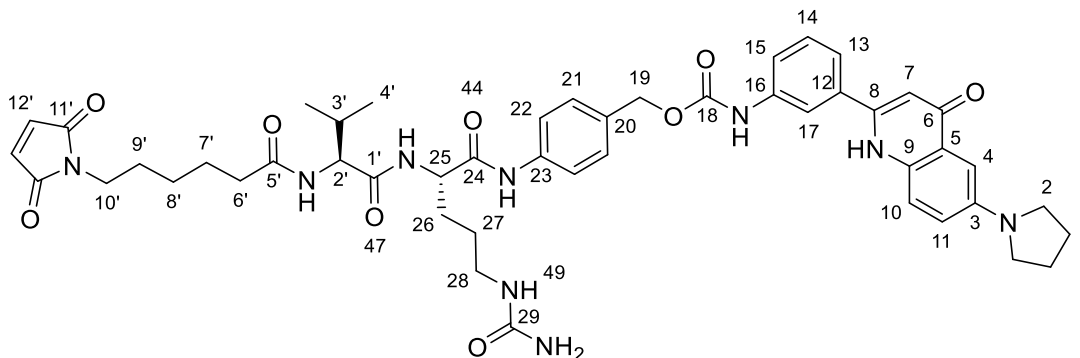
To a solution of L-citrulline methyl ester hydrochloride (1.55 g, 6.88 mmol) in DMF (25 mL) at 0 °C while stirring was added DIPEA (3.3 mL, 18.8 mmol) followed by HOBt (1.15 g, 7.51 mmol) and 2,5-dioxopyrrolidin-1-yl (tert-butoxycarbonyl)-L-valinate (1.97 g, 6.26 mmol) and the reaction mixture was warmed to room temperature and left to stir for 18 hours. The DMF was removed *in vacuo* to give a yellow residue which was dissolved in H₂O. The product was extracted with DCM (3 x 50 mL). The organic extracts were combined and dried over MgSO₄, filtered and concentrated *in vacuo* to give a crude mixture which was purified by flash column chromatography (silica; 0-20% MeOH in DCM) to afford a white solid (1.79 g, 4.63 mmol, 74%) . *R_f* 0.41 (10% MeOH in DCM); IR $\nu_{\max}/\text{cm}^{-1}$ 3445 (NH₂), 3279 (NH), 2684 (NH), 1742 (C=O), 1646 (C=O), 1580 (C=O); M.P. 120.6 – 122.5 °C. ¹H NMR (500 MHz, DMSO-*d*₆) δ_{H} 0.84 (6H, dd, *J* = 6.6, 21.1 Hz, H-14), 1.35-1.39 (11H, m, H-1 and H-8), 1.61-1.66 (2H, m, H-7), 1.89-1.94 (1H, m, H-13), 2.92-2.98 (2H, m, H-9), 3.61 (3H, s, H-12), 3.83 (1H, t, *J* = 8.0 Hz, H-6), 4.18-4.22 (1H, m, H-4), 5.35 (2H, s, NH₂), 5.90-5.92 (1H, m, NH), 6.51 (1H, d, *J* = 9.0 Hz, NH); ¹³C NMR (125 MHz, DMSO-*d*₆) δ_{C} 18.6 (C-14), 19.5 (C-8), 27.1 (C-1), 28.1 (C-7), 31.0 (C-13), 40.6 (C-9), 52.2 (C-12), 59.8 (C-6), 63.9 (C-4), 78.5 (C-2), 159.2 (C-10), 168.4 (C-3), 172.3 (C-5), 173.0 (C-11). LRMS (ES⁺) *m/z* 339.1 [M+H]⁺; HRMS [M+H]⁺ (C₁₇H₃₃N₄O₆) calculated 339.3178 found 389.3137. Data consistent with literature values.²¹⁷

Synthesis of 4-((S)-2-((S)-2-((tert-butoxycarbonyl)amino)-3-methylbutanamido)-5-ureidopentanamido)benzyl (3-(4-oxo-6-(pyrrolidin-1-yl)-1,4-dihydroquinolin-2-yl)phenyl)carbamate, 231



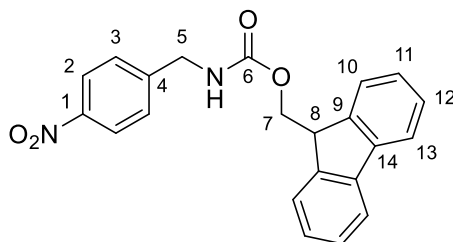
To a solution of tert-butyl ((S)-3-methyl-1-(((S)-1-((4-(((4-nitrophenoxy)carbonyl)oxy)methyl)phenyl)amino)-1-oxo-5-ureidopentan-2-yl)amino)-1-oxobutan-2-yl)carbamate (50 mg, 0.08 mmol) in DMF (2 mL) was added 2-(3-aminophenyl)-6-(pyrrolidin-1-yl)quinolin-4(1H)-one (24 mg, 0.08 mmol) HOBt (13 mg, 0.1 mmol) and DIPEA (42 μ L, 0.24 mmol). The reaction was stirred at RT for 16 hours. The solvent was removed *in vacuo* and the product was purified directly by flash column chromatography (silica; 0-10% MeOH in DCM) followed by reverse phase column chromatography (C-18; 5-95% THF in H₂O) to afford a yellow oil (42 mg, 0.05 mmol, 64%). *R_f* 0.31 (10% MeOH in DCM); UV λ_{max} (EtOH/nm) 286.7, 394.4; IR ν_{max} /cm⁻¹ 3451 (NH), 3314 (NH), 1680 (C=O), 1645 (C=O), 1634 (C=O), 1580 (C=O); ¹H NMR: (500 MHz, DMSO-*d*₆) δ_{H} ; 0.95 (6H, dd, *J* = 7.2, 20.6 Hz, H-4'), 1.45 (9H, s, H-7'), 1.51-1.53 (2H, m, H-27), 1.67-1.71 (2H, m, H-26), 2.81-2.83 (1H, m, H-3'), 3.09-3.11 (2H, m, H-28), 4.20-4.23 (1H, m, H-25), 4.54 (2H, s, H-19), 6.14 (1H, s, H-7), 6.74-6.75 (1H, m, H-15), 6.81-6.83 (1H, m, H-17), 6.90-6.92 (1H, m, H-10), 6.98-7.01 (1H, m, H-11), 7.03-7.04 (1H, m, H-4), 7.11-7.13 (1H, m, H-14), 7.52-7.58 (2H, m, H-21), 7.62-7.71 (3H, H-22, H-13); ¹³C NMR: (125 MHz, DMSO-*d*₆) δ_{C} ; Carbon sample too weak for ¹³C NMR. LRMS (ES⁺) *m/z* 811.9 [M+H]⁺; HRMS [M+H]⁺ (C₄₃H₅₄N₈O₈) calculated 811.7174 found 811.7149.

Synthesis of 4-((S)-2-((S)-2-(6-(2,5-dioxo-2,5-dihydro-1H-pyrrol-1-yl)hexanamido)-3-methylbutanamido)-5-ureidopentanamido)benzyl (3-(4-oxo-6-(pyrrolidin-1-yl)-1,4-dihydroquinolin-2-yl)phenyl)carbamate, 232



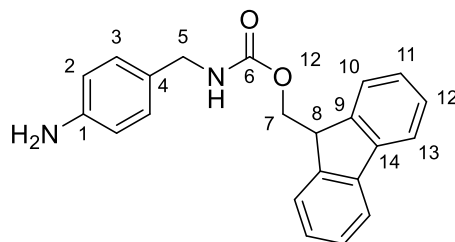
To 4-((S)-2-((S)-2-((tert-butoxycarbonyl)amino)-3-methylbutanamido)-5-ureidopentanamido)benzyl (3-(4-oxo-6-(pyrrolidin-1-yl)-1,4-dihydroquinolin-2-yl)phenyl)carbamate (30 mg, 0.04 mmol) was added 10% TFA in DCM (1 mL). The reaction was left at RT for 5 hours. The solvent was removed *in vacuo* and DMF (1 mL) was added. The solution was cooled to 0 °C and DIPEA (87 μ L, 0.5 mmol) was added followed by HATU (30 mg, 0.08 mmol) and 6-maleimidohexanoic acid (17 mg, 0.08 mmol). The reaction was left to stir for 16 h at RT. The reaction mixture was concentrated *in vacuo* and the crude product was purified by reverse phase column chromatography (C-18; 5-95% THF in H₂O) to give the product as a red oil (20 mg, 0.02 mmol, 56%). *R_f* 0.23 (10% MeOH in DCM); UV λ_{max} (EtOH/nm) 282.7, 246.3 214.1; IR ν_{max} /cm⁻¹ 3456 (NH), 3334 (NH), 1674 (C=O), 1649 (C=O) 1614 (C=O), 1580 (C=O); ¹H NMR: (500 MHz, DMSO-*d*₆) δ_{H} ; 0.99 (6H, dd, *J* = 7.2, 20.1 Hz, H-4'), 1.23-1.29 (4H, m, H-7', H-8'), 1.51-1.58 (4H, m, H-9', H-27), 1.69-1.74 (2H, m, H-26), 2.83-2.85 (1H, m, H-6'), 3.10-3.12 (2H, m, H-28), 3.46-3.50 (2H, m, H-10'), 4.16-4.17 (1H, m, H-2'), 4.24-4.27 (1H, m H-25), 4.53 (2H, s, H-19), 6.11 (1H, s, H-7), 6.73-6.75 (1H, m, H-15), 6.79-6.81 (1H, m, H-17), 6.91-6.93 (1H, m, H-10), 7.01-7.03 (1H, m, H-11), 7.06-7.08 (1H, m, H-4), 7.16-7.21 (1H, m, H-14), 7.51-7.56 (2H, m, H-21), 7.62-7.65 (2H, m, H-22); ¹³C NMR: (125 MHz, DMSO-*d*₆) δ_{C} ; Carbon sample too weak for ¹³C NMR; LRMS (ES⁺) *m/z* 903.1 [M+H]⁺; HRMS [M+H]⁺ (C₄₈H₅₇N₉O₉) calcd 903.0184. found 903.0149.

Synthesis of (9H-fluoren-9-yl)methyl (4-nitrobenzyl)carbamate, 235



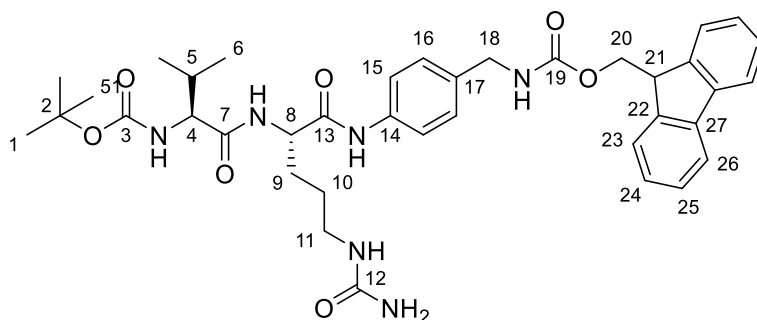
To a solution of 4-nitrobenzyl amine (500 mg, 2.7 mmol) in DCM (50 mL) was added Fmoc-Cl (700 mg, 2.7 mmol) followed by DIPEA (1.4 mL, 8.0 mmol). The reaction was stirred at RT for 6 hours after which the reaction was completed. The organic layer was washed with 1M HCl (30 mL) followed by water (2 x 30 mL). The organic layer was dried over MgSO_4 , filtered and concentrated *in vacuo* to give a white solid (450 mg, 1.2 mmol, 44%). $R_f = 0.35$ (10% MeOH in DCM); m.p. 152.2-153.3 °C; UV λ_{max} (MeOH/nm) 299.6, 264.8; IR $\nu_{\text{max}}/\text{cm}^{-1}$ 3322 (NH), 1697 (C=O) 1525 and 1345 (NO); ^1H NMR (500 MHz CDCl_3) δ_{H} 4.16 (1H, t, $J = 6.0$ Hz, H-8), 4.39 (2H, d, $J = 6.0$ Hz, H-5) 7.23-7.27 (2H, m, H-11), 7.29-7.37 (4H, m, H-10 and H-12), 7.53 (2H, d, $J = 7.5$ Hz, H-3), 7.71 (2H, d, $J = 7.4$ Hz, H-13), 8.11 (2H, d, $J = 7.5$ Hz, H-2); ^{13}C NMR (125 MHz, CDCl_3) δ_{C} 39.6 (C-5), 42.6 (C-8), 61.9 (C-7), 115.3 (C-10), 119.2 (C-2), 120.1 (C-11), 122.3 (C-12), 123.0 (C-3), 136.7 (C-14), 139.0 (C-9), 155.7 (C-6) (C-1 and C-4 not visualized). LRMS (ES^+) m/z 375.4 $[\text{M}+\text{H}]^+$; HRMS $[\text{M}+\text{H}]^+$ ($\text{C}_{22}\text{H}_{19}\text{N}_2\text{O}_4$) calculated 375.3184 found 375.3199. Data consistent with literature values, lit m.p. 149-151 °C.²¹⁸

Synthesis of (9*H*-fluoren-9-yl)methyl (4-aminobenzyl)carbamate, 236



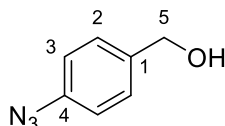
To (9*H*-fluoren-9-yl)methyl (4-aminobenzyl)carbamate (100 mg, 0.27 mmol) in DCM (30 mL) and MeOH (30 mL) was added 10% Pd/C (3 mg, 0.03 mmol). The solution was sparged with H₂ and left in an H₂ atmosphere, stirring for 16 h. The solution was filtered through Celite® and concentrated *in vacuo* to give the product as a white solid (68 mg, 0.19 mmol, 72%). *R_f* = 0.79 (10% MeOH in DCM); m.p. 127-130 °C; UV λ_{max} (MeOH/nm) 299.3, 288.8, 264.6, 254.8; IR ν_{max}/cm⁻¹ 3432 (NH), 3341 (NH), 1697; ¹H NMR (500 MHz CDCl₃) δ_H 4.25 (1H, t, *J* = 6.8 Hz, H-8), 4.29 (2H, d, *J* = 6.0 Hz, H-5), 4.46 (2H, d, *J* = 6.8 Hz, H-7), 6.68 (2H, d, *J* = 7.5 Hz, H-2), 7.10-7.12 (2H, m, H-11), 7.31-7.34 (2H, m, H-12), 7.40-7.43 (2H, m, H-10), 7.61 (2H, d, *J* = 7.5 Hz, H-3), 7.78 (2H, d, *J* = 7.4 Hz, H-13); ¹³C NMR (125 MHz, CDCl₃) δ_C 40.2 (C-5), 43.1 (C-8), 62.4 (C-7), 114.4 (C-2), 118.6 (C-10), 123.8 (C-11), 124.3 (C-13), 124.9 (C-3), 125.2 (C-12) 155.4 (C-6) (C-14, C-9, C-4 and C1 not visualized); LRMS (ES⁺) *m/z* 345.9 [M+H]⁺; HRMS [M+H]⁺ (C₂₂H₂₁N₂O₂) calculated 345.7416 found 345.7454. Data consistent with literature values, lit m.p. 138-139 °C.²¹⁹

Synthesis of (9H-fluoren-9-yl)methyl 4-((S)-2-((S)-2-((tert-butoxycarbonyl)amino)-3-methylbutanamido)-5-ureidopentanamido)benzyl)carbamate, 237



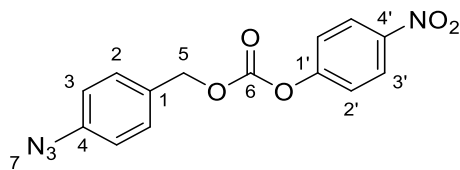
To a solution of (9H-fluoren-9-yl)methyl 4-aminobenzyl)carbamate (50 mg, 0.14 mmol) in dry DCM (1.5 mL) and MeOH (0.5 mL) stirring at RT was added EEDQ (69 mg, 0.28 mmol) and (S)-2-((S)-2-((tert-butoxycarbonyl)amino)-3-methylbutanamido)-5-ureidopentanoic acid (105 mg, 0.28 mmol). The solution was stirred overnight in the dark. The reaction mixture was concentrated *in vacuo* and purified by flash column chromatography (silica; 0-10% MeOH in DCM) to afford a white solid (48 mg, 0.07 mmol, 49% yield). R_f 0.27 (10% MeOH in DCM); m.p. 146-150 °C; UV λ_{max} (MeOH/nm) 292.2, 264.3; IR ν_{max}/cm^{-1} 3286 (NH₂), 2964 (NH), 2930 (NH), 1691 (C=O), 1644 (C=O), 1604 (C=O); ¹H NMR (500 MHz, DMSO-*d*₆) δ_H 0.83-0.85 (6H, m, H-6), 1.21-1.23 (2H, m, H-10), 1.41 (9H, s, H-1), 1.56-1.61 (2H, m, H-9), 1.99-2.03 (1H, m, H-5), 2.91-2.96 (2H, m, H-11), 3.79-3.82 (1H, m, H-8), 4.41-4.43 (1H, m, H-21), 4.66 (2H, d, $J = 6.7$ Hz, H-20), 4.71 (2H, s, H-18), 5.11-5.16 (1H, m, H-4), 5.81 (1H, s, NH), 6.74 (2H, d, $J = 7.3$ Hz, H-15), 7.11-7.13 (2H, m, H-24), 7.40-7.42 (2H, m, H-25), 7.45-7.48 (2H, m, H-23), 7.71 (2H, d, $J = 7.3$ Hz, H-16), 7.81 (2H, d, $J = 7.4$ Hz, H-26); ¹³C NMR (125 MHz, DMSO-*d*₆) δ_C 19.1 (C-6), 20.4 (C-10), 26.4 (C-9), 29.3 (C-1), 31.8 (C-5), 45.4 (C-21), 49.3 (C-11), 53.4 (C-8), 61.1 (C-4), 62.7 (C-20), 65.2 (C-18), 78.6 (C-2), 119.6 (C-15), 120.1 (C-23), 124.9 (C-24), 125.7 (C-26), 126.4 (C-25), 127.5 (C-16), 137.8 (C-14), 138.0 (C-17), 140.3 (C-27), 144.1 (C-22), 156.2 (C-3), 160.2 (C-12), 172.3 (C-7), 173.3 (C-13); LRMS (ES⁺) m/z 700.5 [M+H]⁺; HRMS [M+H]⁺ (C₃₈H₄₉N₆O₇) calculated 700.9647 found 700.9623.

Synthesis of (4-azidophenyl)methanol, 240



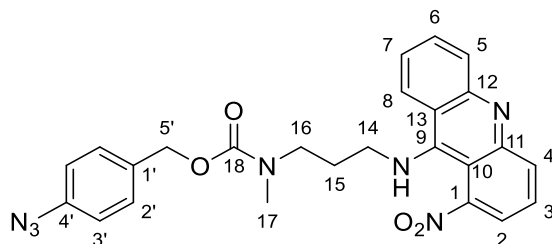
To a solution of sodium nitrite (200 mg, 3.0 mmol), in H₂O (5 mL) at 0 °C was added dropwise 4-aminobenzyl alcohol (246 mg, 2.0 mmol) in 6N HCl (2 mL). The solution was left to stir at 0 °C for 30 mins before sodium azide (520 mg, 8.0 mmol) in H₂O (10 mL) was added slowly dropwise so the temperature did not rise above 5 °C. The reaction mixture was allowed to warm to room temperature and left to stir for 5 hours. The reaction mixture was then poured into 10% aqueous NaHCO₃ solution and extracted into EtOAc (3 x 30 mL). The organic extracts were combined, dried over MgSO₄, filtered and concentrated *in vacuo* and then purified by flash column chromatography (silica; 0-20% EtOAc in petroleum ether) to afford a white solid (207 mg, 1.4 mmol, 69% yield). *R_f* 0.65 (10% MeOH in DCM); m.p. 30-32 °C; UV λ_{\max} (MeOH/nm) 299.4, 265.2, 205.4; IR $\nu_{\max}/\text{cm}^{-1}$ 3379 (OH), 3318 (NH), 2109 (N₃); ¹H NMR (500 MHz, CDCl₃) δ_{H} 4.69 (2H, s, H-5), 7.02-7.05 (2H, m, H-2), 7.36-7.39 (2H, m, H-3); ¹³C NMR (125 MHz, CDCl₃) δ_{C} 64.7 (C-5), 119.1 (C-2), 128.6 (C-3), 137.6 (C-4), 139.4 (C-1). LRMS (ES⁺) *m/z* 150.2 [M+H]⁺; HRMS failed to detect mass. Data consistent with literature values, lit m.p. 27-28 °C.²²⁰

Synthesis of 4-azidobenzyl (4-nitrophenyl) carbonate, 241



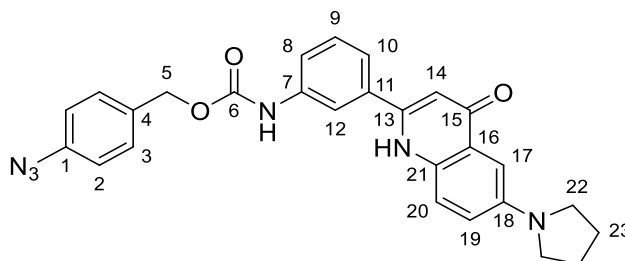
To a solution of 4-nitrophenyl chloroformate (383 mg, 1.9 mmol) in pyridine (0.15 mL, 1.9 mmol) and THF (4 mL) at 0 °C was added (4-azidophenyl)methanol (142 mg, 0.95 mmol) in THF (4 mL) dropwise over 30 mins. The reaction was warmed to RT and left to stir for 6 hours. The reaction mixture was concentrated *in vacuo* and purified by flash column chromatography (silica; 0-20% EtOAc in petroleum ether) to afford a white solid (239 mg, 0.76 mmol, 80%). R_f 0.60 (10% MeOH in DCM); m.p. 94-96 °C; UV λ_{\max} (MeOH/nm) 256.4, 204.8; IR $\nu_{\max}/\text{cm}^{-1}$ 2116 (N₃), 1750 (C=O); ¹H NMR (500 MHz, CDCl₃) δ_{H} 5.26 (2H, s, H-5), 7.05-7.08 (2H, m, H-2), 7.36-7.39 (2H, m, H-3) 7.42-7.46 (2H, m, H-2'), 8.26-8.30 (2H, m, H-3'); ¹³C NMR (125 MHz, CDCl₃) δ_{C} 70.5 (C-5), 119.5 (C-3'), 121.8 (C-2'), 125.3 (C-2), 130.7 (C-3), 139.4 (C-1), 145.6 (C-4), 152.5 (C-4'), 155.6 (C-1'), 158.1 (C=O). LRMS (ES⁺) m/z 315.2 [M+H]⁺; HRMS failed to detect mass. Data consistent with literature values, lit m.p. 101-102 °C.²²¹

Synthesis of 4-azidobenzyl methyl(3-((1-nitroacridin-9-yl)amino)propyl)carbamate, 242



To a solution of 4-azidobenzyl (4-nitrophenyl)carbonate 31 mg, 0.1 mmol) in DMF (1 mL) was added *N*¹-methyl-*N*³-(1-nitroacridin-9-yl)propane-1,3-diamine (30 mg, 0.1 mmol) and Et₃N (27 μL, 0.19 mmol). The solution was stirred for 16 hours and then the solvent removed *in vacuo*. The residue was redissolved in DCM, washed with H₂O (10 mL) and brine (10 mL) before being dried over MgSO₄, filtered and concentrated *in vacuo*. The crude mixture was purified by flash column chromatography (silica; 0-5% MeOH in DCM) to afford a red solid (16 mg, 0.03, 33%). *R*_f 0.45 (10% MeOH in DCM); m.p. 74-77 °C; UV λ_{max} (MeOH/nm) 391.4, 247.0; IR ν_{max}/cm⁻¹ 3284 (NH), 2105 (N₃), 1674 (C=O); ¹H NMR (500 MHz, DMSO-*d*₆) δ_H 1.73 (2H, p, *J* = 6.5 Hz, H-15), 2.83-2.86 (2H, m, H-16), 3.36 (3H, s, H-17), 3.64-3.66 (2H, m, H-14), 4.98 (2H, s, H-5'), 7.00-7.03 (1H, m, H-7), 7.05-7.08 (2H, m, H-3'), 7.11-7.14 (2H, m, H-2'), 7.27-7.31 (1H, m, H-6), 7.33-7.41 (3H, m, H-2, H-3, H-5), 7.86-7.89 (1H, m, H-4), 7.98-8.01 (1H, m, H-8); ¹³C NMR (125 MHz, DMSO-*d*₆) δ_C 29.7 (C-15), 32.4 (C-5'), 34.3 (C-17), 35.2 (C-14), 53.4 (C-16), 113.9 (C-10), 116.1 (C-13), 116.8 (C-5), 117.1 (C-13), 119.1 (C-8), 121.1 (C-7), 127.4 (C-2'), 129.5 (C-3'), 130.9 (C-6), 133.6 (C-4), 133.9 (C-3), 139.5, 139.7 (C-2, C-11), 141.3 (C-4'), 143.4 (C-1'), 144.1 (C-12), 150.1 (C-1), 156.4 (C-9). LRMS (ES⁺) *m/z* 486.7 [M+H]⁺; HRMS [M+H]⁺ failed to detect mass.

Synthesis of 4-azidobenzyl methyl(3-((3-(4-oxo-6-(pyrrolidin-1-yl)-1,4-dihydroquinolin-2-yl)phenyl)amino)propyl)carbamate, 243



To a solution of 4-azidobenzyl (4-nitrophenyl)carbonate 31 mg, 0.1 mmol) in DMF (1 mL) was added 2-(3-aminophenyl)-6-(pyrrolidin-1-yl)quinolin-4(1H)-one (30 mg, 0.1 mmol) and Et₃N (27 μ L, 0.19 mmol). The solution was stirred for 16 hours and then the solvent removed *in vacuo*. The residue was redissolved in DCM, washed with H₂O (10 mL) and brine (10 mL) before being dried over MgSO₄, filtered and concentrated *in vacuo*. The crude mixture was purified by flash column chromatography (silica; 0-5% MeOH in DCM) to afford a red solid (22 mg, 0.05, 46%). *R_f* 0.45 (10% MeOH in DCM); m.p. 91-96 °C; UV λ_{max} (MeOH/nm) 274.4, 384.1; IR ν_{max} /cm⁻¹ 3417 (NH), 3284 (NH), 2105 (N₃), 1674 (C=O), 1581 (C=O); ¹H NMR (500 MHz, DMSO-*d*₆) δ_{H} 1.94-1.97 (4H, m, H-23), 3.31-3.34 (4H, m, H-22), 4.79 (2H, s, H-5), 6.14 (1H, s, H-14), 6.75 (1H, d, *J* = 7.7 Hz, H-8), 6.91 (1H, d, *J* = 6.9 Hz, H-12), 6.97-7.01 (1H, m, H-20), 7.09 (1H, d, *J* = 2.7 Hz, H-17), 7.12 (1H, dd, *J* = 2.7, 8.8 Hz, H-19), 7.19-7.21 (1H, m, H-9), 7.27-7.30 (2H, m, H-2), 7.32-7.36 (2H, m, H-3), 7.66-7.68 (1H, d, *J* = 8.7 Hz, H-10) 11.2 (1H, s, NH); ¹³C NMR (125 MHz, DMSO-*d*₆) δ_{C} 25.4 (C-23), 51.1 (C-22), 58.4 (C-5), 102.6 (C-14), 106.4 (C-12), 111.8 (C-17), 115.4 (C-8), 119.3 (C-10), 121.3 (C-19), 127.4 (C-3), 128.5 (C-16), 128.5 (C-16), 129.4 (C-2), 130.1 (C-9), 132.6 (C-16), 145.1 (C-21), 148.9 (C-7), 177.4 (C-15) (C-19 and C-18 not visualised). LRMS (ES⁺) *m/z* 381.3 [M+H]⁺; HRMS [M+H]⁺ failed to detect mass.

References

1. Cooper, G. M. The Development and Causes of Cancer. In *The Cell: A Molecular Approach*, 2 ed.; Sinauer Associates: Sunderland (MA). **2000**.
2. World Health Organisation. <https://www.who.int/news-room/fact-sheets/detail/cancer> (August 2019).
3. Cancer Research UK. <https://www.cancerresearchuk.org/health-professional/cancer-statistics-for-the-uk> (August 2019).
4. Hanahan, D.; Weinberg, R. A. The Hallmarks of Cancer. *Cell* **2000**, *100*, 57-70.
5. Hanahan, D.; Weinberg, R. A. Hallmarks of cancer: the next generation. *Cell* **2011**, *144*, 646-674.
6. Hanahan, D.; Weinberg, R. A. Hallmarks of cancer: the next generation. *Cell* **2011**, *144*, 646-74.
7. Shay, J. W.; Wright, W. E. Hayflick, his limit, and cellular ageing. *Nature Reviews Molecular Cell Biology* **2000**, *1*, 72-76.
8. Blasco, M. A. Telomeres and human disease: ageing, cancer and beyond. *Nature Reviews Genetics* **2005**, *6*, 611-622.
9. Liberti, M. V.; Locasale, J. W. The Warburg Effect: How Does it Benefit Cancer Cells? *Trends in Biochemical Sciences* **2016**, *41*, 211-218.
10. O'Connor, M. J. Targeting the DNA Damage Response in Cancer. *Mol Cell* **2015**, *60*, 547-60.
11. Underhill, C.; Toulmonde, M.; Bonnefoi, H. A review of PARP inhibitors: from bench to bedside. *Ann Oncol* **2011**, *22*, 268-79.
12. DeNardo, D. G.; Andreu, P.; Coussens, L. M. Interactions between lymphocytes and myeloid cells regulate pro- versus anti-tumor immunity. *Cancer Metastasis Rev* **2010**, *29*, 309-16.
13. DeVita, V. T.; Chu, E. A History of Cancer Chemotherapy. *Cancer research* **2008**, *68*, 8643-8653.
14. Fox, M.; Scott, D. The genetic toxicology of nitrogen and sulphur mustard. *Mutation Research/Reviews in Genetic Toxicology* **1980**, *75*, 131-168.
15. Brock, N. The history of the oxazaphosphorine cytostatics. *Cancer* **1996**, *78*, 542-547.
16. Lokich, J.; Anderson, N. Carboplatin versus cisplatin in solid tumors: An analysis of the literature. *Annals of Oncology* **1998**, *9*, 13-21.
17. Malaviya, A. N. Landmark papers on the discovery of methotrexate for the treatment of rheumatoid arthritis and other systemic inflammatory rheumatic diseases: a fascinating story. *International Journal of Rheumatic Diseases* **2016**, *19*, 844-851.
18. Longley, D. B.; Harkin, D. P.; Johnston, P. G. 5-Fluorouracil: mechanisms of action and clinical strategies. *Nature Reviews Cancer* **2003**, *3*, 330-338.
19. Moudi, M.; Go, R.; Yien, C. Y. S.; Nazre, M. Vinca alkaloids. *Int J Prev Med* **2013**, *4*, 1231-1235.
20. Guenard, D.; Gueritte-Voegelein, F.; Potier, P. Taxol and taxotere: discovery, chemistry, and structure-activity relationships. *Accounts of Chemical Research* **1993**, *26*, 160-167.
21. Bayat Mokhtari, R.; Homayouni, T. S.; Baluch, N.; Morgatskaya, E.; Kumar, S.; Das, B.; Yeger, H. Combination therapy in combating cancer. *Oncotarget* **2017**, *8*, 38022-38043.
22. Iqbal, N.; Iqbal, N. Imatinib: A Breakthrough of Targeted Therapy in Cancer. *Chemotherapy Research and Practice* **2014**, *2014*, 9.
23. Carreau, N. A.; Pavlick, A. C. Nivolumab and ipilimumab: immunotherapy for treatment of malignant melanoma. *Future Oncology* **2019**, *15*, 349-358.
24. Vu, T.; Claret, F. X. Trastuzumab: Updated Mechanisms of Action and Resistance in Breast Cancer. *Frontiers in oncology* **2012**, *2*, 62.

25. Vu, T.; Claret, F. X. Trastuzumab: updated mechanisms of action and resistance in breast cancer. *Frontiers in oncology* **2012**, *2*, 62-62.
26. Breast cancer org. <https://www.breastcancer.org/symptoms/diagnosis/her2> (July 2020).
27. Hudis, C. A. Trastuzumab — Mechanism of Action and Use in Clinical Practice. *New England Journal of Medicine* **2007**, *357*, 39-51.
28. Valeur, E.; Guéret, S. M.; Adihou, H.; Gopalakrishnan, R.; Lemurell, M.; Waldmann, H.; Grossmann, T. N.; Plowright, A. T. New Modalities for Challenging Targets in Drug Discovery. *Angewandte Chemie International Edition* **2017**, *56*, 10294-10323.
29. Bargh, J. D.; Isidro-Llobet, A.; Parker, J. S.; Spring, D. R. Cleavable linkers in antibody–drug conjugates. *Chemical Society Reviews* **2019**, *48*, 4361-4374.
30. Senter, P. D.; Sievers, E. L. The discovery and development of brentuximab vedotin for use in relapsed Hodgkin lymphoma and systemic anaplastic large cell lymphoma. *Nat Biotechnol* **2012**, *30*, 631-637.
31. Staudacher, A. H.; Brown, M. P. Antibody drug conjugates and bystander killing: is antigen-dependent internalisation required? *British Journal of Cancer* **2017**, *117*, 1736-1742.
32. Britannica. <https://www.britannica.com/science/antibody> (August 2019).
33. Vidarsson, G.; Dekkers, G.; Rispen, T. IgG subclasses and allotypes: from structure to effector functions. *Front Immunol* **2014**, *5*, 520-520.
34. Janeway, C. *Immunobiology : the immune system in health and disease*. 5th ed.; Garland Pub.: London ; New York, NY, US, 2001; p xviii, 732 p.
35. Ryman, J. T.; Meibohm, B. Pharmacokinetics of Monoclonal Antibodies. *CPT: pharmacometrics & systems pharmacology* **2017**, *6*, 576-588.
36. Ahmad, A.; Law, K. Strategies for designing antibody-toxin conjugates. *Trends in Biotechnology* **1988**, *6*, 246-251.
37. Köhler, G.; Milstein, C. Continuous cultures of fused cells secreting antibody of predefined specificity. *Nature* **1975**, *256*, 495-497.
38. Kim, E. G.; Kim, K. M. Strategies and Advancement in Antibody-Drug Conjugate Optimization for Targeted Cancer Therapeutics. *Biomol Ther (Seoul)* **2015**, *23*, 493-509.
39. Imai, K.; Takaoka, A. Comparing antibody and small-molecule therapies for cancer. *Nature Reviews Cancer* **2006**, *6*, 714-727.
40. Sau, S.; Alsaab, H. O.; Kashaw, S. K.; Tatiparti, K.; Iyer, A. K. Advances in antibody–drug conjugates: A new era of targeted cancer therapy. *Drug Discovery Today* **2017**, *22*, 1547-1556.
41. Pillay, C. S.; Elliott, E.; Dennison, C. Endolysosomal proteolysis and its regulation. *Biochem J* **2002**, *363*, 417-429.
42. Kalia, J.; Raines, R. T. Hydrolytic stability of hydrazones and oximes. *Angew Chem Int Ed Engl* **2008**, *47*, 7523-7526.
43. Gondi, C. S.; Rao, J. S. Cathepsin B as a cancer target. *Expert opinion on therapeutic targets* **2013**, *17*, 281-291.
44. Dubowchik, G. M.; Firestone, R. A. Cathepsin B-sensitive dipeptide prodrugs. 1. A model study of structural requirements for efficient release of doxorubicin. *Bioorganic & Medicinal Chemistry Letters* **1998**, *8*, 3341-3346.
45. Balaji, K. N.; Schaschke, N.; Machleidt, W.; Catalfamo, M.; Henkart, P. A. Surface cathepsin B protects cytotoxic lymphocytes from self-destruction after degranulation. *J Exp Med* **2002**, *196*, 493-503.
46. Dubowchik, G. M.; Firestone, R. A.; Padilla, L.; Willner, D.; Hofstead, S. J.; Mosure, K.; Knipe, J. O.; Lasch, S. J.; Trail, P. A. Cathepsin B-Labile Dipeptide Linkers for Lysosomal Release of Doxorubicin from Internalizing Immunoconjugates: Model Studies of Enzymatic Drug Release and Antigen-Specific In Vitro Anticancer Activity. *Bioconjugate Chemistry* **2002**, *13*, 855-869.

47. Tranoy-Opalinski, I.; Legigan, T.; Barat, R.; Clarhaut, J.; Thomas, M.; Renoux, B.; Papot, S. β -Glucuronidase-responsive prodrugs for selective cancer chemotherapy: An update. *European Journal of Medicinal Chemistry* **2014**, *74*, 302-313.
48. Michelle de, G.; Epie, B.; Hans, W. S.; Hidde, J. H.; Herbert, M. P. Beta-Glucuronidase-Mediated Drug Release. *Current pharmaceutical design* **2002**, *8*, 1391-1403.
49. Jeffrey, S. C.; Andreyka, J. B.; Bernhardt, S. X.; Kissler, K. M.; Kline, T.; Lenox, J. S.; Moser, R. F.; Nguyen, M. T.; Okeley, N. M.; Stone, I. J.; Zhang, X.; Senter, P. D. Development and Properties of β -Glucuronide Linkers for Monoclonal Antibody-Drug Conjugates. *Bioconjugate Chemistry* **2006**, *17*, 831-840.
50. Jeffrey, S. C.; De Brabander, J.; Miyamoto, J.; Senter, P. D. Expanded Utility of the β -Glucuronide Linker: ADCs That Deliver Phenolic Cytotoxic Agents. *ACS Medicinal Chemistry Letters* **2010**, *1*, 277-280.
51. Saito, G.; Swanson, J. A.; Lee, K.-D. Drug delivery strategy utilizing conjugation via reversible disulfide linkages: role and site of cellular reducing activities. *Advanced Drug Delivery Reviews* **2003**, *55*, 199-215.
52. Su, D.; Chen, J.; Cosino, E.; dela Cruz-Chuh, J.; Davis, H.; Del Rosario, G.; Figueroa, I.; Goon, L.; He, J.; Kamath, A. V.; Kaur, S.; Kozak, K. R.; Lau, J.; Lee, D.; Lee, M. V.; Leipold, D.; Liu, L.; Liu, P.; Lu, G.-L.; Nelson, C.; Ng, C.; Pillow, T. H.; Polakis, P.; Polson, A. G.; Rowntree, R. K.; Saad, O.; Safina, B.; Stagg, N. J.; Tercel, M.; Vandlen, R.; Vollmar, B. S.; Wai, J.; Wang, T.; Wei, B.; Xu, K.; Xue, J.; Xu, Z.; Yan, G.; Yao, H.; Yu, S.-F.; Zhang, D.; Zhong, F.; Dragovich, P. S. Antibody-Drug Conjugates Derived from Cytotoxic seco-CBI-Dimer Payloads Are Highly Efficacious in Xenograft Models and Form Protein Adducts In Vivo. *Bioconjugate Chemistry* **2019**, *30*, 1356-1370.
53. Tolcher, A. W. Antibody drug conjugates: lessons from 20 years of clinical experience. *Annals of Oncology* **2016**, *27*, 2168-2172.
54. Nicolaou, K. C.; Smith, A. L.; Yue, E. W. Chemistry and biology of natural and designed enediynes. *Proceedings of the National Academy of Sciences of the United States of America* **1993**, *90*, 5881-5888.
55. Maiese, W. M.; Lechevalier, M. P.; Lechevalier, H. A.; Korshalla, J.; A. Kuck, N.; Fantini, A.; Wildey, M. J.; Thomas, J.; Greenstein, M. Calicheamicins, a novel family of antitumor antibiotics: Taxonomy, fermentation and biological properties. *The Journal of antibiotics* **1989**, *42*, 558-63.
56. Jones, R. R.; Bergman, R. G. p-Benzyne. Generation as an intermediate in a thermal isomerization reaction and trapping evidence for the 1,4-benzenediyl structure. *Journal of the American Chemical Society* **1972**, *94*, 660-661.
57. Beck, A.; Goetsch, L.; Dumontet, C.; Corvaia, N. Strategies and challenges for the next generation of antibody-drug conjugates. *Nat Rev Drug Discov* **2017**, advance online publication.
58. Nicolaou, K. C.; Hummel, C. W.; Pitsinos, E. N.; Nakada, M.; Smith, A. L.; Shibayama, K.; Saimoto, H. Total synthesis of calicheamicin .gamma.II. *Journal of the American Chemical Society* **1992**, *114*, 10082-10084.
59. Bai, R.; Petit, G. R.; Hamel, E. Dolastatin 10, a powerful cytostatic peptide derived from a marine animal: Inhibition of tubulin polymerization mediated through the vinca alkaloid binding domain. *Biochemical pharmacology* **1990**, *39*, 1941-1949.
60. Pitot, H. C.; McElroy, E. A.; Reid, J. M.; Windebank, A. J.; Sloan, J. A.; Erlichman, C.; Bagniewski, P. G.; Walker, D. L.; Rubin, J.; Goldberg, R. M.; Adjei, A. A.; Ames, M. M. Phase I Trial of Dolastatin-10 (NSC 376128) in Patients with Advanced Solid Tumors. *Clinical Cancer Research* **1999**, *5*, 525-531.
61. Krug, L. M.; Miller, V. A.; Kalemkerian, G. P.; Kraut, M. J.; Ng, K. K.; Heelan, R. T.; Pizzo, B. A.; Perez, W.; McClean, N.; Kris, M. G. Phase II study of dolastatin-10 in patients with advanced non-small-cell lung cancer. *Annals of Oncology* **2000**, *11*, 227-228.

62. Aherne, G. W.; Hardcastle, A.; Valenti, M.; Bryant, A.; Rogers, P.; Pettit, G. R.; Srirangam, J. K.; Kelland, L. R. Antitumour evaluation of dolastatins 10 and 15 and their measurement in plasma by radioimmunoassay. *Cancer Chemotherapy and Pharmacology* **1996**, *38*, 225-232.
63. Doronina, S. O.; Toki, B. E.; Torgov, M. Y.; Mendelsohn, B. A.; Cerveny, C. G.; Chace, D. F.; DeBlanc, R. L.; Gearing, R. P.; Bovee, T. D.; Siegall, C. B.; Francisco, J. A.; Wahl, A. F.; Meyer, D. L.; Senter, P. D. Development of potent monoclonal antibody auristatin conjugates for cancer therapy. *Nature Biotechnology* **2003**, *21*, 778-784.
64. Doronina, S. O.; Mendelsohn, B. A.; Bovee, T. D.; Cerveny, C. G.; Alley, S. C.; Meyer, D. L.; Oflazoglu, E.; Toki, B. E.; Sanderson, R. J.; Zabinski, R. F.; Wahl, A. F.; Senter, P. D. Enhanced Activity of Monomethylauristatin F through Monoclonal Antibody Delivery: Effects of Linker Technology on Efficacy and Toxicity. *Bioconjugate Chemistry* **2006**, *17*, 114-124.
65. Francisco, J. A.; Cerveny, C. G.; Meyer, D. L.; Mixan, B. J.; Klussman, K.; Chace, D. F.; Rejniak, S. X.; Gordon, K. A.; DeBlanc, R.; Toki, B. E.; Law, C.-L.; Doronina, S. O.; Siegall, C. B.; Senter, P. D.; Wahl, A. F. cAC10-vcMMAE, an anti-CD30–monomethyl auristatin E conjugate with potent and selective antitumor activity. *Blood* **2003**, *102*, 1458-1465.
66. H.G. Lerchen, S. H., A. Harrenga, C.C. Kopitz, C.F. Nising, A. Sommer, B. Stelte-Ludwig, C. Mahlert, J. Schuhmacher, S. Golfier, S. Greven, S. Bruder. FGFR Antibody Drug Conjugates (ADCs) and the use thereof., WO2013087716. **2014**.
67. Lavergne, D.; Mordant, C.; Ratovelomanana-Vidal, V.; Genet, J.-P. Stereoselective Synthesis of iso-Dolaproine via Dynamic Kinetic Resolution. *Organic Letters* **2001**, *3*, 1909-1912.
68. Kupchan, S. M.; Komoda, Y.; Court, W. A.; Thomas, G. J.; Smith, R. M.; Karim, A.; Gilmore, C. J.; Haltiwanger, R. C.; Bryan, R. F. Tumor inhibitors. LXXIII. Maytansine, a novel antileukemic ansa macrolide from *Maytenus ovatus*. *Journal of the American Chemical Society* **1972**, *94*, 1354-1356.
69. Widdison, W. C.; Wilhelm, S. D.; Cavanagh, E. E.; Whiteman, K. R.; Leece, B. A.; Kovtun, Y.; Goldmacher, V. S.; Xie, H.; Steeves, R. M.; Lutz, R. J.; Zhao, R.; Wang, L.; Blättler, W. A.; Chari, R. V. J. Semisynthetic Maytansine Analogues for the Targeted Treatment of Cancer. *Journal of Medicinal Chemistry* **2006**, *49*, 4392-4408.
70. Corey, E. J.; Weigel, L. O.; Chamberlin, A. R.; Cho, H.; Hua, D. H. Total synthesis of maytansine. *Journal of the American Chemical Society* **1980**, *102*, 6613-6615.
71. Khalil, M. W.; Sasse, F.; Lünsdorf, H.; Elnakady, Y. A.; Reichenbach, H. Mechanism of Action of Tubulysin, an Antimitotic Peptide from Myxobacteria. *ChemBioChem* **2006**, *7*, 678-683.
72. Chen, H.; Lin, Z.; Arnst, K. E.; Miller, D. D.; Li, W. Tubulin Inhibitor-Based Antibody-Drug Conjugates for Cancer Therapy. *Molecules (Basel, Switzerland)* **2017**, *22*, 1281.
73. Peltier, H. M.; McMahon, J. P.; Patterson, A. W.; Ellman, J. A. The Total Synthesis of Tubulysin D. *Journal of the American Chemical Society* **2006**, *128*, 16018-16019.
74. Kumar, A.; White, J.; James Christie, R.; Dimasi, N.; Gao, C. Chapter Twelve - Antibody-Drug Conjugates. In *Annual Reports in Medicinal Chemistry*, Goodnow, R. A., Ed. Academic Press: 2017; Vol. 50, pp 441-480.
75. Hartley, J. A.; Flynn, M. J.; Bingham, J. P.; Corbett, S.; Reinert, H.; Tiberghien, A.; Masterson, L. A.; Antonow, D.; Adams, L.; Chowdhury, S.; Williams, D. G.; Mao, S.; Harper, J.; Havenith, C. E. G.; Zammarchi, F.; Chivers, S.; van Berkel, P. H.; Howard, P. W. Pre-clinical pharmacology and mechanism of action of SG3199, the pyrrolobenzodiazepine (PBD) dimer warhead component of antibody-drug conjugate (ADC) payload tesirine. *Scientific reports* **2018**, *8*, 10479-10479.

76. Saunders, L. R.; Bankovich, A. J.; Anderson, W. C.; Aujay, M. A.; Bheddah, S.; Black, K.; Desai, R.; Escarpe, P. A.; Hampl, J.; Laysang, A.; Liu, D.; Lopez-Molina, J.; Milton, M.; Park, A.; Pysz, M. A.; Shao, H.; Slingerland, B.; Torgov, M.; Williams, S. A.; Foord, O.; Howard, P.; Jassem, J.; Badzio, A.; Czapiewski, P.; Harpole, D. H.; Dowlati, A.; Massion, P. P.; Travis, W. D.; Pietanza, M. C.; Poirier, J. T.; Rudin, C. M.; Stull, R. A.; Dylla, S. J. A DLL3-targeted antibody-drug conjugate eradicates high-grade pulmonary neuroendocrine tumor-initiating cells in vivo. *Sci Transl Med* **2015**, *7*, 302ra136-302ra136.
77. Pettit, G. R.; Xu, J.-P.; Chapuis, J.-C.; Pettit, R. K.; Tackett, L. P.; Doubek, D. L.; Hooper, J. N. A.; Schmidt, J. M. Antineoplastic Agents. 520. Isolation and Structure of Irciniastatins A and B from the Indo-Pacific Marine Sponge *Ircinia ramosa*. *Journal of Medicinal Chemistry* **2004**, *47*, 1149-1152.
78. Hirano, S.; Quach, H. T.; Watanabe, T.; Kanoh, N.; Iwabuchi, Y.; Usui, T.; Kataoka, T. Irciniastatin A, a pederin-type translation inhibitor, promotes ectodomain shedding of cell-surface tumor necrosis factor receptor 1. *The Journal of Antibiotics* **2015**, *68*, 417-420.
79. Wu, C.-Y.; Feng, Y.; Cardenas, E. R.; Williams, N.; Floreancig, P. E.; De Brabander, J. K.; Roth, M. G. Studies toward the Unique Pederin Family Member Psymberin: Structure–Activity Relationships, Biochemical Studies, and Genetics Identify the Mode-of-Action of Psymberin. *Journal of the American Chemical Society* **2012**, *134*, 18998-19003.
80. Lyon, R. P.; Bovee, T. D.; Doronina, S. O.; Burke, P. J.; Hunter, J. H.; Neff-LaFord, H. D.; Jonas, M.; Anderson, M. E.; Setter, J. R.; Senter, P. D. Reducing hydrophobicity of homogeneous antibody-drug conjugates improves pharmacokinetics and therapeutic index. *Nat Biotechnol* **2015**, *33*, 733-735.
81. Chari, R. V. J. Targeted Cancer Therapy: Conferring Specificity to Cytotoxic Drugs. *Accounts of Chemical Research* **2008**, *41*, 98-107.
82. Lazar, A. C.; Wang, L.; Blättler, W. A.; Amphlett, G.; Lambert, J. M.; Zhang, W. Analysis of the composition of immunoconjugates using size-exclusion chromatography coupled to mass spectrometry. *Rapid Communications in Mass Spectrometry* **2005**, *19*, 1806-1814.
83. Chudasama, V.; Maruani, A.; Caddick, S. Recent advances in the construction of antibody-drug conjugates. *Nat Chem* **2016**, *8*, 114-119.
84. Dan, N.; Setua, S.; Kashyap, V. K.; Khan, S.; Jaggi, M.; Yallapu, M. M.; Chauhan, S. C. Antibody-Drug Conjugates for Cancer Therapy: Chemistry to Clinical Implications. *Pharmaceuticals (Basel)* **2018**, *11*, 32.
85. Wei, C.; Zhang, G.; Clark, T.; Barletta, F.; Tumey, L. N.; Rago, B.; Hansel, S.; Han, X. Where Did the Linker-Payload Go? A Quantitative Investigation on the Destination of the Released Linker-Payload from an Antibody-Drug Conjugate with a Maleimide Linker in Plasma. *Analytical Chemistry* **2016**, *88*, 4979-4986.
86. Dennler, P.; Chiotellis, A.; Fischer, E.; Brégeon, D.; Belmant, C.; Gauthier, L.; Lhospice, F.; Romagne, F.; Schibli, R. Transglutaminase-Based Chemo-Enzymatic Conjugation Approach Yields Homogeneous Antibody–Drug Conjugates. *Bioconjugate Chemistry* **2014**, *25*, 569-578.
87. Behrens, C. R.; Liu, B. Methods for site-specific drug conjugation to antibodies. *MAbs* **2014**, *6*, 46-53.
88. Junutula, J. R.; Raab, H.; Clark, S.; Bhakta, S.; Leipold, D. D.; Weir, S.; Chen, Y.; Simpson, M.; Tsai, S. P.; Dennis, M. S.; Lu, Y.; Meng, Y. G.; Ng, C.; Yang, J.; Lee, C. C.; Duenas, E.; Gorrell, J.; Katta, V.; Kim, A.; McDorman, K.; Flagella, K.; Venook, R.; Ross, S.; Spencer, S. D.; Lee Wong, W.; Lowman, H. B.; Vandlen, R.; Sliwkowski, M. X.; Scheller, R. H.; Polakis, P.; Mallet, W. Site-specific conjugation of a cytotoxic drug to an antibody improves the therapeutic index. *Nature Biotechnology* **2008**, *26*, 925.
89. Shen, B.-Q.; Xu, K.; Liu, L.; Raab, H.; Bhakta, S.; Kenrick, M.; Parsons-Reponte, K. L.; Tien, J.; Yu, S.-F.; Mai, E.; Li, D.; Tibbitts, J.; Baudys, J.; Saad, O. M.; Scales, S. J.; McDonald, P. J.; Hass, P. E.; Eigenbrot, C.; Nguyen, T.; Solis, W. A.; Fuji, R. N.; Flagella, K.

- M.; Patel, D.; Spencer, S. D.; Khawli, L. A.; Ebens, A.; Wong, W. L.; Vandlen, R.; Kaur, S.; Sliwkowski, M. X.; Scheller, R. H.; Polakis, P.; Junutula, J. R. Conjugation site modulates the in vivo stability and therapeutic activity of antibody-drug conjugates. *Nature Biotechnology* **2012**, 30, 184.
90. Kline, T.; Steiner, A. R.; Penta, K.; Sato, A. K.; Hallam, T. J.; Yin, G. Methods to Make Homogenous Antibody Drug Conjugates. *Pharm Res* **2015**, 32, 3480-3493.
91. Tian, F.; Lu, Y.; Manibusan, A.; Sellers, A.; Tran, H.; Sun, Y.; Phuong, T.; Barnett, R.; Hehli, B.; Song, F.; DeGuzman, M. J.; Ensari, S.; Pinkstaff, J. K.; Sullivan, L. M.; Biroc, S. L.; Cho, H.; Schultz, P. G.; DiJoseph, J.; Dougher, M.; Ma, D.; Dushin, R.; Leal, M.; Tchistiakova, L.; Feyfant, E.; Gerber, H.-P.; Sapra, P. A general approach to site-specific antibody drug conjugates. *Proceedings of the National Academy of Sciences of the United States of America* **2014**, 111, 1766-1771.
92. Zimmerman, E. S.; Heibeck, T. H.; Gill, A.; Li, X.; Murray, C. J.; Madlansacay, M. R.; Tran, C.; Uter, N. T.; Yin, G.; Rivers, P. J.; Yam, A. Y.; Wang, W. D.; Steiner, A. R.; Bajad, S. U.; Penta, K.; Yang, W.; Hallam, T. J.; Thanos, C. D.; Sato, A. K. Production of Site-Specific Antibody-Drug Conjugates Using Optimized Non-Natural Amino Acids in a Cell-Free Expression System. *Bioconjugate Chemistry* **2014**, 25, 351-361.
93. VanBrunt, M. P.; Shanebeck, K.; Caldwell, Z.; Johnson, J.; Thompson, P.; Martin, T.; Dong, H.; Li, G.; Xu, H.; D'Hooge, F.; Masterson, L.; Bariola, P.; Tiberghien, A.; Ezeadi, E.; Williams, D. G.; Hartley, J. A.; Howard, P. W.; Grabstein, K. H.; Bowen, M. A.; Marelli, M. Genetically Encoded Azide Containing Amino Acid in Mammalian Cells Enables Site-Specific Antibody-Drug Conjugates Using Click Cycloaddition Chemistry. *Bioconjugate Chemistry* **2015**, 26, 2249-2260.
94. Albers, A. E.; Garofalo, A. W.; Drake, P. M.; Kudirka, R.; de Hart, G. W.; Barfield, R. M.; Baker, J.; Banas, S.; Rabuka, D. Exploring the effects of linker composition on site-specifically modified antibody-drug conjugates. *European Journal of Medicinal Chemistry* **2014**, 88, 3-9.
95. Carrico, I. S.; Carlson, B. L.; Bertozzi, C. R. Introducing genetically encoded aldehydes into proteins. *Nature Chemical Biology* **2007**, 3, 321.
96. Agarwal, P.; van der Weijden, J.; Sletten, E. M.; Rabuka, D.; Bertozzi, C. R. A Pictet-Spengler ligation for protein chemical modification. *Proceedings of the National Academy of Sciences of the United States of America* **2013**, 110, 46-51.
97. Beerli, R. R.; Hell, T.; Merkel, A. S.; Grawunder, U. Sortase Enzyme-Mediated Generation of Site-Specifically Conjugated Antibody Drug Conjugates with High In Vitro and In Vivo Potency. *PLoS one* **2015**, 10, e0131177.
98. Ekholm, F. S.; Pynnönen, H.; Vilkmann, A.; Pitkänen, V.; Helin, J.; Saarinen, J.; Satomaa, T. Introducing Glycolinkers for the Functionalization of Cytotoxic Drugs and Applications in Antibody-Drug Conjugation Chemistry. *ChemMedChem* **2016**, 11, 2501-2505.
99. Zhou, Q.; Stefano, J. E.; Manning, C.; Kyazike, J.; Chen, B.; Gianolio, D. A.; Park, A.; Busch, M.; Bird, J.; Zheng, X.; Simonds-Mannes, H.; Kim, J.; Gregory, R. C.; Miller, R. J.; Brondyk, W. H.; Dhal, P. K.; Pan, C. Q. Site-Specific Antibody-Drug Conjugation through Glycoengineering. *Bioconjugate Chemistry* **2014**, 25, 510-520.
100. Okeley, N. M.; Toki, B. E.; Zhang, X.; Jeffrey, S. C.; Burke, P. J.; Alley, S. C.; Senter, P. D. Metabolic Engineering of Monoclonal Antibody Carbohydrates for Antibody-Drug Conjugation. *Bioconjugate Chemistry* **2013**, 24, 1650-1655.
101. Moolten, F. L.; Cooperband, S. R. Selective Destruction of Target Cells by Diphtheria Toxin Conjugated to Antibody Directed against Antigens on the Cells. *Science* **1970**, 169, 68-70.
102. Saleh, M. N.; Sugarman, S.; Murray, J.; Ostroff, J. B.; Healey, D.; Jones, D.; Daniel, C. R.; LeBherz, D.; Brewer, H.; Onetto, N.; LoBuglio, A. F. Phase I Trial of the Anti-Lewis

- Y Drug Immunoconjugate BR96-Doxorubicin in Patients With Lewis Y–Expressing Epithelial Tumors. *Journal of Clinical Oncology* **2000**, 18, 2282-2292.
103. Tolcher, A. W.; Sugarman, S.; Gelmon, K. A.; Cohen, R.; Saleh, M.; Isaacs, C.; Young, L.; Healey, D.; Onetto, N.; Slichenmyer, W. Randomized Phase II Study of BR96-Doxorubicin Conjugate in Patients With Metastatic Breast Cancer. *Journal of Clinical Oncology* **1999**, 17, 478-478.
104. Ajani, J. A.; P Kelsen, D.; Haller, D.; Hargraves, K.; Healey, D. A multi-institutional phase II study of BMS-182248-01 (BR96-doxorubicin conjugate) administered every 21 days in patients with advanced gastric adenocarcinoma. *Cancer journal (Sudbury, Mass.)* **2000**, 6, 78-81.
105. Tijink, B. M.; Buter, J.; de Bree, R.; Giaccone, G.; Lang, M. S.; Staab, A.; Leemans, C. R.; van Dongen, G. A. M. S. A Phase I Dose Escalation Study with Anti-CD44v6 Bivatuzumab Mertansine in Patients with Incurable Squamous Cell Carcinoma of the Head and Neck or Esophagus. *Clinical Cancer Research* **2006**, 12, 6064-6072.
106. Clinical. Study Report No.: PH-37705/12671, Bayer Healthcare, 2014.
107. Ducry, L.; Stump, B. Antibody–Drug Conjugates: Linking Cytotoxic Payloads to Monoclonal Antibodies. *Bioconjugate Chemistry* **2010**, 21, 5-13.
108. Beck, A.; Goetsch, L.; Dumontet, C.; Corvaia, N. Strategies and challenges for the next generation of antibody–drug conjugates. *Nature Reviews Drug Discovery* **2017**, 16, 315.
109. Egan, P. C.; Reagan, J. L. The return of gemtuzumab ozogamicin: a humanized anti-CD33 monoclonal antibody-drug conjugate for the treatment of newly diagnosed acute myeloid leukemia. *Onco Targets Ther* **2018**, 11, 8265-8272.
110. Petersdorf, S. H.; Kopecky, K. J.; Slovak, M.; Willman, C.; Nevill, T.; Brandwein, J.; Larson, R. A.; Erba, H. P.; Stiff, P. J.; Stuart, R. K.; Walter, R. B.; Tallman, M. S.; Stenke, L.; Appelbaum, F. R. A phase 3 study of gemtuzumab ozogamicin during induction and postconsolidation therapy in younger patients with acute myeloid leukemia. *Blood* **2013**, 121, 4854-4860.
111. Selby, C.; Yacko, L. R.; Glode, A. E. Gemtuzumab Ozogamicin: Back Again. *J Adv Pract Oncol* **2019**, 10, 68-82.
112. Boghaert, E. R.; Khandke, K. M.; Sridharan, L.; Dougher, M.; DiJoseph, J. F.; Kunz, A.; Hamann, P. R.; Moran, J.; Chaudhary, I.; Damle, N. K. Determination of pharmacokinetic values of calicheamicin-antibody conjugates in mice by plasmon resonance analysis of small (5 µl) blood samples. *Cancer Chemotherapy and Pharmacology* **2008**, 61, 1027-1035.
113. Beck, A.; Haeuw, J.-F.; Wurch, T.; Goetsch, L.; Bailly, C.; Corvaia, N. The next generation of antibody-drug conjugates comes of age. *Discov Med* **2010**, 10, 329-339.
114. Bross, P. F.; Beitz, J.; Chen, G.; Chen, X. H.; Duffy, E.; Kieffer, L.; Roy, S.; Sridhara, R.; Rahman, A.; Williams, G.; Pazdur, R. Approval Summary. *Gemtuzumab Ozogamicin in Relapsed Acute Myeloid Leukemia* **2001**, 7, 1490-1496.
115. Hills, R. K.; Castaigne, S.; Appelbaum, F. R.; Delaunay, J.; Petersdorf, S.; Othus, M.; Estey, E. H.; Dombret, H.; Chevret, S.; Ifrah, N.; Cahn, J.-Y.; Récher, C.; Chilton, L.; Moorman, A. V.; Burnett, A. K. Addition of gemtuzumab ozogamicin to induction chemotherapy in adult patients with acute myeloid leukaemia: a meta-analysis of individual patient data from randomised controlled trials. *The Lancet. Oncology* **2014**, 15, 986-996.
116. Uy, N.; Nadeau, M.; Stahl, M.; Zeidan, A. M. Inotuzumab ozogamicin in the treatment of relapsed/refractory acute B cell lymphoblastic leukemia. *J Blood Med* **2018**, 9, 67-74.
117. Tedder, T. F.; Tuscano, J.; Sato, S.; Kehrl, J. H. CD22, A B LYMPHOCYTE–SPECIFIC ADHESION MOLECULE THAT REGULATES ANTIGEN RECEPTOR SIGNALING*. *Annual Review of Immunology* **1997**, 15, 481-504.
118. Piccaluga, P. P.; Arpinati, M.; Candoni, A.; Laterza, C.; Paolini, S.; Gazzola, A.; Sabattini, E.; Visani, G.; Pileri, S. A. Surface antigens analysis reveals significant expression of candidate targets for immunotherapy in adult acute lymphoid leukemia. *Leukemia & Lymphoma* **2011**, 52, 325-327.

119. DiJoseph, J. F.; Dougher, M. M.; Evans, D. Y.; Zhou, B.-B.; Damle, N. K. Preclinical anti-tumor activity of antibody-targeted chemotherapy with CMC-544 (inotuzumab ozogamicin), a CD22-specific immunoconjugate of calicheamicin, compared with non-targeted combination chemotherapy with CVP or CHOP. *Cancer Chemotherapy and Pharmacology* **2011**, *67*, 741-749.
120. de Vries, J. F.; Zwaan, C. M.; De Bie, M.; Voerman, J. S. A.; den Boer, M. L.; van Dongen, J. J. M.; van der Velden, V. H. J. The novel calicheamicin-conjugated CD22 antibody inotuzumab ozogamicin (CMC-544) effectively kills primary pediatric acute lymphoblastic leukemia cells. *Leukemia* **2011**, *26*, 255.
121. Kantarjian, H.; Thomas, D.; Jorgensen, J.; Jabbour, E.; Kebriaei, P.; Rytting, M.; York, S.; Ravandi, F.; Kwari, M.; Faderl, S.; Rios, M. B.; Cortes, J.; Fayad, L.; Tarnai, R.; Wang, S. A.; Champlin, R.; Advani, A.; O'Brien, S. Inotuzumab ozogamicin, an anti-CD22–calicheamicin conjugate, for refractory and relapsed acute lymphocytic leukaemia: a phase 2 study. *The Lancet Oncology* **2012**, *13*, 403-411.
122. Kantarjian, H. M.; DeAngelo, D. J.; Stelljes, M.; Martinelli, G.; Liedtke, M.; Stock, W.; Gökbuget, N.; O'Brien, S.; Wang, K.; Wang, T.; Paccagnella, M. L.; Sleight, B.; Vandendries, E.; Advani, A. S. Inotuzumab Ozogamicin versus Standard Therapy for Acute Lymphoblastic Leukemia. *N Engl J Med* **2016**, *375*, 740-753.
123. Zolot, R. S.; Basu, S.; Million, R. P. Antibody–drug conjugates. *Nature Reviews Drug Discovery* **2013**, *12*, 259.
124. Deutsch, Y. E.; Tadmor, T.; Podack, E. R.; Rosenblatt, J. D. CD30: an important new target in hematologic malignancies. *Leukemia & Lymphoma* **2011**, *52*, 1641-1654.
125. Ansell, S. M.; Horwitz, S. M.; Engert, A.; Khan, K. D.; Lin, T.; Strair, R.; Keler, T.; Graziano, R.; Blanset, D.; Yellin, M.; Fischkoff, S.; Assad, A.; Borchmann, P. Phase I/II Study of an Anti-CD30 Monoclonal Antibody (MDX-060) in Hodgkin's Lymphoma and Anaplastic Large-Cell Lymphoma. *Journal of Clinical Oncology* **2007**, *25*, 2764-2769.
126. Forero-Torres, A.; Leonard, J. P.; Younes, A.; Rosenblatt, J. D.; Brice, P.; Bartlett, N. L.; Bosly, A.; Pinter-Brown, L.; Kennedy, D.; Sievers, E. L.; Gopal, A. K. A Phase II study of SGN-30 (anti-CD30 mAb) in Hodgkin lymphoma or systemic anaplastic large cell lymphoma. *British Journal of Haematology* **2009**, *146*, 171-179.
127. Wahl, A. F.; Klussman, K.; Thompson, J. D.; Chen, J. H.; Francisco, L. V.; Risdon, G.; Chace, D. F.; Siegall, C. B.; Francisco, J. A. The Anti-CD30 Monoclonal Antibody SGN-30 Promotes Growth Arrest and DNA Fragmentation **in Vitro** and Affects Antitumor Activity in Models of Hodgkin's Disease. *Cancer research* **2002**, *62*, 3736-3742.
128. Hamblett, K. J.; Senter, P. D.; Chace, D. F.; Sun, M. M. C.; Lenox, J.; Cervený, C. G.; Kissler, K. M.; Bernhardt, S. X.; Kopcha, A. K.; Zabinski, R. F.; Meyer, D. L.; Francisco, J. A. Effects of Drug Loading on the Antitumor Activity of a Monoclonal Antibody Drug Conjugate. *Clinical Cancer Research* **2004**, *10*, 7063-7070.
129. Kim, K. M.; McDonagh, C. F.; Westendorf, L.; Brown, L. L.; Sussman, D.; Feist, T.; Lyon, R.; Alley, S. C.; Okeley, N. M.; Zhang, X.; Thompson, M. C.; Stone, I.; Gerber, H.-P.; Carter, P. J. Anti-CD30 diabody-drug conjugates with potent antitumor activity. *Molecular Cancer Therapeutics* **2008**, *7*, 2486-2497.
130. Tilly, H.; Morschhauser, F.; Bartlett, N. L.; Mehta, A.; Salles, G.; Haioun, C.; Munoz, J.; Chen, A. I.; Kolibaba, K.; Lu, D.; Yan, M.; Penuel, E.; Hirata, J.; Lee, C.; Sharman, J. P. Polatuzumab vedotin in combination with immunochemotherapy in patients with previously untreated diffuse large B-cell lymphoma: an open-label, non-randomised, phase 1b–2 study. *The Lancet Oncology* **2019**, *20*, 998-1010.
131. Gutierrez, C.; Schiff, R. HER2: biology, detection, and clinical implications. *Arch Pathol Lab Med* **2011**, *135*, 55-62.
132. Boekhout, A. H.; Beijnen, J. H.; Schellens, J. H. Trastuzumab. *Oncologist* **2011**, *16*, 800-10.

133. Iqbal, N.; Iqbal, N. Human Epidermal Growth Factor Receptor 2 (HER2) in Cancers: Overexpression and Therapeutic Implications. *Mol Biol Int* **2014**, 2014, 852748-852748.
134. Diéras, V.; Bachelot, T. The success story of trastuzumab emtansine, a targeted therapy in HER2-positive breast cancer. *Targeted Oncology* **2014**, 9, 111-122.
135. Girish, S.; Gupta, M.; Wang, B.; Lu, D.; Krop, I. E.; Vogel, C. L.; Burris III, H. A.; LoRusso, P. M.; Yi, J.-H.; Saad, O.; Tong, B.; Chu, Y.-W.; Holden, S.; Joshi, A. Clinical pharmacology of trastuzumab emtansine (T-DM1): an antibody–drug conjugate in development for the treatment of HER2-positive cancer. *Cancer Chemotherapy and Pharmacology* **2012**, 69, 1229-1240.
136. Lewis Phillips, G. D.; Li, G.; Dugger, D. L.; Crocker, L. M.; Parsons, K. L.; Mai, E.; Blättler, W. A.; Lambert, J. M.; Chari, R. V. J.; Lutz, R. J.; Wong, W. L. T.; Jacobson, F. S.; Koeppen, H.; Schwall, R. H.; Kenkare-Mitra, S. R.; Spencer, S. D.; Sliwkowski, M. X. Targeting HER2-Positive Breast Cancer with Trastuzumab-DM1, an Antibody–Cytotoxic Drug Conjugate. *Cancer research* **2008**, 68, 9280-9290.
137. Erickson, H. K.; Park, P. U.; Widdison, W. C.; Kovtun, Y. V.; Garrett, L. M.; Hoffman, K.; Lutz, R. J.; Goldmacher, V. S.; Blättler, W. A. Antibody-Maytansinoid Conjugates Are Activated in Targeted Cancer Cells by Lysosomal Degradation and Linker-Dependent Intracellular Processing. *Cancer research* **2006**, 66, 4426-4433.
138. Lewis Phillips, G. D.; Li, G.; Dugger, D. L.; Crocker, L. M.; Parsons, K. L.; Mai, E.; Blattler, W. A.; Lambert, J. M.; Chari, R. V.; Lutz, R. J.; Wong, W. L.; Jacobson, F. S.; Koeppen, H.; Schwall, R. H.; Kenkare-Mitra, S. R.; Spencer, S. D.; Sliwkowski, M. X. Targeting HER2-positive breast cancer with trastuzumab-DM1, an antibody-cytotoxic drug conjugate. *Cancer research* **2008**, 68, 9280-9290.
139. Kung Sutherland, M. S.; Walter, R. B.; Jeffrey, S. C.; Burke, P. J.; Yu, C.; Kostner, H.; Stone, I.; Ryan, M. C.; Sussman, D.; Lyon, R. P.; Zeng, W.; Harrington, K. H.; Klussman, K.; Westendorf, L.; Meyer, D.; Bernstein, I. D.; Senter, P. D.; Benjamin, D. R.; Drachman, J. G.; McEarchern, J. A. SGN-CD33A: a novel CD33-targeting antibody–drug conjugate using a pyrrolbenzodiazepine dimer is active in models of drug-resistant AML. *Blood* **2013**, 122, 1455-1463.
140. Post, T. A. <https://www.ascopost.com/issues/july-10-2017/phase-iii-cascade-trial-of-yadastuximab-talirine-in-front-line-aml-discontinued/> (Aug 2019).
141. Rudin, C. M.; Pietanza, M. C.; Bauer, T. M.; Ready, N.; Morgensztern, D.; Glisson, B. S.; Byers, L. A.; Johnson, M. L.; Burris, H. A., 3rd; Robert, F.; Han, T. H.; Bheddah, S.; Theiss, N.; Watson, S.; Mathur, D.; Vennapusa, B.; Zayed, H.; Lally, S.; Strickland, D. K.; Govindan, R.; Dylla, S. J.; Peng, S. L.; Spigel, D. R.; investigators, S. Rovalpituzumab tesirine, a DLL3-targeted antibody-drug conjugate, in recurrent small-cell lung cancer: a first-in-human, first-in-class, open-label, phase 1 study. *The Lancet. Oncology* **2017**, 18, 42-51.
142. AbbVie. <https://news.abbvie.com/news/press-releases/abbvie-discontinues-rovalpituzumab-tesirine-rova-t-research-and-development-program.htm> (Aug 2019).
143. FierceBiotech. <https://www.fiercebiotech.com/biotech/abbvie-ditches-plans-for-accelerated-rova-t-review-after-weak-phase-2-data> (Accessed September 2019).
144. Goldenberg, D. M.; Stein, R.; Sharkey, R. M. The emergence of trophoblast cell-surface antigen 2 (TROP-2) as a novel cancer target. *Oncotarget* **2018**, 9, 28989-29006.
145. Nijman, S. M. B. Synthetic lethality: general principles, utility and detection using genetic screens in human cells. *FEBS letters* **2011**, 585, 1-6.
146. Bardia, A.; Mayer, I. A.; Vahdat, L. T.; Tolaney, S. M.; Isakoff, S. J.; Diamond, J. R.; O’Shaughnessy, J.; Moroosse, R. L.; Santin, A. D.; Abramson, V. G.; Shah, N. C.; Rugo, H. S.; Goldenberg, D. M.; Sweidan, A. M.; Iannone, R.; Washkowitz, S.; Sharkey, R. M.; Wegener, W. A.; Kalinsky, K. Sacituzumab Govitecan-hziy in Refractory Metastatic Triple-Negative Breast Cancer. *New England Journal of Medicine* **2019**, 380, 741-751.

147. Chari, R. V. J.; Miller, M. L.; Widdison, W. C. Antibody–Drug Conjugates: An Emerging Concept in Cancer Therapy. *Angewandte Chemie International Edition* **2014**, *53*, 3796-3827.
148. Kovtun, Y. V.; Audette, C. A.; Mayo, M. F.; Jones, G. E.; Doherty, H.; Maloney, E. K.; Erickson, H. K.; Sun, X.; Wilhelm, S.; Ab, O.; Lai, K. C.; Widdison, W. C.; Kellogg, B.; Johnson, H.; Pinkas, J.; Lutz, R. J.; Singh, R.; Goldmacher, V. S.; Chari, R. V. J. Antibody-Maytansinoid Conjugates Designed to Bypass Multidrug Resistance. *Cancer research* **2010**, *70*, 2528-2537.
149. Li, J. Y.; Perry, S. R.; Muniz-Medina, V.; Wang, X.; Wetzel, L. K.; Rebelatto, M. C.; Hinrichs, M. J. M.; Bezabeh, B. Z.; Fleming, R. L.; Dimasi, N.; Feng, H.; Toader, D.; Yuan, A. Q.; Xu, L.; Lin, J.; Gao, C.; Wu, H.; Dixit, R.; Osbourn, J. K.; Coats, S. R. A Biparatopic HER2-Targeting Antibody-Drug Conjugate Induces Tumor Regression in Primary Models Refractory to or Ineligible for HER2-Targeted Therapy. *Cancer Cell* **2016**, *29*, 117-129.
150. Wallqvist, A.; Rabow, A. A.; Shoemaker, R. H.; Sausville, E. A.; Covell, D. G. Linking the growth inhibition response from the National Cancer Institute's anticancer screen to gene expression levels and other molecular target data. *Bioinformatics* **2003**, *19*, 2212-2224.
151. Chen, Y. C.; Lu, P. H.; Pan, S. L.; Teng, C. M.; Kuo, S. C.; Lin, T. P.; Ho, Y. F.; Huang, Y. C.; Guh, J. H. Quinolone analogue inhibits tubulin polymerization and induces apoptosis via Cdk1-involved signaling pathways. *Biochem Pharmacol* **2007**, *74*, 10-9.
152. Gorlewska, K.; Mazerska, Z.; Sowiński, P.; Konopa, J. Products of Metabolic Activation of the Antitumor Drug Ledakrin (Nitracrine) in Vitro. *Chemical Research in Toxicology* **2001**, *14*, 1-10.
153. Slaska, K.; Szmigiero, L.; Jaros-Kaminska, B.; Ciesielska, E.; Gniazdowski, M. The mechanism of inhibition of DNA transcription *in vitro* by nitracrine (Ledakrin, C-283). *Molecular pharmacology* **1979**, *16*, 287-296.
154. Gniazdowski, M.; Szmigiero, L. Nitracrine and its Congeners-An overview. *Gen. Pharmac.* **1995**, *26*, 473-481.
155. Peter, W. Electron Transfer and Oxidative Stress as Key Factors in the Design of Drugs Selectively Active in Hypoxia. *Current medicinal chemistry* **2001**, *8*, 739-761.
156. Denny, W. A.; Atwell, G. J.; Anderson, R. F.; Wilson, W. R. Hypoxia-Selective Antitumor Agents. 4. Relationships between Structure, Physicochemical Properties, and Hypoxia-Selective Cytotoxicity for Nitracrine Analogues with Varying Side Chains: The "Iminoacridan Hypothesis". *J. Med. Chem.* **1990**, *33*, 1288-1295.
157. Pawlak, K.; Pawlak, J. W.; Konopa, J. Cytotoxic and Antitumor Activity of 1-Nitroacridines as an Aftereffect of Their Interstrand DNA Cross-Linking. *Cancer research* **1984**, *44*, 4289-4296.
158. Xia, Y.; Yang, Z. Y.; Xia, P.; Bastow, K. F.; Tachibana, Y.; Kuo, S. C.; Hamel, E.; Hackl, T.; Lee, K. H. Antitumor Agents. 181. Synthesis and Biological Evaluation of 6,7,2',3',4'-Substituted-1,2,3,4-tetrahydro-2-phenyl-4-quinolones as a New Class of Antimitotic Antitumor Agents. *J. Med. Chem.* **1998**, *41*, 1155-1162.
159. Huang, S.-M.; Cheng, Y.-Y.; Chen, M.-H.; Huang, C.-H.; Huang, L.-J.; Hsu, M.-H.; Kuo, S.-C.; Lee, K.-H. Design and synthesis of 2-(3-alkylaminophenyl)-6-(pyrrolidin-1-yl)quinolin-4-ones as potent antitumor agents. *Bioorganic & Medicinal Chemistry Letters* **2013**, *23*, 699-701.
160. Li, L.; Wang, H. K.; Kuo, S. C.; Wu, T. S.; Mauger, A.; Lin, C. M.; Hamel, E.; Lee, K. H. Antitumor Agents 155. Synthesis and Biological Evaluation of 3',6,7-Substituted 2-Phenyl-4-quinolones as Antimicrotubule Agents. *J. Med. Chem.* **1994**, *37*, 3400-3407.
161. Mishra, V.; Pandeya, S. N.; Pannecouque, C.; Witvrouw, M.; De Clercq, E. Anti-HIV Activity of Thiosemicarbazone and Semicarbazone Derivatives of (±)-3-Menthone. *Archiv der Pharmazie* **2002**, *335*, 183-186.

162. Walcourt, A.; Loyevsky, M.; Lovejoy, D. B.; Gordeuk, V. R.; Richardson, D. R. Novel aroylhydrazone and thiosemicarbazone iron chelators with anti-malarial activity against chloroquine-resistant and -sensitive parasites. *The international journal of biochemistry & cell biology* **2004**, 36, 401-407.
163. Richardson, D. R.; Kalinowski, D. S.; Richardson, V.; Sharpe, P. C.; Lovejoy, D. B.; Islam, M.; Bernhardt, P. V. 2-Acetylpyridine Thiosemicarbazones are Potent Iron Chelators and Antiproliferative Agents: Redox Activity, Iron Complexation and Characterization of their Antitumor Activity. *Journal of Medicinal Chemistry* **2009**, 52, 1459-1470.
164. Yu, Y.; Suryo Rahmanto, Y.; Richardson, D. R. Bp44mT: an orally active iron chelator of the thiosemicarbazone class with potent anti-tumour efficacy. *British journal of pharmacology* **2012**, 165, 148-166.
165. Whitnall, M.; Howard, J.; Ponka, P.; Richardson, D. R. A class of iron chelators with a wide spectrum of potent antitumor activity that overcomes resistance to chemotherapeutics. *Proceedings of the National Academy of Sciences of the United States of America* **2006**, 103, 14901-14906.
166. Jansson, P. J.; Sharpe, P. C.; Bernhardt, P. V.; Richardson, D. R. Novel Thiosemicarbazones of the ApT and DpT Series and Their Copper Complexes: Identification of Pronounced Redox Activity and Characterization of Their Antitumor Activity. *Journal of Medicinal Chemistry* **2010**, 53, 5759-5769.
167. Kalinowski, D. S.; Yu, Y.; Sharpe, P. C.; Islam, M.; Liao, Y.-T.; Lovejoy, D. B.; Kumar, N.; Bernhardt, P. V.; Richardson, D. R. Design, Synthesis, and Characterization of Novel Iron Chelators: Structure–Activity Relationships of the 2-Benzoylpyridine Thiosemicarbazone Series and Their 3-Nitrobenzoyl Analogues as Potent Antitumor Agents. *Journal of Medicinal Chemistry* **2007**, 50, 3716-3729.
168. Girisha, H. R.; Srinivasa, G. R.; Gowda, D. C. A simple and environmentally friendly method for the synthesis of N-phenylanthranilic acid derivatives. *J. Chem. Res.* **2006**, 5, 342-344.
169. Nishihama, Y.; Ishikawa, Y.; Nishiyama, S. Total synthesis of (±)-megistophylline I. *Tetrahedron Letters* **2009**, 50, 2801-2804.
170. Satyanarayana, B.; Muralikrishna, P.; Kumar, D. R.; Ramachandran, D. Preparation and biological evaluation of phenothiazine derivatives. *J. Chem. Pharm. Res.* **2013**, 5, 262-266.
171. Chen, G.-L.; Zeng, B.; Eastmond, S.; Elsenussi, S. E.; Boa, A. N.; Xu, S.-Z. Pharmacological comparison of novel synthetic fenamate analogues with econazole and 2-APB on the inhibition of TRPM2 channels. *British journal of pharmacology* **2012**, 167, 1232-1243.
172. Goldberg, A. A.; Kelly, W. 29. Synthesis of diaminoacridines. Part I. *J. Chem. Soc.* **1946**, 102-111.
173. Monnier, F.; Taillefer, M. Catalytic C–C, C–N, and C–O Ullmann-Type Coupling Reactions. *Angewandte Chemie International Edition* **2009**, 48, 6954-6971.
174. O'Connor, C. J.; Mclennan, D. J.; Denny, W. A.; Sutton, B. M. Substituent Effects on the Hydrolysis of Analogues of Nitracrine {9-[3-(N,Ndimethylamino) propylamino] -1 - nitroacridine}. *J. Chem. Soc. Perkin Trans. 2* **1990**, 1637-1641.
175. Isaev, S. G.; Yeryomina, H. O.; Zhukova, T. V.; Kryuchkova, T. M.; Zhegunova, G. P. Synthesis, structure and research of the pharmacological activity of methyl esters of 6-nitro-N-phenylanthranilic acids. *News of Pharmacy* **2014**, 2, 29-33.
176. Routier, S.; Saugé, L.; Ayerbe, N.; Coudert, G.; Mérour, J.-Y. A mild and selective method for N-Boc deprotection. *Tetrahedron Letters* **2002**, 43, 589-591.
177. Byun, J. S.; Sohn, J. M.; Leem, D. G.; Park, B.; Nam, J. H.; Shin, D. H.; Shin, J. S.; Kim, H. J.; Lee, K.-T.; Lee, J. Y. In vitro synergistic anticancer activity of the combination of T-type calcium channel blocker and chemotherapeutic agent in A549 cells. *Bioorganic & Medicinal Chemistry Letters* **2016**, 26, 1073-1079.

178. Jae Yeol Lee, K.-T. L. 3,4-dihydroquinazoline derivative and complex preparation containing same **2015**, EP3150584A4.
179. Li, H.; Hao, M.-a.; Wang, L.; Liang, W.; Chen, K. Preparation of Mono Boc-Protected Unsymmetrical Diamines. *Organic Preparations and Procedures International* **2009**, 41, 301-307.
180. Wolfe, S.; Hasan, S. Five-membered rings. II. Inter and intramolecular reactions of simple amines with N-substituted phthalimides. Methylamine as a reagent for removal of a phthaloyl group from nitrogen. *Canadian Journal of Chemistry* **2011**, 48, 3572-3579.
181. Wee, A. Ceric ammonium nitrate oxidation of N-(p-methoxybenzyl) lactams: Competing formation of N-(hydroxymethyl) δ -lactams. *Arkivoc* **2014**, 2014, 108.
182. Nickel, A.; Maruyama, T.; Tang, H.; Murphy, P. D.; Greene, B.; Yusuff, N.; Wood, J. L. Total Synthesis of Ingenol. *Journal of the American Chemical Society* **2004**, 126, 16300-16301.
183. Wang, S.-Y.; Lee, Y.-L.; Lai, Y.-H.; Chen, J. J. W.; Wu, W.-L.; Yuann, J.-M. P.; Su, W.-L.; Chuang, S.-M.; Hou, M.-H. Spermine Attenuates the Action of the DNA Intercalator, Actinomycin D, on DNA Binding and the Inhibition of Transcription and DNA Replication. *PloS one* **2012**, 7, e47101.
184. Risinger, A. L.; Mooberry, S. L. Cellular studies reveal mechanistic differences between taccalonolide A and paclitaxel. *Cell cycle (Georgetown, Tex.)* **2011**, 10, 2162-2171.
185. Pei, H.; Peng, Y.; Zhao, Q.; Chen, Y. Small molecule PROTACs: an emerging technology for targeted therapy in drug discovery. *RSC Advances* **2019**, 9, 16967-16976.
186. Klayman, D. L.; Bartosevich, J. F.; Griffin, T. S.; Mason, C. J.; Scovill, J. P. 2-Acetylpyridine thiosemicarbazones. 1. A new class of potential antimalarial agents. *Journal of Medicinal Chemistry* **1979**, 22, 855-862.
187. Berg, C. A convenient synthesis of N-isothiocyanatoimines. *Journal of the Chemical Society, Chemical Communications* **1974**, 122-123.
188. Radics, U.; Liebscher, J.; Ziemer, B.; Rybakov, V. Ring-chain transformations, IX[1] Synthesis and ring-chain tautomerism of 2-(ω -aminoalkyl)-1,3,4-thiadiazoles. *Chemische Berichte* **1992**, 125, 1389-1395.
189. Serda, M.; Kalinowski, D. S.; Rasko, N.; Potůčková, E.; Mrozek-Wilczkiewicz, A.; Musiol, R.; Małeck, J. G.; Sajewicz, M.; Ratuszna, A.; Muchowicz, A.; Gołąb, J.; Šimůnek, T.; Richardson, D. R.; Polanski, J. Exploring the Anti-Cancer Activity of Novel Thiosemicarbazones Generated through the Combination of Retro-Fragments: Dissection of Critical Structure-Activity Relationships. *PloS one* **2014**, 9, e110291.
190. West, D. X.; Ives, J. S.; Krejci, J.; Salberg, M. M.; Zumbahlen, T. L.; Bain, G. A.; Liberta, A. E.; Valdes-Martinez, J.; Hernandez-Ortiz, S.; Toscano, R. A. Copper(II) complexes of 2-benzoylpyridine 4N-substituted thiosemicarbazones. *Polyhedron* **1995**, 14, 2189-2200.
191. Chapkanov, A.; Dzimbova, T.; Ivanova, B. A facile synthesis and IR-LD spectral elucidation of N-acetyl amino acid derivatives. *Bulgarian Chemical Communications 0324-1130* **2012**, 44, 228 – 232.
192. Mitsumori, T. S., Takayuki Preparation of isothiazole compounds as industrial antibactericides, JP 2009298717. **2009**.
193. Lanigan, R. M.; Starkov, P.; Sheppard, T. D. Direct Synthesis of Amides from Carboxylic Acids and Amines Using B(OCH₂CF₃)₃. *The Journal of Organic Chemistry* **2013**, 78, 4512-4523.
194. Li, B.; Berliner, M.; Buzon, R.; Chiu, C. K. F.; Colgan, S. T.; Kaneko, T.; Keene, N.; Kissel, W.; Le, T.; Leeman, K. R.; Marquez, B.; Morris, R.; Newell, L.; Wunderwald, S.; Witt, M.; Weaver, J.; Zhang, Z.; Zhang, Z. Aqueous Phosphoric Acid as a Mild Reagent for Deprotection of tert-Butyl Carbamates, Esters, and Ethers. *The Journal of Organic Chemistry* **2006**, 71, 9045-9050.

195. Michinori, O.; Keiji, K. The Reaction of Sulfenyl Chlorides with Thioethers. I. The Scope of the Reactions. *Bulletin of the Chemical Society of Japan* **1970**, 43, 1223-1229.
196. Duane Brown, W. Reduction of protein disulfide bonds by sodium borohydride. *Biochimica et biophysica acta* **1960**, 44, 365-367.
197. Anderson, G. W.; Zimmerman, J. E.; Callahan, F. M. N-Hydroxysuccinimide Esters in Peptide Synthesis. *Journal of the American Chemical Society* **1963**, 85, 3039-3039.
198. Joullié, M. Evolution of amide bond formation. *Arkivoc* **2010**, 2010, 189.
199. Lippert III, J. W. Amide bond formation by using amino acid fluorides. *Arkivoc* **2005**, 2005, 87-95.
200. TEUFEL, G. B. D. P. COMPOUNDS FOR TREATING CANCER. WO2018/127699. **2018**.
201. Belkheira, M.; El Abed, D.; Pons, J.-M.; Bressy, C. Organocatalytic Synthesis of 1,2,3-Triazoles from Unactivated Ketones and Arylazides. *Chemistry – A European Journal* **2011**, 17, 12917-12921.
202. Thompson, P.; Fleming, R.; Bezabeh, B.; Huang, F.; Mao, S.; Chen, C.; Harper, J.; Zhong, H.; Gao, X.; Yu, X.-Q.; Hinrichs, M. J.; Reed, M.; Kamal, A.; Strout, P.; Cho, S.; Woods, R.; Hollingsworth, R. E.; Dixit, R.; Wu, H.; Gao, C.; Dimasi, N. Rational design, biophysical and biological characterization of site-specific antibody-tubulysin conjugates with improved stability, efficacy and pharmacokinetics. *Journal of Controlled Release* **2016**, 236, 100-116.
203. Kaltenbronn, J. S.; Scherrer, R. A.; Short, F. W.; Jones, E. M.; Beatty, H. R.; Saka, M. M.; Winder, C. V.; Wax, J.; Williamson, W. R. Structure-activity relationships in a series of anti-inflammatory N-arylanthranilic acids. *Arzneimittelforschung* **1983**, 33, 621-7.
204. Jackson, A.; Guilbert, B. B.; Plant, S. D.; Goggi, J.; Battle, M. R.; Woodcraft, J. L.; Gaeta, A.; Jones, C. L.; Bouvet, D. R.; Jones, P. A.; O'Shea, D. M.; Zheng, P. H.; Brown, S. L.; Ewan, A. L.; Trigg, W. The development of potential new fluorine-18 labelled radiotracers for imaging the GABAA receptor. *Bioorganic & Medicinal Chemistry Letters* **2013**, 23, 821-826.
205. Allegretti, M.; Bertini, R.; Cesta, M. C.; Bizzarri, C.; Di Bitondo, R.; Di Cioccio, V.; Galliera, E.; Berdini, V.; Topai, A.; Zampella, G.; Russo, V.; Di Bello, N.; Nano, G.; Nicolini, L.; Locati, M.; Fantucci, P.; Florio, S.; Colotta, F. 2-Arylpropionic CXC Chemokine Receptor 1 (CXCR1) Ligands as Novel Noncompetitive CXCL8 Inhibitors. *Journal of Medicinal Chemistry* **2005**, 48, 4312-4331.
206. Reuillon, T.; Bertoli, A.; Griffin, R. J.; Miller, D. C.; Golding, B. T. Efficacious N-protection of O-aryl sulfamates with 2,4-dimethoxybenzyl groups. *Organic & Biomolecular Chemistry* **2012**, 10, 7610-7617.
207. Jiang, C.; Yang, L.; Wu, W.-T.; Guo, Q.-L.; You, Q.-D. De novo design, synthesis and biological evaluation of 1,4-dihydroquinolin-4-ones and 1,2,3,4-tetrahydroquinazolin-4-ones as potent kinesin spindle protein (KSP) inhibitors. *Bioorganic & Medicinal Chemistry* **2011**, 19, 5612-5627.
208. Shi, H.-B.; Hu, W.-X.; Zhang, W.-M.; Wu, Y.-F. Synthesis of 5-acetyl-2-arylamino-4-methylthiazole Thiosemicarbazones under Microwave Irradiation and their in Vitro Anticancer Activity. *Journal of Chemical Research* **2016**, 40, 67-72.
209. Cao, S.; Duan, W. Microwave assisted solvent-free CH amination by silica-supported manganese dioxide. *Tetrahedron Letters* **2016**, 57, 2390-2394.
210. Sabatino, D.; Proulx, C.; Klocek, S.; Bourguet, C. B.; Boeglin, D.; Ong, H.; Lubell, W. D. Exploring Side-Chain Diversity by Submonomer Solid-Phase Aza-Peptide Synthesis. *Organic Letters* **2009**, 11, 3650-3653.
211. Martin, T. A.; Causey, D. H.; Sheffner, A. L.; Wheeler, A. G.; Corrigan, J. R. Amides of N-Acylcysteines as Mucolytic Agents. *Journal of Medicinal Chemistry* **1967**, 10, 1172-1176.

212. Uttamsingh, V.; Keller, D. A.; Anders, M. W. Acylase I-Catalyzed Deacetylation of N-Acetyl-L-cysteine and S-Alkyl-N-acetyl-L-cysteines. *Chemical Research in Toxicology* **1998**, *11*, 800-809.
213. Keller, M.; Erdmann, D.; Pop, N.; Pluym, N.; Teng, S.; Bernhardt, G.; Buschauer, A. Red-fluorescent argininamide-type NPY Y1 receptor antagonists as pharmacological tools. *Bioorganic & Medicinal Chemistry* **2011**, *19*, 2859-2878.
214. Skwarecki, A. S.; Skarbek, K.; Martynow, D.; Serocki, M.; Bylińska, I.; Milewska, M. J.; Milewski, S. Molecular Umbrellas Modulate the Selective Toxicity of Polyene Macrolide Antifungals. *Bioconjugate Chemistry* **2018**, *29*, 1454-1465.
215. Jahani, F.; Tajbakhsh, M.; Golchoubian, H.; Khaksar, S. Guanidine hydrochloride as an organocatalyst for N-Boc protection of amino groups. *Tetrahedron Letters* **2011**, *52*, 1260-1264.
216. Cregge, R. J.; Durham, S. L.; Farr, R. A.; Gallion, S. L.; Hare, C. M.; Hoffman, R. V.; Janusz, M. J.; Kim, H.-O.; Koehl, J. R.; Mehdi, S.; Metz, W. A.; Peet, N. P.; Pelton, J. T.; Schreuder, H. A.; Sunder, S.; Tardif, C. Inhibition of Human Neutrophil Elastase. 4. Design, Synthesis, X-ray Crystallographic Analysis, and Structure–Activity Relationships for a Series of P2-Modified, Orally Active Peptidyl Pentafluoroethyl Ketones. *Journal of Medicinal Chemistry* **1998**, *41*, 2461-2480.
217. Ahmad Omar, K.; Brown Stephen, P.; Dirico Kenneth, J.; Dushin, R.; Filzen Gary, F.; Puthenveetil, S.; Strop, P.; Subramanyam, C.; Tumej Lawrence, N. Calicheamicin Derivatives And Antibody Drug Conjugates Thereof. WO 2018/138591 A1, 2018/01/10, 2018.
218. Pfister, R.; Ihalainen, J.; Hamm, P.; Kolano, C. Synthesis, characterization and applicability of three isotope labeled azobenzene photoswitches. *Organic & Biomolecular Chemistry* **2008**, *6*, 3508-3517.
219. Murawska, G. M.; Poloni, C.; Simeth, N. A.; Szymanski, W.; Feringa, B. L. Comparative Study of Photoswitchable Zinc-Finger Domain and AT-Hook Motif for Light-Controlled Peptide–DNA Binding. *Chemistry – A European Journal* **2019**, *25*, 4965-4973.
220. Spletstoser, J. T.; Flaherty, P. T.; Himes, R. H.; Georg, G. I. Synthesis and Anti-Tubulin Activity of a 3'-(4-Azidophenyl)-3'-dephenylpaclitaxel Photoaffinity Probe. *Journal of Medicinal Chemistry* **2004**, *47*, 6459-6465.
221. Griffin, R. J.; Evers, E.; Davison, R.; Gibson, A. E.; Layton, D.; Irwin, W. J. The 4-azidobenzoyloxycarbonyl function; application as a novel protecting group and potential prodrug modification for amines. *Journal of the Chemical Society, Perkin Transactions 1* **1996**, 1205-1211.